Title
Development of mutually orthogonal chemistries for multicomponent biomolecule labeling

Author
Kamber, David N.

Publication Date
2015

Peer reviewed|Thesis/dissertation

UNIVERSITY OF CALIFORNIA, IRVINE

Development of mutually orthogonal chemistries for multicomponent biomolecule labeling

DISSERTATION

submitted in partial satisfaction of the requirements for the degree of

DOCTOR OF PHILOSOPHY

in Chemistry

by

David N. Kamber

Dissertation Committee:

Professor Jennifer A. Prescher, Chair

Professor Larry E. Overman

Professor Shiou-Chuan (Sheryl) Tsai

2015

DEDICATION

To

my family, friends, and mentors

for their support and inspiration.

Like everything metaphysical

the harmony between thought and reality

is to be found in the grammar of the language.

-Wittgenstein

TABLE OF CONTENTS

LIST OF FIGURES

LIST OF TABLES

David N. Kamber

EDUCATION

University of California, Irvine Irvine, CA, 2011–2015

- Ph.D., Chemistry

Benedictine University Lisle, IL, 2008–2011

- B.S., Biochemistry and Molecular Biology, *magna cum laude*

RESEARCH EXPERIENCE

Graduate Student with Prof. Jennifer Prescher, UC-Irvine 2011–2015

Thesis project: Development of mutually orthogonal chemistries for multicomponent labeling.

- *Developed 1,2,4-triazines as highly selective and tunable dienes for bioorthogonal chemistry. 1,2,4-Triazine amino acid was synthesized and utilized in recombinant protein production.*
- *Developed isomeric cyclopropenes for sequential labeling of biomolecules. First example of tandem [4+2] IED-DA and 1,3-dipolar cycloaddition for dual labeling.*

Undergraduate Researcher with Prof. Kari Stone, Benedictine University 2009–2011

worked on the synthesis of transition metal complexes with redox-active ligands for the purpose of nitrogen activation.

PUBLICATIONS

5) Kamber, D.N.; Liang, Y.; Briggs, J.; Houk, K.N.; Prescher, J. A: Scope and reactivity of 1,2,4-triazines in inverse electron demand Diels-Alder. *In preparation.*

4) Kamber, D.N.; Liang, Y.; Blizzard, R. J.; Liu, F.; Mehl, Y.; Houk, K.N.; Prescher, J. A. 1,2,4-Triazines are versatile bioorthogonal reagents. *J. Am. Chem. Soc*. **2015**, *137*, 8388.

3) Shih, H-W.*; Kamber, D.N.*; Prescher, J. A. Building better bioorthogonal reactions. *Curr. Opin. Chem. Biol*. **2014,** *21*, 103. [*denotes equal contribution]

2) Kamber, D.N.; Nazarova, L.A.; Liang, Y.; Lopez, S.A.; Patterson, D.M.; Shih, H-W.; Houk, K.N.; Prescher, J.A. Isomeric cyclopropenes exhibit unique bioorthogonal reactivities. *J. Am. Chem. Soc*. **2013**, *135*, 13680.

1) Patterson, D. M.; Nazarova, L. A.; Xie, B.; Kamber, D. N.; Prescher, J. A. Functionalized cyclopropenes as bioorthogonal chemical reporters. *J. Am. Chem. Soc.* **2012**, *134*, 18638.

PRESENTATIONS

4) David N. Kamber, Yong Liang, Robert J. Blizzard, Fang Liu, Ryan A. Mehl, K. N. Houk, and Jennifer A. Prescher, "Development of mutually orthogonal chemistries for multicomponent labeling," oral presentation, Bader Awards Symposium, Milwaukee, WI, August 13, 2015.

3) David N. Kamber, Lidia A. Nazarova, Yong Liang, Steven A. Lopez, David M. Patterson, Hui-Wen Shih, K. N. Houk , and Jennifer A. Prescher, "Design and synthesis of isomeric cyclopropenes for bioorthogonal chemistry," poster presentation, *248th ACS National Meeting*, San Francisco, CA, August 10-14, 2014.

2) David N. Kamber and Kari L. Stone, "Synthesis of First Row Transition Metal Complexes with Redox-active Ligands," oral presentation, 44th *Associated Colleges of the Chicago Area* student symposium, Chicago, IL, April 9, 2011.

1) Jonathan Pollock, David N. Kamber, and Allison K. Wilson, "Investigation of McCune-Albright syndrome using 2B2 cells with mutation D223E," oral presentation, 44th *Associated Colleges of the Chicago Area* student symposium, Chicago, IL, April 9, 2011.

AWARDS

- UC Regents Dissertation Fellowship, 2015
- Aldrich Alfred R. Bader Award for Student Innovation, 2015
- Kappa Gamma Pi, 2011
- ACS Division of Inorganic Chemistry Undergraduate Award, 2011
- Benedictine University Scholars Program (campus-wide honors program), 2008-2010

ABSTRACT OF THE DISSERTATION

Development of mutually orthogonal chemistries for multicomponent biomolecule labeling

By

David N. Kamber

Doctor of Philosophy in Chemistry

University of California, Irvine, 2015

Professor Jennifer A. Prescher, Chair

The bioorthogonal chemical reporter strategy provides a method for selectively labeling biomolecules with detectable probes. This strategy relies on the incorporation of a unique reporter into a biomolecule, followed by a covalent ligation with a secondary reagent. This approach can be used to visualize or retrieve biomolecules in complex environments. Over the past decade, the bioorthogonal chemical reporter strategy has been successfully applied to label and study various biomolecules in complex systems. However, the scope of this method has been hindered by a lack of reactions that are compatible with each other. Most of the popular bioorthogonal reagents to date cross react, precluding multicomponent imaging studies and other applications. To address this issue and expand the scope of the chemical reporter strategy, new reagents and chemistries were developed and their reactivities were analyzed.

In Chapter 1, I highlight the most commonly used bioorthogonal reactions, discuss the reactivity of the different reactions, and emphasize areas of improvements and sources of inspiration for thinking about bioorthogonal reactions. In Chapter 2, I focus on the development of new candidate reactions for biomolecule labeling. More specifically, the reactivity of 1,3-disubstituted and 3,3-disubstituted cyclopropenes with tetrazines and nitrile imines is discussed.

3,3-Disubstituted cyclopropenes were shown to exhibit orthogonal reactivity with tetrazines, but still react robustly with nitrile imine probes. In Chapter 3, I discuss the development of 1,2,4-triazine as a novel diene for bioorthogonal labeling applications. 1,2,4-Triazines were synthesized via an expedient route, and their reactivity and stability were analyzed. 1,2,4-Triazines were shown to exhibit robust stability and selective reactivity with *trans*-cyclooctene over other commonly used strained dienophiles. Additionally, a non-canonical amino acid comprising the triazine motif was synthesized and successfully used to tag model proteins. In Chapter 4, the reactivity profile of the triazine scaffold is discussed. I analyzed the reactivity of isomeric 1,2,4-triazines with a panel of commonly used bioorthogonal reagents. A combination of steric and electronic perturbations was applied to the development of cycloaddition reactions that could be used simultaneously.

Collectively, this thesis explores novel chemical reagents for bioorthogonal chemistry. New chemical reagents that exhibit mutually orthogonal reactivity are developed and used to label biomolecules. Looking ahead, the chemistries described here will advance the scope of the chemical reporter strategy for multicomponent studies.

CHAPTER 1: Building better bioorthogonal reactions

Hui-Wen Shih contributed to the work presented in this chapter.

1.1 Introduction

Our understanding of living systems is being continually shaped and refined by unique chemical tools. Included in this group are selective, covalent reactions that can be used to target large biopolymers, small molecule metabolites, and other cellular species with probes for visualization or identification [1]. These reactions are minimally perturbing to biological systems and, thus, have been collectively termed 'bioorthogonal'. Bioorthogonal chemistries were initially employed to examine glycans and other biopolymers in cells, but they have since been applied in numerous other contexts. The early successes of these transformations also inspired nearly two decades of research toward building faster and more exquisitely selective reactions. Impressively, there are now over twenty unique chemistries suitable for tagging isolated biomolecules, with nearly half being reported within the past five years [2].

While the bioorthogonal toolkit continues to expand at a rapid pace, the seamless transition of these chemistries into the most complex settings — live cells and organisms — has not been fully realized. This is due, in part, to a lack of functional groups that operate under the most extreme conditions. These groups must be stable in aqueous environments, yet robustly reactive with complementary probes. The motifs must also be sufficiently bioavailable to reach their targets, yet remain inert to surrounding molecules, cells, and even tissues. Only a handful of bioorthogonal chemistries — out of the dozens

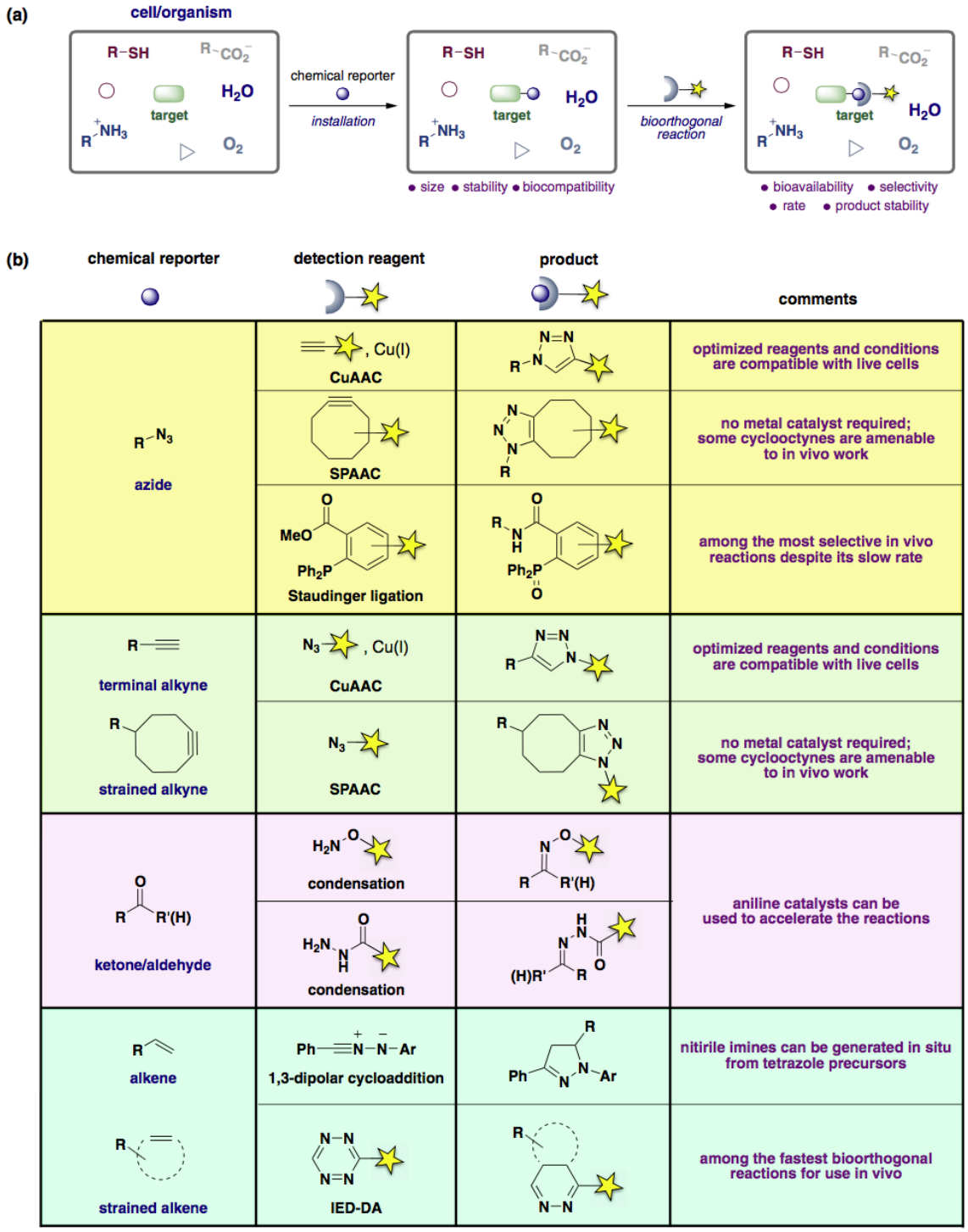

Figure 1-1. Chemical reporters and bioorthogonal chemistries for biomolecule tagging *in vivo*. (A) Considerations for bioorthogonal reaction development. Chemical reporters (blue circles) must be installed onto target biomolecules and remain stable in cellular environments. The covalent labeling reaction with a complementary functional groups (blue arc) must also provide stable adducts and be minimally perturbing to surrounding biomolecules (shapes). (B) Popular bioorthogonal reagents and reactions for *in vivo* use.

reported to date — satisfy these stringent criteria [2]. And, among these, no one reaction has emerged as a perfect fit for all applications.

Designing and building better bioorthogonal reactions thus remain important goals in chemical biology. Such efforts require exceptional functional groups that interface well with biological systems and exhibit reliable, biocompatible reactivities. In this chapter, individual functional groups that underlie the most successful bioorthogonal reactions *in vivo* are highlighted. Recent efforts to tune the reactivities and stabilities of these motifs using physical organic chemistry principles are also discussed. Last, ongoing work to not only identify improved bioorthogonal chemistries, but also *combinations* of reactions that are orthogonal to one another and can be used in concert for biomolecule tracking are discussed. An arsenal of such reactions will enable more complex biological networks to be examined in real time and paint a more complete picture of living systems.

1.2 Paving the way with 'privileged' scaffolds

Applications of bioorthogonal chemistries *in vivo* typically involve two steps. First, a metabolic substrate, biomolecule (e.g., antibody), or other target is outfitted with a biocompatible functional group (i.e., a 'chemical reporter') and introduced into the cell or organism (Figure 1-1a). Once the reporter has reached its target, the second step involves a selective (bioorthogonal) reaction with a complementary probe. In most cases, the secondary probe is outfitted with a visual tag or affinity agent to facilitate either the direct detection or isolation of the target biomolecule (Figure 1-1a) [3]. While both the reporter and its partner probe must be compatible with living systems, the criteria placed on the reporter are often more stringent. This group must be minimally perturbing to the target structure to avoid interfering with its normal activity. The

reporter must also tolerate cellular environments for extended periods of time. Few functional groups satisfy these requirements, and most are quite stable and small in size (Figure 1-1b). These 'privileged' scaffolds and their associated bioorthogonal reactions are briefly described below [4].

1.2a Azides

The organic azide is arguably the most recognized chemical reporter to date. This functional group is remarkably compatible with cells and nascent biosynthetic pathways owing to its small size and stability [5]. Azides can be readily detected with soft nucleophiles and dipolarophiles — motifs that are similarly bioorthogonal [6,7]. The most popular azide-specific ligation is the Huisgen 1,3-dipolar cycloaddition with terminal alkynes. This reaction requires alkyne activation (often via a Cu (I) catalyst) to proceed under physiological conditions [8]. The copper-catalyzed azide-alkyne cycloaddition (CuAAC) is ubiquitous in chemical biology, but has been historically difficult to apply *in vivo* due to its tri-component nature and concerns over copper cytotoxicity [9]. However, new metal-chelating reagents obviate the need for large quantities of copper [10,11] and are broadening the scope of CuAAC *in vivo* [12,13]. Other azide- alkyne cycloadditions eliminate metal catalysts altogether, relying instead on strain energies to promote reactivity (*vide infra*) [14]. Combinations of these reactions have recently been used to track biomolecules in human pathogens [15], visualize neuronal proteins [16] and examine cell wall biosynthesis [17,18].

1.2b Terminal alkynes

In addition to being popular reaction partners for azides, terminal alkynes are also 'privileged' chemical reporters. These functional groups are small and compatible with a variety

of enzymatic pathways and cellular environments [19,20]. Terminal alkynes are also found in various natural products, indicating that these motifs possess some degree of metabolic stability. Unlike their azido counterparts, though, fewer bioorthogonal transformations exist to detect alkynes. CuAAC with azido probes remains the reaction of choice, and this chemistry has been slower to transition into live cells and organisms.

1.2c Ketones and aldehydes

Ketones and aldehydes rival azides and alkynes in terms of size, and were among the first reagents pursued for bioorthogonal reaction development. These functional groups, while abundant inside cells in the form of monosaccharides, are virtually absent on cell surfaces and in extracellular spaces. Thus, ketones and aldehydes achieve bioorthogonality by being used in *unnatural* contexts. Both motifs can be affixed to surface biomolecules using metabolic probes or other reagents, and then subsequently detected via covalent reaction with hydrazides or aminooxy probes. Aldehydes can also be tagged using a recently reported Pictet–Spengler-type reaction [21]. This transformation offers improved kinetics and more stable oxacarboline adducts than traditional aldehyde ligations.

1.2d Alkenes

Alkenes are the newest members of the bioorthogonal toolkit. They are attractive chemical reporters owing to their small size, stability, and propensity to react with either 1,3-dipoles or dienes. These latter cycloadditions typically require heating or high pressures to proceed at reasonable rates, but can also be driven using electronically modified or strained alkenes [22,23]. Indeed, the reaction between strained *trans*-cyclooctene (TCO) and tetrazines proceeds readily in biological solutions and live cells. This inverse electron-demand Diels–Alder

(IED-DA) reaction is among the fastest bioorthogonal reactions reported to date, with second-order rate constants now approaching 10^5 M^{-1} s^{-1} in some cases [24]. IED-DA reactions with TCO and tetrazine have been used to visualize biological processes that occur on rapid time scales in preclinical models, where only minimal amounts of reagent can be used [24,25].

1.2e Tetrazines

Like alkenes, some tetrazines are both small and stable enough to be used as chemical reporters in living systems. Most harbor fewer electron-withdrawing substituents than tetrazines typically employed for IED-DA reactions. Electron-rich tetrazines are less susceptible to hydrolysis and attack by biological nucleophiles, and are thus more desirable for use *in vivo* and intracellular environments, in particular. Stabilized tetrazines have recently been introduced into recombinant proteins via unnatural amino acid mutagenesis. The heterocyclic amino acid derivatives survived prolonged incubation times in cellular media and could be covalently detected with strained alkenes (*vide infra*).

1.3 Tuning reagent reactivities and biocompatibilities

As noted above, bioorthogonal functional groups must often be tuned to achieve suitable reaction rates or biocompatibilities for use *in vivo*. Rapid transformations are essential for numerous imaging and drug delivery studies, as only small doses of probe can typically be used [25,26,27]. Reagents must also be sufficiently hydrophilic to avoid 'sticking' to surrounding biomolecules. Fortunately, most bioorthogonal functional groups can be readily modified to achieve desired properties (Figure 1-2).

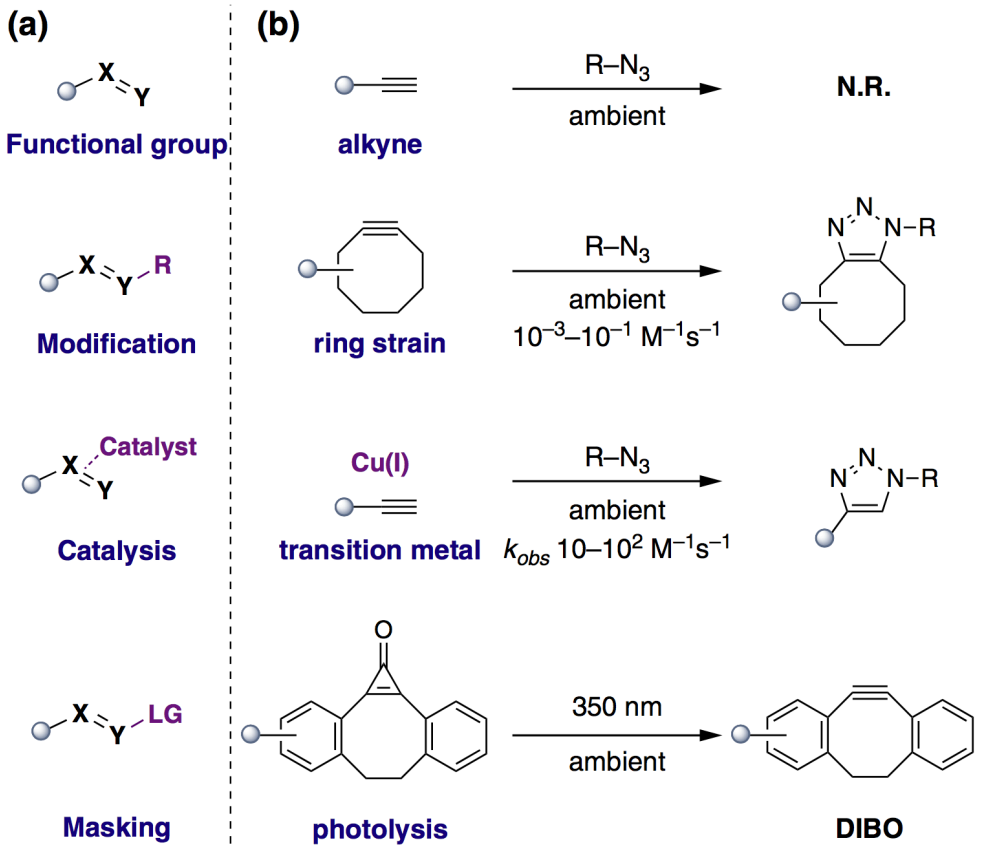

Figure 1-2. Functional group tuning for improved bioorthogonal reactivity. (A) Strategies to "activate" functional groups for efficient bioorthogonal ligation. (B) Examples of strategies used to activate alkynes for covalent reaction with organic azides. Under ambient conditions, no reaction between the functional groups is observed. Alkynes activated via ring strain or metal catalysis, though, are poised to undergo rapid bioorthogonal cycloaddition with azides. Reactive strained alkynes (e.g., DIBO) can also be liberated "on demand" via photolysis.

1.3a Modifying intrinsic properties

One of the most common methods to enhance bioorthogonal reactivity exploits ring strain. As noted above, alkenes and terminal alkynes are attractive chemical reporters based on size and stability. However, these motifs do not react with complementary bioorthogonal functional groups under mild conditions. Several groups have shown that alkene-based and

alkyne-based reactions can be driven via ring strain (Figure 1-2b) [28]. For example, the strained alkenes TCO and cyclopropene react with electron-deficient dienes via IED-DA reactions in physiological environments. Similarly, over twelve different strained cycloalkynes have been reported to react with azides under ambient conditions and in live cells [1].

In recent years, efforts to further tune different classes of strained reagents have revealed even more rapid bioorthogonal ligations. For example, Fox demonstrated that when TCO is fused to a cyclopropane ring, the reagent is forced to adopt a highly strained half-chair conformation. This constrained alkene reacts more rapidly in IED-DA reactions than TCO itself [29] and is especially advantageous for detecting the electron-rich (and less reactive) tetrazines used in recombinant protein production [30]. Chin and Lemke also showed that cyclopropane-fused cyclooctynes (i.e., bicyclononynes) offer improved reaction speeds for protein tagging applications in live cells [31,32]. Most recently, Lin and colleagues reported a strained spirocyclic alkene that exhibits accelerated cycloaddition rates relative to parental cyclopropenes [33]. Such small, hydrophilic, and fast-reacting bioorthogonal reagents are desirable for cellular and *in vivo* imaging where excess probe and non-specific binding must be avoided.

In addition to reaction speed, steric and electronic modifications can also dramatically influence bioorthogonal reagent stability and lipophilicity [27,28]. Indeed, optimizing for ligation speed often comes at the expense of probe stability or biocompatibility. In the case of tetrazines, Hilderbrand and coworkers demonstrated that small, electron-withdrawing substituents enhanced IED-DA reactivity (due to favorable FMO interactions in the transition state); however, these same modifications also promoted hydrolytic degradation of the tetrazine scaffold [34]. Similarly, some of the fastest reacting TCO motifs are the least stable *in vitro* and *in vivo* [24,30,34], while many of the most stable alkenes exhibit the slowest IED-DA rates

[35,36]. Striking the right balance of stability and reactivity is an ongoing challenge in bioorthogonal reaction development. However, systematic tuning will continue to refine bioorthogonal reagents for applications in cells and organisms, and perhaps reveal entirely new classes of reactions. Indeed, efforts to modulate cycloalkynes uncovered new manifolds of reactivity between cyclooctynes and various 1,3-dipoles [37,38,39].

1.4 Engineering reagents for 'on demand' reactivity

Bioorthogonal reagents can also be tuned for desired levels of reactivity and stability using extrinsic controls. Many current strategies involve liberating bioorthogonal groups with mild chemistries or exposure to light. These exogenous triggers enable highly reactive (and perhaps unstable) functional groups to be generated only when needed.

1.4a Chemical activation

One straightforward approach to controlling bioorthogonal chemistries involves synthesizing the reactants 'on demand'. For example, nitrones are attractive chemical reporters owing to their small size and rapid reactivity with strained alkynes. However, some nitrones are chemically unstable and not amenable to long-term storage. These 1,3-dipoles can be generated *in situ* from more stable precursors, including aldehydes and methylhydroxylamine. Boons and van Delft used this strategy to introduce nitrones into model proteins for subsequent reaction with cyclooctynes [40]. Similar chemical activation strategies have been reported for nitrile oxides [41], some diazo compounds [38,39], and oxidation-prone dienes [42]. Catalytic chemical activation strategies are also possible (Figure 1-2b). The most well known example, of course, is alkyne activation via CuAAC, although other metal catalysts have been recently explored [43]. Metal catalysts can also promote alkene reactivity. In a recent example, Davis and co-workers

utilized a Ru(II) catalyst to drive cross-metathesis reactions with allylselenides and allylsulfides on model proteins [44]. Further developments in catalytic activation are expected following recent reports on biocompatible palladium-mediated reactions [45,46,47]. Ongoing work in organocatalysis will also obviate the need for toxic metals in generating bioorthogonal agents 'on demand' [48,49].

1.4b Photoactivation

In addition to exogenous chemicals, light can be used to activate bioorthogonal motifs for reactivity. Popik and Boons reported one of the earliest examples of this approach, using cyclopropenone to conceal a strained alkyne (dibenzocyclooctyne or DIBO, Figure 1-2b). DIBO reacts rapidly with organic azides, but is prone to nucleophilic attack by endogenous thiols. Cyclopropenone protects the alkyne from such non-specific reactivity, and upon exposure to UV light, the mask is released (as CO) and functional DIBO is generated. Photoactivation thus enables exquisite temporal and spatial control over the labeling reaction [50,51,52]. Lin and others exploited a similar strategy to generate reactive nitrile imines (for 1,3-dipolar cycloaddition with unactivated alkenes) from tetrazoles [53,54]. Some recently reported tetrazoles can be photolyzed with near-IR light, improving the *in vivo* compatibility of this approach [55].

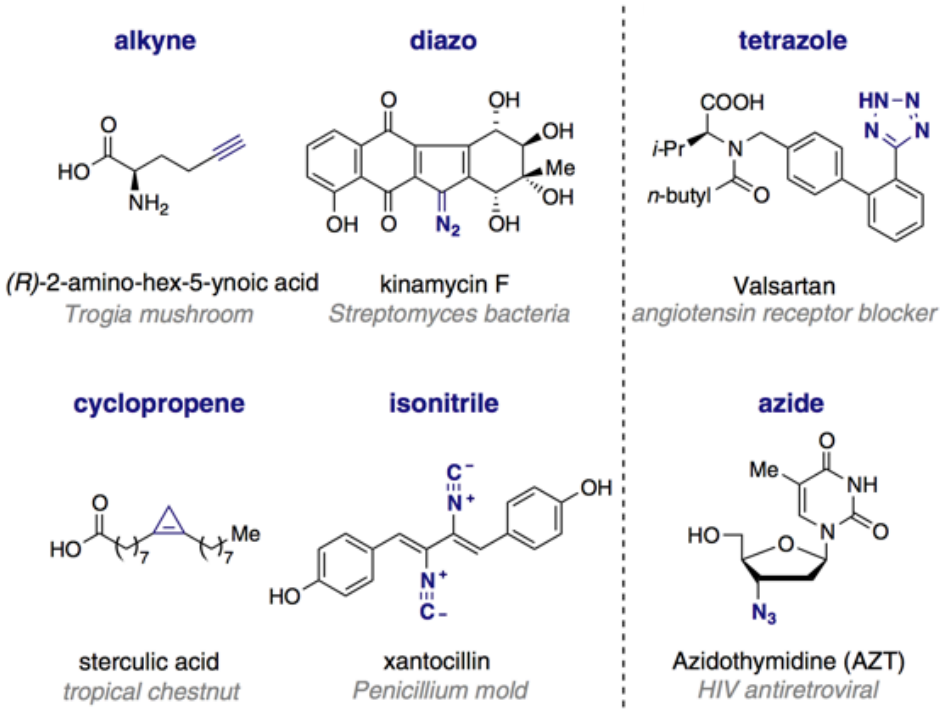

Figure 1-3. Inspiration for new bioorthogonal reagent discovery. Structures of representative natural products and therapeutic drugs harboring "bioorthogonal" functional groups (highlighted in blue).

1.5 Unfinished work

The majority of bioorthogonal functional groups are not 'bioorthogonal' in the truest sense of the word. Many are prone to hydrolysis over time, and some react with endogenous thiols or other biomolecules at high concentrations [20]. Additionally, many of the most popular bioorthogonal motifs are incompatible with one another and cannot be used concurrently to probe multiple biomolecules or cellular processes in vivo [2]. These limitations underscore the need for continued optimization of existing bioorthogonal reagents, along with efforts to discover new ones.

1.5a Establishing new platforms of reactivity

The hunt for new bioorthogonal functionality can take important cues from complex natural products. Microbes and other species produce an array of richly functionalized molecules harboring motifs not present in higher eukaryotes (Figure 1-3a). Translating such naturally occurring, 'privileged' groups into unnatural settings (e.g., mammalian cells) can be a fruitful starting point for reaction development. Indeed, popular bioorthogonal motifs, including terminal alkynes, have been identified in microbial metabolites and other natural products [56]. Several newly minted bioorthogonal reagents, including cyclopropenes and cyanobenzothiazoles, also have precedence in nature [57–59]. Careful analysis of natural product structures will likely reveal even more promising bioorthogonal functional groups.

Further inspiration for bioorthogonal motifs can be gleaned from drug discovery efforts [60]. Small molecule drugs are subjected to rigorous assays for toxicity, lipophilicity, and bioavailability-parameters relevant to bioorthogonality. The remarkable biocompatibility of organic azides was suggested over 30 years ago during preclinical work on azidothymidine (AZT). Similar data exist for tetrazoles, syndones, and other pharmacophores now gaining prominence in bioorthogonal reactions (Figure 1-3b) [61]. Efforts to improve reagent stabilities and reactivities will also benefit from drug discovery practices, where optimization of 'lead' scaffolds is routine. Indeed, Taran and colleagues recently employed modern screening techniques to rapidly identify new reaction partners for established bioorthogonal motifs [62].

1.5b Designing better reactions in silico

In parallel with new reaction discovery, efforts to improve existing bioorthogonal transformations will be beneficial. Toward this end, computational labs have identified algorithms that can reliably predict activation energy barriers for various bioorthogonal

cycloadditions. Already, these approaches have revealed insights into improved cyclooctyne and cyclopropene structures, reactivities, and stabilities [33,63,64,65]. Equally as important, computational methods can provide information on scaffolds to avoid in designing new bioorthogonal chemistries.

1.5c Identifying 'orthogonal' bioorthogonal reactions

In silico analyses are also aiding in the identification of pairs and even groups of bioorthogonal chemistries that are compatible with one another and applicable to multi-component tracking. A complete understanding of biological networks requires methods to track not just individual biomolecules, but combinations of molecules simultaneously. Unfortunately, many bioorthogonal reagents (especially strained alkenes and alkynes) are ill suited for such studies due to cross-reactivities [31]. Thus, identifying reactions that not only work well *in vivo*, but that also perform well in concert with established transformations is a major challenge (Figure 1-4a) [66,67,68]. Several efforts to map out pairs — and even groups — of mutually orthogonal reactions are well underway [66,69,70,71]. In 2012, we demonstrated that IED-DA with cyclopropenes and SPAAC with azides are mutually orthogonal and can be used concurrently for biomolecule visualization [36]. Others have since employed these mutually orthogonal reactions for the production of non-natural proteins and other applications [72,73]. Aided by computational work, we further identified a pair of regioisomeric cyclopropenes that exhibit unique cycloaddition preferences (Figure 1-4b) [63]. These and other 'orthogonal' bioorthogonal chemistries will enable more detailed looks into multi-component biological processes.

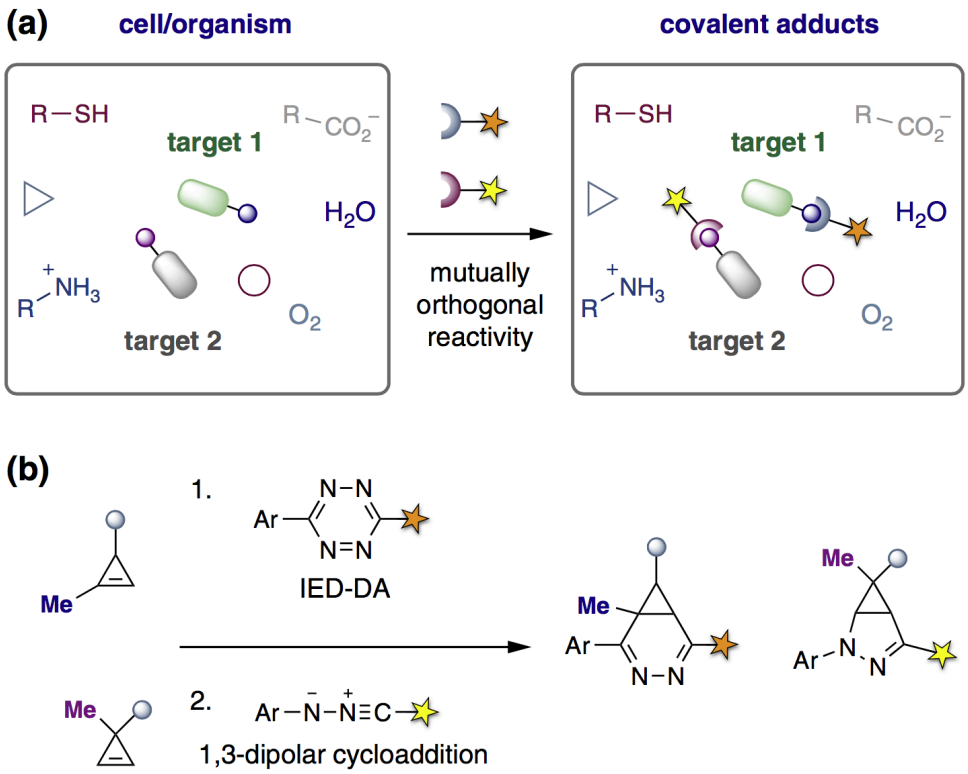

Figure 1-4. Expanding the bioorthogonal toolkit. (A) Compatible and "orthogonal" bioorthogonal reactions enable the detection of multiple biomolecules in complex environments. (B) Regioisomeric cyclopropenes exhibit unique cycloaddition reactivities and can be used in tandem for multi-component labeling experiments. 1,3-Disubstituted cyclopropenes can be selectively ligated with tetrazines via IED-DA ligation. 3,3-Disubstituted cyclopropenes can be readily reacted with nitrile imines via 1,3-dipolar cycloaddition.

1.6 Conclusions

Bioorthogonal reactions have provided unprecedented views of biomolecule structures and functions in complex environments. Despite their success in revealing new facets of biology, limitations remain: (1) many bioorthogonal reagents are too large or unstable for tagging native biomolecules in live cells, and (2) many of the most common reactions are incompatible with one another, limiting their utility for studies of multiple biomolecules in tandem. Thus,

identifying new bioorthogonal reagents and reactions that are not only suitable for use *in vivo* — but that also work well in tandem — remain important goals. A handful of 'privileged' motifs for in vivo use have been identified over the years, and efforts to improve their reactivities and biocompatibilities have benefited from a combi- nation of experimental work and computational chemistry. Continued, systematic optimization of these reagents and newly discovered ones will further expand the bioorthogonal toolkit.

In this thesis, new reagents and chemistries that expand the scope of the chemical reporter strategy are discussed. By tuning the steric properties of cyclopropenes, sequential labeling of biomolecules is accomplished. Additionally, 1,2,4-triazines are developed as alternative dienes for bioorthogonal chemistry. Furthermore, steric tuning of 1,2,4-triazines facilitated the development of compatible [4+2] cycloadditions. Collectively, these chemical transformations expand the bioorthogonal toolbox for multicomponent labeling.

1.7 References

(1) Ramil, C. P.; Lin, Q: Bioorthogonal chemistry: Strategies and recent developments. *Chem. Commun.* **2013**, *49*, 11007.

(2) Patterson, D. M.; Nazarova, L. A.; Prescher, J. A: Finding the right (bioorthogonal) chemistry. *ACS Chem. Biol.* **2014**, *9*, 592.

(3) Grammel, M.; Hang, H. C: Chemical reporters for biological discovery. *Nat. Chem. Biol.* **2013**, *9*, 475.

(4) Welsch, M. E.; Snyder, S. A.; Stockwell, B. R: Privileged scaffolds for library design and drug discovery. *Curr. Opin. Chem. Biol.* **2010**, *14*, 347.

(5) Bianco, A.; Townsley F. M.; Greiss, S.; Lang, K.; Chin, J. W: Expanding the genetic code of drosophila melanogaster. *Nat. Chem. Biol.* **2012**, *8*, 748.

(6) Debets, M. F.; van der Doelen, C. W.; Rutjes, P.; van Delft, F. L: Azide: A unique dipole for metal-free bioorthogonal ligations. *ChemBioChem* **2010**, *11*, 1168.

(7) van Berkel, S. S.; van Eldijk, M. B.; van Hest, J. C. M: Staudinger ligation as a method for bioconjugation. *Angew. Chem. Int. Ed.* **2011**, *50*, 8806.

(8) Worrell, B. T.; Malik, J. A.; Fokin, V. V: Direct evidence of a dinuclear copper intermediate in cu(i)-catalyzed azide-alkyne cycloadditions. *Science* **2013**, *340*, 457.

(9) Kennedy, D. C.; McKay, C. S.; Legault, M. C.; Danielson, D. C.; Blake, J. A.; Pegoraro, A. F.; Stolow, A.; Mester, Z.; Pezacki, J. P: Cellular consequences of copper complexes used to catalyze bioorthogonal click reactions. *J. Am. Chem. Soc.* **2011**, *133*, 17993.

(10) Uttamapinant, C.; Tangpeerachaikul, A.; Grecian, S.; Clarke, S.; Singh, U.; Slade, P.; Gee, K. R.; Ting, A. Y: Fast, cell-compatible click chemistry with copper-chelating azides for biomolecular labeling. *Angew. Chem. Int. Ed.* **2012**, *51*, 5852.

(11) Rudolf, G. C.; Sieber, S. A: Copper-assisted click reactions for activity-based proteomics: Fine-tuned ligands and refined conditions extend the scope of application. *ChemBioChem* **2013**, *14*, 2447.

(12) Jiang, H.; Zheng, T.; Lopez-Aguilar, A.; Feng, L.; Kopp, F.; Marlow, F, L.; Wu, P: Monitoring dynamic glycosylation in vivo using supersensitive click chemistry. *Bioconjug. Chem.* **2014**, *25*, 698.

(13) Lin, W.; Du, Y.; Zhu, Y.; Chen, X: A cis-membrane FRET-based method for protein-specific imaging of cell-surface glycans. *J. Am. Chem. Soc.* **2014**, *136*, 679.

(14) Jewett, J. C.; Bertozzi, C. R: Cu-free click cycloaddition reactions in chemical biology. *Chem. Soc. Rev.* **2010**, *39*, 1272.

(15) Tra, V. N.; Dube, D. H: Glycans in pathogenic bacteria - potential for targeted covalent

therapeutics and imaging agents. *Chem. Commun.* **2014**, *50*, 4659.

(16) Hinz, F. I.; Dieterich, D. C.; Tirrell, D. A.; Schuman, E. M: Non-canonical amino acid labeling in vivo to visualize and affinity purify newly synthesized proteins in larval zebrafish. *ACS. Chem. Neurosci.* **2012**, *3,* 40.

(17) Siegrist, M. S.; Whiteside, S.; Jewett, J. C.; Aditham, A.; Cava, F.; Bertozzi, C. R: D-Amino acid chemical reporters reveal peptidoglycan dynamics of an intracellular pathogen. *ACS Chem. Biol.* **2013**, *8,* 500.

(18) Liechti, G. W.; Kuru, E.; Hall, E.; Kalinda, A.; Brun, Y. V.; VanNieuwenhze, M.; Maurelli, A. T: A new metabolic cell-wall labelling method reveals peptidoglycan in *Chlamydia Trachomatis*. *Nature* **2014**, *506*, 507.

(19) Bateman, L. A.; Zaro, B. W.; Chuh, K. N.; Pratt, M. R: N-Propargyloxycarbamate monosaccharides as metabolic chemical reporters of carbohydrate salvage pathways and protein glycosylation. *Chem. Commun.* **2013**, *49*, 4328.

(20) Ekkebus, R.; van Kasteren, S. I.; Kulathu, Y.; Scholten, A.; Berlin, I.; Geurink, P. P.; de Jong, A.; Goerdayal, S.; Neefjes, J.; Heck, A. J.; Komander, D.; Ovaa, H: On terminal alkynes that can react with active-site cysteine nucleophiles in proteases. *J. Am. Chem. Soc.* **2013**, *135*, 2867.

(21) Agarwal, P.; van der Weijden, J.; Sletten, E. M.; Rabuka, D.; Bertozzi, C. R: A Pictet-Spengler ligation for protein chemical modification. *Proc. Natl. Acad. Sci. USA* **2013**, *110*, 46.

(22) Devaraj, N. K.; Weissleder, R: Biomedical applications of tetrazine cycloadditions. *Acc. Chem. Res.* **2011**, *44*, 816.

(23) Selvaraj, R.; Fox, J. M: *Trans*-cyclooctene- a stable, voracious dienophile for bioorthogonal labeling. *Curr. Opin. Chem. Biol.* **2013**, *17*, 753.

(24) Rossin, R.; van den Bosch, S. M.; Ten Hoeve, W.; Carvelli, M.; Versteegen, R. M.; Lub J.; Robillard, M. S: Highly reactive *trans*-cyclooctene tags with improved stability for Diels-Alder chemistry in living systems. *Bioconjug. Chem.* **2013**, *24*, 1210.

(25) Zeglis, B. M.; Sevak, K. K.; Reiner, T.; Mohindra, P.; Carlin, S. D.; Zanzonico, P.; Weissleder, R.; Lewis, J. S: A pretargeted PET imaging strategy based on bioorthogonal Diels-Alder click chemistry. *J. Nucl. Med.* **2013**, *54*, 1389.

(26) Lee, S.; Koo, H.; Na, J. H.; Han, S. J.; Min, H. S.; Lee, S. J.; Kim, S. H.; Yun, S. H.; Jeong, S. Y.; Kwon, I. C.; Choi, K.; Kim, K: Chemical tumor-targeting of nanoparticles based on metabolic glycoengineering and click chemistry. *ACS. Nano.* **2014**, *8*, 2048.

(27) van den Bosch, S. M.; Rossin, R.; Renart Verkerk, P.; Ten Hoeve, W.; Janssen, H. M.; Lub, J.; Robillard, M. S: Evaluation of strained alkynes for Cu-free click reaction in live mice. *Nucl. Med. Biol.* **2013**, *40*, 415.

(28) Debets, M. F.; van Berkel, S. S.; Dommerholt, J.; Dirks, A. T.; Rutjes, F. P.; van Delft, F. L: Bioconjugation with strained alkenes and alkynes. *Acc. Chem. Res.* **2011**, *44*, 805.

(29) Taylor, M. T.; Blackman, M. L.; Dmitrenko, O.; Fox, J. M: Design and synthesis of highly reactive dienophiles for the tetrazine-*trans*-cyclooctene ligation. *J. Am. Chem. Soc.* **2011**, *133*, 9646.

(30) Seitchik, J. L.; Peeler, J. C.; Taylor, M. T.; Blackman, M. L.; Rhoads, T. W.; Cooley, R. B.; Refakis, C.; Fox, J. M.; Mehl, R. A: Genetically encoded tetrazine amino acid directs rapid site-specific in vivo bioorthogonal ligation with *trans*-cyclooctenes. *J. Am. Chem. Soc.* **2012**, *134*, 2898.

(31) Borrmann, A.; Milles, S.; Plass, T.; Dommerholt, J.; Verkade, J. M.; Wiessler, M.; Schultz, C.; van Hest, J. C.; van Delft, F. L.; Lemke, E. A: Genetic encoding of a bicyclo[6.1.0]nonyne-

charged amino acid enables fast cellular protein imaging by metal-free ligation. *ChemBioChem* **2012**, *13*, 2094.

(32) Lang, K.; Davis, L.; Wallace, S.; Mahesh, M.; Cox, D. J.; Blackman, M. L.; Fox, J. M.; Chin, J. W: Genetic encoding of bicyclononynes and trans-cyclooctenes for site-specific protein labeling *in vitro* and in live mammalian cells via rapid fluorogenic Diels-Alder reactions. *J. Am. Chem. Soc.* **2012**, *134*, 10317.

(33) Yu, Z.; Lin, Q: Design of spiro[2.3]hex-1-ene, a genetically encodable double-strained alkene for superfast photoclick chemistry. *J. Am. Chem. Soc.* **2014**, *136*, 4153.

(34) Karver, M. R.; Weissleder, R.; Hilderbrand, S. A: Synthesis and evaluation of a series of 1,2,4,5-tetrazines for bioorthogonal conjugation. *Bioconjug. Chem.* **2011**, *22*, 2263.

(35) Yang, J.; Seckute, J.; Cole, C. M.; Devaraj, N. K: Live-cell imaging of cyclopropene tags with fluorogenic tetrazine cycloadditions. *Angew. Chem. Int. Ed.* **2012**, *51*, 7476.

(36) Patterson, D. M.; Nazarova, L. A.; Xie, B.; Kamber, D. N.; Prescher, J. A: Functionalized cyclopropenes as bioorthogonal chemical reporters. *J. Am. Chem. Soc.* **2012**, *134*, 18638.

(37) Sanders, B. C.; Friscourt, F.; Ledin, P. A.; Mbua, N. E.; Arumugam, S.; Guo, J.; Boltje, T. J.; Popik, V. V.; Boons, G. J: Metal-free sequential [3 + 2]-dipolar cycloadditions using cyclooctynes and 1,3-dipoles of different reactivity. *J. Am. Chem. Soc.* **2011**, *133*, 949.

(38) McGrath, N. A.; Raines, R. T: Diazo compounds as highly tunable reactants in 1,3-dipolar cycloaddition reactions with cycloalkynes. *Chem. Sci.* **2012**, *3*, 3237.

(39) Chou, H. H.; Raines, R. T: Conversion of azides into diazo compounds in water. *J. Am. Chem. Soc.* **2013**, *135*, 14936.

(40) Ning, X.; Temming, R. P.; Dommerholt, J.; Guo, J.; Ania, D. B.; Debets, M. F.; Wolfert, M. A.; Boons, G. J.; van Delft, F. L: Protein modification by strain-promoted alkyne-nitrone

cycloaddition. *Angew. Chem. Int. Ed.* **2010**, *49*, 3065.

(41) Chen, S. J.; Ren, J.; Wang, Z. W: A highly regioselective tandem 1,3-dipolar cycloaddition of cyclopropene 1,1-diesters and nitrile oxides: Synthesis of highly functionalized isoxazoles. *Tetrahedron* **2009**, *65*, 9146.

(42) Li, Q.; Dong, T.; Liu, X.; Lei, X: A bioorthogonal ligation enabled by click cycloaddition of O-quinolinone quinone methide and vinyl thioether. *J. Am. Chem. Soc.* **2013**, *135*, 4996.

(43) Li, J.; Lin, S.; Wang, J.; Jia, S.; Yang, M.; Hao, Z.; Zhang, X.; Chen, P. R: Ligand-free palladium-mediated site-specific protein labeling inside gram-negative bacterial pathogens. *J. Am. Chem. Soc.* **2013**, *135*, 7330.

(44) Lin, Y. A.; Boutureira, O.; Lercher, L.; Bhushan, B.; Paton, R. S.; Davis, B. G: Rapid cross-metathesis for reversible protein modifications via chemical access to Se-allyl-selenocysteine in proteins. *J. Am. Chem. Soc.* **2013**, *135*, 12156.

(45) Lercher, L.; McGouran, J. F, Kessler, B. M.; Schofield, C. J.; Davis B, G: DNA modification under mild conditions by Suzuki-Miyaura cross-coupling for the generation of functional probes. *Angew. Chem. Int. Ed.* **2013**, *52*, 10553.

(46) Yusop, R. M.; Unciti-Broceta A.; Johansson E, M, Sanchez-Martin R, M.; Bradley M: Palladium-mediated intracellular chemistry. *Nat. Chem.* **2011**, *3*, 239.

(47) Chankeshwara, S. V.; Indrigo, E.; Bradley, M: Palladium-mediated chemistry in living cells. *Curr. Opin. Chem. Biol.* **2014**, *21*, 128.

(48) Crisalli, P.; Kool, E. T: Water-soluble organocatalysts for hydrazone and oxime formation. *J. Org. Chem.* **2013**, *78*, 1184.

(49) Wendeler, M.; Gringberg, L.; Wang, X.; Dawson, P. E.; Baca, M: Enhanced catalysis of oxime-based bioconjugations by substituted anilines. *Bioconjug. Chem.* **2013**, *25*, 93.

(50) Arumugam, S.; Popik, V. V: Sequential "click" - "photo-click" cross-linker for catalyst-free ligation of azide-tagged substrates. *J. Org. Chem.* **2014**, *79*, 2702.

(51) Poloukhtine, A. A.; Mbua, N. E.; Wolfert, M. A.; Boons, G. J.; Popik, V. V: Selective labeling of living cells by a photo-triggered click reaction. *J. Am. Chem. Soc.* **2009**, *131*, 15769.

(52) Ramil, C. P.; Lin, Q: Photoclick chemistry: A fluorogenic light-triggered *in vivo* ligation reaction. *Curr. Opin. Chem. Biol.* **2014**, *21*, 89.

(53) Yu, Z.; Pan, Y.; Wang, Z.; Wang, J.; Lin, Q: Genetically encoded cyclopropene directs rapid, photoclick-chemistry-mediated protein labeling in mammalian cells. *Angew. Chem. Int. Ed.* **2012**, *51*, 10600.

(54) Lee, Y. J.; Wu, B.; Raymond, J. E.; Zeng, Y.; Fang, X, Q.; Wooley, K, L.; Liu, W, R, S: A genetically encoded acrylamide functionality. *ACS Chem. Biol.* **2013**, *8,* 1664.

(55) Yu, Z.; Ohulchanskyy, T. Y.; An, P.; Prasad, P. N.; Lin, Q: Fluorogenic, two-photon-triggered photoclick chemistry in live mammalian cells. *J. Am. Chem. Soc.* **2013**, *135*, 16766.

(56) Minto, R. E.; Blacklock, B. J: Biosynthesis and function of polyacetylenes and allied natural products. *Prog. Lipid. Res.* **2008**, *47*, 233.

(57) Wainman, Y. A.; Neves, A. A.; Stairs, S.; Stockmann, H.; Ireland-Zecchini, H.; Brindle, K, M.; Leeper, F, J: Dual-sugar imaging using isonitrile and azido-based click chemistries. *Org. Biomol. Chem.* **2013**, *11*, 7297.

(58) Matsuura, M.; Saikawa, Y.; Inui, K.; Nakae, K.; Igarashi, M.; Hashimoto, K.; Nakata, M: Identification of the toxic trigger in mushroom poisoning. *Nat. Chem. Biol.* **2009**, *5*, 465.

(59) Nguyen, D. P.; Elliott, T; Holt, M.; Muir, T. W.; Chin, J. W: Genetically encoded 1,2-aminothiols facilitate rapid and site-specific protein labeling via a bio-orthogonal cyanobenzothiazole condensation. *J. Am. Chem. Soc.* **2011**, *133*, 11418.

(60) Newman, D, J.; Cragg, G. M: Natural products as sources of new drugs over the 30 years from 1981 to 2010. *J. Nat. Prod.* **2012**, *75*, 311.

(61) Wallace, S.; Chin, J, W: Strain-promoted sydnone bicyclo-[6.1.0]-nonyne cycloaddition. *Chem. Sci.* **2014**, *5*, 1742.

(62) Kolodych, S.; Rasolofonjatovo, E.; Chaumontet, M.; Nevers, M, C.; Creminon, C.; Taran, F: Discovery of chemoselective and biocompatible reactions using a high-throughput immunoassay screening. *Angew. Chem. Int. Ed.* **2013**, *52*, 12056.

(63) Kamber, D. N.; Nazarova, L. A.; Liang, Y.; Lopez, S. A.; Patterson, D. M.; Shih, H-W.; Houk, K. N.; Prescher, J, A: Isomeric cyclopropenes exhibit unique bioorthogonal reactivities. *J. Am. Chem. Soc.* **2013**, *135*, 13680.

(64) Liang, Y.; Mackey, J. L.; Lopez, S. A.; Liu, F.; Houk, K. N: Control and design of mutual orthogonality in bioorthogonal cycloadditions. *J. Am. Chem. Soc.* **2012**, *134*, 17904.

(65) Gold, B.; Dudley, G. B.; Alabugin, I. V: Moderating strain without sacrificing reactivity: Design of fast and tunable noncatalyzed alkyne-azide cycloadditions via stereoelectronically controlled transition state stabilization. *J. Am. Chem. Soc.* **2013**, *135*, 1558.

(66) Willems, L. I.; Li, N.; Florea, B. I.; Ruben, M.; van der Marel, G. A.; Overkleeft, H. S: Triple bioorthogonal ligation strategy for simultaneous labeling of multiple enzymatic activities. *Angew. Chem. Int. Ed.* **2012**, *51*, 4431.

(67) Hudak, J. E.; Barfield, R. M.; de Hart, G. W.; Grob, P.; Nogales, E.; Bertozzi, C. R.; Rabuka, D: Synthesis of heterobifunctional protein fusions using copper-free click chemistry and the aldehyde tag. *Angew. Chem. Int. Ed.* **2012**, *51*, 4161.

(68) Chang, P. V.; Prescher, J. A.; Hangauer, M. J.; Bertozzi, C. R: Imaging cell surface glycans with bioorthogonal chemical reporters. *J. Am. Chem. Soc.* **2007**, *129*, 8400.

(69) Nikic, I.; Plass, T.; Schraidt, O.; Szymanski, J.; Briggs, J, A.; Schultz, C.; Lemke, E. A: Minimal tags for rapid dual-color live-cell labeling and super-resolution microscopy. *Angew. Chem. Int. Ed.* **2014**, *53*, 2245.

(70) Neves, A. A.; Stockmann, H.; Wainman, Y. A.; Kuo, J. C.; Fawcett, S.; Leeper, F. J.; Brindle, K. M: Imaging cell surface glycosylation in vivo using "double click" chemistry. *Bioconjug. Chem.* **2013**, *24*, 934.

(71) Karver, M. R.; Weissleder, R.; Hilderbrand, S. A: Bioorthogonal reaction pairs enable simultaneous, selective, multi-target imaging. *Angew. Chem. Int. Ed.* **2012**, *51*, 920.

(72) Sachdeva, A.; Wang, K.; Elliott, T.; Chin, J, W: Concerted, rapid, quantitative, and site-specific dual labeling of proteins. *J. Am. Chem. Soc.* **2014**, *136*, 7785.

(73) Cole, C. M.; Yang, J.; Seckute, J.; Devaraj, N. K: Fluorescent live-cell imaging of metabolically incorporated unnatural cyclopropene-mannosamine derivatives. *ChemBioChem* **2013**, *14*, 205.

CHAPTER 2: Isomeric cyclopropenes exhibit unique reactivities

Lidia A. Nazarova, Yong Liang, Steven A. Lopez, David M. Patterson, and Hui-Wen Shih contributed to the work presented in this chapter.

2.1 Introduction

The bioorthogonal chemical reporter strategy introduced in chapter 1, has been widely used to interrogate glycans and other biopolymers in living systems [1-5]. This approach relies on the introduction of a uniquely reactive functional group (i.e., a "chemical reporter") into a biomolecule of interest. The chemical reporter can be ligated to probes for visualization or retrieval using highly selective (i.e., "bioorthogonal") chemistries [2,6]. While powerful, this two-step strategy has been largely limited to examining one biological feature at a time in live cells and tissues. This is because many bioorthogonal reactions are incompatible with one another and cannot be used in tandem to monitor multiple species [7-12].

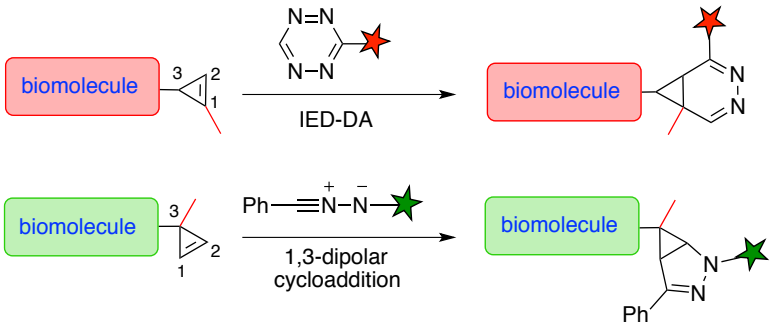

Figure 2-1. Cyclopropene scaffolds undergo bioorthogonal cycloadditions. 1,3-Disubstituted cyclopropenes (top) react with tetrazines. 3,3-Disubstituted scaffolds (bottom) react with 1,3-dipoles to afford covalent adducts.

Our long-term goal is to identify transformations that can be used concurrently to tag biomolecules in complex environments. As a starting point, we were drawn to the cycloaddition reactions of cyclopropenes. Functionalized cyclopropenes are stable in physiological environments, yet readily reactive with dienes and other biocompatible motifs [13-17]. We and others have shown that 1,3-disubstituted cyclopropenes can be metabolically incorporated into cellular glycans and selectively ligated via inverse-electron demand Diels–Alder (IED-DA) reactions with tetrazines (Figure 2-1) [14-16,18]. In related work, Lin and colleagues demonstrated that 3,3-disubstituted cyclopropenes can be introduced into proteins and ultimately detected via 1,3-dipolar cycloaddition with nitrile imines (Figure 2-1) [16]. This reaction, similar to the cyclopropene-tetrazine ligation, proceeds readily in cellular environments.

We were intrigued by cyclopropene IED-DA and dipolar cycloadditions for an additional reason: these reactions had the potential to be orthogonal to one another and, thus, applicable to multi-component biomolecule labeling. In earlier work, we observed that 1,3-disubstituted cyclopropenes react with tetrazines at the least-hindered face of the three-membered ring (i.e., the side bearing the C-3 H atom) [14]. Additional steric bulk at this position (as in the case of 3,3-disubstituted cyclopropenes) would, in theory, impede IED-DA reactivity but not impact cycloadditions with less sterically encumbered reactants (e.g., 1,3-dipoles).

2.2 Computational analysis on the reactivity of isomeric cyclopropenes

To predict whether cyclopropene reactivity could be tuned with steric modifications at C-3, we examined the reactions of 1,3- and 3,3-dimethylcyclopropene (Cp(1,3) and Cp(3,3)) with diphenyl-substituted nitrile imine (NI) and tetrazine (Tz), using density functional theory (DFT) calculations [19]. M06-2X [20,21], a density functional that provides relatively accurate

energetics for cycloadditions [22,23], was used to generate the transition-state structures shown in Figure 2-2. We also analyzed activation barriers using the distortion/interaction model [24,25], in which the activation energy (E_{act}) is analyzed in terms of the distortion energy (E_{dist}) required for the reactants to achieve their transition-state geometries, and the interaction energy (E_{int}) arising from orbital overlap between the two distorted reactants in the transition state. The computed activation free energies in water (G_{water}), relative rate constants (k_{rel}), and distortion/interaction energies are provided in Figure 2-2 and Table S2.1.

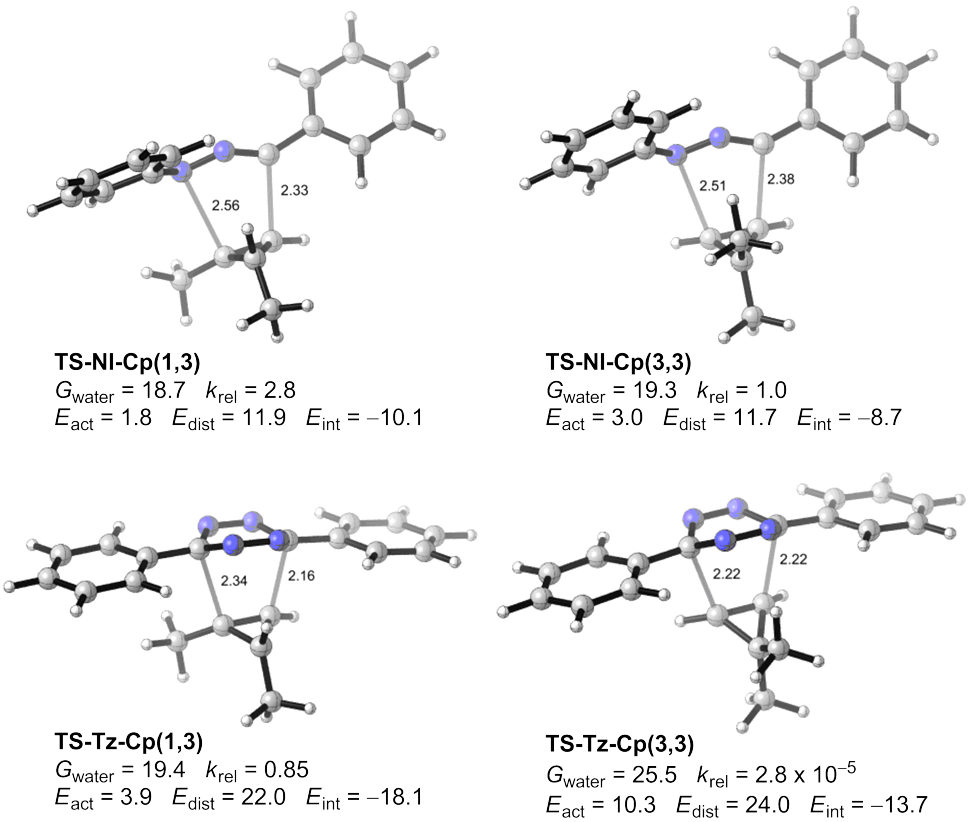

Figure 2-2. M06-2X/6-31G(d)-optimized transition-state structures for the cycloadditions of 1,3- and 3,3-dimethylcyclopropene [Cp(1,3) and Cp(3,3)] with diphenyl-substituted nitrile imine (NI) and tetrazine (Tz). M06-2X/6-311+G(d,p)//6-31G(d)-computed energies and relative rate constants (distances in Å, energies in kcal/mol, k_{rel} based on G_{water} at 298 K) are also shown.

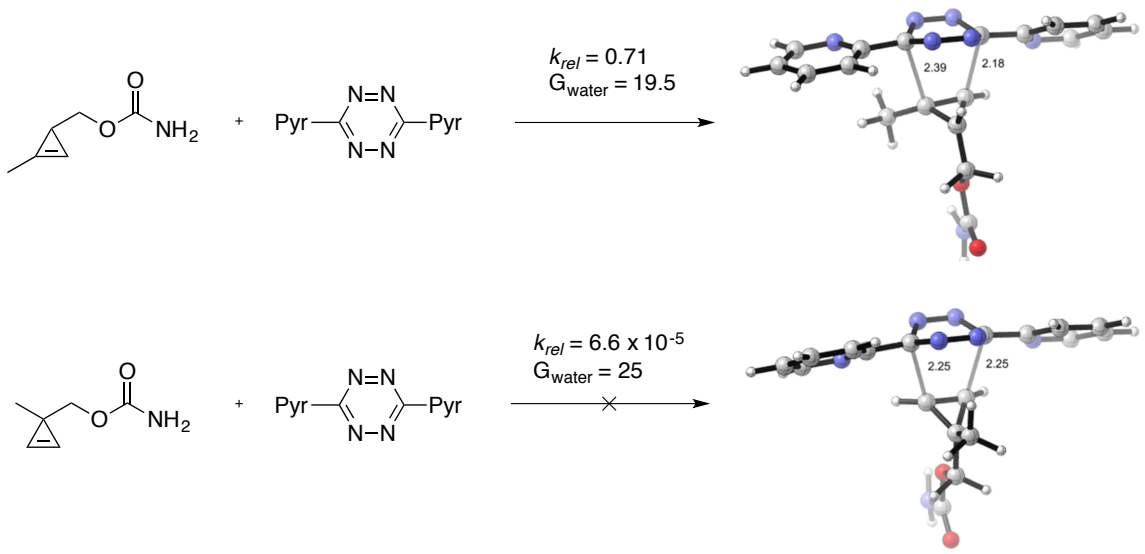

Figure 2-3. M06-2X/6-31G(d)-optimized transition-state structures for the cycloadditions of 3-carbamoyloxymethyl-1-methylcyclopropene and 3-carbamoyloxymethyl-3-methylcyclopropene with dipyridyl-substituted tetrazine. M06-2X/6-311+G(d,p)//6-31G(d)-computed activation free energies and relative rate constants (distances in Å, energies in kcal/mol, k_{rel} based on G_{water} at 298 K) are also shown.

Our calculations indicated that for the sterically less encumbered nitrile imine, 1,3-dimethylcyclopropene reacts only 2.8 times faster than 3,3-dimethylcyclopropene. The distortion and interaction energies are very close, suggesting that increased steric bulk at C-3 of the cyclopropene does not dramatically influence reactivity with linear 1,3-dipoles (Figure 2-3). However, for the bulkier tetrazine, placement of a single methyl group at C-3 reduces cyclopropene reactivity by over four orders of magnitude in the IED-DA reaction (Figure 2-3). In the transition state **TS-Tz-Cp(3,3)**, to avoid steric clashes between the C-3 methyl and tetrazine nitrogens, the dihedral angle between the cyclopropene plane and the C-C bonds-forming plane increases to 120°, about 15° larger than the corresponding value in **TS-Tz-Cp(1,3)**. In Figure 2-2, note how the cyclopropene C-3 and methyl groups are tilted away from the tetrazine. This results in increased distortion energy (24.0 versus 22.0 kcal/mol) and less favorable interaction energy (13.7 versus 18.1 kcal/mol) due to poorer orbital overlap. Similar

reactivities were predicted for more functionalized cyclopropenes and tetrazines (Figure 2-3). Collectively, these data suggest that isomeric cyclopropenes possess unique bioorthogonal reactivities: 3,3-disubstitued cyclopropenes should react readily with nitrile imines, but not tetrazines, under physiological conditions; 1,3-disubstituted cyclopropenes, by contrast, should react readily with both.

2.3 Synthesis and reactivity of isomeric cyclopropenes

To test these predictions, we synthesized a panel of disubstituted cyclopropenes bearing methyl groups at either C-1 or C-3. The scaffolds also comprise amide or carbamate groups as these linkages mimic those found in numerous bioconjugates. The amide-functionalized probes **2.1a-b** were synthesized similarly to previous reports (Scheme 2-1) [14-16]. In brief, esters **2.3a-b** were first subjected to base-catalyzed hydrolysis. The resulting acids (**2.4a-b)** were subsequently treated with PFP-TFA, followed by isopropylamine to access the desired probes. To prepare the carbamate scaffolds, esters **2.3a-b** were first reduced with DIBAL-H. The reaction with **2.3b** was prone to cyclopropane formation; over-reduction was avoided at -78 °C. Alcohols **2.5a-b** were ultimately converted to the desired carbamates (**2.2a-b**) via CDI coupling with isopropylamine, followed by TMS removal.

Scheme 2-1. Synthesis of disubstituted cyclopropenes.

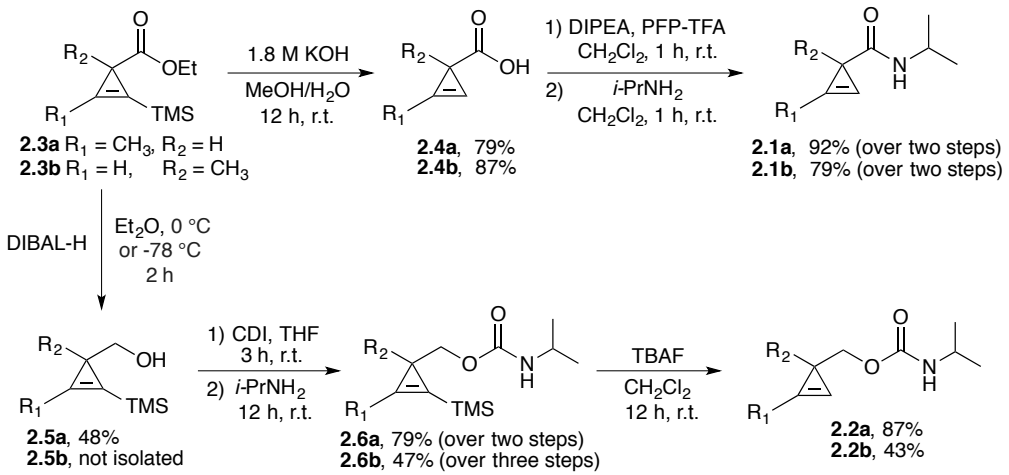

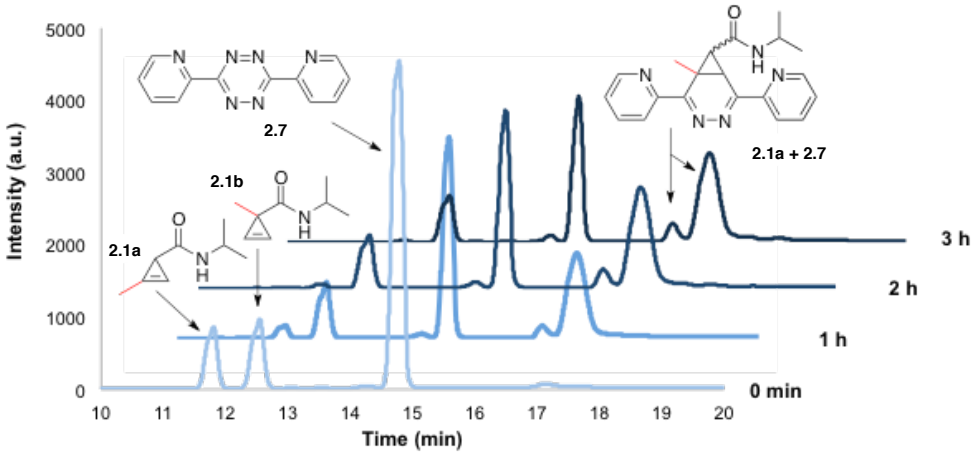

Figure 2-4. Tetrazines react selectively with 1,3-disubstitued cyclopropenes. Cyclopropenes **2.1a-b** (5 mM in 15% MeCN/PBS) were treated with tetrazine **2.7** (10 mM) and monitored by HPLC. The initial cycloadduct formed between **2.1a** and **2.7** can undergo further intramolecular cyclization in aqueous solution [14].

Table 2-1. Second-order rate constants for the cyclopropene-tetrazine ligation. All rate constants were measured in 15% DMSO/PBS. *No reaction observed after 90 min.

Cyclopropene		Tetrazine		k_2 (x 10^{-2} M^{-1} s^{-1})
2.1a	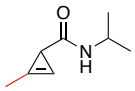	**2.7**	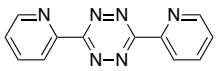	3.91 ± 0.45
2.1b	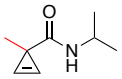	**2.7**	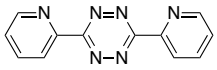	N/R*
2.1b	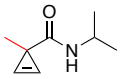	**2.8**	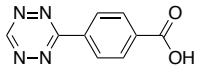	N/R*
2.2a	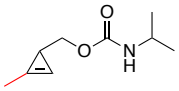	**2.7**	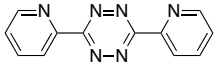	277.8 ± 36.6
2.2b	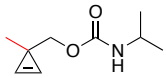	**2.7**	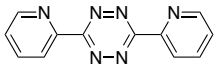	N/R*
2.2b	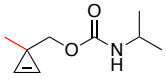	**2.8**	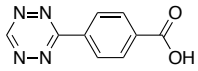	N/R*

With the desired cyclopropenes in hand, we analyzed their reactivity with model tetrazines (Figure 2-4) (Table 2-1). Tetrazines **2.7-2.8** were incubated with excess cyclopropene, and the cycloadditions were monitored by the change in tetrazine absorbance over time (Table 2-1). Robust IED-DA reactivity was observed with the 1,3-disubstituted scaffolds **2.1a** and **2.2a**, while no reactivity was detected with their 3,3-disubstituted counterparts in organic or aqueous solvents (**2.1b** and **2.2b**) (Figure 2-5). It should also be noted that the tetrazine-cyclopropene ligations revealed the expected trends, with the more electron-rich carbamates and less sterically hindered tetrazine exhibiting the fastest rates (Table 2-2 and Figure 2-6) [26-27].

Despite their extremely sluggish reaction kinetics with tetrazines, 3,3-disubstituted cyclopropenes react readily with nitrile imines in "photo-click" reactions [16]. Indeed, when micromolar concentrations of **2.1b** and **2.9** were subjected to UV light (generating **2.10** *in situ*), the fluorescent cycloadduct **2.11** was formed (Scheme 2-2). The corresponding 1,3-cyclopropene **2.1a** also reacted rapidly with **2.10** to provide the rearranged cycloadduct **2.12**. Similar rearrangements have been observed in cycloadditions with cyclopropenes and nitrile oxides [28]. Both ligation products **2.11** and **2.12** were found to be stable in aqueous solution for over three days. Importantly, nitrile imine **2.10** could also be generated in the presence of tetrazine **2.7** with no observable side reactivity, highlighting the compatibility of these reagents (Figure 2-7).

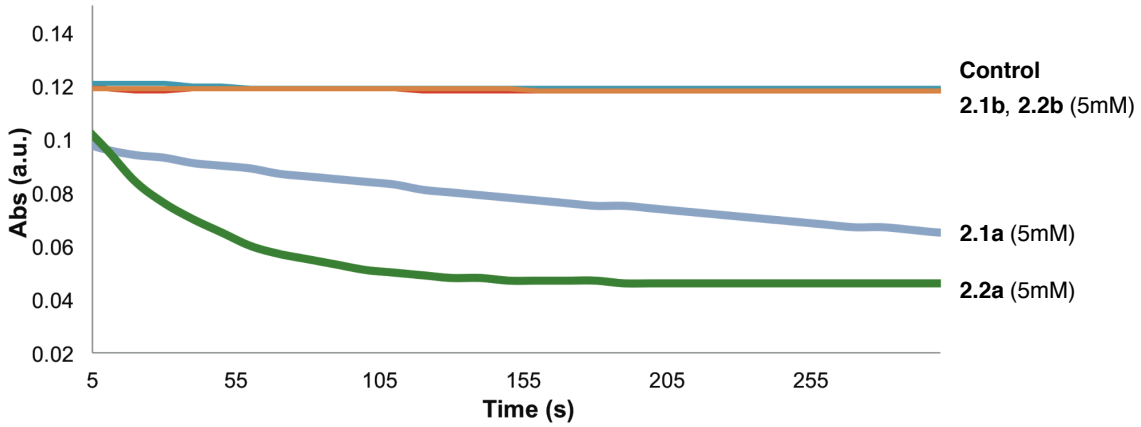

Figure 2-5. Tetrazines react selectively with 1,3-disubstitued cyclopropenes. (A) Reaction of cyclopropenes **2.1-2.2** (5 mM in 15% DMSO/PBS) with tetrazine **2.7** (0.2 mM) monitored by UV-visible spectroscopy

Table 2-2. Selective IED-DA reactivity observed between cyclopropene and tetrazine scaffolds. *No reaction observed after 90 min.

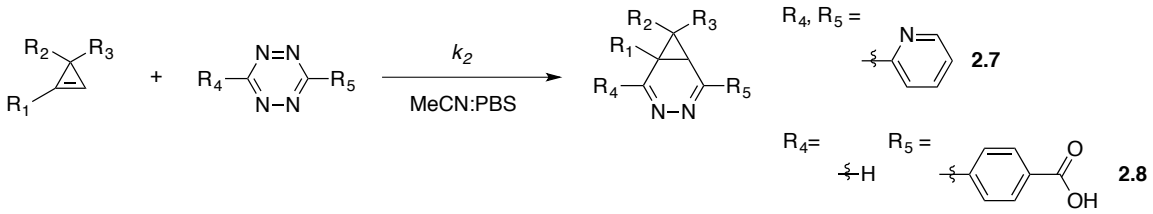

Entry	Cyclopropene	R_1	R_2	R_3	Tetrazine	k_2 (x 10^{-2} $M^{-1}s^{-1}$)
5	**2.2a**	CH_3	H	carbamate	**2.7**	11.5 ± 2.2
6	**2.2a**	CH_3	H	carbamate	**2.8**	29.5 ± 5.0
7	**2.2b**	H	CH_3	carbamate	**2.7**	N/R*
8	**2.2b**	H	CH_3	carbamate	**2.8**	N/R*

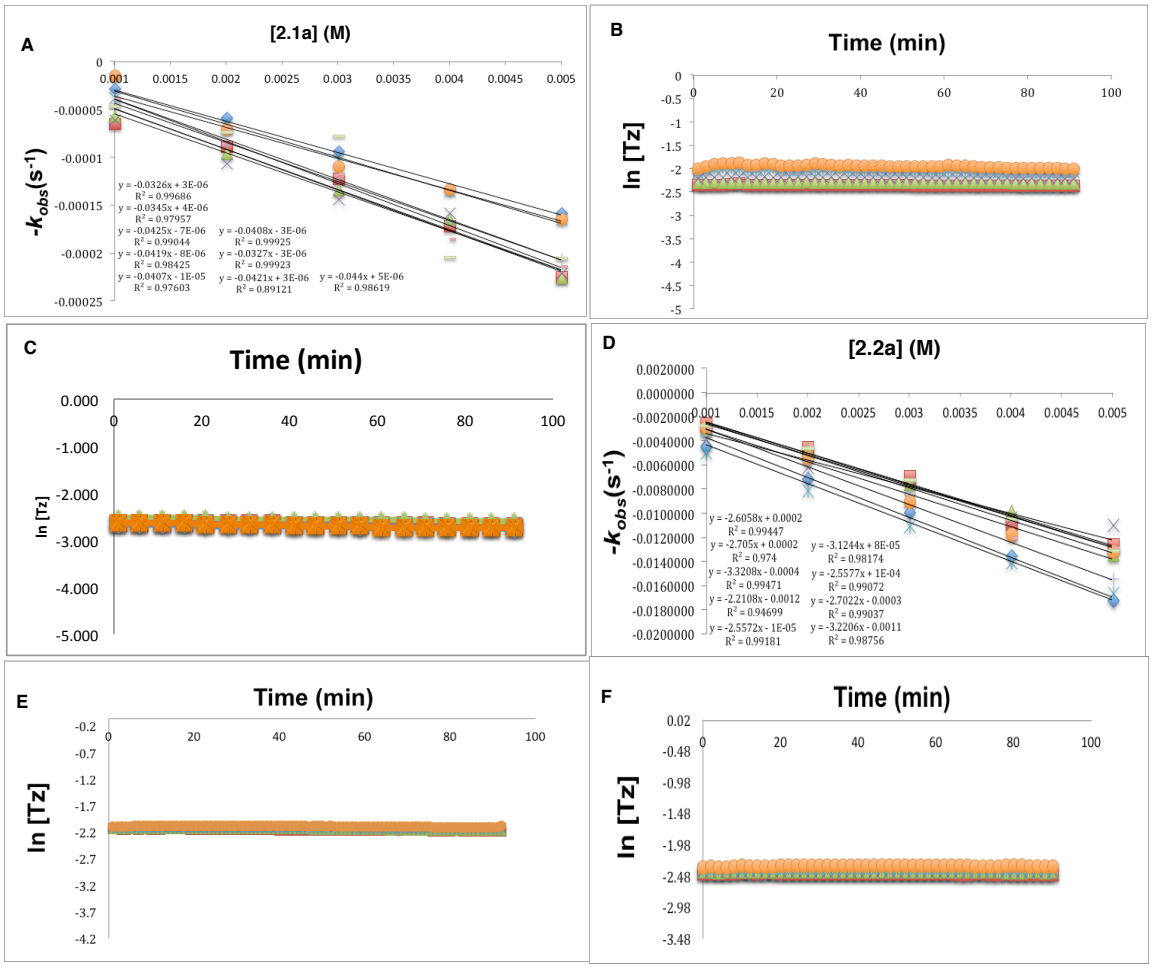

Figure 2-6. Plots used to calculate second-order rate constants (k_2) between: (A) **2.1a** and **2.7** in 15% DMSO/PBS, (B) **2.1b** and **2.7** in 1:1 MeCN:PBS, (C) **2.1a** and **2.8** in 1:1 MeCN:PBS, (D) **2.2a** and **2.7** in 15% DMSO/PBS, (E) **2.2b** and **2.7** in 15% DMSO/PBS, (F) **2.2b** and **2.8** in 1:1 MeCN:PBS,

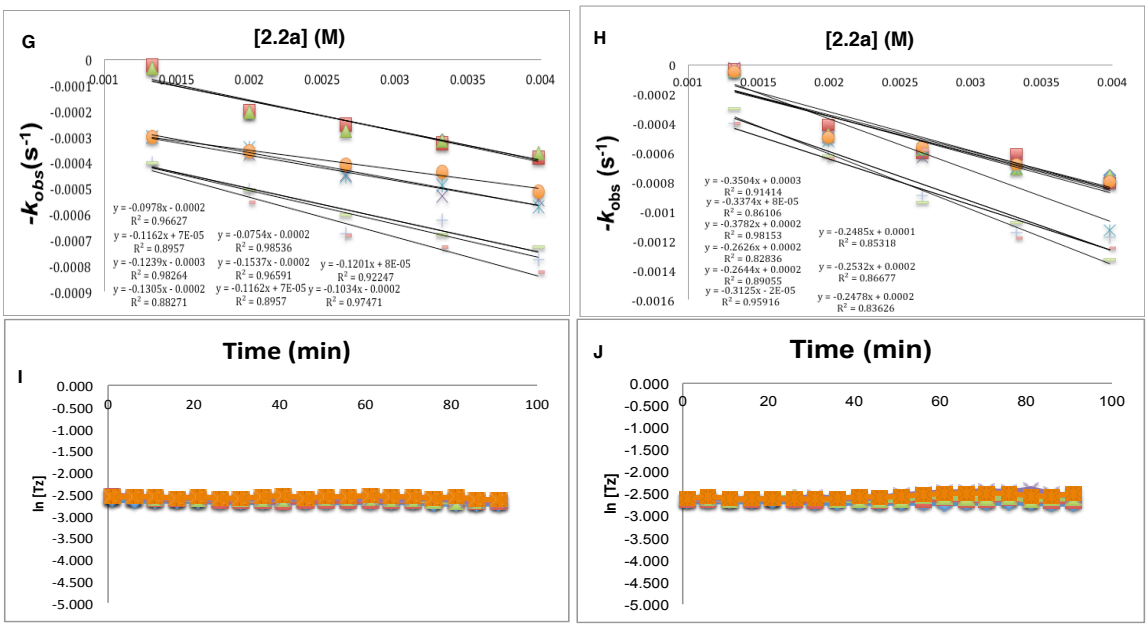

Figure 2-6. Plots used to calculate second-order rate constants (k_2) between: (G) **2.2a** and **2.7** in 1:1 MeCN:PBS, (H) **2.2a** and **2.8** in 1:1 MeCN:PBS, (I) **2.2b** and **2.7** in 1:1 MeCN:PBS, and (J) **2.2b** and **2.8** in 1:1 MeCN:PBS.

Scheme 2-2. Cyclopropenes react with nitrile imines to generate stable cycloadducts.

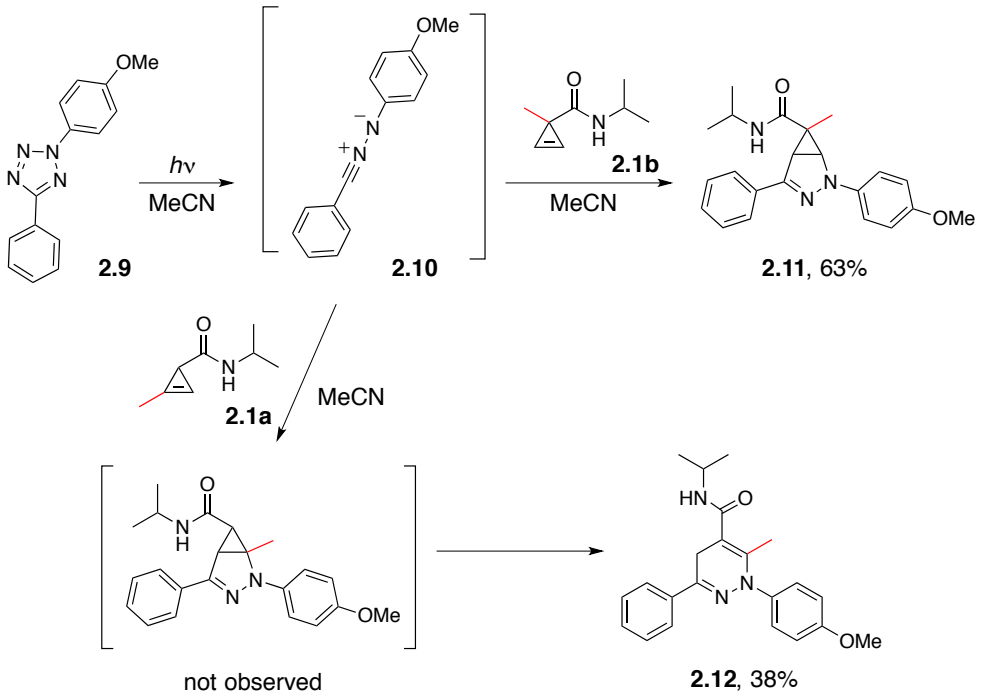

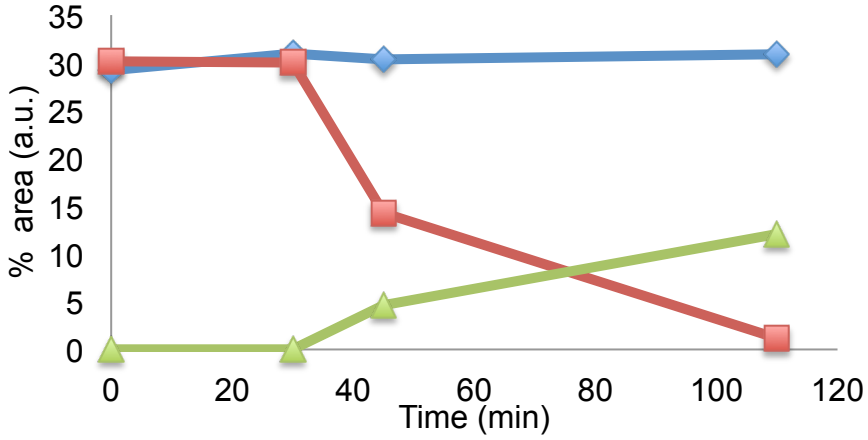

Figures 2-7. Nitrile imines and tetrazines exhibit no side reactivity. Tetrazole **2.9** (red) (2.2 mM), tetrazine **2.7** (blue) (2.2 mM), and cyclopropene **2.1b** (6 mM) were stirred for 30 min in a quartz test tube at RT prior to photoirradiation with a handheld UV lamp (110 min, 302 nm, Zilla, 20 watts). Reaction aliquots were analyzed by HPLC. The disappearance of tetrazole **2.9** was concurrent with the appearance of cycloadduct **2.11** (green). No change in peak area was observed for tetrazine **2.7**.

2.4 Chemical labeling of model proteins using isomeric cyclopropenes

The unique reactivity profiles of 1,3- and 3,3-disubstituted cyclopropenes suggested that the probes could be used in tandem for biomolecule labeling. To test this hypothesis, we functionalized model proteins (BSA and lysozyme) with the isomeric cyclopropenes **2.13a-b** using standard coupling conditions (Figure 2-8). Mass spectrometry analysis was used to verify that equivalent numbers of cyclopropenes were appended to the biomolecules (Figure 2-8). When the proteins were treated with a tetrazine-rhodamine conjugate (**Tz-Rho**), only samples functionalized with 1,3-disubstituted cyclopropenes (**Cp (1,3)**) showed robust dose- and time-dependent labeling, in agreement with our kinetic data (Figures 2-9B, 2-10, 2-12A-B). No labeling above background was observed with proteins outfitted with 3,3-disubstituted cyclopropenes (**Cp (3,3)**). Both **Cp (1,3)** and **Cp (3,3)** samples were covalently modified with nitrile imines using "photo-click" conditions (Figures 2-9C, 2-12C). The fluorescent intensities of the **Cp (1,3)** adducts were somewhat reduced, though, likely due to the decreased absorption efficiency of the products (**2.12** versus **2.11**, Figure 2-11). When conjugates **Cp (1,3)** and **Cp (3,3)** were subjected to both cycloaddition reactions (treatment with **Tz-Rho**, followed by **2.10**), tetrazine labeling was again only observed for **Cp (1,3)** samples. The **Cp (3,3)** samples, along with unmodified scaffolds on **Cp (1,3)**, were detected following nitrile imine generation (Figures 2-9D, 2-12D).

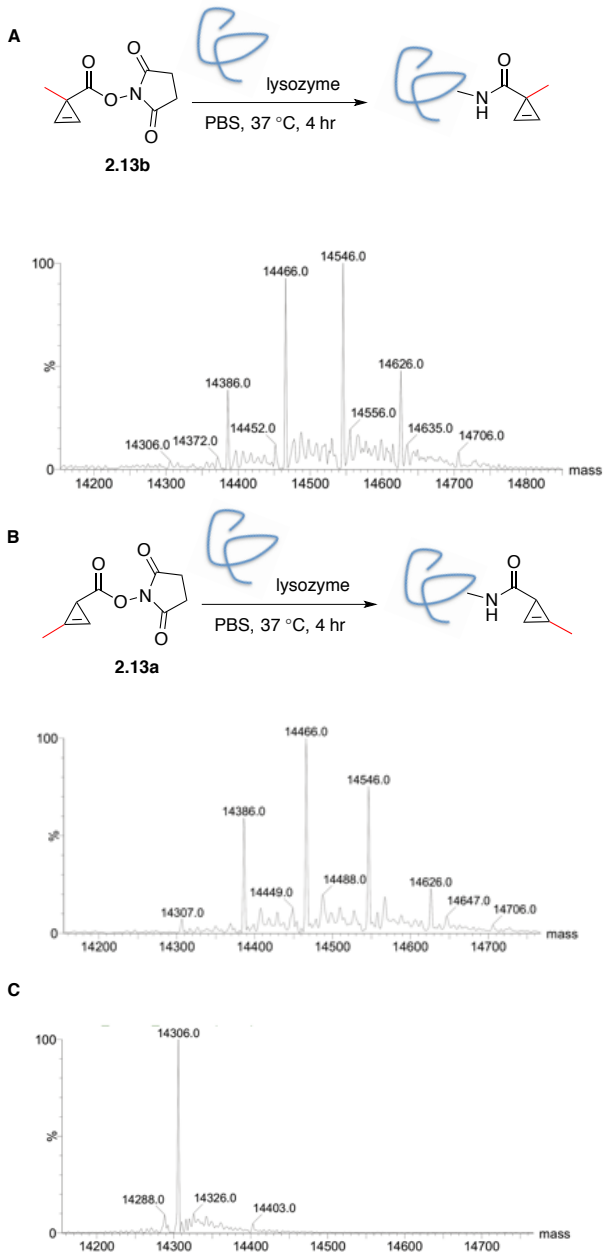

Figure 2-8. Mass spectrometry analysis of lysozyme treated with (A) 3,3-disubstituted cyclopropene **2.13b**, (B) 1,3-disubstituted cyclopropene **2.13a**, or (C) or no reagent.

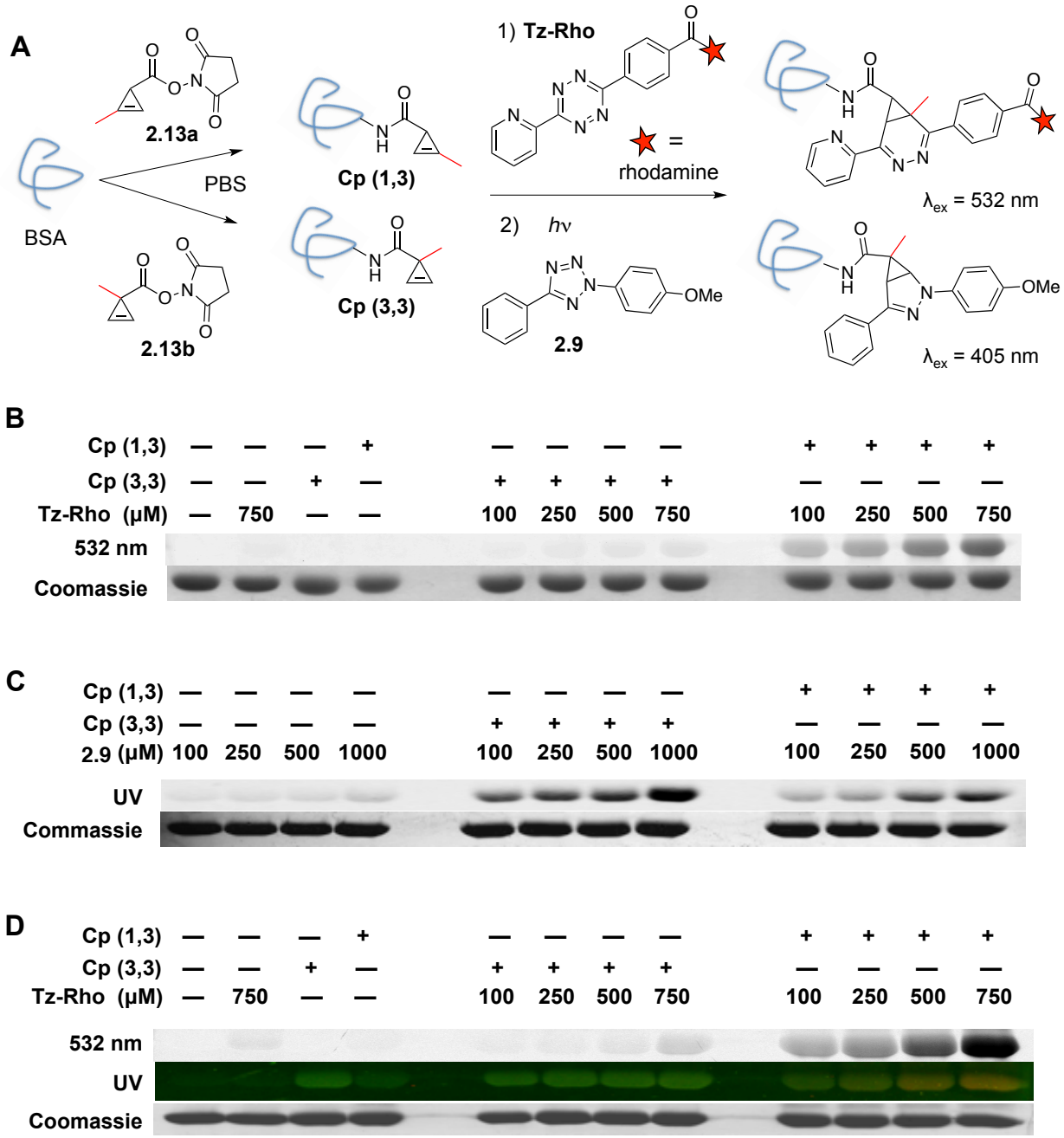

Figure 2-9. Cyclopropenes can be selectively detected on model proteins. (A) Cyclopropenes were appended to BSA. The modified proteins **Cp (1,3)** and **Cp (3,3)** were subsequently reacted with either a tetrazine-rhodamine conjugate (**Tz-Rho**) or **nitrile imine** (generated via photolysis of tetrazole). (B) Gel analysis of **Cp (1,3)** or **Cp (3,3)** incubated with **Tz-Rho** (100-750 μM) or no reagent (—) for 1 h. (C) Gel analysis of **Cp (1,3)** or **Cp (3,3)** treated with **tetrazole** (100-1000 μM) and UV irradiation. (D) Analysis of samples treated with **Tz-Rho** (100-750 μM) or no reagent (—), followed by tetrazole (5 mM) and UV irradiation (in gel). The gel was scanned at 532 nm (top) to visualize rhodamine, and also illuminated with UV light (middle) to visualize nitrile imine cycloadducts (green). The red color in the UV-illuminated gel (middle) is due to rhodamine fluorescence. For B-D, protein loading was assessed with Coomassie stain.

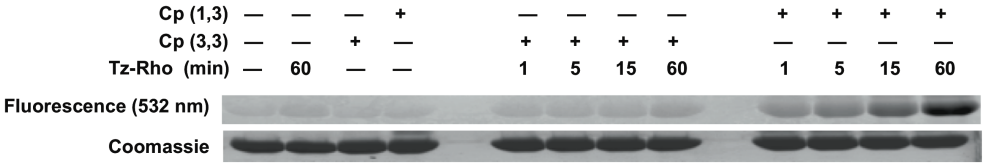

Figure 2-10. Proteins can be labeled with **Tz-Rho** in a time-dependent manner. Gel analysis of **Cp (1,3)** or **Cp (3,3)** incubated with **Tz-Rho** (500 μM) for 0-60 min.

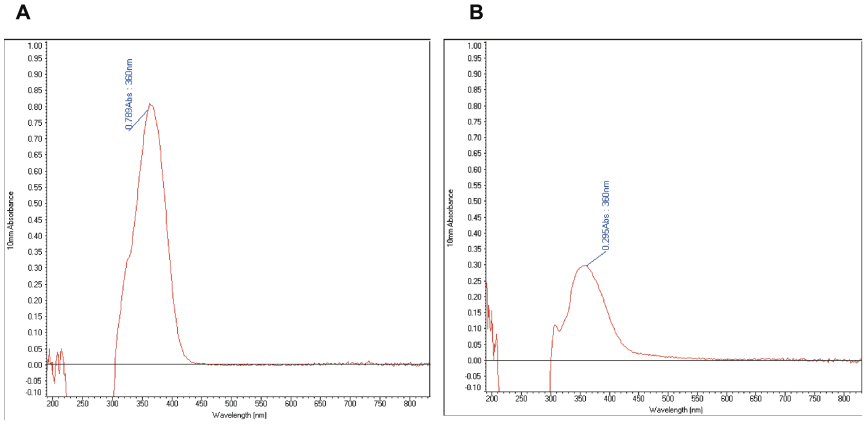

Figure 2-11. UV-Vis absorption traces for 100 μM solutions of **2.11** (A) and **2.12** (B) in MeCN.

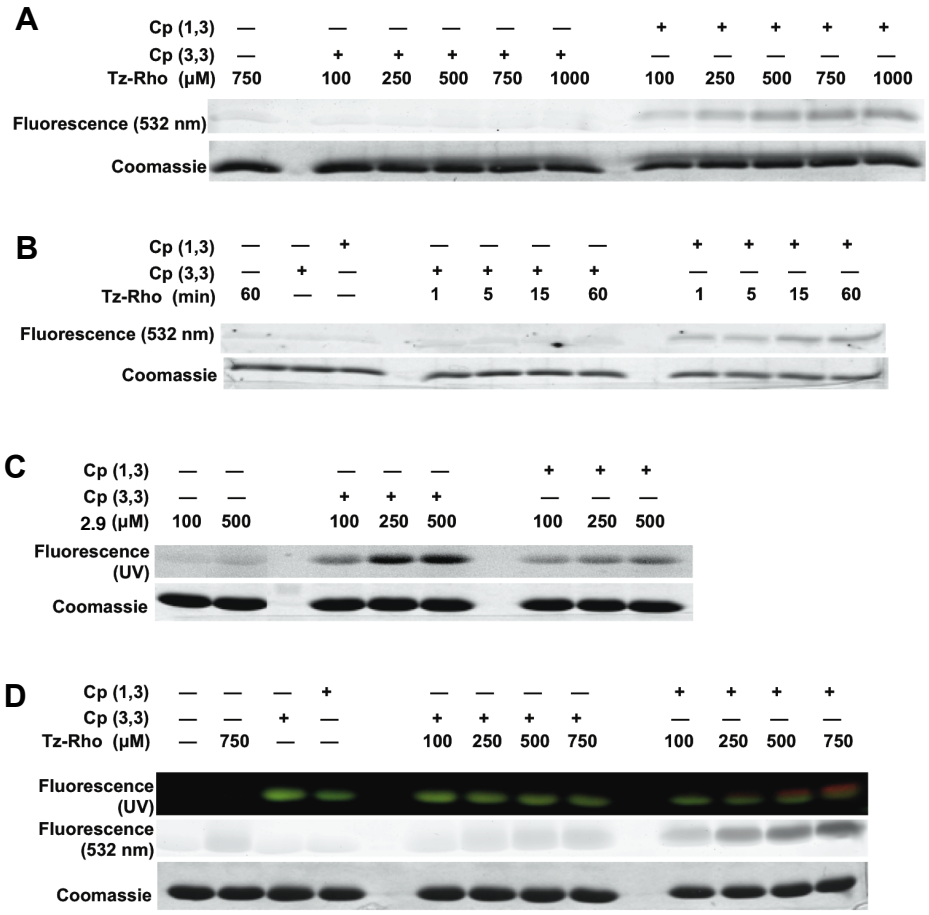

Figure 2-12. Selective cyclopropene reactivity observed with lysozyme conjugates. (A) Gel analysis of the cyclopropene-modified proteins **Cp (1,3)** or **Cp (3,3)** incubated with **Tz-Rho** (100-750 μM) or no reagent (—) for 60 min. (B) Gel analysis of **Cp(1,3)** or **Cp(3,3)** treated with **Tz-Rho** (500 μM) for 0-60 min. (C) Gel analysis of **Cp (1,3)** or **Cp (3,3)** treated with tetrazole (100-500 μM) and irradiated with UV light. (D) Gel analysis of **Cp (1,3)** or **Cp (3,3)** treated with **Tz-Rho** (100-750 μM) or no reagent (—), followed by tetrazole (500 μM) and UV irradiation. The gel was illuminated with UV light (top panel) to visualize nitrile imine cycloadducts (green) and scanned at 532 nm (middle panel) to visualize rhodamine fluorescence. For B-D, protein loading was assessed with Coomassie stain (lower panels).

2.5 Conclusions and future work

In sum, we identified cyclopropenes that exhibit unique modes of bioorthogonal reactivity. Computational analyses predicted that 1,3-disubstituted cyclopropenes would undergo facile IED-DA reactions, while 3,3-disubstituted scaffolds would be minimally reactive with tetrazines. Upon synthesis and *in vitro* characterization of a panel of modified cyclopropenes, we discovered that scaffolds that differ in the placement of a single methyl group (C-1 vs. C-3) exhibit vastly different IED-DA reaction profiles: 1-methyl cyclopropenes can be selectively ligated with tetrazine probes in the presence of 3-methyl cyclopropenes; the unmodified 3-methyl substituted scaffolds can be efficiently ligated via dipolar cycloaddition. The ability to selectively modify isomeric cyclopropenes—and ultimately target them to discrete biomolecules—will facilitate multi-component imaging studies *in vitro* and in live cells. The cyclopropene scaffold also offers unique opportunities for further biocompatible reaction development, including selective nucleophilic additions and normal-demand Diels–Alder reactions. An arsenal of such orthogonal reactions will continue to provide insight into complex biological systems [29,30].

2.6 Materials and Methods

2.6a Computational studies

All calculations were performed with Gaussian 09 [19]. The geometry optimization of all minima and transition states involved was carried out at the M06-2X level of theory [20,21] with the 6-31G(d) basis set [31]. The vibrational frequencies were computed at the same level to check whether each optimized structure is an energy minimum or a transition state and to

evaluate zero-point vibration energy (ZPVE) and thermal corrections at 298 K. A quasiharmonic correction was applied during the entropy calculation by setting all positive frequencies that are less than 100 cm^{-1} to 100 cm^{-1} [32, 33]. Solvent effects in water were computed at the M06-2X/6-311+G(d,p) level using the gas-phase optimized structures at the M06-2X/6-31G(d) level. Solvation energies were evaluated by a self-consistent reaction field (SCRF) using the CPCM model [33], where UFF radii were used. Fragment distortion and interaction energies were computed at the M06-2X/6- 311+G(d,p) level using the M06-2X/6-31G(d) geometries.

2.6b Rate studies

The reactions between cyclopropenes **2.1-2** and tetrazines **2.7-8** were conducted in 96-well plates and monitored by the change in tetrazine absorbance at 536 nm. All runs were conducted in triplicate under pseudo-first order conditions and repeated at least three times. For each measurement, 150 μL of a 0.2 mM tetrazine solution (in 1:1 MeCN:PBS or 15% DMSO/PBS) was added to a well containing 150 μL of cyclopropene solution (2- 10 mM in 1:1 MeCN:PBS or 15% DMSO/PBS). The cyclopropene concentration at the start of each reaction ranged from 1.0-5.0 mM, while the tetrazine concentration was held at 0.1 mM. For reactions with **2.1a** and **2.2a** in 15% DMSO/PBS, the tetrazine concentration was held at 0.4 mM, and cyclopropene concentrations ranged from 2.0-10.0 mM. Absorbance values were recorded every 5 min over a 90 min interval or every 4 seconds over a 30 min interval for faster reactions (using a BioTek Epoch plate reader).

2.6c Cyclopropene conjugation to protein scaffolds

Bovine serum albumin (BSA) or lysozyme conjugates were prepared by treating the proteins with cyclopropene esters **2.13a-b** as previously described [14]. In brief, BSA or

lysozyme (400 μL of a 20 mg/mL solution in PBS, pH 7.4) was treated with **2.13a-b** (100 μL of a 25 mM solution in DMSO). The lysozyme solutions were incubated at 37 °C (with shaking) for 4 h, while the BSA solutions were allowed to stand at RT for 12 h. The modified proteins were isolated using P-10 BioGel® (BioRad), eluting with nanopure water.

2.6d In-gel fluorescence analysis of cyclopropene-tetrazine reactivity

Purified protein conjugates were diluted to 2 mg/mL with PBS (pH 7.4), treated with **Tz-Rho** (1-7.5 μL of a 5 mM DMSO/PBS solution), and combined with additional PBS to total 50 μL. The labeling reactions were run for 1-60 min, and protein isolates (4-9 μg) were analyzed on SDS-PAGE as previously described [14]. Gels were analyzed by in-gel fluorescence scanning (GE Typhoon TRIO+ Variable Mode Imager, 532 nm excitation/580 nm emission). Gels were also stained with Coomassie Brilliant Blue.

Purified protein conjugates (40 μL of 2 mg/mL solutions in PBS) were treated with **Tz-Rho** (1-7.5 μL of a 5 mM stock solution in 1:1 DMSO:PBS), and combined with additional PBS to total volume of 50 μL. The labeling reactions were run for 1-60 min, and protein isolates (4-9 μg) were analyzed on SDS-PAGE as previously described [14]. The gels were rinsed in destain buffer for 10 min, then in water for 10 min

2.6e In-gel fluorescence analysis of nitrile imine reactivity

Protein conjugates were labeled with nitrile imines using a procedure reported by Lin and coworkers [9]. Purified proteins (40 μL of 2 mg/mL solutions in PBS) were added to a 96- well plate and treated with tetrazole **2.9** (1-10 μL of a 5 mM solution in DMSO). The samples were irradiated with a UV lamp (302 nm, Zilla UVB 20 watts) for 5 min. For these experiments, the

lamp was placed directly on top of the 96-well plate. The labeled samples were subsequently analyzed via SDS-PAGE as described previously [14]. Gels were visualized with a UV-transilluminator (MultiDoc-It Digital Imaging System) and stained with Coomassie Brilliant Blue.

2.6f Dual protein modification

2.6g Solution reactions

Protein conjugates (40 μL of 2 mg/mL solutions in PBS) were added to a 96-well plate and treated with **Tz-Rho** (1-7.5 μL of a 5 mM stock in 1:1 DMSO/PBS solution) for 1 h at RT. Tetrazole **2.9** (5.6 μL of a 5 mM solution in DMSO) or no reagent was added to each well, and the mixtures were irradiated with a UV lamp for 5 min (302 nm, Zilla UVB 20 watts). For these experiments, the lamp was placed directly on top of the 96- well plate. The samples were then analyzed via SDS-PAGE as described [14]. Gels were visualized using a fluorescence scanner (GE Typhoon TRIO+ Variable Mode Imager, 532 nm excitation/580 nm emission) and a UV-transilluminator (MultiDoc-It Digital Imaging System) prior to staining with Coomassie Brilliant Blue.

2.6h In-gel labeling

Following reaction with **Tz-Rho**, some protein samples were analyzed via SDS-PAGE and visualized by in-gel fluorescence scanning (GE Typhoon TRIO+ Variable Mode Imager, 532 nm excitation/580 nm emission). The gels were then soaked in a solution of **2.9** (5 mM in DMSO) for 1 h at RT, rinsed in destain buffer (10% AcOH, 40% MeOH), and photoirradiated (302 nm, Zilla UVB 20 watts). Gels were visualized using a UV- transilluminator (MultiDoc-It

Digital Imaging System) and stained with Coomassie Brilliant Blue.

2.6i General synthetic procedures

Compounds **2.1a** [14], **2.3a** [34], **2.3b** [16], **2.4a** [14, 34], **2.4b** [16], **2.5a** [15], **2.8** [27], **2.9** [35], **2.13a** [14], **2.13b** [16], and **Tz-Rho** [14] were synthesized as previously reported, and spectroscopic data were consistent with literature values. All other reagents were obtained from commercial sources and used without further purification. Reactions were run under an inert atmosphere of nitrogen, unless otherwise indicated. Tetrahydrofuran (THF), diethyl ether (Et_2O), triethylamine (Net_3), dichloromethane (CH_2Cl_2), *N,N*-dimethylformamide (DMF), and methanol (CH3OH) were degassed with argon and run through two 4 x 36 inch columns of anhydrous neutral A-2 (8 x 14 mesh; LaRoche Chemicals; activated under a flow of argon at 350 °C for 12 h). Thin-layer chromatography was performed using Silica Gel 60 F254-coated glass plates (0.25 mm thickness), and visualization was realized with KMnO4 stain, CAM stain, and/or UV irradiation. Chromatography was accomplished with 60 Å (240-400 mesh) silica gel, commercially available from Sorbent Technologies. HPLC purifications were performed on a Varian ProStar equipped with 325 Dual Wavelength UV-Vis Detector. Analytical runs were performed using an Agilent C18 Scalar column (4.6 x 150 mm, 5 μm) with a 1 mL/min flow rate. Semi-preparative runs were performed using an Agilent Prep-C18 Scalar column (9.4 x 150 mm, 5 μm) with a 5 mL/min flow rate. NMR spectra were collected on a Bruker DRX-400 (400 MHz ^{1}H, 100 MHz ^{13}C, 376.5 MHz ^{19}F) or CRYO-500 (500 MHz ^{1}H, 125.7 MHz ^{13}C) instrument. All spectra were collected at 298 K. Chemical shifts are reported in ppm values relative to tetramethylsilane or residual non-deuterated NMR solvent, and coupling constants (*J*) are reported in Hertz (Hz). High-resolution mass spectrometry was performed by the University

of California, Irvine Mass Spectrometry Center.

2.6j Synthetic procedures

***N*-Isopropyl-1-methylcycloprop-2-enecarboxamide (2.1b)**: To an oven-dried round- bottom flask was added **2.4b** (58 mg, 0.59 mmol) and CH_2Cl_2 (5.0 mL). *N,N*-Diisopropylethylamine (0.25 mL, 1.4 mmol) was added to the solution, followed by pentafluorophenyl trifluoroacetate (0.20 mL, 1.2 mmol). The reaction was stirred for 1 h, then concentrated *in vacuo*. The resulting crude residue was dissolved in CH_2Cl_2 (5.0 mL), and isopropylamine (0.50 mL, 5.8 mmol) was slowly added. The solution was stirred for 1 h, then filtered, concentrated, and purified by flash chromatography (eluting with 5% MeOH in CH_2Cl_2) to provide **2.1b** (65 mg, 79% yield) as a light yellow solid. 1H NMR (400 MHz, $CDCl_3$): δ 7.10 (s, 2H), 5.15 (bs, 1H), 4.05-3.99 (m, 1H), 1.40 (s, 3H), 1.09 (d, J = 6.8 Hz, 6H). 13C NMR (125 MHz, $CDCl_3$) δ 176.4, 112.2, 41.5, 23.0, 22.5, 21.2 HRMS (ESI) *m/z* calcd for $C_8H_{13}NONa$ $[M+Na]^+$ 162.0895, found 162.0894.

(2-Methylcycloprop-2-en-1-yl)methyl isopropylcarbamate (2.2a): To an oven-dried round-bottom flask was added **2.6a** (0.10 g, 0.41 mmol) in THF (7.0 mL), followed by TBAF (0.50 mL of a 1.0 M solution in hexanes, 0.50 mmol). The reaction was stirred overnight, then diluted with H_2O and extracted with Et_2O (2 x 15 mL). The organic layers were combined and dried over $MgSO_4$, filtered, and concentrated *in vacuo.* The crude organic residue was purified by flash chromatography (eluting with 20% Et_2O in hexanes) to provide **2.2a** (61 mg, 87% yield) as a yellow oil. ^{1}H NMR (400 MHz, $CDCl_3$): δ 6.57 (s, 1H), 4.50 (bs, 1H), 3.91-3.90 (m, 2H), 3.81-3.80 (m, 1H), 2.14 (s, 3H), 1.64 (t, J = 4.8 Hz, 1H), 1.16 (d, J = 6.6 Hz, 6H). ^{13}C NMR (125 MHz, $CDCl_3$) δ 156.1, 120.8, 102.2, 72.0, 43.0, 23.2, 17.3, 11.7. HRMS (ESI) *m/z* calcd for

$C_9H_{15}NO_2Na$ $[M+Na]^+$ 192.1001, found 192.0997.

(1-Methylcycloprop-2-en-1-yl)methyl isopropylcarbamate (2.2b): To an oven-dried round-bottom flask was added **2.6b** (0.14 g, 0.58 mmol) in THF (8.6 mL), followed by TBAF (1.8 mL of a 1.0 M solution in hexanes, 1.8 mmol). The reaction was stirred overnight, then diluted with H_2O and extracted with Et_2O (2 x 15 mL). The organic layers were combined and dried over $MgSO_4$, filtered, and concentrated *in vacuo.* The resulting crude residue was purified by flash chromatography (eluting with 20% Et_2O in hexanes) to provide **2.2b** (42 mg, 43% yield) as a yellow oil. ^{1}H NMR (400 MHz, $(CD_3)_2CO$): δ 7.43 (s, 2H), 5.90 (bs, 1H), 3.86 (s, 2H), 3.72-3.70 (m, 1H), 1.13 (m, 9H). ^{13}C NMR (125 MHz, (CD3)2CO) δ 155.7, 119.0, 72.4, 43.0, 23.1, 22.1, 18.9. HRMS (ESI) *m/z* calcd for $C_9H_{16}NO_2$ $[M+H]^+$ 170.1181, found 170.1178.

(1-Methyl-2-(trimethylsilyl)cycloprop-2-en-1-yl)methanol (2.5b): To an oven-dried round-bottom flask was added **2.3b** (0.13 g, 0.67 mmol) in Et2O (3 mL). The solution was chilled to -78 °C, and 0.70 mL DIBAL-H in hexanes (1.0 M, 0.70 mmol) was slowly added. The reaction mixture was stirred for 2 h at -78 °C, then quenched with Rochelle's salt solution. The mixture was diluted with H_2O, extracted with Et_2O (2 x 25 mL), dried over $MgSO_4$, filtered, and concentrated slightly *in vacuo.* The crude organic residue was carried on without further purification due to volatility issues.

2-Methyl-3-(trimethylsilyl)cycloprop-2-en-1-yl)methyl isopropylcarbamate (2.6a): To an oven-dried round-bottom flask was added carbonyldiimidazole (CDI, 0.18 g, 1.1 mmol) and THF (6.0 mL). Compound **2.5a** (0.14 g, 0.90 mmol) was then added, and the resulting solution was stirred for 3 h. Isopropylamine (0.15 mL, 1.7 mmol) was added to the reaction mixture, and the solution was stirred overnight. The reaction was then diluted with H_2O, extracted with Et_2O (2 x

10 mL), dried over $MgSO_4$, filtered, and concentrated *in vacuo.* The crude organic residue was purified by flash chromatography (eluting with 30% Et_2O in hexanes) to provide **2.6a** (0.17 g, 79% yield over two steps) as a clear oil. ^{1}H NMR (400 MHz, $CDCl_3$): δ 4.47 (bs, 1H), 3.95-3.92 (m, 1H), 3.82-3.76 (m, 2H), 2.19 (s, 3H), 1.53 (t, J = 4.6 Hz, 1H), 1.15 (d, J = 6.8 Hz, 6H), 0.15 (s, 9H). ^{13}C NMR (125 MHz, $CDCl_3$) δ 156.3, 134.7, 111.0, 73.1, 42.9, 23.2, 18.7, 13.3, -1.2. HRMS (ESI) *m*/*z* calcd for $C_{12}H_{23}NO_2SiNa$ $[M+Na]^+$ 264.1396, found 264.1406.

(1-Methyl-2-(trimethylsilyl)cycloprop-2-en-1-yl)methyl isopropylcarbamate (2.6b): To an oven-dried round-bottom flask was added CDI (0.11 g, 0.68 mmol) and THF (5.0 mL). Crude cyclopropene **2.5b** (isolated from the reduction of 0.67 mmol **2.3b**) was then added, and the resulting solution was stirred for 2 h. Isopropylamine (0.10 mL, 1.1 mmol) was subsequently added, and the solution was stirred overnight. The reaction was then diluted with H_2O, extracted with Et_2O (3 x 20 mL), dried over $MgSO_4$, filtered, and concentrated *in vacuo.* The crude organic residue was purified by flash chromatography (eluting with 30% Et_2O in hexanes) to provide **2.6b** (77 mg, 47% yield over three steps) as a yellow oil. ^{1}H NMR (400 MHz, $CDCl_3$): δ 7.89 (s, 1H), 4.50 (bs, 1H), 4.02-3.94 (m, 1H), 3.94-3.75 (m, 2H), 1.16 (m, 9H), 0.17 (s, 9H). ^{13}C NMR (125 MHz, $CDCl_3$) δ 156.8, 131.9, 129.6, 75.1, 42.9, 23.9, 23.1, 20.2, -1.1. HRMS (ESI) *m*/*z* calcd for $C_{12}H_{23}NO_2SiNa$ $[M+Na]^+$ 264.1396, found 264.1405.

***N*-Isopropyl-2-(4-methoxyphenyl)-6-methyl-4-phenyl-2,3-diazabicyclo[3.1.0]hex-3- ene-6-carboxamide (2.11):** A solution of **2.1b** (22 mg, 0.16 mmol) and tetrazole **2.9** (20 mg, 0.079 mmol) in MeCN (15 mL) was added to a quartz test tube. The reaction was photoirradiated with a UV lamp (302 nm, Zilla UVB 20 watts) for 2 h. The reaction was then concentrated *in vacuo*, and purified by preparative HPLC, eluting with 0-95% MeCN in water over 30 min. The desired

fractions were collected and concentrated *in vacuo* to provide **2.11** (18 mg, 63% yield) as a yellow solid. ^{1}H NMR (400 MHz, $CDCl_3$): δ 7.80 (d, *J* = 7.2 Hz, 2H), 7.42-7.30 (m, 3H), 7.25 (d, *J* = 9.2 Hz, 2H), 6.90 (d, *J* = 8.9 Hz, 2H), 5.75 (d, *J* = 7.1 Hz, 1H), 4.66 (d, *J* = 6.9 Hz, 1H), 4.21-4.16 (m, 1H), 3.81 (s, 3H), 3.72 (d, *J* = 7.1 Hz, 1H), 1.24 (dd, *J* = 6.4, 2.5 Hz, 6H), 0.77 (s, 3H). ^{13}C NMR (125 MHz, $CDCl_3$) δ 172.7, 154.5, 146.8, 137.4, 133.0, 128.6, 128.4, 125.8, 114.8, 114.7, 55.8, 55.0, 42.1, 40.0, 23.1, 23.0, 15.8, 7.7. HRMS (ESI) *m*/*z* calcd for $C_{22}H_{25}N_3O_2Na$ $[M+Na]^+$ 386.1844, found 386.1844.

***N*-Isopropyl-2-(4-methoxyphenyl)-3-methyl-6-phenyl-2,5-dihydropyridazine-4-carboxamide (2.12):** A solution of **2.1a** (23 mg, 0.17 mmol) and tetrazole **2.9** (21 mg, 0.083 mmol) in MeCN (26 mL) was added to a quartz test tube. The reaction was photoirradiated with a UV lamp (302 nm, Zilla UVB 20 watts) for 3 h. The reaction was then concentrated *in vacuo* and purified by preparative HPLC, eluting with 0-95% MeCN in water over 30 min. The desired fractions were collected and concentrated *in vacuo* to provide **2.12** (12 mg, 38% yield) as a yellow solid. ^{1}H NMR (400 MHz, $CDCl_3$): δ 7.78 (d, *J* = 7.9 Hz, 2H), 7.39 (m, 3H), 7.29 (d, *J* = 7.1 Hz, 2H), 6.94 (d, *J* = 8.7 Hz, 2H), 5.29 (d, *J* = 7.5 Hz, 1H), 4.24-4.16 (m, 1H), 3.84 (s, 3H), 3.41 (s, 2H), 2.07 (s, 3H), 1.22 (d, *J* = 6.8, 6H). ^{13}C NMR (125 MHz, CDCl3) δ 168.1, 158.2, 141.8, 141.7, 137.8, 136.3, 129.3, 128.5, 127.7, 126.2, 114.2, 97.9, 55.7, 41.7, 25.4, 23.2, 17.0. HRMS (ESI) *m*/*z* calcd for $C_{22}H_{25}N_3O_2Na$ $[M+Na]^+$ 386.1844, found 386.1840.

2.7 References

(1) Chang, P. V.; Prescher, J. A.; Hangauer, M. J.; Bertozzi, C. R: Imaging cell surface glycans with bioorthogonal chemical reporters. *J. Am. Chem. Soc.* **2007**, *129*, 8400.

(2) Prescher, J. A.; Bertozzi, C. R: Chemistry in living systems. *Nat. Chem. Biol.* **2005**, *1*, 13.

(3) Prescher, J. A.; Dube, D. H.; Bertozzi, C. R: Chemical remodelling of cell surfaces in living animals. *Nature* **2004**, *430*, 873.

(4) Hang, H. C.; Wilson, J. P.; Charron, G: Bioorthogonal chemical reporters for analyzing protein lipidation and lipid trafficking. *Acc. Chem. Res.* **2011**, *44*, 699.

(5) Haun, J. B.; Devaraj, N. K.; Hilderbrand, S. A.; Lee, H.; Weissleder, R: Bioorthogonal chemistry amplifies nanoparticle binding and enhances the sensitivity of cell detection. *Nat. Nanotechnol.* **2010**, *5*, 660.

(6) Sletten, E. M.; Bertozzi, C. R: Bioorthogonal chemistry: fishing for selectivity in a sea of functionality. *Angew. Chem. Int. Ed.* **2009**, *48*, 6974.

(7) Debets, M. F.; van Berkel, S. S.; Dommerholt, J.; Dirks, A. J.; Rutjes, F. P. J. T.; van Delft, F. L: Bioconjugation with strained alkenes and alkynes. *Acc. Chem. Res.* **2011**, *44*, 805.

(8) Lang, K.; Davis, L; Wallace, S.; Mahesh, M.; Cox, D. J.; Blackman, M. L.; Fox, J. M.; Chin, J. W: Genetic Encoding of bicyclononynes and trans-cyclooctenes for site-specific protein labeling in vitro and in live mammalian cells via rapid fluorogenic Diels-Alder reactions. *J. Am. Chem. Soc.* **2012**, *134*, 10317.

(9) Chen, W.; Wang, D.; Dai, C.; Hamelberg, D.; Wang, B: Clicking 1,2,4,5-tetrazine and cyclooctynes with tunable reaction rates. *Chem. Commun.* **2012**, *48*, 1736.

(10) Plass, T.; Milles, S.; Koehler, C.; Schultz, C.; Lemke E. A: Genetically encoded copper-free click chemistry. *Angew. Chem. Int. Ed.* **2011**, *50*, 3878.

(11) Liang, Y.; Mackey, J. L.; Lopez, S. A.; Liu, F.; Houk, K. N: Control and design of mutual orthogonality in bioorthogonal cycloadditions. *J. Am. Chem. Soc*. **2012**, *134*, 17904.

(12) Sanders, B. C.; Friscourt, F.; Ledin, P. A.; Mbua, N. E.; Arumugam, S.; Guo, J.; Boltje, T. J.; Popik, V. V.; Boons, G. J: Metal-free sequential [3+2]-dipolar cycloadditions using

cyclooctynes and 1,3-dipoles of different reactivity. *J. Am. Chem. Soc.* **2011**, *133*, 949.

(13) Zhu, Z.-B.; Wei, Y.; Shi, M: Recent developments of cyclopropene chemistry. *Chem. Soc. Rev.* **2011**, *40*, 5534.

(14) Patterson, D. M.; Nazarova, L. A.; Xie, B.; Kamber, D. N.; Prescher, J. A: Functionalized cyclopropenes as bioorthogonal chemical reporters. *J. Am. Chem. Soc.* **2012**, *134*, 18638.

(15) Yang, J.; Šečkutė, J.; Cole, C. M.; Devaraj, N. K: Live-cell imaging of cyclopropene tags with fluorogenic tetrazine cycloadditions. *Angew. Chem. Int. Ed.* **2012**, *51*, 7476.

(16) Yu, Z.; Pan, Y.; Wang, Z.; Wang, J.; Lin, Q: Genetically encoded cyclopropene directs rapid, photoclick-chemistry-mediated protein labeling in mammalian cells. *Angew. Chem. Int. Ed.* **2012**, *51*, 10600.

(17) Thalhammer, F.; Wallfahrer, U.; Sauer, J: Reaktivität einfacher offenkettiger und cyclischer dienophile bei Diels-Alder-reaktionen mit inversem elektronenbedarf. *Tetrahedron Lett.* **1990**, *31*, 6851.

(18) Cole, C. M.; Yang, J.; Šečkutė, J.; Devaraj, N. K: Fluorescent live-cell imaging of metabolically incorporated unnatural cyclopropene-mannosamine derivatives. *ChemBioChem* **2013**, *14*, 205.

(19) Frisch, M. J., *et al*. *Gaussia 09*, revision C.01; Gaussian, Inc.: Wallingford, CT, **2010**.

(20) Zhao, Y.; Truhlar, D. G: Density functionals with broad applicability in chemistry *Acc. Chem. Res.* **2008**, *41*, 157.

(21) Zhao, Y.; Truhlar, D. G: The M06 suite of density functionals for main group thermochemistry, thermochemical kinetics, noncovalent interactions, excited states, and transition elements: two new functionals and systematic testing of four M06-class functionals and 12 other functionals. *Theor. Chem. Acc.* **2008**, *120*, 215.

(22) Lan, Y.; Zou, L.; Cao, Y.; Houk, K. N: Computational methods to calculate accurate activation and reaction energies of 1,3-dipolar cycloadditions. *J. Phys. Chem. A.* **2011**, *115*, 13906.

(23) Paton, R. S.; Mackey, J. L; Kim, W. H.; Lee, J. H.; Danishefsy, S. J.; Houk, K. N: Origins of stereoselectivity in the *trans* Diels−Alder paradigm. *J. Am. Chem. Soc.* **2010**, *132*, 9335.

(24) Ess, D. H.; Houk, K. N: Distortion/interaction energy control of 1,3-dipolar cycloaddition reactivity. *J. Am. Chem. Soc.* **2007**, *129*, 10646.

(25) Gordon, C. G.; Mackey, J. L; Jewett, J. C.; Sletten, E. M.; Houk, K. N.; Bertozzi, C. R: Reactivity of biarylazacyclooctynones in Copper-free click chemistry. *J. Am. Chem. Soc.* **2012**, *134*, 9199.

(26) Diev, V. V.; Kostikov, R. R.; Gleiter, R.; Molchanov, A. P: Cyclopropenes in the 1,3-dipolar cycloaddition with carbonyl ylides: experimental and theoretical evidence for the enhancement of σ-withdrawal in 3-substituted-cyclopropenes. *J. Org. Chem.* **2006**, *71*, 4066.

(27) Karver, M. R.; Weissleder, R.; Hilderbrand, S. A: Synthesis and evaluation of a series of 1,2,4,5-tetrazines for bioorthogonal conjugation. *Bioconjugate Chem.* **2011**, *22*, 2263.

(28) Chen, S.; Ren, J.; Wang, Z: A highly regioselective tandem 1,3-dipolar cycloaddition of cyclopropene 1,1-diesters and nitrile oxides: synthesis of highly functionalized isoxazoles. *Tetrahedron* **2009**, *65*, 9146.

(29) Willems, L. I.; Li, N.; Florea, B. I.; Ruben, M.; van der Marel, G. A.; Overkleeft, H. S: Triple bioorthogonal ligation strategy for simultaneous labeling of multiple enzymatic activities. *Angew. Chem. Int. Ed.* **2012**, *51*, 4431.

(30) Sletten, E. M.; Bertozzi, C. R: A Bioorthogonal quadricyclane ligation. *J. Am. Chem. Soc.* **2011**, *133*, 17570.

(31) W. J. Hehre, L. Radom, P. v. R. Schleyer, J. A. Pople: *Ab initio molecular orbital theory*, Wiley: New York, **1986**.

(32) (a) Zhao, Y.; Truhlar, D. G: Computational characterization and modeling of buckyball tweezers: density functional study of concave–convex π···π interactions. *Phys. Chem. Chem. Phys.* **2008**, *10*, 2813. (b) Ribeiro, R. F.; Marenich, A. V.; Cramer, C. J.; Truhlar, D. G: Use of solution-phase vibrational frequencies in continuum models for the free energy of solvation. *J. Phys. Chem. B* **2011**, *115*, 14556.

(33) (a) Barone, V.; Cossi, M: Quantum calculation of molecular energies and energy gradients in solution by a conductor solvent model. *J. Phys. Chem. A.* **1998**, *102*, 1995. (b) Cossi, M.; Rega, N.; Scalmani, G.; Barone, V: Energies, structures, and electronic properties of molecules in solution with the C-PCM solvation model. *J. Comput. Chem.* **2003**, *24*, 669.

(34) (a) Zefirov, N. S.; Averina, N.V.; Boganov, A. M.; Laryukova, M.V.; Rashchupkina, Z.A.; Terent'ev, P.B.; Sharbatyan, P.A. *J. Org. Chem. USSR (English. Transl.)* **1981**, 1291–13001. (b) Liao, L.; Zhang, F.; Yan, N.; Golen, J.; Fox, J: An efficient and general method for resolving cyclopropene carboxylic acids. *Tetrahedron* **2004**, *60*, 1803-1816.

(35) Wang, Y.; Song, W.; Hu, W. J.; Lin, Q: Fast alkene functionalization *in vivo* by photoclick chemistry: HOMO-lifting of nitrile imine dipoles. *Angew. Chem. Int. Ed.* **2009**, *48*, 5330-5333.

Chapter 3: 1,2,4-Triazines are versatile bioorthogonal reagents

Yong Liang, Robert J. Blizzard, and Fang Liu contributed to the work presented in this chapter.

3.1 Introduction

As introduced in Chapter 1, numerous chemical reporters and bioorthogonal reactions have been reported in recent years, but significant limitations remain [1-3]. Many of the reagents are too bulky for general use or prone to hydrolysis in cellular environments [4]. Moreover, several popular bioorthogonal reagents cross-react with one another and cannot be used concurrently to visualize collections of biomolecules [4]. To address these issues and expand the scope of the chemical reporter strategy, new bioorthogonal reactions and combinations of reactions are being pursued. In recent years, we and others have developed compatible chemistries based on cyclopropenes and other strained alkenes [5-8]. In Chapter 2, our efforts tuning the reactivity of the cyclopropene scaffold were discussed. By strategically tuning the reactivity at C3 of the cyclopropene ring, we developed a strategy for sequential labeling of distinct biomolecules.

The cyclopropene motifs are stable in physiological environments and have been used to target numerous biomolecules in live cells [9-12]. In nearly all cases, the strained alkenes were detected via inverse electron demand Diels−Alder (IED-DA) reactions with 1,2,4,5-tetrazines. A handful of tetrazine ligations can also be used simultaneously with azide−alkyne cycloadditions [5,11], setting the stage for multicomponent bioorthogonal imaging in vivo [8,11,13]. While much attention has been paid to strained alkenes for bioorthogonal reaction development, less attention has been given to the other half of the IED-DA reaction: the electron-deficient dienes.

To date, tetrazines have dominated the IED- DA landscape [14]. These moieties react robustly with trans-cyclooctene (TCO) and other strained dienophiles in a variety of settings [15]. Unfortunately, the most rapid-reacting tetrazines also tend to be the least stable in cells and *in vivo* [16]. Tetrazines are prone to hydrolysis and side reactions with endogenous thiols, limiting their applications in the most stringent environments (e.g., inside cells) [17-19]. More stable tetrazines are being pursued, but these reagents are generally large in size [20].

3.2 Computational analysis on reactivity profile of tetrazines and triazines

To develop improved bioorthogonal IED-DA reactions, we were drawn to triazine scaffolds. 1,2,4-Triazines have been identified in microbial natural products and pigments, suggesting that they are stable in physiological environments [21-23]. These motifs also react efficiently with electron-rich alkenes in IED-DA reactions [24-29]. Boger further showed that 1,2,3-triazines react with electron-rich dienophiles [30]. To compare the intrinsic DA reactivities of 1,2,3- and 1,2,4- triazines with that of 1,2,4,5-tetrazine, we evaluated the activation free energies for their reactions with ethylene by density functional theory (DFT) calculations (Figure 3-1A, Table 3-2) [31-33]. The computational analysis suggested that 1,2,4- triazine is much more reactive than 1,2,3-triazine (activation free energy: 29.3 versus 41.0 kcal/mol), but less reactive than 1,2,4,5-tetrazine (29.3 versus 21.9 kcal/mol). This is consistent with the inverse electron demand nature of the cycloaddition: the LUMO+1 (the π^* orbital that interacts with the dienophile HOMO in the DA reaction) of 1,2,4-triazine is increased by 0.49 eV as compared to 1,2,4,5-tetrazine (2.18 versus 1.69 eV, Figures 3-1A and 3-2). While highly reactive, tetrazines are prone to decomposition by biological nucleophiles [18-20]. Seitz and co-workers found that thiols rapidly decompose tetrazines via 1,4-addition and subsequent release of nitrogen [34]. DFT calculations revealed that formation of the 1,4-adduct of 3-phenyl- 1,2,4,5-tetrazine and

methanethiol is endergonic by 23.4 kcal/ mol in water and that the overall barrier for N_2 release is 28.6 kcal/mol (Figure 3-1B). However, the corresponding adduct and transition state of 6-phenyl-1,2,4-triazine are significantly higher in energy. This implies that 6-aryl-1,2,4-triazine is inert to thiols relative to monoaryl tetrazine, although both are very similar in size. Thus, while 1,2,4-triazine is less reactive in the IED-DA reaction, considering the extremely fast rates of the tetrazine−TCO cycloaddition (k_2 = 10^2−10^4 M^{-1} s^{-1}) [17,18], we hypothesized that triazines would be good candidates for bioorthogonal reaction development based on their size and stability.

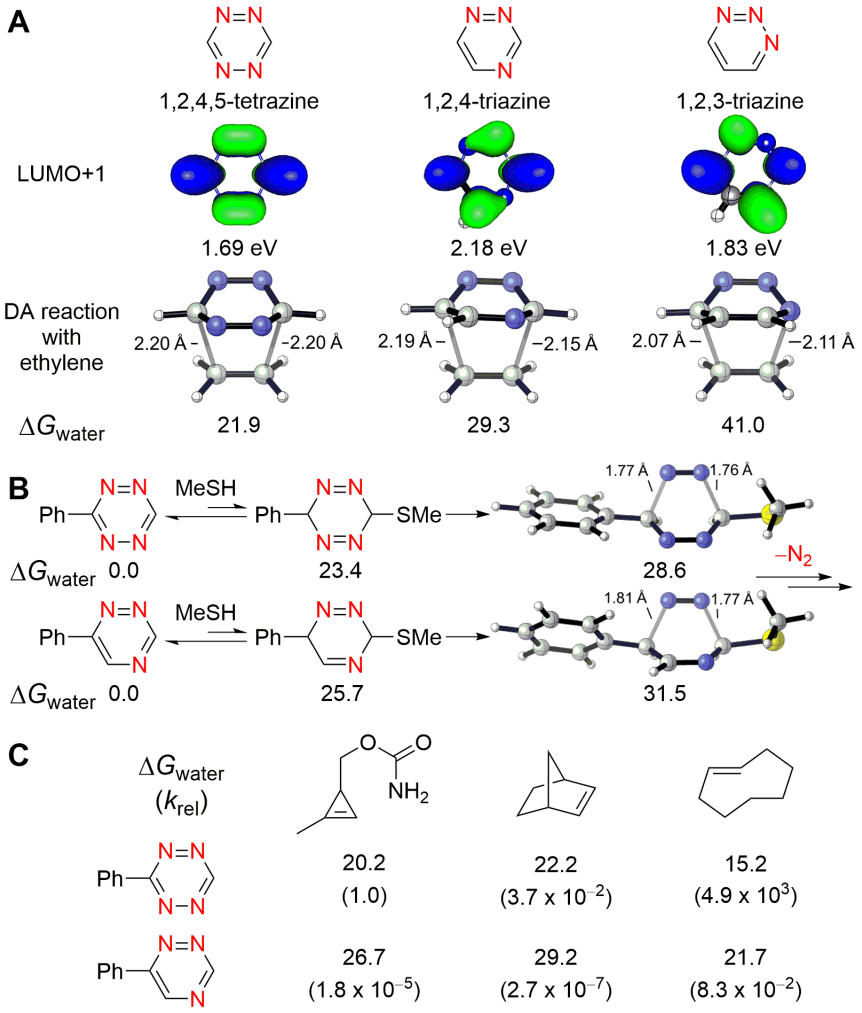

Figure 3-1. (A) Diels-Alder reactions of 1,2,4,5-tetrazine, 1,2,4-triazine, and 1,2,3-triazine with ethylene. LUMO+1 energies were computed with HF/6-311+G(d,p)//M06-2X/6-31G(d), and activation free energies (in kcal/mol) in water were computed with CPCM(water)-M06-2X/6-311+G(d,p)//M06-2X/6-31G(d). (B) Energetics of 1,4-adduct formation and subsequent N_2 release transition state for methanethiol and 3-phenyl-1,2,4,5-tetrazine or 6-phenyl-1,2,4-triazine. (C) DFT-computed activation free energies and predicted relative rate constants for tetrazine or triazine cycloaddition with 3-carbamoyloxymethyl-1-methylcyclopropene, norbornene, or *trans*-cyclooctene, in water at 25 °C.

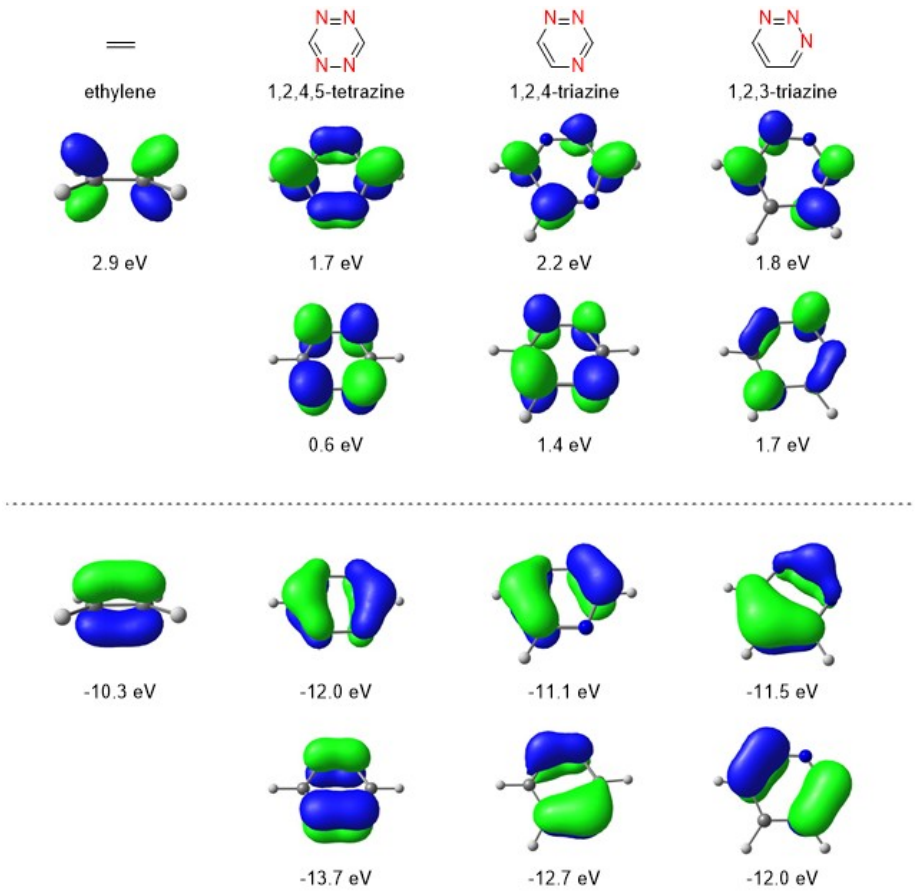

Figure 3-2. Frontier π orbitals of ethylene, 1,2,4,5-tetrazine, 1,2,4-triazine, and 1,2,3-triazine. The orbital energies were computed with HF/6-311+G(d,p)//M06-2X/6-31G(d).

We also predicted relative rate constants for the DA reactions of 3-phenyl-1,2,4,5-tetrazine or 6-phenyl-1,2,4-triazine with 3-carbamoyloxymethyl-1-methylcyclopropene, norbornene, and trans-cyclooctene (Figures 3-1C and 3-3). These data suggest that 6-aryl-1,2,4-triazines react efficiently with TCO, yet remain inert to other bioorthogonal scaffolds, including cyclopropene and norbornene. This unique reactivity profile could potentially be exploited for "orthogonal" bioorthogonal cycloaddition development [35-37].

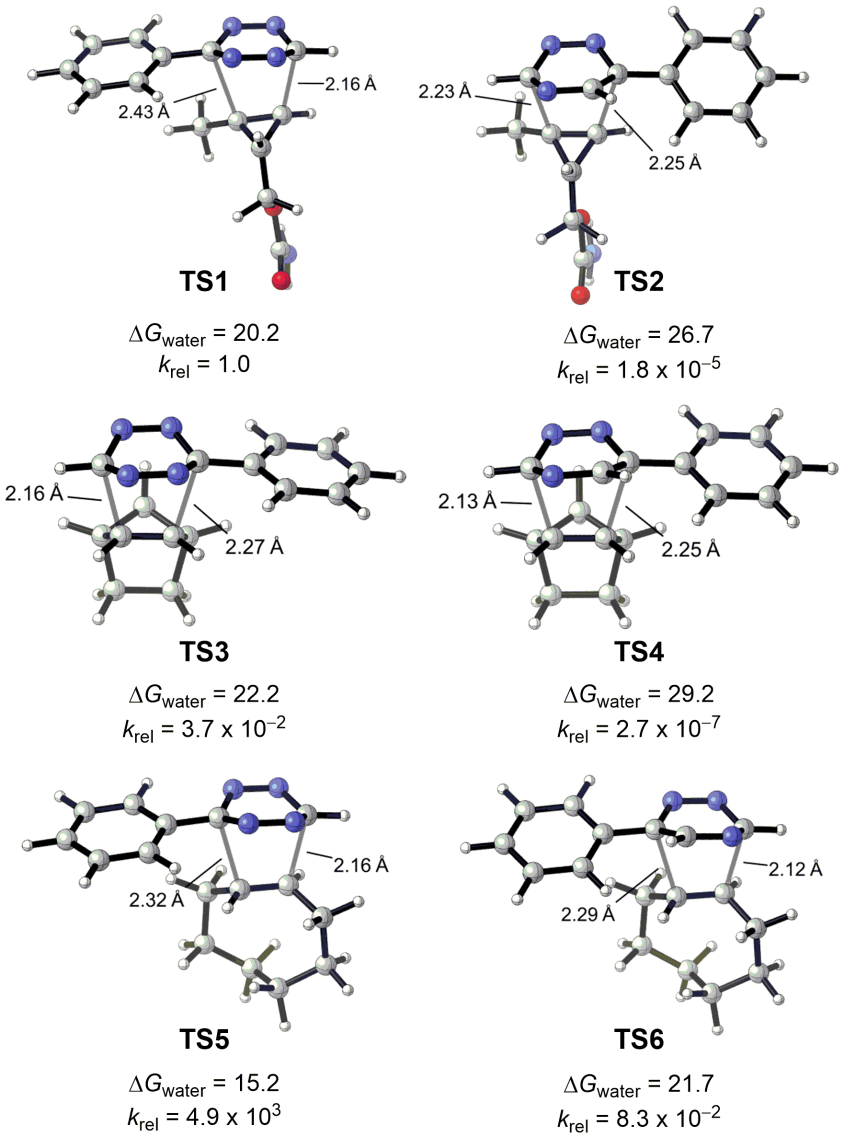

Figure 3-3. DFT-computed transition states **TS1-6** for tetrazine or triazine cycloaddition with 3-carbamoyloxymethyl-1-methylcyclopropene, norbornene, or *trans*-cyclooctene.

3.3 Synthesis and reactivity of 6-substituted-1,2,4-triazines

To test these hypotheses, we synthesized a panel of substituted 1,2,4-triazines using the reaction sequence pictured in Scheme 1. In brief, glyoxal was condensed with amino-guanidine to afford 3-amino-1,2,4-triazine (**3.1**). Bromination of this scaffold provided a convenient handle for diversification, and triazine **3.2** ultimately underwent Suzuki couplings with a variety of commercially available boronic acids (Schemes 3-1, top). Subsequent deamination of the products afforded triazines **3.4−3.9**, **3.13-3.19**. To access triazines containing nucleophilic substituents (**3.10-3.12** and **3.19**), the reverse sequence, deamination/Suzuki coupling, was employed (Schemes 3-1, bottom). This short reaction scheme can be used to access 6-substituted triazines with a broad array of functionality. By contrast, traditional syntheses of tetrazines are typically not compatible with free amino groups owing to the harsh oxidants employed, although milder conditions have recently been reported [38,39].

With the panel of triazines in hand, we analyzed their reactivities with TCO **3.20** (Table 3-1). The reactions were monitored by ^{1}H-NMR, and air oxidized cycloadducts were observed (Figures 3-5, 3-6, and 3-8). As expected, the most electron-poor triazine **3.4** exhibited the fastest rate (Table 1, entry 8), consistent with the inverse-electron-demand nature of the reaction. No reactivity was observed when electron-rich scaffolds **3.1** and **3.2** were incubated with TCO **3.20** (Figures 3-9 and 3-10). The triazine−TCO reaction is significantly slower than many of the tetrazine−TCO ligations [18], but on par with several copper- free click chemistries [40,41], and some IED-DA reactions with stabilized tetrazines [20,39]. Hammett analysis of the triazine−TCO rate constants gave a slope of $\rho = 0.49$ (Figure 3-4). This value is consistent with concerted IED-DA reactions and suggests that only partial charge separation occurs during the reaction.

Scheme 3-1. Synthesis of functionalized 1,2,4-triazines.

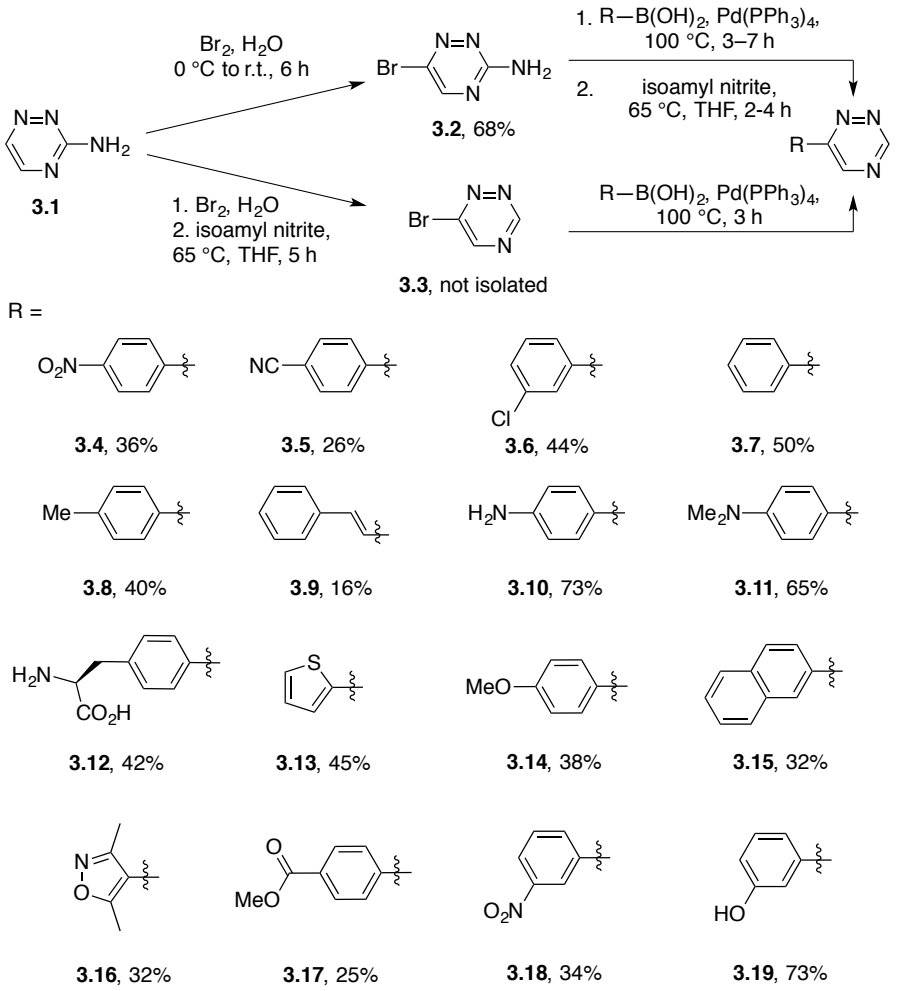

Table 3-1. Second-order rate constants for the triazine-TCO Ligation.

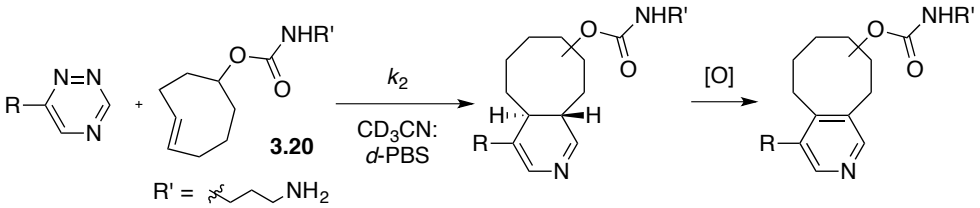

Entry	R =	k_2 (x 10^{-2} M^{-1} s^{-1})	Entry	R =	k_2 (x 10^{-2} M^{-1} s^{-1})
1	Me_2N	1.2 ± 0.1	5		3.4 ± 0.5
2	H_2N	1.3 ± 0.2	6	Cl	4.7 ± 0.2
3		2.3 ± 0.1	7	NC	6.4 ± 0.2
4	Me	3.4 ± 0.4	8	O_2N	7.5 ± 2.0

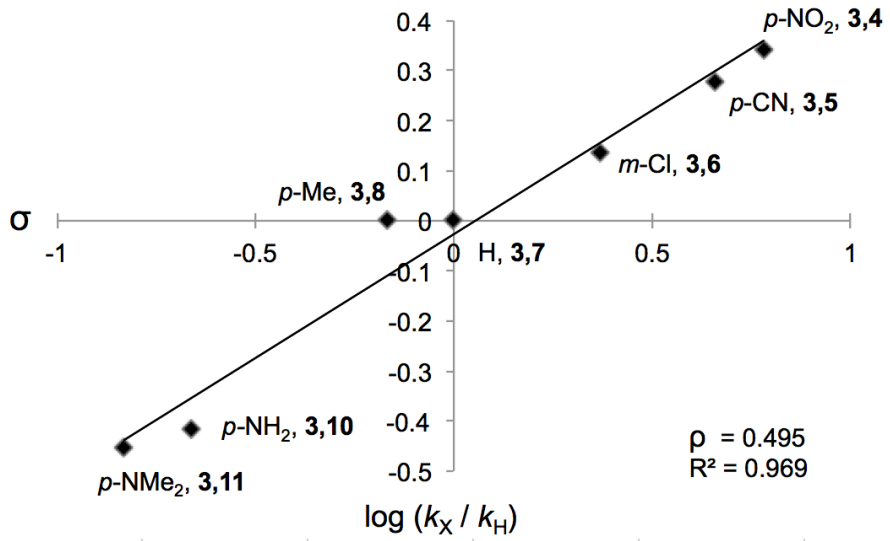

Figure 3-4. Hammet plot for the reactions between TCO **3.20** and a panel of 1,2,4-triazines. Sigma (σ) values derive from ref 42.

As predicted by our DFT calculations, no ligation was observed between the more reactive triazines (**3.4** and **3.9**) and other strained alkenes, including norbornene (**3.23**) and cyclopropene **3.22** (Scheme 3-2, Figures 3-11, 3-11, S3-1, S3-2). These alkenes do react robustly with the common tetrazine reagent **3.21** (Figure 3-7), suggesting that triazines and combinations of other bioorthogonal reagents can be used in tandem.

Scheme 3-2. Comparison of Tetrazine and Triazine Cycloadditions with Norbornene or 1,3-Disubstituted Cyclopropene[a]

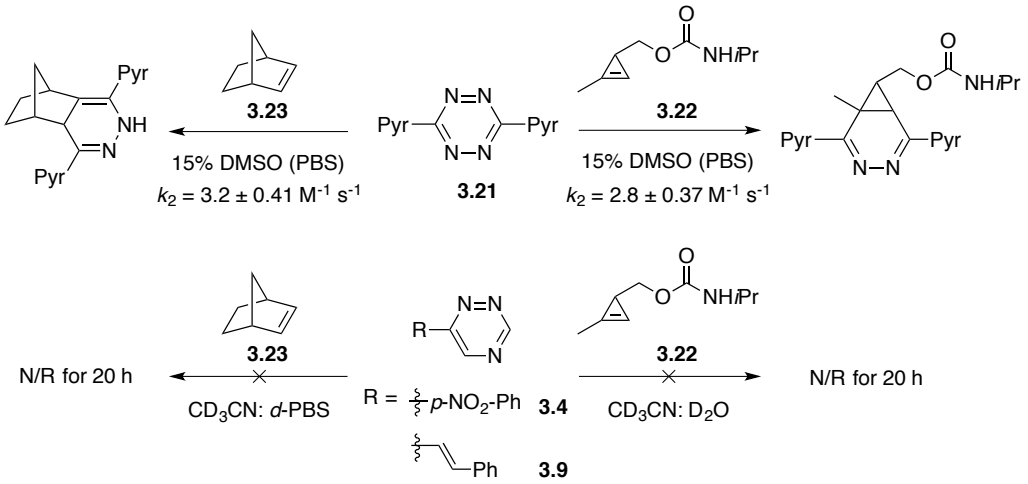

[a] The rate constant for 3.21 + 3.22 is from ref [8]

The triazine scaffold also excels in a key aspect of bioorthogonality: stability. When monosubstituted triazines were dissolved in a mixture of d-PBS and CD_3CN, they remained stable for over 1 week at 37 °C (Figures 3-13, 3-14, S3-3, and S3-4). Triazine scaffolds were also inert to cysteine over a similar time period (Figures 3-15 to 3-17, S3-4 to S3-6). These results are in sharp contrast to monosubstituted tetrazines that have been observed to hydrolyze and/or react with cysteine under similar conditions (Figure 3-18) [17-20,39].

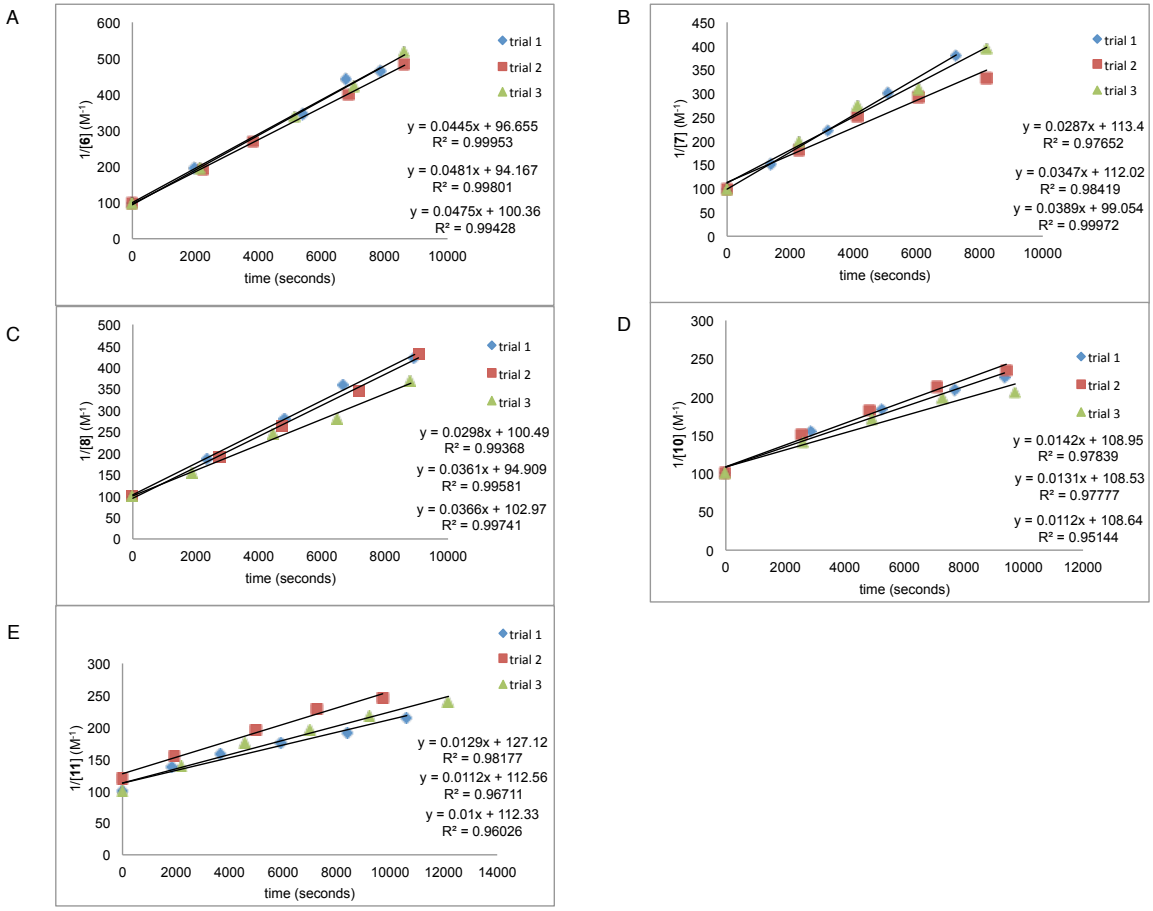

Figure 3-5. Kinetic data used to calculate second-order rate constants (k_2) for: (A) **3.6** and **3.20** in 1:1 CD_3CN: *d*-PBS, (B) **3.7** and **3.20** in 1:1 CD_3CN: *d*-PBS, (C) **3.8** and **3.20** in 1:1 CD_3CN: *d*-PBS, (D) **3.10** and **3.20** in 1:1 CD_3CN: *d*-PBS, (E) **3.11** and **3.20** in 1:1 CD_3CN: *d*-PBS. The reactions between triazines **3.6-3.8, 3.10-3.11** and TCO **3.20** were run in 1:1 ratios and monitored by ^{1}H-NMR.

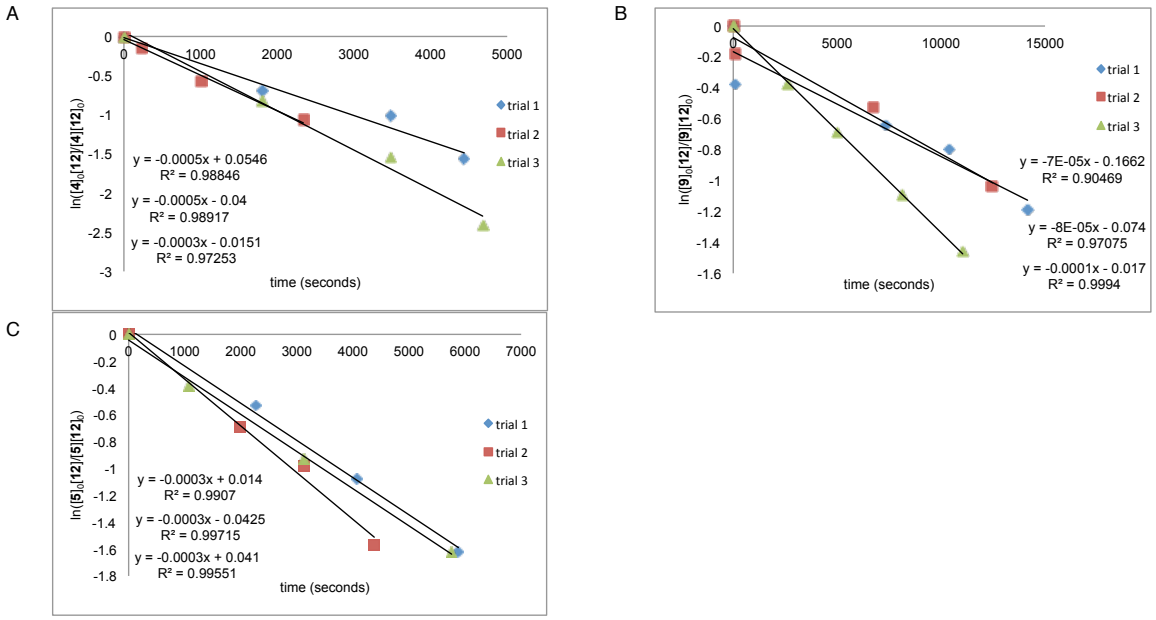

Figure 3-6. Kinetic data used to calculate second-order rate constants (k_2) for: (A) **3.4** and **3.20** in 1:1 CD_3CN: *d*-PBS, (B) **3.9** and **3.20** in 1:1 CD_3CN: *d*-PBS, (C) **3.5** and **3.20** in 1:1 CD_3CN: *d*-PBS. The reactions between triazines **3.4-3.5, 3.9** and TCO **3.20** were run in roughly 1:2 (triazine:TCO) ratios and monitored by ^{1}H-NMR.

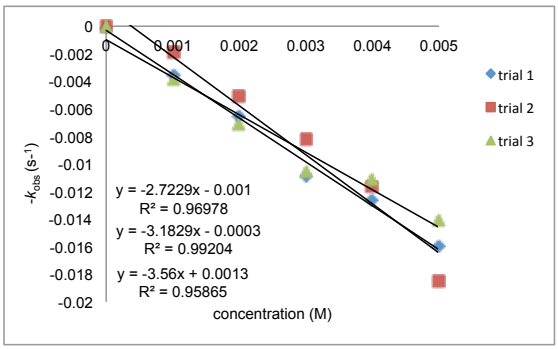

Figure 3-7. Kinetic data used to calculate second-order rate constants (k_2) for: **3.21** and **3.23** in 15% DMSO (PBS). The reactions between tetrazine **3.21** and norbornene **3.23** were run in 96-well plates and monitored by the change in tetrazine absorbance at 536 nm.

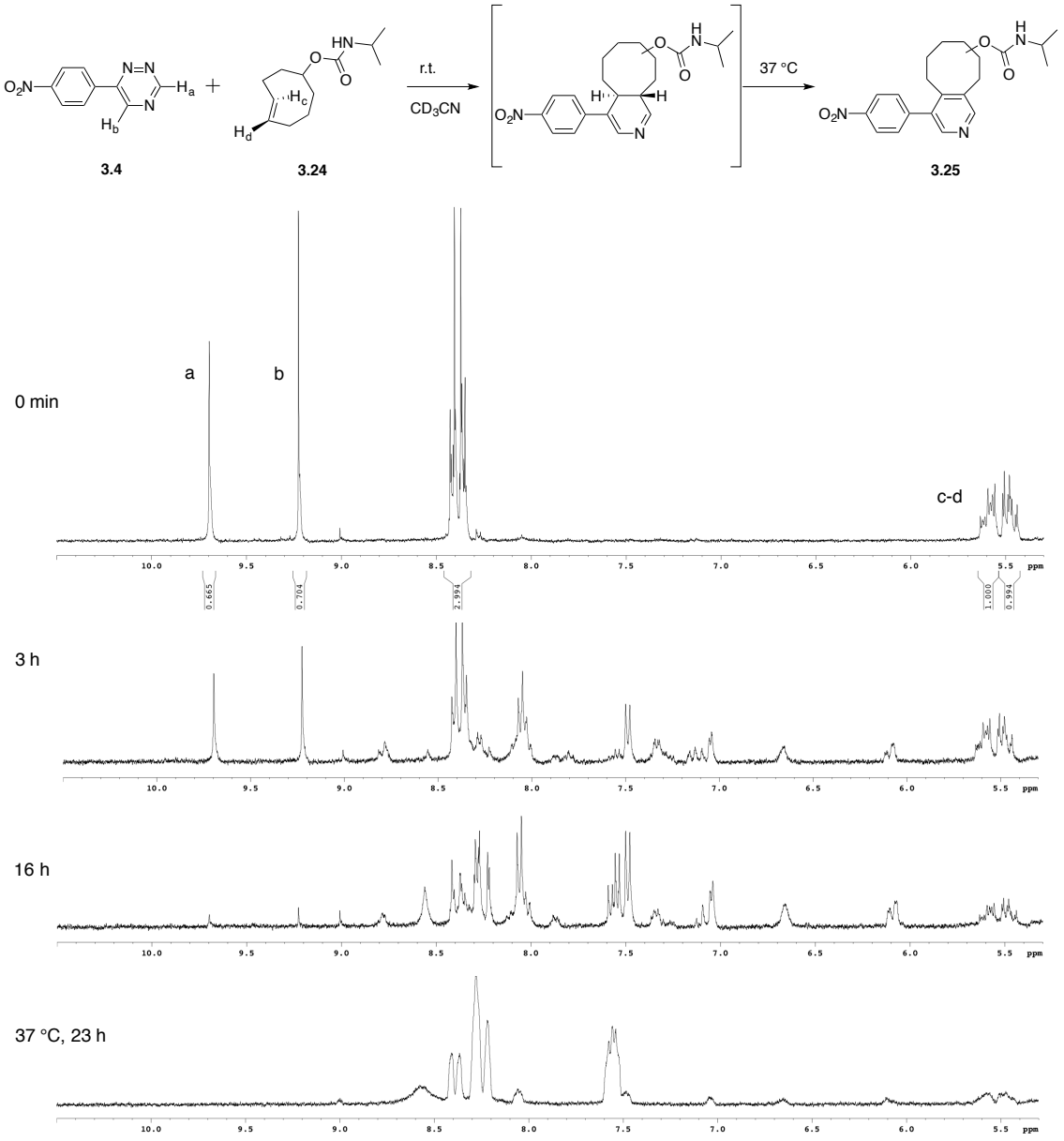

Figure 3-8. Formation of the initial dihydropyridine adduct and subsequent aromatization. Triazine **3.4** (0.3 mL of a 14 mM solution in CD_3CN) was added to a solution containing TCO **3.24** (0.24 mL of a 25 mM solution in CD_3CN) and diluted to 0.6 mL with CD_3CN. The reaction was monitored over time by ^{1}H-NMR.

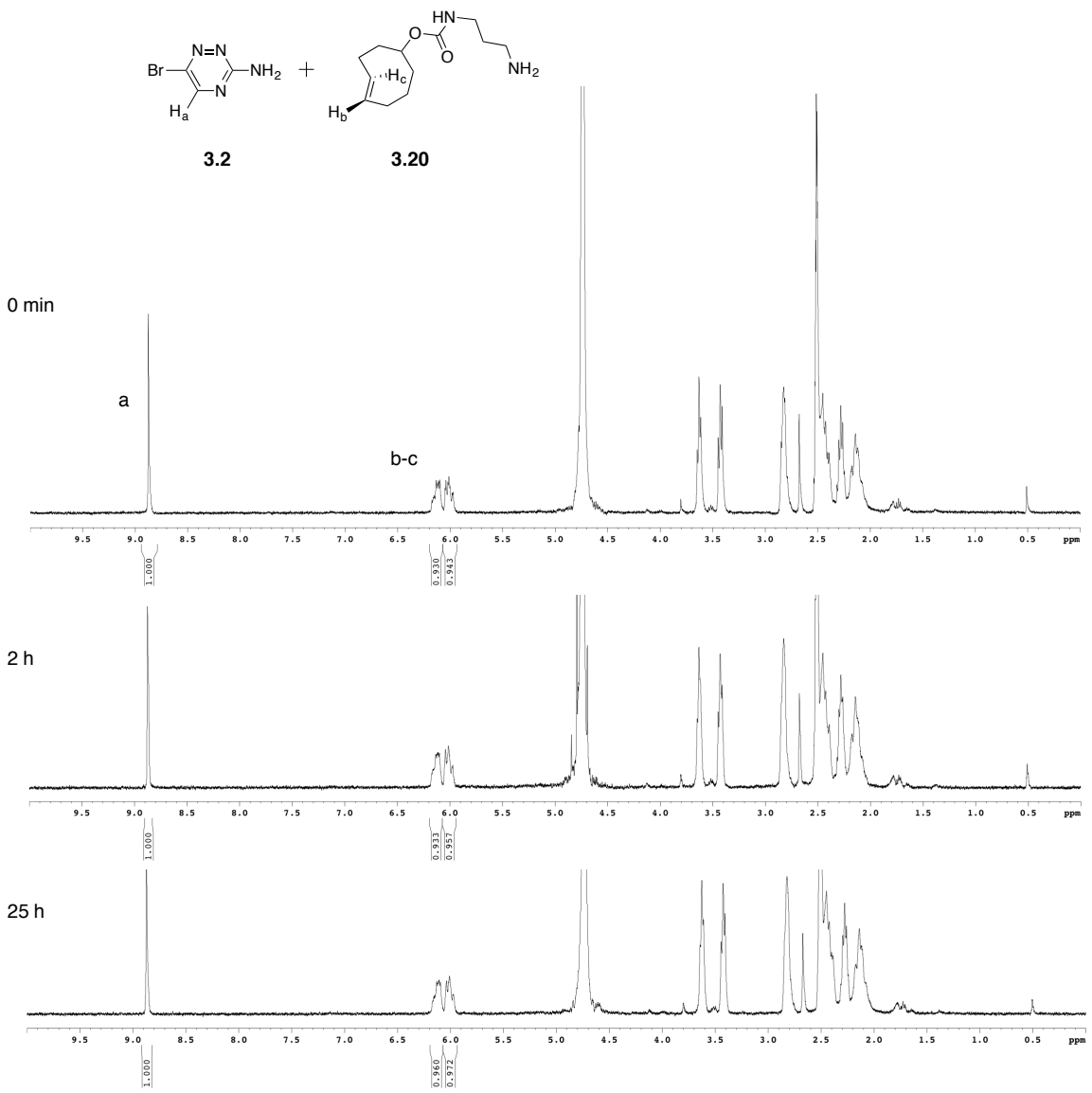

Figure 3-9. Triazine **3.2** does not react with TCO **3.20.** To a solution of triazine **3.2** (0.3 mL of a 20 mM solution in CD_3CN) was added TCO **3.20** (0.3mL of a 20 mM solution in *d*-PBS). The reaction was monitored over time by ^{1}H-NMR.

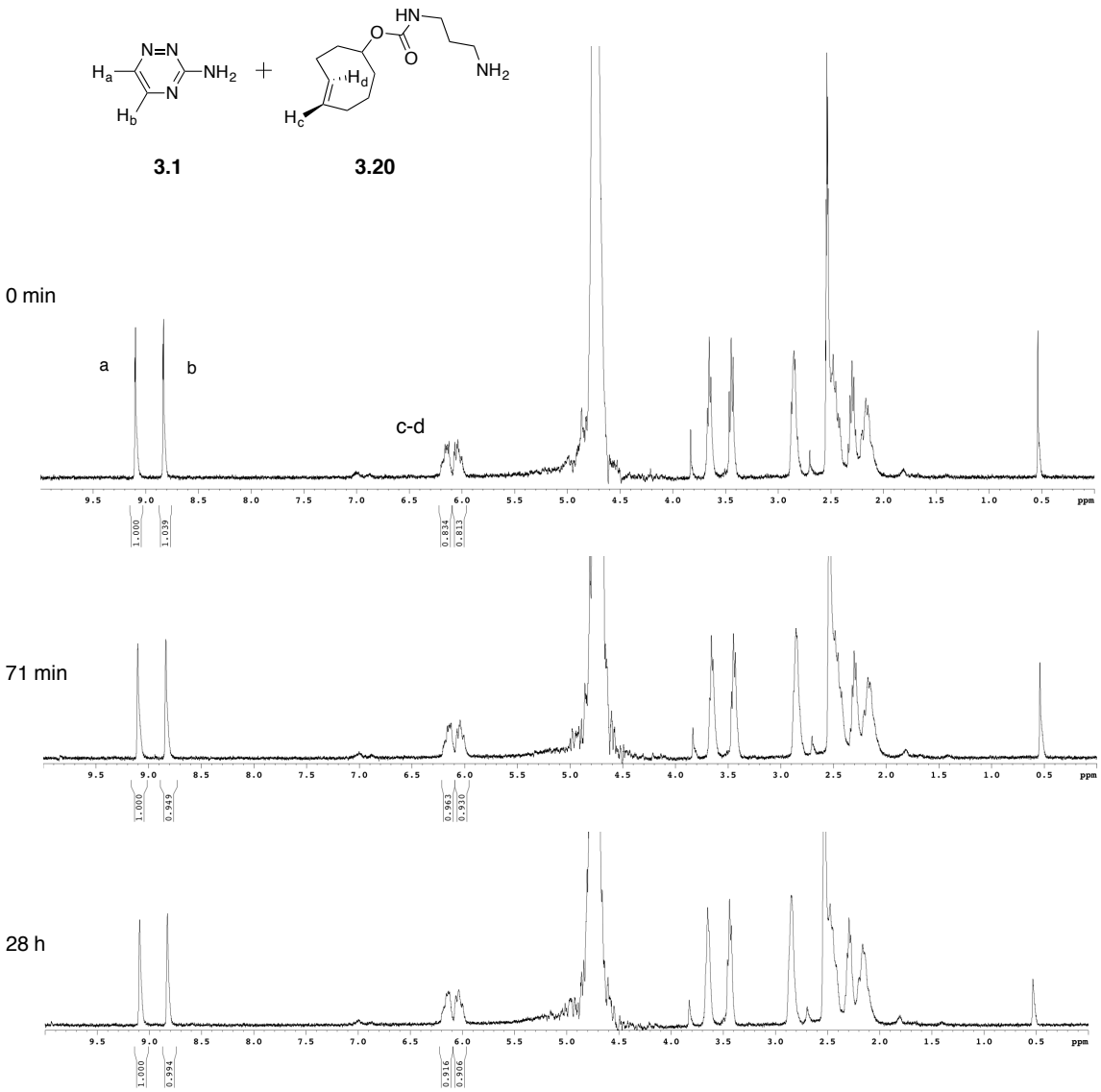

Figure 3-10. Triazine **3.1** does not react with TCO **3.20.** To a solution of triazine **3.1** (0.3 mL of a 20 mM solution in CD_3CN) was added TCO **3.20** (0.3mL of a 17 mM solution in *d*-PBS). The reaction was monitored over time by ^{1}H-NMR.

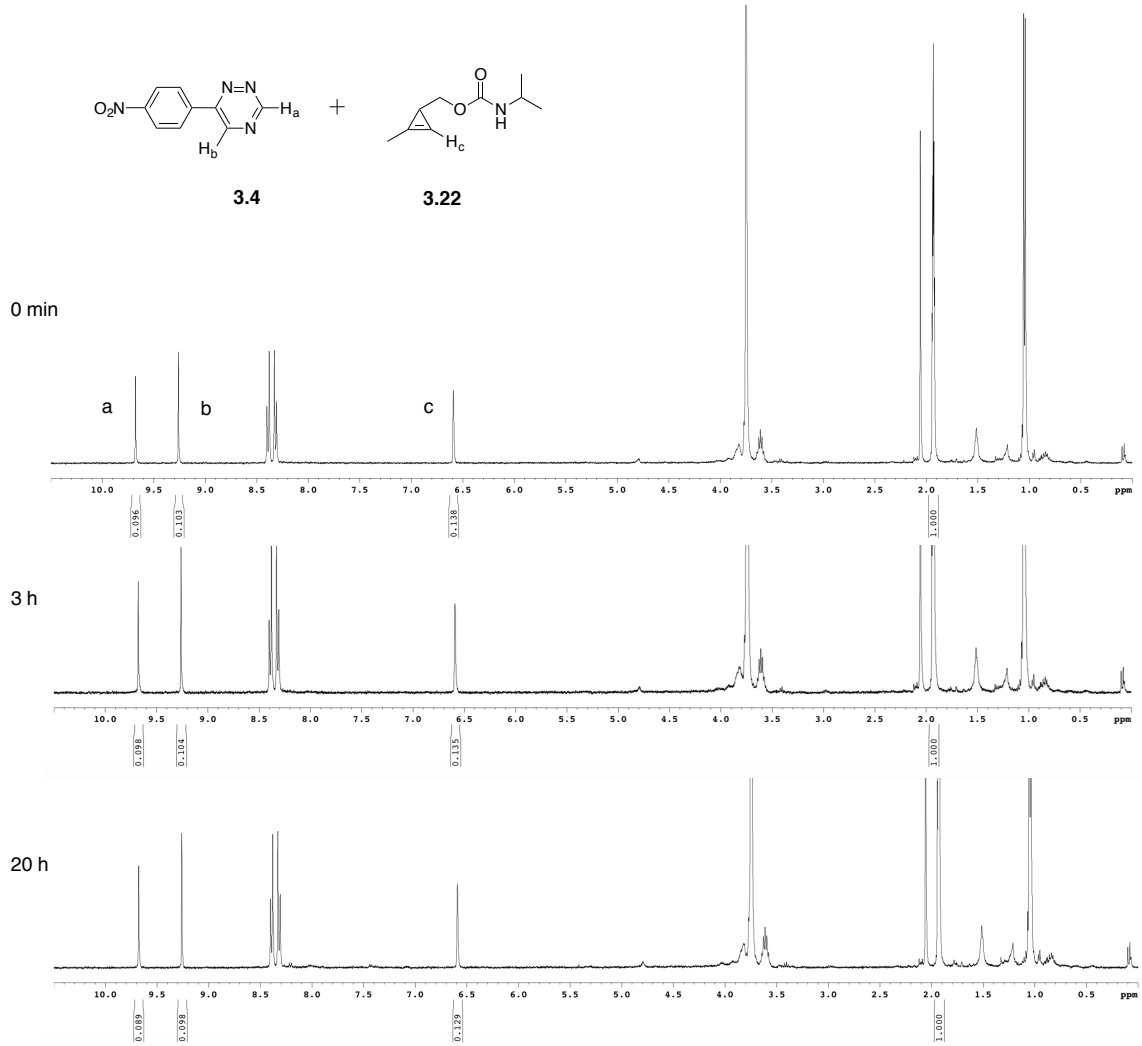

Figure 3-11. Triazine **3.4** does not react with cyclopropene **3.22.** To a solution of triazine **3.4** (0.3 mL of a 20 mM solution in CD_3CN) was added cyclopropene **3.22** (0.3 mL of a 20 mM in 1:1 CD_3CN:D_2O). The reaction was monitored over time by ^{1}H-NMR.

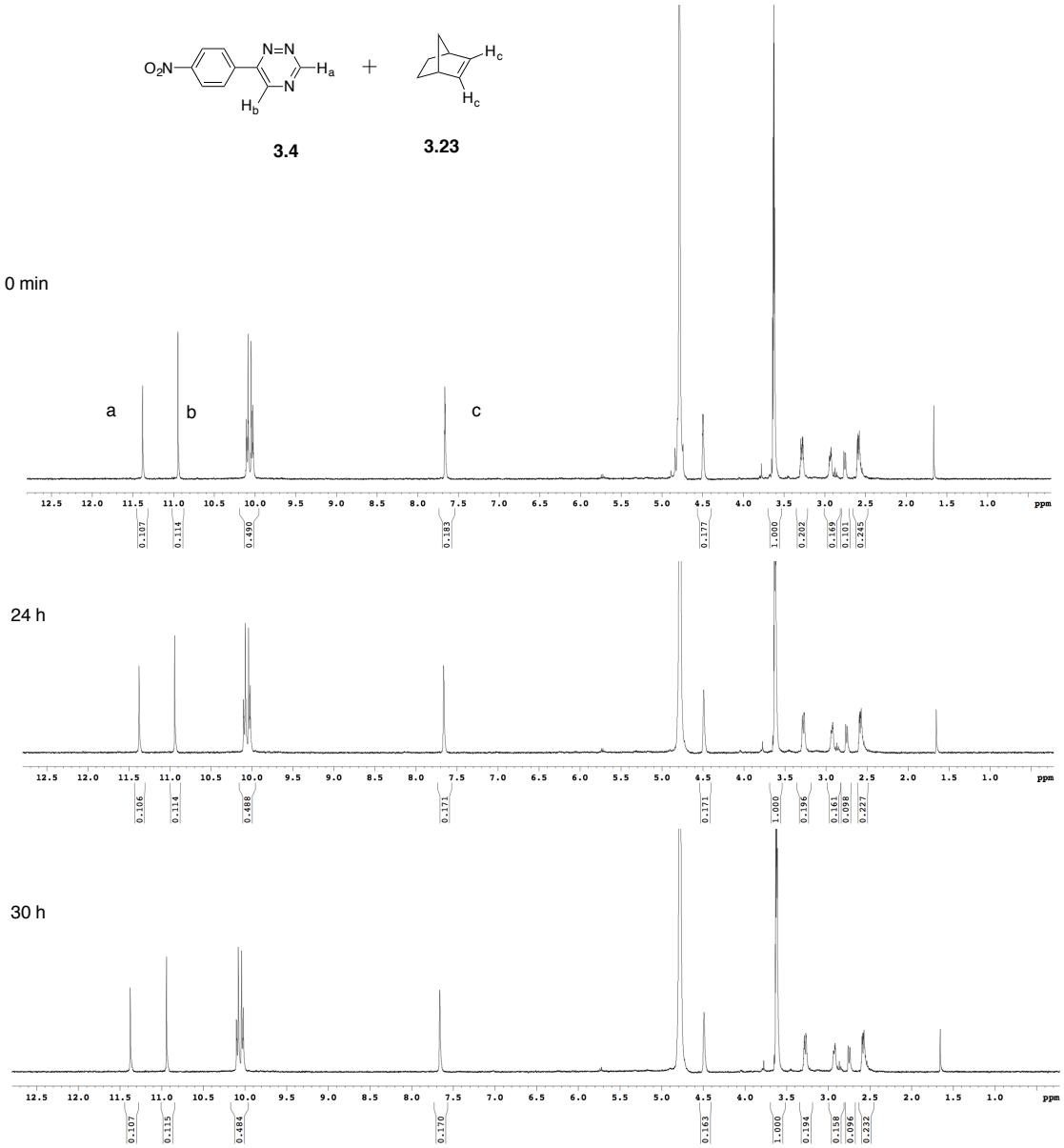

Figure 3-12. Triazine **3.4** does not react with norbornene **3.23.** To a solution of triazine **3.4** (0.24 mL of a 25 mM solution in CD_3CN) was added norbornene **3.23** (0.12 mL of a 40 mM solution in 1:1 CD_3CN:*d*-PBS) and diluted with 0.12 mL CD_3CN and 0.12 mL *d*-PBS to a final volume of 0.6 mL. The reaction was monitored over time by ^{1}H-NMR.

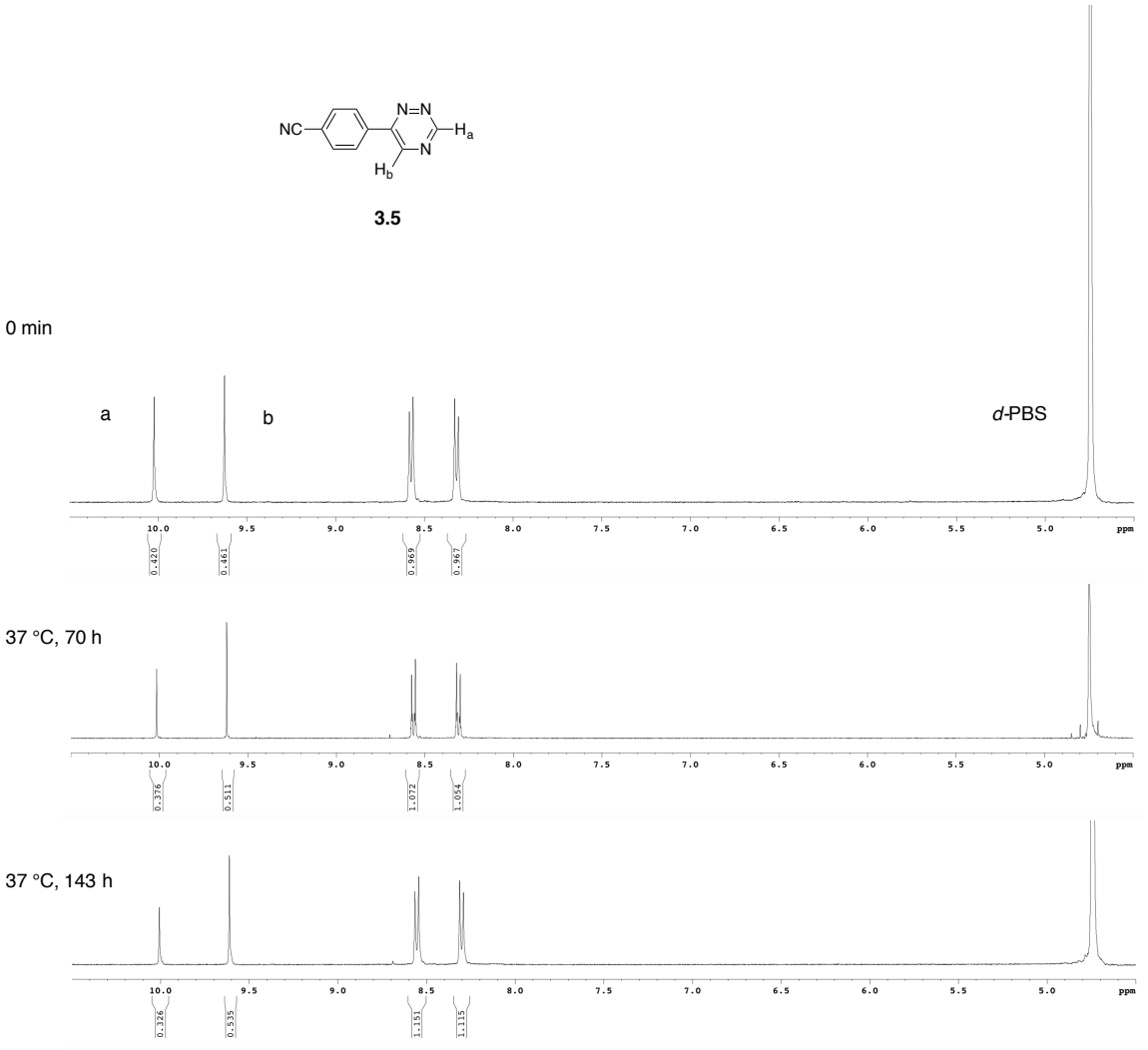

Figure 3-13. Triazine **3.5** is stable in aqueous buffer. A solution of triazine **3.5** (0.2 mL of a 50 mM solution in CD_3CN) was diluted with 0.4 mL *d*-PBS. The reaction was incubated at 37 °C for 0-143 h. The reaction was monitored over time by ^{1}H-NMR.

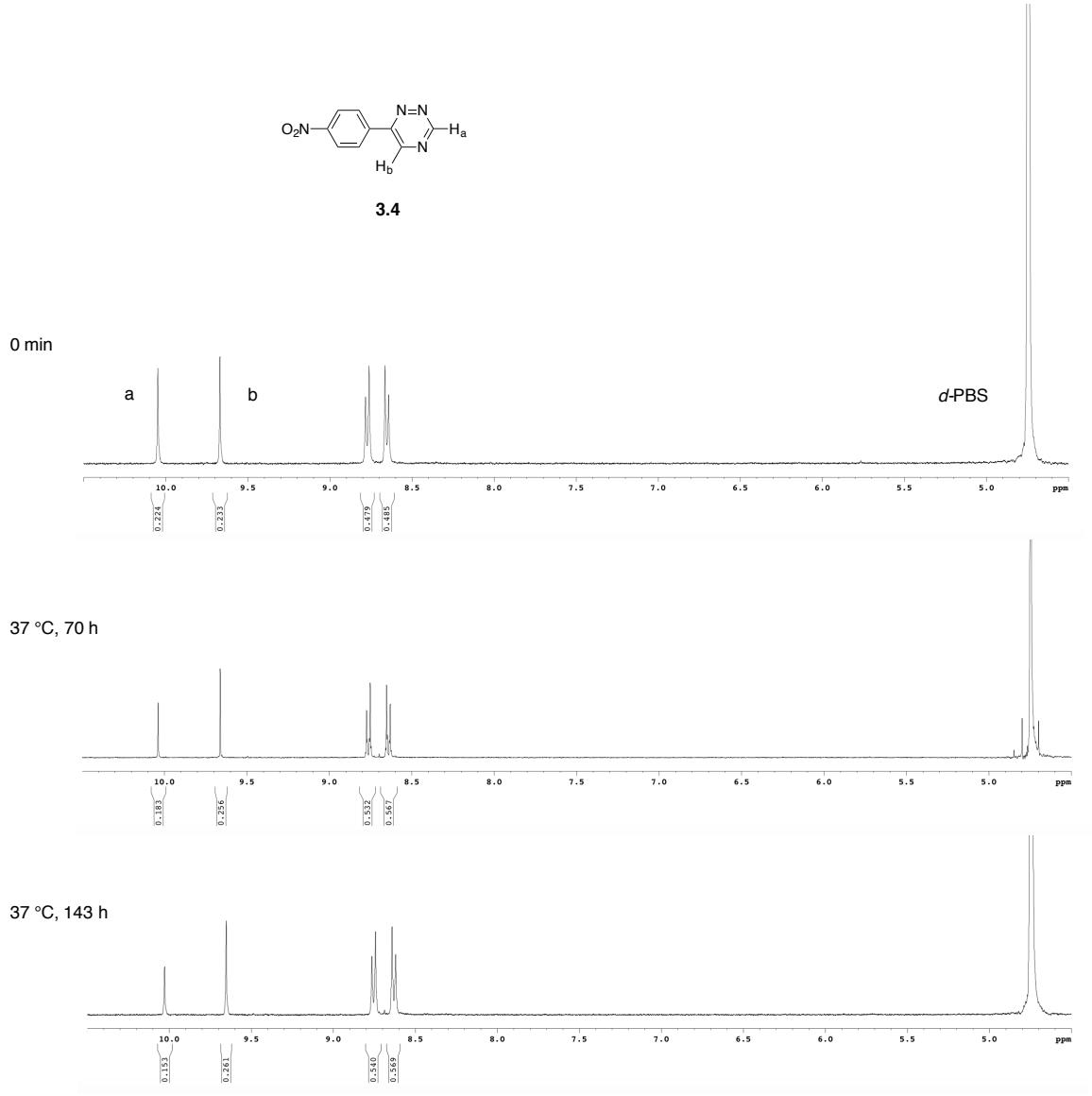

Figure 3-14. Triazine **3.4** is stable in aqueous buffer. A solution of triazine **3.4** (0.2 mL of a 25 mM solution in CD_3CN) was diluted with 0.4 mL *d*-PBS. The reaction was incubated at 37 °C for 0-143 h. The reaction was monitored over time by ^{1}H-NMR.

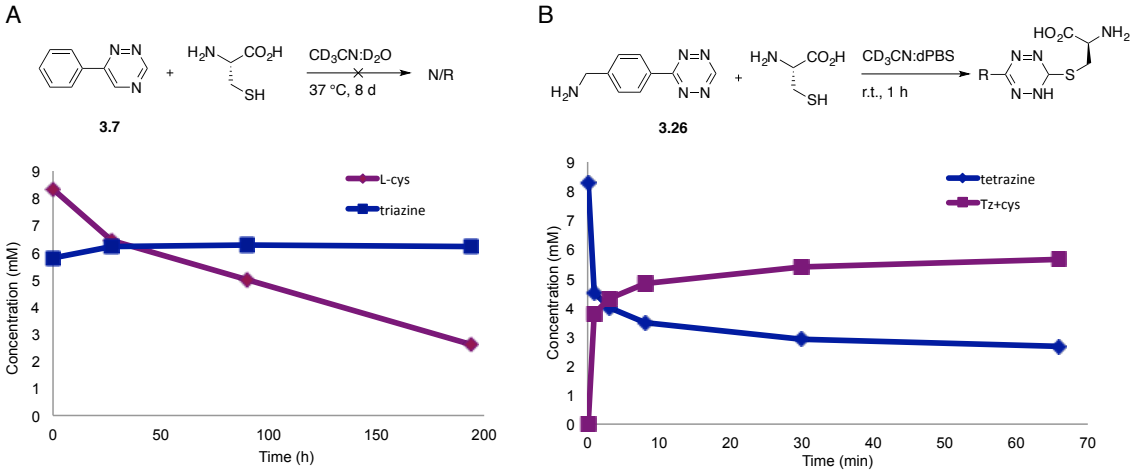

Figure 3-15. Stability profiles of model triazine and tetrazine probes. (A) Triazine **3.7** (0.1 mL of a 35 mM solution in CD_3CN) and cysteine (0.1 mL of a 50 mM solution in D_2O) were incubated at 37 °C for 8 d. Additionally, no cysteine reactivity was observed with a related triazine in solutions containing PBS (see Figure 3-22). (B) Tetrazine **3.26** (0.2 mL of a 25 mM solution in *d*-PBS) and cysteine (0.1 mL of a 50 mM solution in D_2O) were incubated at r.t. for 1 h.

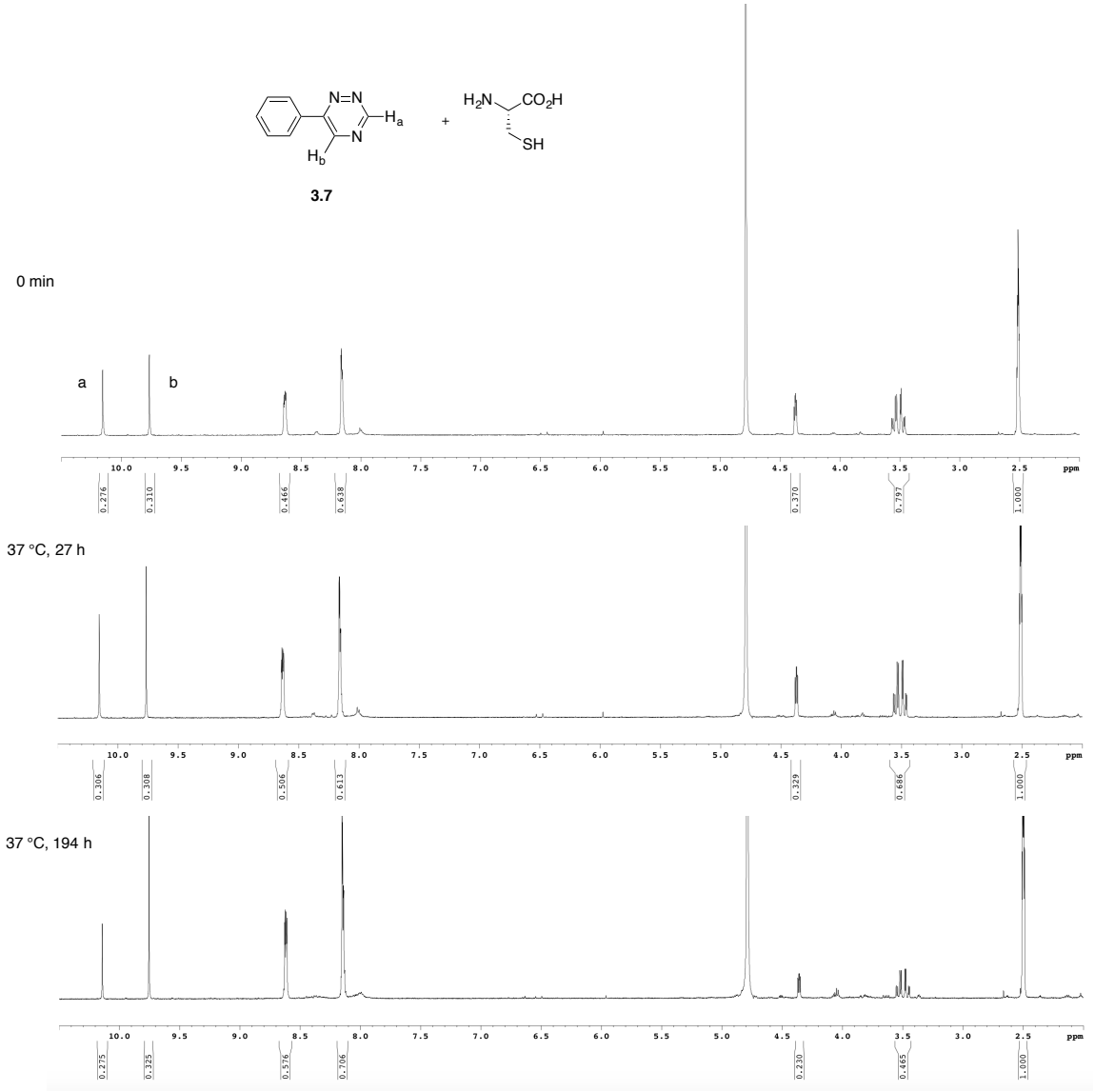

Figure 3-16. Triazine **3.7** is stable in the presence of cysteine. To a solution of triazine **3.7** (0.1 mL of a 35 mM solution in CD_3CN) was added L-cys (0.1 mL of a 50 mM solution in D_2O). The reaction was further diluted with 1:1 CD_3CN:D_2O to a final volume of 0.6 mL. The reaction was incubated at 37 °C and monitored over time by ^{1}H-NMR.

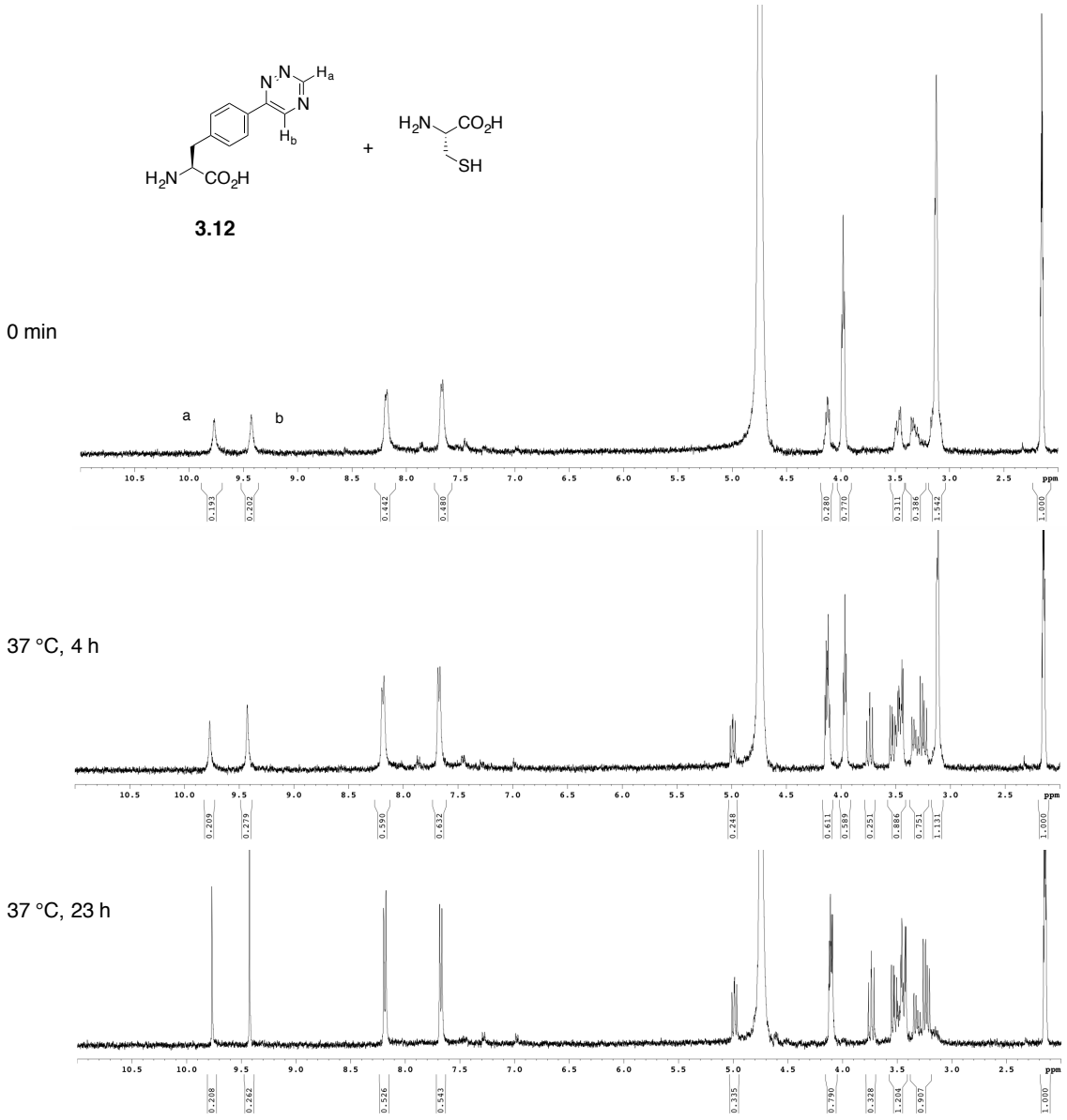

Figure 3-17. Triazine **3.12** is stable in the presence of cysteine. To a solution of triazine **3.12** (0.3 mL of a 4.2 mM solution in D_2O) was added L-cysteine (96 μL of a 50 mM solution in *d*-PBS). The reaction was further diluted with 1:1 CD_3CN:*d*-PBS to a final volume of 0.6 mL. The reaction was incubated at 37 °C and monitored over time by ^{1}H-NMR.

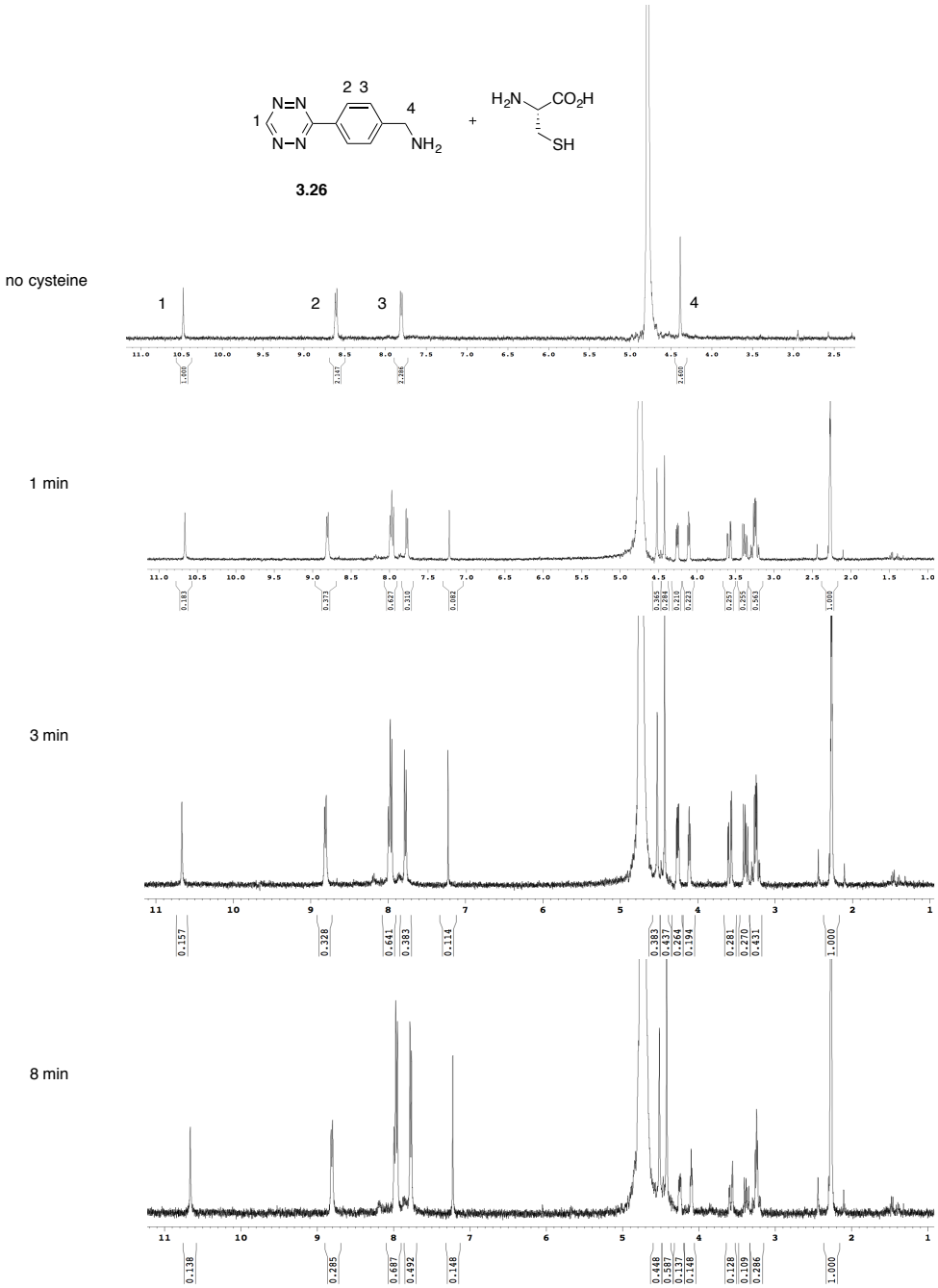

Figure 3-18. Monosubstituted tetrazine **3.26** reacts with cysteine. To a solution of tetrazine **3.26** (0.2 mL of a 25 mM solution in *d*-PBS) was added L-cysteine (0.1 mL of a 50 mM solution in D_2O), along with additional D_2O (0.1 mL) and CD_3CN (0.2 mL) to a final volume of 0.6 mL. The reaction was monitored over time by ^{1}H-NMR.

3.4 Incorporation of a triazine non-canonical amino acid into recombinant protein

The remarkable stability of the triazine scaffold suggested immediate application in environs that have been difficult to access with bioorthogonal reagents, including recombinant protein production in intracellular environments. Disubstituted tetrazines and cyclopropenes have been previously incorporated into recombinant proteins and tagged with TCO or tetrazine probes, respectively [9,43]. However, monosubstituted tetrazines have been more difficult to incorporate directly into proteins, due to the length of time required for protein production and the instability of the scaffolds [19,43]. Monosubstituted triazines offer unique advantages in terms of their size and stability.

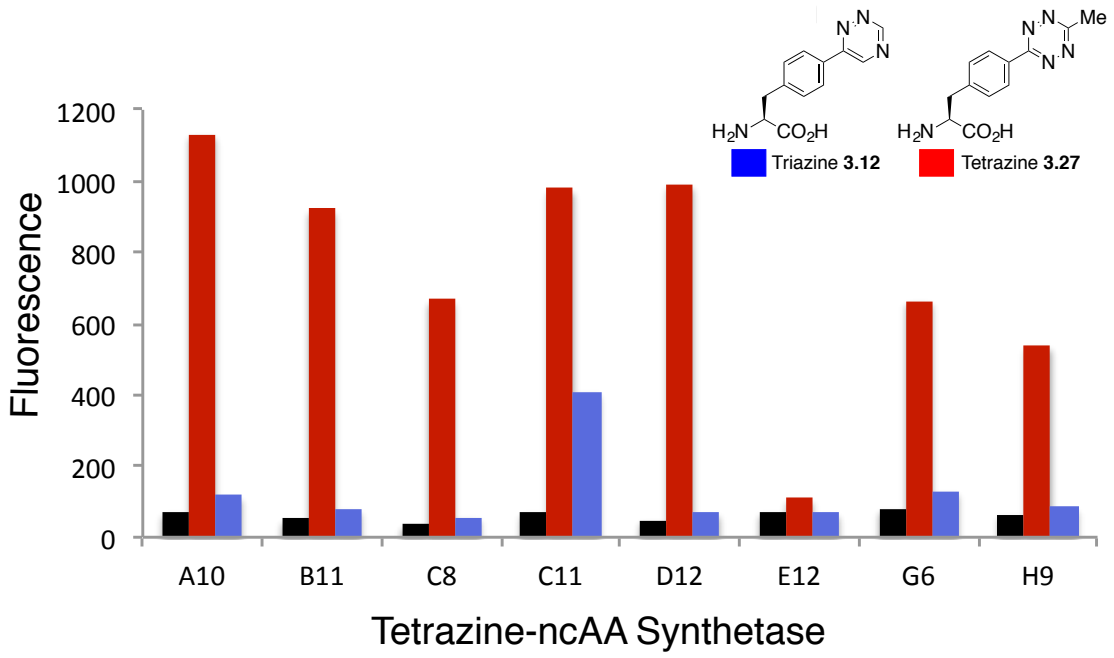

Figure 3-19. ncAA-GFP Expression. Fluorescence measurements of seven synthetases with GFP ncAA reporter. Blue bars represents colonies induced in media containing 1 mM triazine **3.12**, red bars represent 1 mM tetrazine **3.27**, while black represents colonies induced in the absence of ncAA.

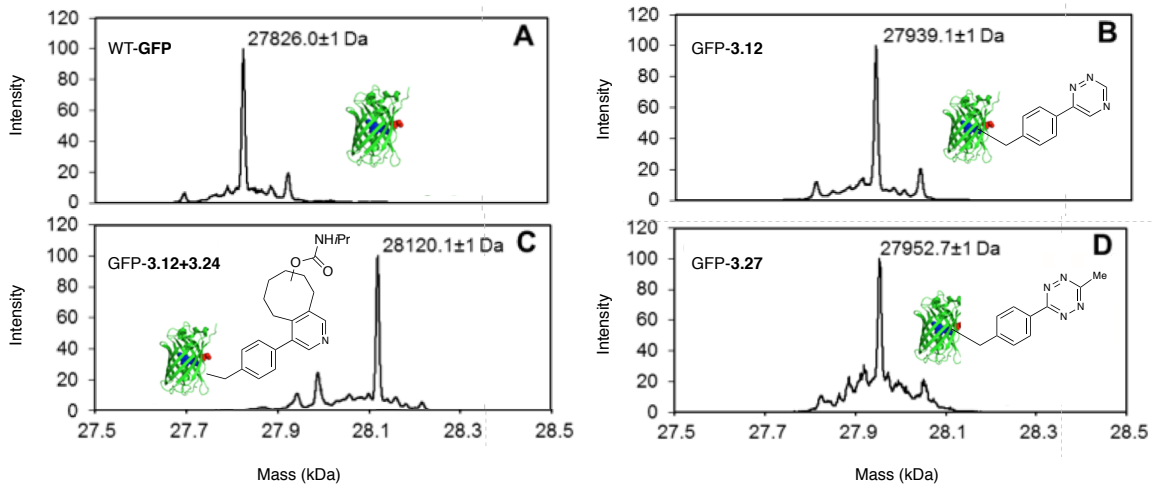

Figure 3-20. ESI-MS of amber codon interrupted GFP. (A) ESI-MS of WT GFP conforms to the expected mass, showing a single major peak at 27826.0±1 Da (expected mass 27827.3). (B) ESI-MS of GFP-**3.12** shows a single major peak at 27939.1±1 Da (expected mass 27939.4 Da). (C) ESI-MS of GFP-**3.12**+**3.24** demonstrates a mass of 28120.1±1 Da (expected mass 28120.7 Da). The mass difference (181.0 Da) between GFP-**3.12** and GFP-**3.12**+**3.24** is consistent with the expected mass increase (181.3 Da) through addition of TCO **3.24**. (D) ESI-MS of GFP-**3.27** shows a mass of 27952.7±1 Da and conforms to the expected mass of 27954.5 Da. Each sample showed a small secondary peak at -131 Da indicating cleavage of N-terminal methionines.

To demonstrate that monosubstituted triazines are compatible with protein labeling and sufficiently stable for genetic code expansion, we synthesized triazine amino acid **3.12** (Scheme 3-1). We screened a panel of seven *Methanocaldococcus jannaschii* tyrosyl tRNA synthetase (RS)/$tRNA_{CUA}$ pairs for permissivity toward **3.12**, while maintaining fidelity against canonical AAs (Figure 3-25) [43,44]. The M. *jannaschii* (RS)/$tRNA_{CUA}$ pairs were previously evolved to incorporate noncanonical amino acids (ncAAs) of similar structure (**3.27**, Figure 3-26) in response to an amber codon [45]. One of the seven RS/$tRNA_{CUA}$ pairs efficiently incorporated **3.12** in response to an amber codon- disrupted GFP gene, resulting in expression of 18.8 mg/L of GFP-**3.12** in the presence of **3.12** (Figure 3-27, lane 3).

To verify that **3.12** is stable in complex media and can be incorporated into recombinant proteins, we compared the masses of GFP-**3.12** to GFP-wt using ESI-Q mass analysis. Native GFP-wt has a mass of 27826.0 ± 1 Da and GFP-**3.12** exhibited the expected increase to 27939.1 ± 1 Da, verifying that **3.12** is incorporated at a single site (Figures 3-26 and 3-27). To determine whether the triazine/TCO ligation is also quantitative on proteins, pure GFP-**3.12** (10 μM) was incubated with TCO **3.24** (1 mM) in PBS (pH 7.0). ESI-Q mass analysis confirmed quantitative conversion of GFP-**3.12** to GFP-**3.12**+**3.24** (expected 28120.7 Da; observed 28120.1 ± 1 Da, Figure 3C). These results demonstrate that triazines are stable in cells and can be incorporated into proteins efficiently and with high fidelity using genetic code expansion. Furthermore, the triazine/TCO ligation is suitable for site-specific protein labeling applications.

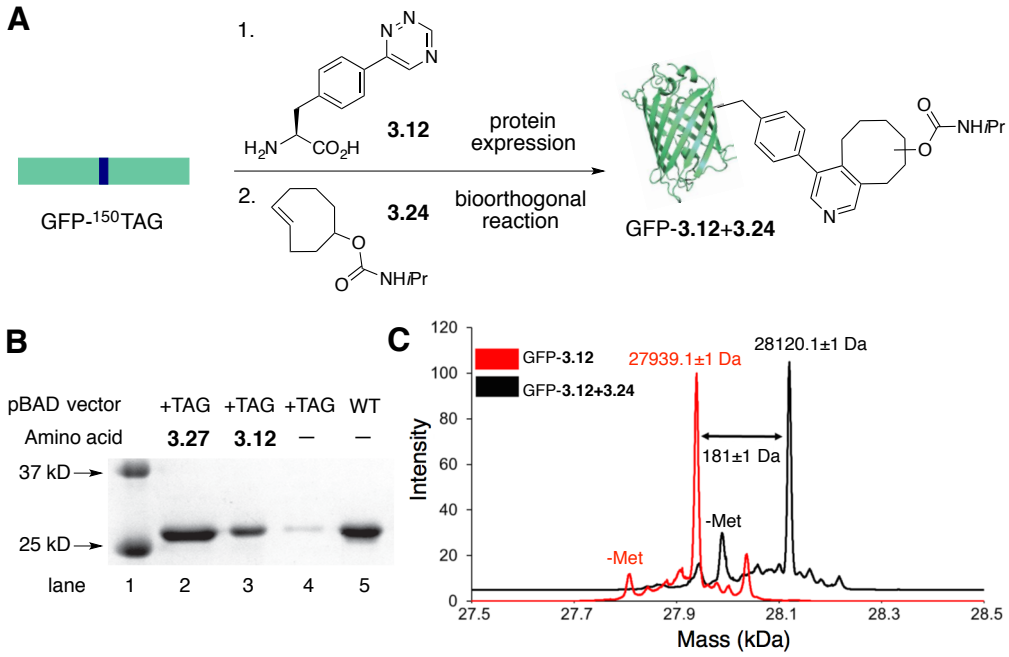

Figure 3-21. Triazines are suitable for recombinant protein production. (A) Genetic incorporation of **3.12** into proteins and reaction with TCO (B) SDS-PAGE analysis of site-specific incorporation in response to amber codon 150 in GFP. (C) MS analysis of GFP-**3.12** shows a single major peak at 27939.1±1 Da. Reaction of GFP-**3.12** with TCO **3.24** shows a single major peak at 28120.1±1 Da, consistent with the expected mass increase from selective reaction with TCO.

3.5 Conclusions and future work

In summary, we identified 1,2,4-triazines as a new class of bioorthogonal reagents. These scaffolds are remarkably stable in aqueous buffers, in the presence of biological nucleophiles, and in cells. Triazines can be easily assembled and decorated with diverse functional groups to tune reactivities. Triazines also react efficiently and selectively with TCO. These features render triazines suitable for a variety of intracellular applications, and we showed that a triazine amino

acid can be efficiently incorporated into recombinant proteins and labeled site-specifically with TCO. Triazines are also compatible with other strained alkenes and will enable different types of IED-DA reactions to be performed in tandem in cellular environments.

3.6 Materials and methods

3.6a Computational studies

Calculations were performed with Gaussian 09 [31]. The geometry optimization of all the minima and transition states involved was carried out at the M06-2X level of theory [32,33] with the 6-31G(d) basis set [46]. The vibrational frequencies were computed at the same level to check whether each optimized structure was an energy minimum or a transition state and to evaluate its zero-point vibration energy (ZPVE) and thermal corrections at 298 K. A quasiharmonic correction was applied during the entropy calculation by setting all positive frequencies that were less than 100 cm^{-1} to 100 cm^{-1} [47]. The single-point energies and solvent effects in water were computed at the M06-2X/6-311+G(d,p) level using the gas-phase optimized structures at the M06-2X/6-31G(d) level. Solvation energies were evaluated by a self-consistent reaction field (SCRF) using the CPCM model [48], where UFF radii were used. The frontier molecular orbitals (FMOs) and their energies were computed at the HF/6-311+G(d,p) level using the M06-2X/6-31G(d) geometries.

3.6b Rate studies

The reactions between triazines and strained alkenes were monitored by ^{1}H-NMR. All runs were conducted at least three times. For *trans*-cyclooctene (TCO)-triazine reactions, 0.3 mL

of a 20 mM solution of TCO in *d*-PBS was added to a solution of the appropriate triazine in CD_3CN (0.12-0.24 mL), then diluted to a final volume of 0.6 mL. The final concentrations of all reactants were 5-10 mM. For cyclopropene-triazine reactions, 0.3 mL of a 20 mM solution of cyclopropene in CD_3CN: D_2O (1:1) was added to a solution of triazine in CD_3CN (0.12 mL of a 50 mM solution or 0.24 mL of a 25 mM solution), and diluted with CD_3CN to a final volume of 0.6 mL. For norbornene-triazine reactions, 0.12 mL of a 40 mM of norbornene solution in CD_3CN:*d*-PBS (1:1) was added to a solution of triazine in CD_3CN (0.12 mL of a 50 mM solution or 0.24 mL of a 25 mM solution), and diluted with CD_3CN:*d*-PBS (1:1) to a final volume of 0.6-7.2 mL. Representative spectra for each reaction are shown in the accompanying figures.

3.6c Stability studies

The stability studies for triazines in PBS or in the presence of cysteine were monitored by ^{1}H-NMR. For stability studies in PBS, each triazine stock solution (0.2 mL of a 25-50 mM solution in CD_3CN) was diluted with *d*-PBS to a final volume of 0.6 mL. For stability studies with cysteine, each triazine stock solution (0.12-0.24 mL of a 25-50 mM solution in CD_3CN) was added to a solution of cysteine (0.1 mL of a 50 mM solution in *d*-PBS or D_2O) and diluted to a volume of 0.6 mL. The samples were incubated at r.t. or 37 °C for 0-150 h. Representative spectra for each reaction are shown in the accompanying figures.

3.6d Permissivity screening of selected synthetases for triazine-ncAA

A *pALS* plasmid containing TAG 150-interrupted superfolder GFP (sfGFP) under an AraBAD promoter and an orthogonalized copy of the *Methanocaldococcus jannaschii* tyrosine $tRNA_{CUA}$ under an lpp promoter, was transformed into DH10b cells with a *pBK* plasmid

containing one of seven *M. jannaschii* aminoacyl tyrosyl-tRNA synthetases selected to incorporate tetrazine **3.27**. Colonies of the transformed cells were picked and grown in 2XYT media containing kanamycin (50 μg/mL) and tetracycline (25 μg/mL) for 24 h before adding glycerol (18% v/v) and storing at -80 °C. Cell stocks were used to inoculate 5 mL Non-Inducing Media (NIM) containing kanamycin (50 μg/mL) and tetracycline (25 μg/mL). After 24 h of growth, 50 μL NIM was used to inoculate 5 mL Auto-Inducing Media (AIM) containing **3.12** (1 mM), kanamycin (50 μg/mL), and tetracycline (25 μg/mL) for efficiency measurements and the same AIM without **3.12** for fidelity measurements. Fluorescence readings of the cultures were obtained at 36 h using a Turner Biosystems PicoFluor fluorimeter. Fluorescence of the media indicated that of the seven synthetases screened, only the C11 synthetase effectively incorporated **3.12**.

3.6e Characterization of GFP-3.12

Pure proteins were diluted to 10 μM and reacted for 16 h with TCO **3.24** (1 mM in 300 mM NaCl, 50 mM NaH_2PO_4, pH 7.0). GFP-wt, GFP-**3.12**, and GFP-**3.12**+**3.24** were desalted using Vivaspin spin concentrators (500 μL, 10kDa Molecular weight cut off) into ammonium acetate buffer (25 mM, pH 7.0). The concentrations of the resulting solutions were measured using a Bradford assay. The proteins were diluted to 10 μM and were analyzed using an FT LTQ mass spectrometer and Millipore C_4 zip tips at the Oregon State University mass spectrometry facility.

3.6f SDS-PAGE of GFP-3.12 incorporation

Purified GFP-**3.12**, GFP-**3.27**, WT GFP, and TAG-interrupted GFP (GFP-^{150}TAG)

expressed in the presence of the C11 synthetase, but without **3.12** present, were diluted to equal volumes. Samples were mixed with 2X Laemmli Buffer and heated at 95 °C for 15 min. The samples were then analyzed by SDS-PAGE (15 % gel, 200 V, 60 minutes).

3.6g General synthetic procedures

Compounds **3.22** [8], **3.26** [18], and **3.27** [45] were synthesized as previously reported. All other reagents were obtained from commercial sources and used without further purification. Reactions were run under an inert atmosphere of nitrogen, unless otherwise indicated. Tetrahydrofuran (THF), diethyl ether (Et_2O), dichloromethane (CH_2Cl_2), and methanol (CH_3OH) were degassed with argon and run through two 4 x 36 inch columns of anhydrous neutral A-2 (8 x 14 mesh; LaRoche Chemicals; activated under a flow of argon at 350 °C for 12 h). Thin-layer chromatography was performed using Silica Gel 60 F_{254}-coated glass plates (0.25 mm thickness), and visualization was performed with $KMnO_4$ stain and/or UV irradiation. Chromatography was accomplished with 60 Å (240-400 mesh) silica gel, commercially available from Sorbent Technologies. HPLC purifications were performed on a Varian ProStar equipped with 325 Dual Wavelength UV-Vis Detector. Analytical runs were performed using an Agilent C18 Scalar column (4.6 x 150 mm, 5 μm) with a 1 mL/min flow rate. Semi-preparative runs were performed using an Agilent Prep-C18 Scalar column (9.4 x 150 mm, 5 μm) with a 5 mL/min flow rate. NMR spectra were collected on a Bruker DRX-400 (400 MHz ^{1}H, 100 MHz ^{13}C, 376.5 MHz ^{19}F) or CRYO-500 (500 MHz ^{1}H, 125.7 MHz ^{13}C) instrument. All spectra were collected at 298 K. High-resolution mass spectrometry was performed by the University of California, Irvine Mass Spectrometry Center.

3.6h Synthetic procedures

3-Amino-1,2,4-triazine (3.1): To a solution of aminoguanidine (0.500 g, 4.52 mmol) in H_2O (20.0 mL) was added $NaHCO_3$ (0.417 g, 4.97 mmol) at 0 °C, followed by a solution of 8.8 M glyoxal in H_2O (0.570 mL, 5.01 mmol). The reaction was stirred overnight, then extracted with EtOAc (3 x 100 mL). The organic layers were combined and dried over $MgSO_4$, then filtered and concentrated *in vacuo* to provide **3.1** (0.25 g, 59%) as a light-yellow solid. ^{1}H NMR (400 MHz, $CDCl_3$): δ 8.70 (d, J = 2.0 Hz, 2H), 8.22 (d, J = 2.0 Hz, 1H), 5.41 (bs, 2H). Spectral data were consistent with literature values [49].

3-Amino-6-bromo-1,2,4-triazine (3.2): To a solution of **3.1** (53.0 mg, 0.552 mmol) in H_2O (6 mL) was added bromine (70.0 µL, 1.38 mmol) at 0 °C. The mixture was stirred for 6 h, then the pH was adjusted to ~10 by addition of sat. $NaHCO_3$. The crude solution was then extracted with EtOAc (3 x 40 mL). The organic layers were combined and dried over $MgSO_4$, then filtered and concentrated *in vacuo.* The crude product was purified by flash column chromatography (eluting with 10-30% EtOAc in CH_2Cl_2) to provide **3.2** (66 mg, 68%) as a yellow solid. ^{1}H NMR (500 MHz, $(CD_3)_2SO$): δ 8.40 (s, 1H), 7.48 (bs, 2 H). ^{13}C NMR (125 MHz, $(CD_3)_2SO$) δ 162.8, 153.0, 135.9. HRMS (ESI) *m/z* calcd for $C_3H_2BrN_4$ $[M-H]^-$ 172.9463, found 172.9467. Spectral data were consistent with literature values [50].

6-Bromo-1,2,4-triazine (3.3): To a pressure tube was added a solution of triazine **3.2** (120 mg, 0.685) in THF (5 mL) and isopentyl nitrite (0.280 mL, 2.08 mmol). The tube was flushed with nitrogen, sealed, and heated at 65 °C for 5 h. The crude product was gently concentrated *in vacuo* and purified by flash column chromatography (eluting with 10% EtOAc in CH_2Cl_2) to provide

3.3 as a volatile yellow oil. This material was immediately carried on to the next step.

(*E*)-Cyclooct-4-en-1-yl isopropylcarbamate (3.24): To a round-bottom flask containing a solution of commercially available TCO-NHS ester (12.0 mg, 0.0449 mmol) in 2.0 mL CH_2Cl_2 was added excess isopropylamine (0.10 mL, 1.2 mmol). The solution was gently stirred for 5 h. The crude product was concentrated *in vacuo* and purified by flash column chromatography (eluting with 0-10% EtOAc in CH_2Cl_2) to provide **3.24** (9.0 mg, 95%) as a white solid. ^{1}H NMR (400 MHz, $CDCl_3$): δ 5.53 (m, 2H), 4.35 (m, 2H), 3.78 (m, 1H), 2.35 (m, 3H), 1.67-2.04 (m, 6H), 1.51 (m, 1H), 1.13 (d, J = 6.4 Hz, 6H). ^{13}C NMR (125 MHz, $CDCl_3$) δ 155.5, 134.9, 133.1, 80.3, 42.9, 41.2, 38.7, 34.4, 32.6, 31.0, 23.2. HRMS (ESI) *m/z* calcd for $C_{12}H_{21}NO_2Na$ $[M+Na]^+$ 234.1470, found 234.1463.

4-(4-Nitrophenyl)-5,6,7,8,9,10-hexahydrocycloocta[*c*]pyridin-8-yl isopropylcarbamate (3.25): To a vial containing TCO **3.24** (8.00 mg, 0.0379 mmol) was added a solution of triazine **3.4** (8.00 mg, 0.0396 mmol) in 2 mL MeCN. The vial was placed in a 37 °C incubator for 2 d. The solution color changed from light yellow to red, then back to yellow over the course of the reaction. The crude product was concentrated *in vacuo* and purified by flash column chromatography (eluting with 10-20% EtOAc in CH_2Cl_2) to provide aromatized cycloadduct **3.25** as a mixture of two-regioisomers (12.0 mg, 83%) as a light-yellow oil. ^{1}H NMR (500 MHz, $CDCl_3$): δ 8.45 (s, 1H), 8.40 (s, 1H), 8.25-8.32 (m, 6H), 7.51 (d, J = 7.5 Hz, 2H), 7.45 (d, J = 8.4 Hz, 2H), 4.30-4.52 (m, 4H), 3.74 (bs, 2H), 2.64-2.95 (m, 8H), 1.53-2.11 (m, 12H), 1.12 (m, 12H). ^{13}C NMR (125 MHz, $CDCl_3$) δ 155.2, 155.0, 150.6, 150.4, 148.1, 147.9, 147.5, 146.2, 145.8, 145.3, 145.3, 136.4, 136.3, 135.5, 130.6, 130.5, 123.6, 74.4, 74.1, 43.1, 37.1, 35.6, 34.0, 33.1, 30.1, 29.7, 27.9, 27.7, 26.4, 26.3, 24.4, 23.1. HRMS (ESI) *m/z* calcd for $C_{21}H_{25}N_3O_4Na$

[M+Na]$^+$ 406.1743, found 406.1742.

General procedure to access mono-substituted triazines (Scheme 1, top):

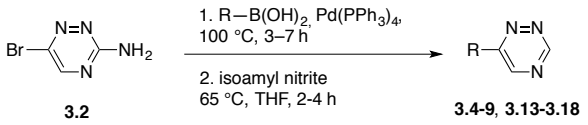

6-(4-Nitrophenyl)-1,2,4-triazine (3.4): To a pressure tube was added (4-nitrophenyl)boronic acid (55.0 mg, 0.329 mmol), $Pd(PPh_3)_4$ (38.0 mg, 0.0329 mmol), a solution of **3.2** (116 mg, 0.663 mmol) in 6.5 mL of 4:2.5 tol:EtOH, and Cs_2CO_3 (91.0 mg, 0.279 mmol) in 1 mL H_2O. The tube was flushed with nitrogen, sealed, and heated at 100 °C for 7 h. The reaction was then diluted with 40 mL H_2O and extracted with EtOAc (2 x 50 mL). The organic layers were combined and dried over $MgSO_4$, then filtered and concentrated *in vacuo.* The crude product was purified by flash column chromatography (eluting with 0-30% EtOAc in CH_2Cl_2). The isolated material (81.0 mg, 0.373 mmol) was dissolved in THF (9 mL), then isopentyl nitrite (0.150 mL, 1.11 mmol) was added. The reaction was heated at 65 °C for 3 h, using a reflux condenser. The crude product was concentrated *in vacuo*, then purified by flash column chromatography (eluting with 10-20% EtOAc in CH_2Cl_2) to provide **3.4** (24 mg, 36% over two steps) as a yellow solid. ^{1}H NMR (400 MHz, CD_3CN): δ 9.70 (s, 1H), 9.23 (s, 1H), 8.41 (d, J = 9.2 Hz, 2H), 8.35 (d, J = 9.0 Hz, 2H). ^{13}C NMR (125 MHz, $CDCl_3$) δ 156.9, 156.1, 149.6, 146.9, 138.9, 128.0, 124.7. HRMS (ESI) *m*/*z* calcd for $C_9H_7N_4O_2$ [M+H]$^+$ 203.0569, found 203.0575.

4-(1,2,4-Triazin-6-yl)benzonitrile (3.5): To a pressure tube was added (4-cyanophenyl)boronic acid (78.0 mg, 0.531 mmol), $Pd(PPh_3)_4$ (61.0 mg, 0.0528 mmol), a solution of **3.2** (93.0 mg,

0.531 mmol) in 5.5 mL of 4.5:1 tol:EtOH, and K_2CO_3 (146 mg, 1.06 mmol) in 1.4 mL H_2O. The tube was flushed with nitrogen, sealed, and heated at 110 °C for 5 h. The reaction was then diluted with 40 mL H_2O and extracted with EtOAc (2 x 60 mL). The organic layers were combined and dried over $MgSO_4$, then filtered and concentrated *in vacuo.* The crude product was purified by flash column chromatography (eluting with 20-40% EtOAc in CH_2Cl_2). The isolated material (62.0 mg, 0.314 mmol) was dissolved in THF (4 mL), then isopentyl nitrite (80.0 μL, 0.595 mmol) was added and the reaction was heated at 65 °C for 3 h, using a reflux condenser. The crude product was concentrated *in vacuo*, then purified by flash column chromatography (eluting with 20% EtOAc in CH_2Cl_2) to provide **3.5** (25 mg, 26% over two steps) as a yellow solid. ^{1}H NMR (400 MHz, $CDCl_3$): δ 9.74 (s, 1H), 9.08 (s, 1H), 8.26 (d, J = 8.8 Hz, 2H), 7.89 (d, J = 8.7 Hz, 2H). ^{13}C NMR (125 MHz, $CDCl_3$) δ 156.8, 156.4, 146.8, 137.2, 133.2, 127.6, 118.1, 115.0 HRMS (ESI) *m/z* calcd for $C_{10}H_{10}N_5$ $[M+NH_4]^+$ 200.0936, found 200.0938.

6-(3-Chlorophenyl)-1,2,4-triazine (3.6): To a pressure tube was added (3-chlorophenyl)boronic acid (113 mg, 0.723 mmol), $Pd(PPh_3)_4$ (84.0 mg, 0.0727 mmol), a solution of **3.2** (127 mg, 0.726 mmol) in 7 mL of 4:3 tol:EtOH, and Cs_2CO_3 (200 mg, 0.613 mmol) in 1 mL H_2O. The tube was flushed with nitrogen, sealed, and heated at 100 °C for 3 h. The reaction was then diluted with 50 mL H_2O and extracted with EtOAc (2 x 60 mL). The organic layers were combined and dried over $MgSO_4$, then filtered and concentrated *in vacuo.* The crude product was purified by flash column chromatography (eluting with 20-40% EtOAc in CH_2Cl_2). The isolated material (127 mg, 0.615 mmol) was dissolved in THF (7 mL), then isopentyl nitrite (0.250 mL, 1.86 mmol) was added and the reaction was heated at 65 °C for 4 h, using a reflux condenser. The crude

product was concentrated *in vacuo*, then purified by flash column chromatography (eluting with 20% EtOAc in CH_2Cl_2) to provide **3.6** (62 mg, 45% over two steps) as a yellow solid. ^{1}H NMR (400 MHz, CD_3CN): δ 9.63 (s, 1H), 9.14 (s, 1H), 8.17 (m, 1H), 8.07 (dt, J = 6.8, 1.9 Hz, 1H), 7.53-7.62 (m, 2H) . ^{13}C NMR (125 MHz, CD_3CN) δ 156.7, 156.5, 147.6, 135.6, 134.8, 130.9, 130.8, 126.9, 125.5. HRMS (ESI) *m*/*z* calcd for $C_9H_6ClN_3Na$ $[M+Na]^+$ 214.0148, found 214.0157.

6-Phenyl-1,2,4-triazine (3.7): To a pressure tube was added phenylboronic acid (89.0 mg, 0.730 mmol), $Pd(PPh_3)_4$ (84.0 mg, 0.0727 mmol), a solution of **3.2** (128 mg, 0.731 mmol) in 7 mL of 4:3 tol:EtOH, and a solution of Cs_2CO_3 (202 mg, 0.620 mmol) in 1 mL of H_2O. The tube was flushed with nitrogen, sealed, and heated at 100 °C for 4 h. The reaction was then diluted with 40 mL H_2O and extracted with EtOAc (2 x 60 mL). The organic layers were combined and dried over $MgSO_4$, then filtered and concentrated *in vacuo.* The crude product was purified by flash column chromatography (eluting with 10-30% EtOAc in CH_2Cl_2). The isolated material (122 mg, 0.708 mmol) was dissolved in THF (7 mL), then isopentyl nitrite (0.280 mL, 2.08 mmol) was added. The reaction was heated at 65 °C for 3 h, using a reflux condenser. The crude product was concentrated *in vacuo,* then purified by flash column chromatography (eluting with 20% EtOAc in CH_2Cl_2) to provide **3.7** (57 mg, 50% over two steps) as a yellow solid. ^{1}H NMR (400 MHz, $CDCl_3$): δ 9.66 (s, 1H), 9.03 (s, 1 H), 8.11 (m, 2H), 7.58 (m, 3H). ^{13}C NMR (125 MHz, $CDCl_3$) δ 157.9, 156.2, 146.7, 133.1, 131.3, 129.5, 127.0. HRMS (ESI) *m*/*z* calcd for $C_9H_7N_3Na$ $[M+Na]^+$ 180.0538, found 180.0537.

6-(*p*-Tolyl)-1,2,4-triazine (3.8): To a pressure tube was added *p*-tolylboronic acid (97.0 mg,

0.713 mmol), $Pd(PPh_3)_4$ (82.0 mg, 0.0710 mmol), a solution of **3.2** (125 mg, 0.714 mmol) in 7 mL of 4:3 tol:EtOH, and Cs_2CO_3 (197 mg, 0.605 mmol) in 1 mL H_2O. The tube was flushed with nitrogen, sealed, and heated at 100 °C for 3 h. The reaction was then diluted with 40 mL H_2O and extracted with EtOAc (2 x 60 mL). The organic layers were combined and dried over $MgSO_4$, then filtered and concentrated *in vacuo.* The crude product was purified by flash column chromatography (eluting with 20-40% EtOAc in CH_2Cl_2). The isolated material (130 mg, 0.698 mmol) was dissolved in THF (10 mL), then isopentyl nitrite (0.280 mL, 2.08 mmol) was added. The reaction was heated at 65 °C for 3 h, using a reflux condenser. The crude product was concentrated *in vacuo*, then purified by flash column chromatography (eluting with 20% EtOAc in CH_2Cl_2) to provide **3.8** (49 mg, 40% over two steps) as a yellow solid. ^{1}H NMR (400 MHz, CD_3OD): δ 9.59 (s, 1H), 9.24 (s, 1H), 8.05 (d, J = 8.7 Hz, 2H), 7.40 (d, J = 8.4 Hz, 2H), 2.43 (s, 3H). ^{13}C NMR (125 MHz, CD_3OD) δ 157.8, 155.6, 147.6, 141.7, 130.3, 129.7, 126.7, 20.1. HRMS (ESI) *m/z* calcd for $C_{10}H_{10}N_3$ $[M+H]^+$ 172.0875, found 172.0868.

(*E*)-6-Styryl-1,2,4-triazine (3.9): To a pressure tube was added (*E*)-styrylboronic acid (176 mg, 1.19 mmol), $Pd(PPh_3)_4$ (92 mg, 0.080 mmol), a solution of **3.2** (139 mg, 0.794 mmol) in 5 mL of 4:3 tol:EtOH, and Cs_2CO_3 (388 mg, 1.19 mmol) in 1 mL H_2O. The tube was flushed with nitrogen, sealed, and heated at 100 °C for 6 h. The reaction was then quenched with 40 mL H_2O and extracted with EtOAc (2 x 50 mL). The organic layers were combined and dried over $MgSO_4$, then filtered and concentrated *in vacuo.* The crude product was purified by flash column chromatography (eluting with 20-40% EtOAc in CH_2Cl_2). The isolated material (114 mg, 0.575 mmol) was dissolved in THF (6 mL), then isopentyl nitrite (0.150 mL, 1.12 mmol) was added and the reaction was heated at 65 °C for 2 h, using a reflux condenser. The crude product was

concentrated *in vacuo*, then purified by flash column chromatography (eluting with 10% EtOAc in CH_2Cl_2) to provide **3.9** (24 mg, 16% over two steps) as a yellow solid. ^{1}H NMR (400 MHz, $CDCl_3$): δ 9.54 (s, 1H), 8.76 (s, 1 H), 7.86 (d, *J* = 16.5 Hz, 1H), 7.63 (m, 2H), 7.36-7.47 (m, 3H), 7.26 (d, *J* = 3.2 Hz, 1H). ^{13}C NMR (125 MHz, CD_3CN) δ 157.1, 155.6, 147.9, 136.6, 135.7, 129.6, 129.0, 127.6, 121.9. HRMS (ESI) *m*/*z* calcd for $C_{11}H_9N_3Na$ $[M+Na]^+$ 206.0694, found 206.0693.

6-(Thiophen-2-yl)-1,2,4-triazine (3.13): To a pressure tube was added thiophen-2-ylboronic acid (116 mg, 0.907 mmol), $Pd(PPh_3)_4$ (52.0 mg, 0.045 mmol), a solution of **3.2** (79.0 mg, 0.451 mmol) in 5 mL of 3:2 tol:EtOH, and Cs_2CO_3 (294 mg, 0.903 mmol) in 0.5 mL H_2O. The tube was flushed with nitrogen, sealed, and heated at 100 °C for 4 h. The reaction was then diluted with 50 mL H_2O and extracted with EtOAc (2 x 60 mL). The organic layers were combined and dried over $MgSO_4$, then filtered and concentrated *in vacuo.* The crude product was purified by flash column chromatography (eluting with 0-20% EtOAc in CH_2Cl_2). The isolated material (85.0 mg, 0.477 mmol) was dissolved in THF (6 mL), then isopentyl nitrite (0.200 mL, 1.49 mmol) was added and the reaction was heated at 65 °C for 4 h, using a reflux condenser. The crude produt was concentrated *in vacuo*, then purified by flash column chromatography (eluting with 0-10% EtOAc in CH_2Cl_2) to provide **3.13** (33 mg, 45% over two steps) as a light orange solid. ^{1}H NMR (400 MHz, $CDCl_3$): δ 9.54 (s, 1H), 8.95 (s, 1H), 7.80 (d, *J* = 3.5 Hz, 1H), 7.62 (d, *J* = 5.1 Hz, 1H), 7.23 (t, *J* = 4.4 Hz, 1H). ^{13}C NMR (125 MHz, $CDCl_3$) δ 155.8, 154.1, 145.3, 137.0, 130.9, 128.7, 127.6. HRMS (ESI) *m*/*z* calcd for $C_7H_6N_3S$ $[M+H]^+$ 164.0282, found 164.0282.

6-(4-Methoxyphenyl)-1,2,4-triazine (3.14): To a pressure tube was added (4-methoxyphenyl)boronic acid (78.0 mg, 0.513 mmol), $Pd(PPh_3)_4$ (59.0 mg, 0.051 mmol), a solution of **3.2** (90.0 mg, 0.514 mmol) in 7 mL of 4:3 tol:EtOH, and Cs_2CO_3 (142 mg, 0.436 mmol) in 1.0 mL H_2O. The tube was flushed with nitrogen, sealed, and heated at 100 °C for 4 h. The reaction was then diluted with 50 mL H_2O and extracted with EtOAc (2 x 60 mL). The organic layers were combined and dried over $MgSO_4$, then filtered and concentrated *in vacuo.* The crude product was purified by flash column chromatography (eluting with 40% EtOAc in CH_2Cl_2). The isolated material (102 mg, 0.504 mmol) was dissolved in THF (6 mL), then isopentyl nitrite (0.200 mL, 1.49 mmol) was added and the reaction was heated at 65 °C for 3 h, using a reflux condenser. The crude product was concentrated *in vacuo*, then purified by flash column chromatography (eluting with 0-20% EtOAc in CH_2Cl_2) to provide **3.14** (37 mg, 38% over two steps) as a yellow solid. ^{1}H NMR (500 MHz, $CDCl_3$): δ 9.57 (s, 1H), 8.98 (s, 1H), 8.08 (d, J = 8.8 Hz, 2H), 7.08 (d, J = 8.8 Hz, 2H), 3.90 (s, 3H). ^{13}C NMR (125 MHz, $CDCl_3$) δ 162.3, 157.4, 155.6, 146.1, 128.5, 125.4, 114.9, 55.6. HRMS (ESI) *m/z* calcd for $C_{10}H_{10}N_3O$ $[M+H]^+$ 188.0824, found 188.0827.

6-(Naphthalen-2-yl)-1,2,4-triazine (3.15): To a pressure tube was added naphthalen-2-ylboronic acid **2** (149 mg, 0.866 mmol), $Pd(PPh_3)_4$ (50.0 mg, 0.0433 mmol), a solution of **3.2** (76.0 mg, 0.434 mmol) in 5 mL of 3:2 tol:EtOH, and Cs_2CO_3 (283 mg, 0.869 mmol) in 0.5 mL H_2O. The tube was flushed with nitrogen, sealed, and heated at 100 °C for 4 h. The reaction was then diluted with 40 mL H_2O and extracted with EtOAc (2 x 50 mL). The organic layers were combined and dried over $MgSO_4$, then filtered and concentrated *in vacuo.* The crude product was purified by flash column chromatography (eluting with 0-30% EtOAc in CH_2Cl_2). The isolated

material (88.0 mg, 0.398 mmol) was dissolved in THF (5 mL), then isopentyl nitrite (0.160 mL, 1.19 mmol) was added and the reaction was heated with a reflux condenser at 65 °C for 4 h. The crude product was concentrated *in vacuo*, then purified by flash column chromatography (eluting with 0-10% EtOAc in CH_2Cl_2) to provide **3.15** (29 mg, 32% over two steps) as a yellow solid. ^{1}H NMR (400 MHz, CD_3CN): δ 9.63 (s, 1H), 9.29 (s, 1 H), 8.69 (s, 1H), 8.69 (dd, J = 9.0, 1.7 Hz, 1H), 7.59-8.11 (m, 3H), 7.60-7.65 (m, 2H). ^{13}C NMR (125 MHz, CD_3CN) δ 157.8, 156.1, 147.7, 134.4, 133.2, 130.9, 129.1, 128.9, 128.9, 127.8, 127.3, 127.1, 123.6. HRMS (ESI) *m/z* calcd for $C_{13}H_{10}N_3$ $[M+H]^+$ 208.0875, found 208.0868.

(3,5-Dimethylisoxazol-4-yl)boronic acid (3.16): To a pressure tube was added (3,5-dimethylisoxazol-4-yl)boronic acid (101 mg, 0.717 mmol), $Pd(PPh_3)_4$ (55.0 mg, 0.0480 mmol), a solution of **3.2** (84.0 mg, 0.480 mmol) in 5 mL of 3:2 tol:EtOH, and Cs_2CO_3 (172 mg, 0.528 mmol) in 0.5 mL H_2O. The tube was flushed with nitrogen, sealed, and heated at 100 °C for 4 h. The reaction was then diluted with 40 mL H_2O and extracted with EtOAc (2 x 50 mL). The organic layers were combined and dried over $MgSO_4$, then filtered and concentrated *in vacuo.* The crude product was purified by flash column chromatography (eluting with 40% EtOAc in CH_2Cl_2). The isolated material (103 mg, 0.538 mmol) was dissolved in THF (7 mL), then isopentyl nitrite (0.220 mL, 1.64 mmol) was added and the reaction was heated at 65 °C for 4 h, using a reflux condenser. The crude product was concentrated *in vacuo*, then purified by flash column chromatography (eluting with 0-30% EtOAc in CH_2Cl_2) to provide **3.16** (27 mg, 32% over two steps) as a yellow solid. ^{1}H NMR (500 MHz, $CDCl_3$): δ 9.63 (s, 1H), 8.72 (s, 1H), 2.70 (s, 3H), 2.52 (s, 3H). ^{13}C NMR (125 MHz, $CDCl_3$) δ 169.9, 158.4, 155.5, 153.3, 147.3, 110.6, 13.1, 11.9. HRMS (ESI) *m/z* calcd for $C_8H_9N_4O$ $[M+H]^+$ 177.0776, found 177.0770.

Methyl-4-(1,2,4-triazin-6-yl)benzoate (3.17): To a pressure tube was added (4-(methoxycarbonyl)phenyl)boronic acid (98.0 mg, 0.545 mmol), $Pd(PPh_3)_4$ (63.0 mg, 0.0545 mmol), a solution of **3.2** (96.0 mg, 0.549 mmol) in 7 mL of 5:2 tol:EtOH, and K_2CO_3 (151 mg, 1.09 mmol) in 1 mL H_2O. The tube was flushed with nitrogen, sealed, and heated at 110 °C for 4 h. The reaction was then diluted with 40 mL H_2O and extracted with EtOAc (2 x 60 mL). The organic layers were combined and dried over $MgSO_4$, then filtered and concentrated *in vacuo.* The crude product was purified by flash column chromatography (eluting with 30-40% EtOAc in CH_2Cl_2). The isolated material (88.0 mg, 0.382 mmol) was dissolved in THF (7 mL), then isopentyl nitrite (0.150 mL, 1.12 mmol) was added and the reaction was heated at 65 °C for 3 h, using a reflux condenser. The crude product was concentrated *in vacuo*, then purified by flash column chromatography (eluting with 20% EtOAc in CH_2Cl_2) to provide **3.17** (29 mg, 25% over two steps) as a yellow solid. ^{1}H NMR (400 MHz, $CDCl_3$): δ 9.71 (s, 1H), 9.09 (s, 1H), 8.25 (d, J = 8.4 Hz, 2H), 8.20 (d, J = 8.6 Hz, 2H), 3.99 (s, 3H). ^{13}C NMR (125 MHz, $CDCl_3$) δ 166.4, 157.1, 156.6, 146.9, 137.1, 132.6, 130.6, 127.0, 126.9, 52.5. HRMS (ESI) *m*/*z* calcd for $C_{11}H_{13}N_4O_2$ $[M+NH_4]^+$ 233.1039, found 233.1038.

6-(3-Nitrophenyl)-1,2,4-triazine (3.18): To a pressure tube was added (3-nitrophenyl)boronic acid (100 mg, 0.599 mmol), $Pd(PPh_3)_4$ (63.0 mg, 0.0545 mmol), a solution of **3.2** (95.0 mg, 0.543 mmol) in 7 mL of 4:3 tol:EtOH, and Cs_2CO_3 (150 mg, 0.460 mmol) in 1 mL H_2O. The tube was flushed with nitrogen, sealed, and heated at 100 °C for 5 h. The reaction was then diluted with 50 mL H_2O and extracted with EtOAc (2 x 60 mL). The organic layers were combined and dried over $MgSO_4$, then filtered and concentrated *in vacuo.* The crude product was

purified by flash column chromatography (eluting with 10-40% EtOAc in CH_2Cl_2). The isolated material (92.0 mg, 0.423 mmol) was dissolved in THF (8 mL), then isopentyl nitrite (0.170 mL, 1.27 mmol) was added and the reaction was heated at 65 °C for 4 h, using a reflux condenser. The crude product was concentrated *in vacuo*, then purified by flash column chromatography (eluting with 20% EtOAc in CH_2Cl_2) to provide **3.18** (38 mg, 34% over two steps) as a yellow solid. ^{1}H NMR (400 MHz, CD_3CN): δ 9.69 (s, 1H), 9.25 (s, 1H), 8.95 (m, 1H), 8.52 (m,1H), 8.40 (m, 1H), 7.86 (t, J = 7.9 Hz, 1H). ^{13}C NMR (125 MHz, CD_3CN) δ 156.8, 156.2, 149.1, 147.8, 135.3, 133.0, 130.7, 125.4, 121.8. HRMS (ESI) *m/z* calcd for $C_9H_5N_4O_2$ $[M-H]^-$ 201.0412, found 201.0419.

General procedure to access mono-substituted triazines (Scheme 1, bottom):

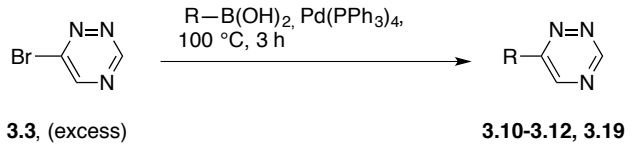

4-(1,2,4-Triazin-6-yl)aniline (3.10): To a pressure tube was added 4-aminophenylboronic acid pinacol ester (42.0 mg, 0.192 mmol), $Pd(PPh_3)_4$ (22.0 mg, 0.0190 mmol), a solution of **3.3** (91.0 mg, 0.569 mmol) in 5 mL of 3:2 tol:EtOH, and Cs_2CO_3 (185 mg, 0.568 mmol) in 1 mL H_2O. The tube was flushed with nitrogen, sealed, and heated at 100 °C for 3 h. The reaction was then diluted with 40 mL H_2O and extracted with EtOAc (2 x 60 mL). The organic layers were combined and dried over $MgSO_4$, then filtered and concentrated *in vacuo.* The crude product was purified by flash column chromatography (eluting with 20-40% EtOAc in CH_2Cl_2) to provide

3.10 (24 mg, 73%) as yellow solid. ^{1}H NMR (400 MHz, CD_3CN): δ 9.42 (s, 1H), 8.99 (s, 1H), 7.93 (d, *J* = 8.6 Hz, 2H), 6.78 (d, *J* = 8.6 Hz, 2H), 4.64 (bs, 2H). ^{13}C NMR (125 MHz, CD_3CN) δ 158.4, 155.8, 152.0, 147.1, 129.0, 122.4, 115.3. HRMS (ESI) *m*/*z* calcd for $C_9H_8N_4Na$ $[M+Na]^+$ 195.0647, found 195.0643.

***N*,*N*-Dimethyl-4-(1,2,4-triazin-6-yl)aniline (3.11)**: To a pressure tube was added (4-(dimethylamino)phenyl)boronic acid (48.0 mg, 0.291 mmol), $Pd(PPh_3)_4$ (34.0 mg, 0.0294 mmol), a solution of triazine **3.3** (92.0 mg, 0.575 mmol) in 5 mL of 3:2 tol:EtOH, and Cs_2CO_3 (120 mg, 0.368 mmol) in 1.0 mL H_2O. The tube was flushed with nitrogen, sealed, and heated at 100 °C for 3 h. The reaction was then diluted with 40 mL H_2O, extracted with EtOAc (2 x 60 mL). The organic layers were combined and dried over $MgSO_4$, then filtered and concentrated *in vacuo.* The crude product was purified by flash column chromatography (eluting with 0-10 % EtOAc in CH_2Cl_2) to provide **3.11** (38.0 mg, 65%) as yellow solid.^{1}H NMR (400 MHz, $CDCl_3$): δ 9.47 (s, 1H), 8.93 (s, 1H), 8.04 (d, *J* = 9.0 Hz, 2H), 6.83 (d, *J* = 9.0 Hz, 2H), 3.09 (s, 6H). ^{13}C NMR (125 MHz, CD_3Cl) δ 157.6, 154.8, 152.3, 145.7, 127.9, 119.9, 112.3, 40.2. HRMS (ESI) *m*/*z* calcd for $C_{11}H_{12}N_4Na$ $[M+Na]^+$ 223.0960, found 223.0965.

3-(1,2,4-Triazin-6-yl)phenol (3.19): To a pressure tube was added (3-hydroxyphenyl)boronic acid (46.0 mg, 0.334 mmol), $Pd(PPh_3)_4$ (38.0 mg, 0.0329 mmol), a solution of **3.3** (159 mg, 0.994) in 7 mL of 4:3 tol:EtOH, and Cs_2CO_3 (216 mg, 0.663 mmol) in 1 mL H_2O. The tube was flushed with nitrogen, sealed, and heated at 100 °C for 3 h. The reaction was then diluted with 40 mL H_2O and extracted with EtOAc (2 x 60 mL). The organic layers were combined and dried over $MgSO_4$, then filtered and concentrated *in vacuo* The crude product was purified by flash

column chromatography (eluting with 10-40 % EtOAc in CH_2Cl_2) to provide **3.19** (42.0 mg, 73%) as a light-yellow solid.^{1}H NMR (400 MHz, CD_3OD): δ 9.60 (s, 1H), 9.20 (s, 1H), 7.58 (m, 2H), 7.36 (t, *J* = 7.8, 1H), 6.99 (apparent dd, *J* = 7.0, 2.1 Hz, 1H). ^{13}C NMR (125 MHz, CD_3OD) δ 158.2, 157.9, 155.9, 147.8, 134.3, 130.2, 117.9, 117.8, 113.2. HRMS (ESI) *m*/*z* calcd for $C_9H_8N_3O$ $[M+H]^+$ 174.0667, found 174.0667.

(*S*)-3-(4-(1,2,4-Triazin-6-yl)phenyl)-2-aminopropanoic acid (3.12): To a pressure tube was added (*S*)-2-amino-3-(4 boronophenyl)propanoic acid (30.0 mg, 0.144 mmol), $Pd(PPh_3)_4$ (16.0 mg, 0.0138 mmol), a solution of **3.3** (70.0 mg, 0.438) in 5 mL of 3:2 tol:EtOH, and Cs_2CO_3 (143 mg, 0.437 mmol) in 1 mL H_2O. The tube was flushed with nitrogen, sealed, and heated at 100 °C for 3 h. The reaction was then quenched with 40 mL H_2O, extracted with EtOAc (2 x 40 mL). The aqueous layer was concentrated *in vacuo* and purified by preparative HPLC, eluting with 0-95% MeCN in water over 30 min. The desired fractions were collected and concentrated *in vacuo* to provide **3.12** (15 mg, 42%) as light-orange solid.^{1}H NMR (400 MHz, D_2O): δ 9.59 (s, 1H), 9.25 (s, 1H), 7.98 (d, *J* = 8.2 Hz, 2H), 7.49 (d, *J* = 8.1 Hz, 2H), 3.69 (t, *J* = 6.6 Hz, 1H), 3.14 (dd, *J* = 13.4, 5.4 Hz, 1H), 3.02 (dd, *J* = 13.7, 7.3 Hz, 1H). ^{13}C NMR (125 MHz, D_2O) δ 175.4, 158.2, 155.4, 149.5, 139.5, 131.6, 130.5, 127.9, 56.2, 37.2. HRMS (ESI) *m*/*z* calcd for $C_{12}H_{11}N_4O_2$ $[M-H]^-$ 243.0882, found 243.0889.

3.7 References

(1) Grammel, M.; Hang, H. C: Chemical reporters for biological discovery. *Nat. Chem. Biol.* **2013**, *9,* 475.

(2) Patterson, D.M.; Nazarova, L. A.; Prescher J.A: Finding the right (bioorthogonal) chemistry.

ACS Chem Biol. **2014**, *9*, 592.

(3) Lang, K.; Chin, J. W: Bioorthogonal reagents for labeling proteins. *ACS Chem. Biol.* **2014**, *9*, 16.

(4) Shih, H-W.; Kamber, D. N.; Prescher, J. A: Building better bioorthogonal reactions. *Curr. Opin. Chem. Biol.* **2014**, *21*, 103.

(5) Patterson, D. M.; Nazarova, L. A.; Xie, B.; Kamber, D. N.; Prescher, J. A: Functionalized cyclopropenes as bioorthogonal chemical reporters. *J. Am. Chem. Soc.* **2012**, *134*, 18638.

(6) Yang, J.; Šečkutė, J.; Cole, C. M.; Devaraj, N. K: Live-cell imaging of cyclopropene tags with fluorogenic tetrazine cycloadditions. *Angew. Chem., Int. Ed.* **2012**, *51*, 7476.

(7) Yu, Z.; Pan, Y.; Wang, Z.; Wang, J.; Lin, Q: Genetically encoded cyclopropene directs rapid, photoclick-chemistry-mediated protein labeling in mammalian cells. *Angew. Chem., Int. Ed.* **2012**, *51*, 10600.

(8) Kamber, D. N.; Nazarova, L. A.; Liang, Y.; Lopez, S. A.; Patterson, D. M.; Shih, H-W.; Houk, K. N.; Prescher, J. A: Isomeric cyclopropenes exhibit unique bioorthogonal reactivities. *J. Am. Chem. Soc.* **2013**, *135*, 13680.

(9) Elliott, T. S.; Townsley, F. M.; Bianco, A.; Ernst, R. J.; Sachdeva, A.; Elsasser, S. J.; Davis, L.; Lang, K.; Pisa, R.; Greiss, S.; Lilley, K. S.; Chin, J. W: Proteome labeling and protein identification in specific tissues and at specific developmental stages in an animal. *Nat. Biotechnol.* **2014**, *32*, 465.

(10) Šečkutė, J.; Yang, J.; Devaraj, N. K: Rapid oligonucleotide-templated fluorogenic tetrazine ligations. *Nucleic Acids Res.* **2013**, *41*, e148.

(11) Patterson, D. M.; Jones, K. A.; Prescher, J. A: Improved cyclopropene reporters for probing protein glycosylation**.** *Mol. BioSyst.* **2014**, *10*, 1693.

(12) Xiong, D. C.; Zhu, J.; Han, M. J.; Luo, H. X.; Wang, C.; Yu, Y.; Ye, Y.; Tai, G.; Ye, X. S: Rapid probing of sialylated glycoproteins in vitro and in vivo via metabolic oligosaccharide engineering of a minimal cyclopropene reporter. *Org. Biomol. Chem.* **2015**, *13*, 3911.

(13) Sachdeva A, Wang K, Elliott T, Chin JW: Concerted, rapid, quantitative, and site-specific dual labeling of proteins. *J. Am. Chem. Soc.* **2014**, *136*, 7785.

(14) Devaraj, N. K.; Weissleder, R: Biomedical applications of tetrazine cycloadditions *Acc. Chem. Res.* **2011**, *44*, 816.

(15) Liu, F.; Liang, Y.; Houk, K. N: Theoretical elucidation of the origins of substituent and strain effects on the rates of Diels-Alder reactions of 1,2,4,5-tetrazines. *J. Am. Chem. Soc.* **2014**, *136*, 11483.

(16) Šečkutė, J.; Devaraj, N. K: Expanding room for tetrazine ligations in the in vivo chemistry toolbox *Curr. Opin. Chem. Biol.* **2013**, *17*, 761.

(17) Blackman, M. L.; Royzen, M.; Fox, J. M: The tetrazine ligation: Fast bioconjugation based on Inverse-electron-demand Diels-Alder reactivity. *J. Am. Chem. Soc.* **2008**, *130*, 13518.

(18) Karver, M. R.; Weissleder, R.; Hilderbrand, S. A: Synthesis and evaluation of a series of 1,2,4,5-tetrazines for bioorthogonal conjugation. *Bioconjug. Chem.* **2011**, *22*, 2263.

(19) Liu, D. S.; Tangpeerachaikul, A.; Selvaraj, R.; Taylor, M. T.; Fox, J. M.; Ting, A. Y: Diels-Alder cycloaddition for fluorophore targeting to specific proteins inside living cells. *J. Am. Chem. Soc.* **2012**, *134*, 792.

(20) Yang, J.; Liang, Y.; Šečkutė, J.; Houk, K. N.; Devaraj, N. K: Synthesis and reactivity comparisons of 1-methyl-3-substituted cyclopropene minitags for tetrazine bioorthogonal reactions. *Chem. Eur. J.* **2014**, *20*, 3365.

(21) Daves, G. D.; Robins, R. K.; Cheng, C. C: The total synthesis of toxoflavin *J. Am. Chem.*

Soc. **1961**, *83*, 3904.

(22) Liao, T. K.; Baiocchi, F.; Cheng, C. C: Synthesis of 1-demethyltoxoflavin (8-demethylfervenulin). *J. Org. Chem.* **1966**, *31*, 900.

(23) Taylor, E. C.; Sowinski, F: Synthesis of the pyrimido[5,4-e]-as-triazine antibiotics fervenulin and 2-methylfervenulone. *J. Org. Chem.* **1975**, *40*, 2321.

(24) Boger, D. L.; Panek, J. S: Diels-Alder reaction of heterocyclic azadienes. I. Thermal cycloaddition of 1,2,4-triazine with enamines: simple preparation of substituted pyridines. *J. Org. Chem.* **1981**, *46*, 2179.

(25) Steigel, A.; Sauer, J. (4+2)-Cycloadditionen 6-gliedriger heterocyclen mit inaminen. *Tetrahedron Lett.* **1970**, 3357.

(26) Boger, D. L: Diels-Alder cycloaddition reactions of heterocyclic azadienes: scope and applications. *Chem. Rev.* **1986**, *86*, 781.

(27) Boger, D. L: Diels-alder reactions of azadienes. *Tetrahedron.* **1983**, *39*, 2869.

(28) Neunhoeffer, H.; Frühauf, H.-W: Zur chemie der 1, 2, 4-triazine I reaktion von 1, 2, 4-triazinen mit 1-diäthylaminopropin. *Tetrahedron Lett.* **1969**, *10*, 3151.

(29) Dittmar, W.; Sauer, J.; Steigel, A: (4+2)-Cycloadditionen der 1.2.4-Triazine - ein neuer weg zu 4-H-Azepinen. *Tetrahedron Lett.* **1969**, *10*, 5171.

(30) Anderson, E. D.; Boger, D. L: Inverse electron demand Diels–Alder reactions of 1,2,3-triazines: Pronounced substituent effects on reactivity and cycloaddition scope. *J. Am. Chem. Soc.* **2011**, *133*, 12285.

(31) Frisch, M. J. T., *et al.* Gaussian 09, revision D.01; . *Gaussian Inc.: Wallingford, CT* **2013**.

(32) Zhao, Y.; Truhlar, D. G: The M06 suite of density functionals for main group thermochemistry, thermochemical kinetics, noncovalent interactions, excited states, and

transition elements: two new functionals and systematic testing of four M06-class functionals and 12 other functionals. *Theor. Chem. Acc.* **2008**, *120*, 215.

(33) Zhao, Y.; Truhlar, D. G: Density functionals with broad applicability in chemistry *Acc. Chem. Res.* **2008**, *41*, 157.

(34) Kämpchen, T. M., W.; Massa, W.; Overheu, W.; Schmidt, R.; Seitz, G: Zur Kenntnis von Reaktionen des 1,2,4,5-Tetrazin-3,6-dicarbonsäure-dimethylesters mit Nucleophilen. *Chem. Ber.* **1982**, *115*, 683.

(35) Karver, M. R.; Weissleder, R.; Hilderbrand, S. A: Bioorthogonal reaction pairs enable simultaneous, selective, multi-target imaging. *Angew. Chem., Int. Ed.* **2012**, *51*, 920.

(36) Liang, Y.; Mackey, J. L.; Lopez, S. A.; Liu, F.; Houk, K. N: Control and design of mutual orthogonality in bioorthogonal cycloadditions. *J. Am. Chem. Soc.* **2012**, *134*, 17904.

(37) Debets, M. F.; van Hest, J. C. M.; Rutjes, F. P. J. T: Bioorthogonal labelling of biomolecules: new functional handles and ligation methods. *Org. Biomol. Chem.* **2013**, *11*, 6439.

(38) Selvaraj, R.; Fox, J. M: An efficient and mild oxidant for the synthesis of s-tetrazines. *Tetrahedron Lett.* **2014**, *55*, 4795.

(39) Wu, H.; Yang, J.; Šečkutė, J.; Devaraj, N. K: In situ synthesis of alkenyl tetrazines for highly fluorogenic bioorthogonal live-cell imaging probes. *Angew. Chem., Int. Ed.* **2014**, *53*, 5805.

(40) Sletten, E. M.; Nakamura, H.; Jewett, J. C.; Bertozzi, C. R: Difluorobenzocyclooctyne: Synthesis, reactivity, and stabilization by β-cyclodextrin. *J. Am. Chem. Soc.* **2010**, *132*, 11799.

(41) Debets, M. F.; van Berkel, S. S.; Dommerholt, J.; Dirks, A. T.; Rutjes, F. P. J. T.; van Delft, F. L. Bioconjugation with strained alkenes and alkynes. *Acc. Chem. Res.* **2011**, *44*, 805.

(42) Hansch, C.; Leo, A.; Taft, R. W: A survey of Hammett substituent constants and resonance

and dield parameters. *Chem. Rev*. **1991**, *91*, 165.

(43) Seitchik, J. L.; Peeler, J. C.; Taylor, M. T.; Blackman, M. L.; Rhoads, T. W.; Cooley, R. B.; Refakis, C.; Fox, J. M.; Mehl, R. A: Genetically encoded tetrazine amino acid directs rapid site-specific *in vivo* bioorthogonal ligation with *trans*-cyclooctenes. *J. Am. Chem. Soc.* **2012**, *134*, 2898.

(44) Darko, A.; Wallace, S.; Dmitrenko, O.; Machovina, M. M.; Mehl, R. A.; Chin, J. W.; Fox, J. M: Conformationally strained *trans*-cyclooctene with improved stability and excellent reactivity in tetrazine ligation. *Chem. Sci*. **2014**, *5*, 3770.

(45) Blizzard, R. J.; Brown, W.; Bazewicz, C. G.; Backus, D. R.; Li, Y.; Mehl, R. A. J. Am. Chem. Soc., Blizzard, R. J.; Brown, W.; Bazewicz, C.G.; Backus, D.R.; Li, Y.; Mehl, R. A*:* Ideal bioorthogonal reactions using a site-specifically encoded tetrazine amino acid. *J. Am. Chem. Soc.* **2015**, *137*, 10044.

(46) Hehre, W. J.; Radom, L.; Schleyer, P. v. R.; Pople, J. A. *Ab Initio Molecular Orbital Theory*, Wiley: New York, 1986.

(47) (a) Zhao, Y.; Truhlar, D. G: Computational characterization and modeling of buckyball tweezers: density functional study of concave–convex π···π interactions. *Phys. Chem. Chem. Phys.* **2008**, *10*, 2813. (b) Ribeiro, R. F.; Marenich, A. V.; Cramer, C. J.; Truhlar, D. G: Use of solution-phase vibrational frequencies in continuum models for the free energy of solvation. *J. Phys. Chem. B* **2011**, *115*, 14556.

(48) (a) Barone, V.; Cossi, M: Quantum calculation of molecular energies and energy gradients in solution by a conductor solvent model. *J. Phys. Chem. A.* **1998**, *102*, 1995. (b) Cossi, M.; Rega, N.; Scalmani, G.; Barone, V: Energies, structures, and electronic properties of molecules in solution with the C-PCM solvation model. *J. Comput. Chem.* **2003**, *24*, 669. (c) Takano, Y.;

Houk, K. N: Benchmarking the Conductor-like Polarizable Continuum Model (CPCM) for Aqueous Solvation Free Energies of Neutral and Ionic Organic Molecules. *J. Chem. Theory Comput.* **2005**, *1*, 70.

(49) Erickson, J. G: 3-Amino-*as*-triazines. *J. Am. Chem. Soc.* **1952**, *74*, 4706.

(50) Peake, C. J.; Cullen, T. G. (FMC corporation., USA). 6-Substituted-3,5-diamino-1,2,4-triazines as insecticides. US patent 5,502,054, **1995**.

Chapter 4: Isomeric 1,2,4-triazines exhibit distinct profiles of bioorthogonal reactivity

Yong Liang, Fang Liu, Jeffrey Briggs, and Hui-Wen Shih contributed to the work presented in this chapter.

4.1 Introduction

In the previous chapter, I discussed the reactivity of 6-substituted 1,2,4-triazines. These motifs react robustly with *trans*-cyclooctene (TCO), but are orthogonal to other bioorthogonal alkenes and are stable in cells (in contrast to structurally related tetrazine scaffolds). In this chapter, I will discuss our efforts to tune 1,2,4-triazines to exhibit unique reaction profiles with strained alkenes and alkynes.

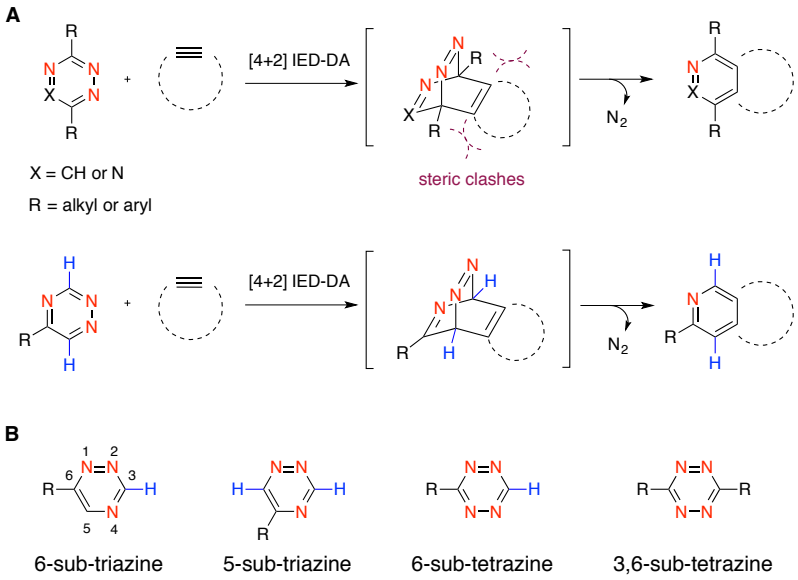

Figure 4-1. Inverse electron-demand Diels-Alder (IED-DA) reactivity of substituted tetrazine and triazine scaffolds. (A) Model IED-DA reactivity of strained alkynes with tetrazine or 1,2,4-traizine motifs. (B) Isomeric triazines and tetrazines examined in this work.

The success of bioorthogonal transformations is critically dependent on the reagents being exquisitely stable in cells and tissues, yet robustly reactive with complementary probes [1, 2]. This chemical paradox has often frustrated efforts to develop reagents that exhibit selective reactivity, let alone multiple reactions that can function in concert. In fact, there are only a handful of bioorthogonal reaction pairs that can be used simultaneously [3], and of these, none involve concurrent [4+2] cycloadditions [4-10].

To address this void, we are developing "privileged" scaffolds that not only meet the requirements for bioorthogonality, but also are compatible with each other for simultaneous reactivity [11]. Such mutually orthogonal reagents will enable selective and concurrent chemical tagging of multiple biomolecules [12]. One such "privileged" scaffold is 1,2,4-triazine. As I highlighted in Chapter 3, triazines offer robust reactivity and exquisite stability for biomolecule labeling.

To capitalize on the unique features of triazines and further explore reactivity, we aimed to synthesize and analyse isomeric scaffolds (Figure 4-1). 1,2,4-Triazines react with alkene and alkyne dienophiles via inverse electron-demand Diels-Alder (IED-DA) cycloaddition across C3-C6 (Figure 4-1) [25]. The regioselectivity of this addition could potentially be exploited for orthogonal reaction development: bulky dienophiles would be more likely to react with 5-substituted triazines than their 6-substituted counterparts (Figure 4-1). Similar steric "tuning" tactics have been used to develop mutually compatible reactions with strained alkynes and alkenes [10, 14, 26]. For example, C3- and C6-substituted tetrazines exhibit differential reactivities with sterically modified cyclooctynes [26]. Cyclooctynes with substitutents near the reactive alkyne center react

exclusively with mono-substituted (versus di-substitued tetrazines) due to steric clashes in the transition state.

4.2 Computational analysis of 1,2,4-triazine reactivity

We hypothesized that 1,2,4-triazine reactivity could be similarly modulated to generate mutually orthogonal reactions. To examine this possibility, we first used density-functional theory (DFT) calculations to evaluate the reactivity of model 1,2,4- triazines with a series of strained dienophiles and known bioorthogonal motifs (Table 4-1) [20-24].

Table 4-1. DFT-computed activation free energies (kcal/mol) and predicted relative rate constants (M^{-1} s^{-1}) for tetrazine and triazines cycloadditions with strained dienophiles, in water at 25 °C.

$\Delta G^{\ddagger}$ (k_{rel})	Cp	NB	TCO	DIFO	DIBAC	TMTH
6-sub-triazine	26.7 (1.8×10^{-5})	29.2 (2.7×10^{-7})	21.7 (8.3×10^{-2})	26.1 (5.4×10^{-5})	33.2 (3.0×10^{-10})	25.6 (1.1×10^{-4})
5-sub-triazine	26.5 (2.4×10^{-5})	29.9 (7.7×10^{-8})	22.7 (1.6×10^{-2})	26.7 (1.8×10^{-5})	32.3 (1.5×10^{-9})	21.1 (2.4×10^{-1})
3-sub-triazine	26.5 (2.4×10^{-5})	30.0 (6.8×10^{-8})	23.1 (7.6×10^{-3})	27.0 (1.1×10^{-5})	35.1 (1.2×10^{-11})	26.8 (1.4×10^{-5})
6-sub-tetrazine	20.2 (1.0)	22.2 (3.7×10^{-2})	15.2 (4.9×10^{3})	20.6 (5.5×10^{-1})	26.7 (1.8×10^{-5})	19.6 (3.2)
3,6-disub-tetrazine	21.4 (1.5×10^{-1})	22.0 (4.8×10^{-2})	15.9 (1.5×10^{3})	25.6 (1.1×10^{-4})	30.8 (1.7×10^{-8})	30.8 (1.7×10^{-8})

Isomeric 1,2,4-triazines differed in the placement of subsitutents, either at the sites of new bond formation (C3 or C6) or removed from these sites (C5). Similar calculations were

performed with substituted tetrazines. In agreement with our previous work, 6-substituted-triazines were predicted to react robustly with TCO, although slower than their tetrazine counterparts. Minimal or no triazine reactivity was predicted with strained alkenes, including cyclopropene and norbornene. These results are in stark contrast to tetrazines, which harbor lower LUMO+1 energies and thus react robustly with a variety of strained alkenes [14].

A surprising result emerged in the predicted reactivity profiles of triazines with strained alkynes. The 5-substituted-triazine and monosubstituted tetrazine were predicted to be robustly reactive with tetramethylthiacycloheptyne (TMTH), one of the most sterically encumbered strained alkynes. TMTH was previously developed by the Bertozzi group for strain-promoted azide-alkyne cycloaddition [32]. TMTH can also react with dienes, though, including minimally substituted tetrazines [32,33]. As expected, the 3- and 6-subsituted triazine isomers were predicted to react slowly with TMTH due to steric clashes at the reactive centers. Calculations further suggested that 5-substituted-triazines would not react efficiently other bioorthogonal strained alkynes, including DIBAC and DIFO (molecules with lower HOMO energies). Monosubstituted tetrazines are also predicted to react with TMTH. However, due to their instability, monosubstituted tetrazines are not utilized as the primary labelling reagent [17].

4.3 Reactivity profile of isomeric 1,2,4-triazines

The predicted rate data were verified experimentally. We synthesized the panel of reagents shown in Table 4-2, and monitored the relevant reactions by ^{1}H-NMR. The measured bimolecular rate constants closely matched the DFT predictions (Table 4-2).

As expected, the 6-substituted triazine **4.1** reacted exclusively with TCO **4.8**. The 5-phenyl triazine isomer **4.2** was similarly reactive with TCO **4.8** (Figure 4-2), but also underwent cycloaddition (albeit minimally) with carbamate-cyclopropenes **4.4-4.5** (Figure 4-3) and DIFO **4.9** (Figure S4-2). Minimal reactivity was also observed between tetrazine **4.3** and DIFO **4.9** (Figure S4-3). Triazine **4.2** was also stable in the presence of L-cysteine at 37 °C (Figure S4-4). Importantly, the most tantalizing prediction—robust reactivity between TMTH **4.11** and 5-phenyl triazine **4.2**—was also validated experimentally (Table 4-2 and Figure S4-5). Disubstituted tetrazine **4.3** did not react with TMTH **4.11** for up to 2 d- likely due to steric clashes between the methyl groups on TMTH **4.11** and dipyridyl groups on tetrazine **4.3** (Figure S4-6). 6-Phenyl-triazine also did not react with TMTH for 2 d (Figure S4-7), and only minimal reactivity was observed with *para*-nitrophenyl-triazine over 2 d (Figure S4-8). Our experimental data correlate with the computational values (Table 4-1 and Figures S4-5 to S4-8).

Table 4-2. Second order rate constants (M^{-1} s^{-1}) for tetrazine and triazine cycloadditions with strained dienophiles. All rates were monitored by ^{1}H-NMR at 25 °C. N/R indicates no reaction after 24 h and a rate constant < $k_2 = 10^{-4}$ M^{-1} s^{-1}. Calculated rate constants: *k_2 = 2.29 ± 0.16 x 10^{-4} M^{-1} s^{-1}, ** k_2 = 3.35 ± 0.80 x 10^{-4} M^{-1} s^{-1}.

k_2(M^{-1} s^{-1})	4.4 / 4.5	4.6	4.7	4.8	4.9	4.10	4.11
4.1	N/R	N/R	N/R	0.034 ± 0.005	N/R	N/R	N/R
4.2	15% conv. after 24 h	N/R	N/R	0.046 ± 0.001	20% conv. after 24 h*	N/R	0.22 ± 0.01
4.3	2.78 ± 0.37	0.032 ± 0.005	3.16 ± 0.41	2000 ± 400	25% conv. after 24 h**	N/R	N/R

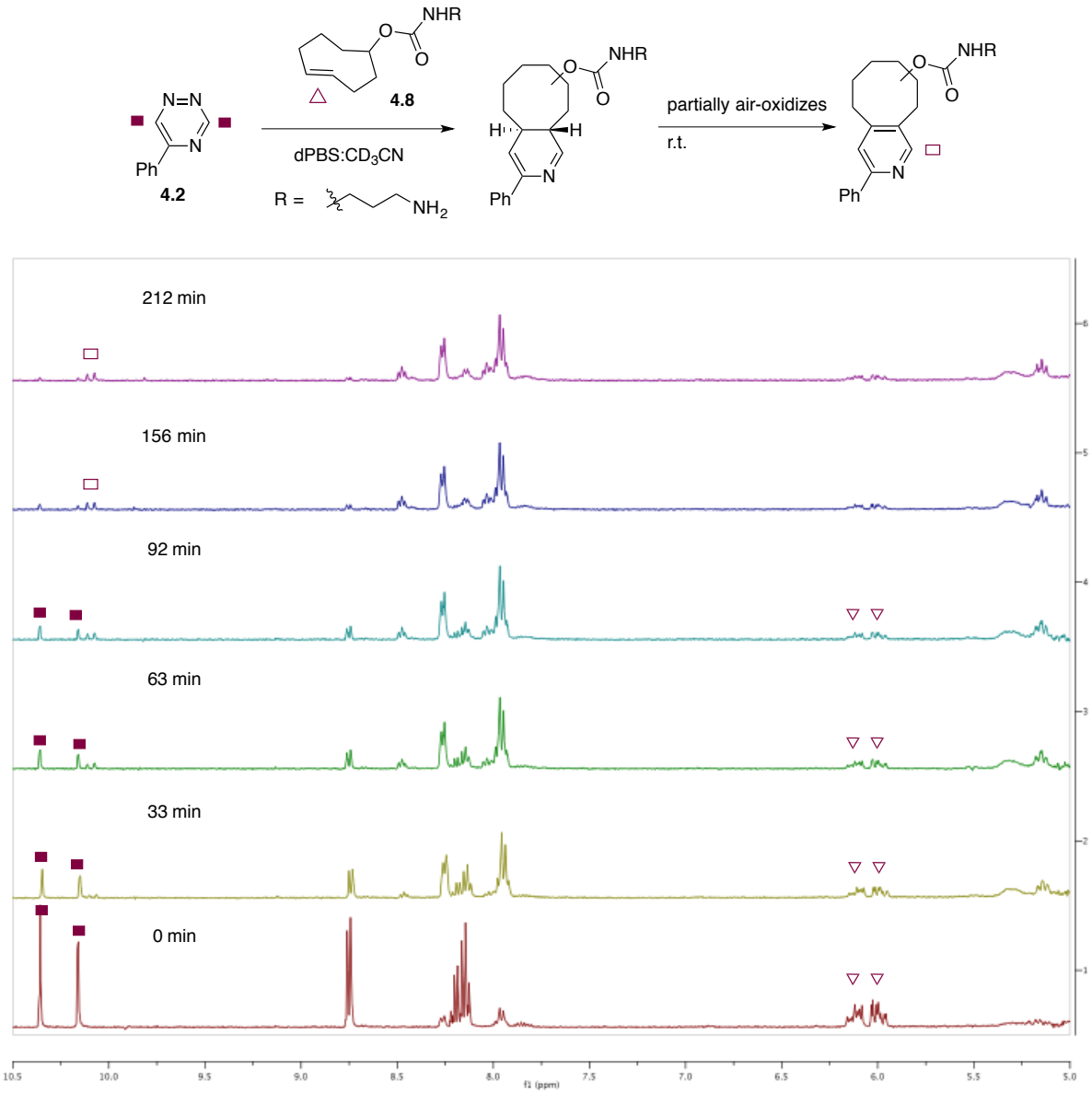

Figure 4-2. Reaction between triazine **4.2** and TCO **4.8**. Triazine **4.2** (0.30 mL of a 20 mM solution in CD_3CN) was added a solution of TCO **4.8** (0.30 mL of a 20 mM solution in dPBS). The reaction was monitored over time by ^{1}H-NMR.

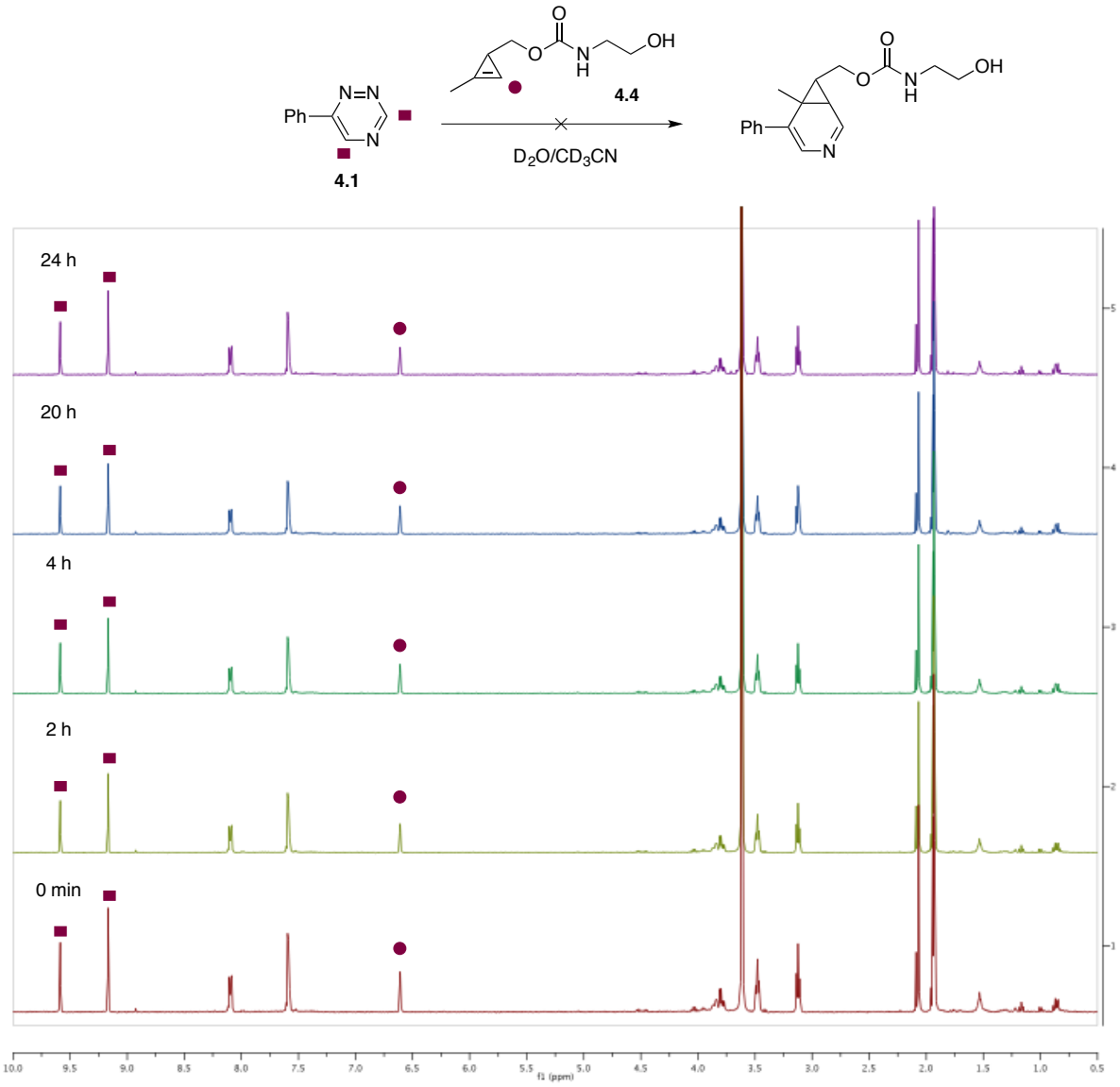

Figure 4-3. Triazine **4.1** is orthogonal to cyclopropene **4.4**. Triazine **4.1** (0.24 mL of a 25 mM solution in CD_3CN) was added a solution of cyclopropene **4.4** (0.24 mL of a 25 mM solution in 25% D_2O in CD_3CN) and diluted with 0.12 mL CD_3CN. The reaction was monitored over time by ^{1}H-NMR.

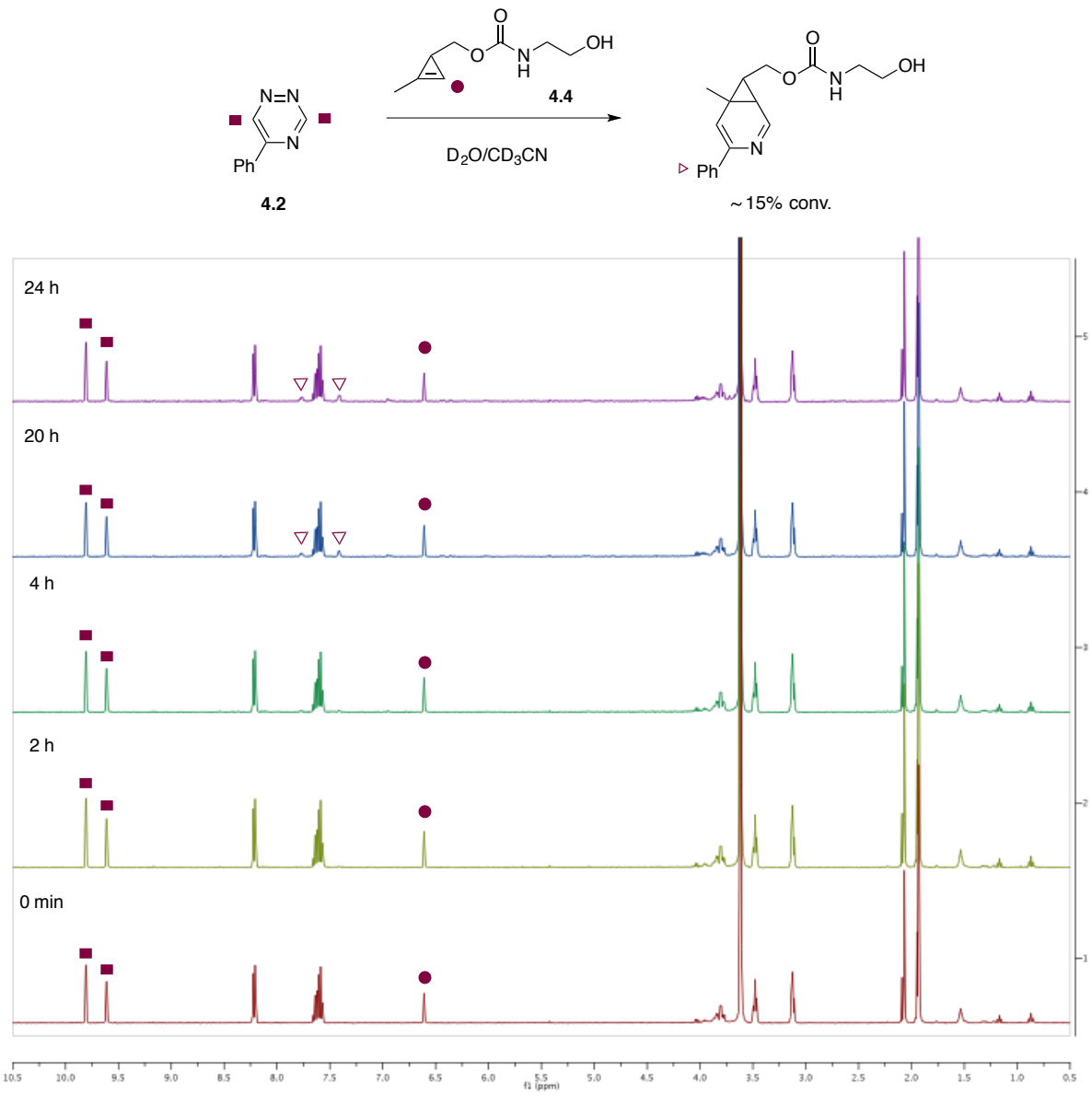

Figure 4-4. Minimum reactivity is observed between triazine **4.2** and cyclopropene **4.4**. Triazine **4.2** (0.30 mL of a 20 mM solution in CD_3CN) was added a solution of cyclopropene **4.4** (0.24 mL of a 25 mM solution in 25% D_2O in CD_3CN) and diluted with 60 µL CD_3CN. The reaction was monitored over time by ^{1}H-NMR.

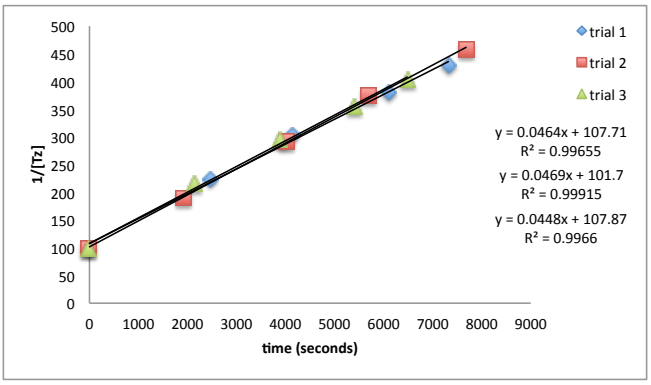

Figure 4-5. Kinetic data used to calculate second-order rate constants (k_2) for **4.2** and **4.8** in 1:1 CD_3CN: *d*-PBS. The reactions between triazine **4.2** and TCO **4.8** were run in 1:1 ratios and monitored by ^{1}H-NMR.

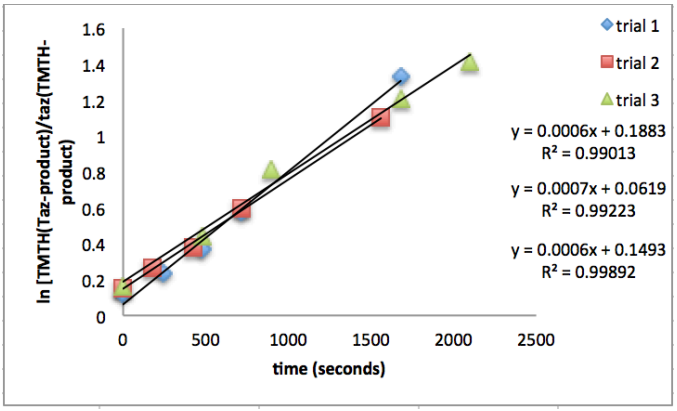

Figure 4-6. Kinetic data used to calculate second-order rate constants (k_2) for **4.2** and **4.11** CD_3CN. The reactions between triazine **4.2** and TMTH **4.11** were run in roughly 1:2 (triazine:TMTH) ratios and monitored by ^{1}H-NMR.

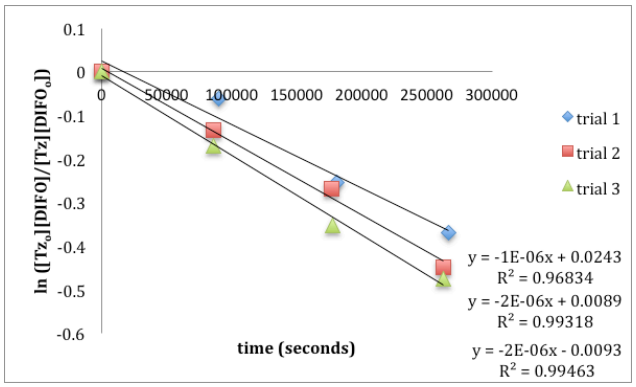

Figure 4-7. Kinetic data used to calculate second-order rate constants (k_2) for **4.3** and **4.9** in CD_3CN. The reactions between tetrazine **4.3** and DIFO **4.9** were run in roughly 1:2 (tetrazine:DIFO) ratios and monitored by ^{1}H-NMR.

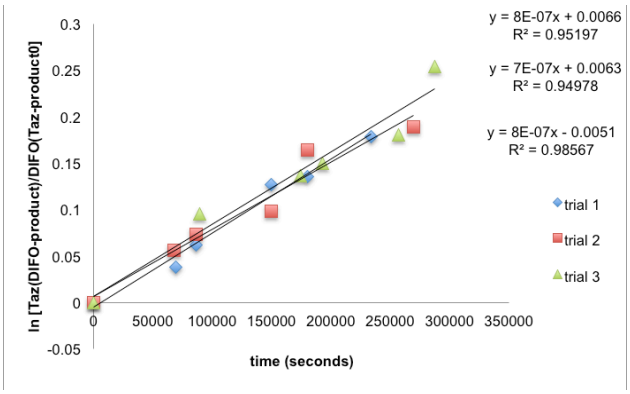

Figure 4-8. Kinetic data used to calculate second-order rate constants (k_2) for **4.2** and **4.9** in CD_3CN. The reactions between triazine **4.2** and DIFO **4.9** were run in roughly 1:2 (triazine:DIFO) ratios and monitored by ^{1}H-NMR.

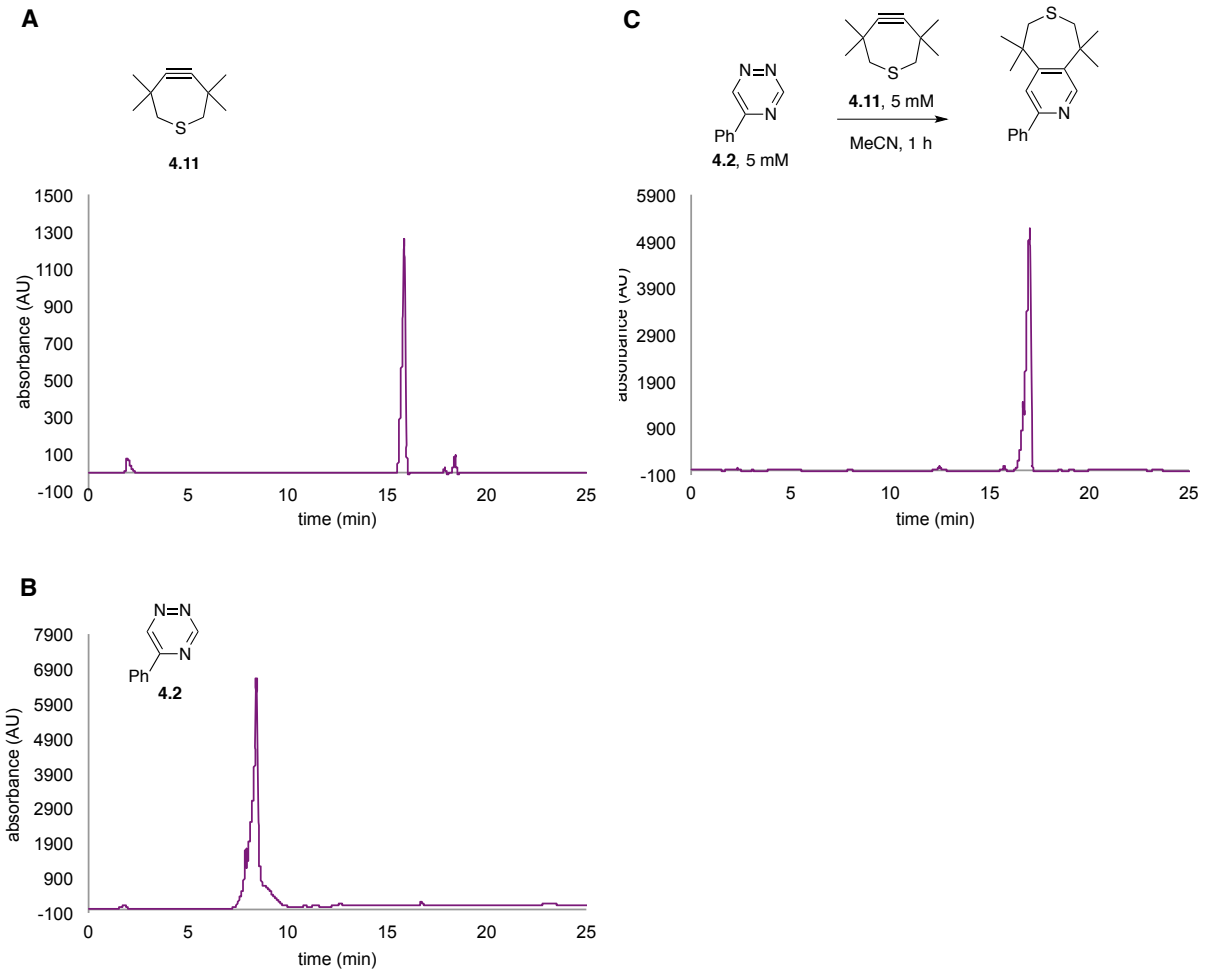

Figure 4-9. 5-Phenyl-1,2,4-triazine **4.2** reacts quantitatively with TMTH **4.11**. (A) HPLC trace of starting TMTH **4.11** reagent. (B) HPLC trace of starting triazine **4.2** trace. (C) Triazine **4.2** (5mM in MeCN) was reacted with TMTH **4.11** (5 mM in MeCN) for 1 h, and monitored by HPLC. HPLC traces are monitored at 210 nm wavelength.

The unique reactivity profile of 5-phenyl triazine suggested further opportunities for mutually orthogonal reaction development. The reaction between TMTH **4.11** and 5-phenyl-1,2,4-triazine **4.2** proceeded with a rate constant of $k_2 = 0.22 \pm 0.01\ M^{-1}\ s^{-1}$ (Figure 4-6). This rate is on par with many commonly used strain promoted azide-alkyne cycloadditions [2,34,35]. The reactivity of 5-substituted triazine with TMTH in the presence of 6-substituted triazine was further analysed by ^{1}H-NMR (Figure 4-10).

Isomeric triazines were mixed at equal concentrations with excess TMTH. Over the course of the reaction, the concentration of TMTH and 5-phenyl-triazine decreased concurrently (Figure 4-10). By contrast, 6-phenyl-triazine was not consumed.

4.4 Dual [4+2] IED-DA reactions

The 5-substituted isomer (**4.2**) is also non-reactive with cyclopropene **4.6** (a scaffold known to react robustly with tetrazines), setting the stage for dual [4+2] IED-DA reactions. To examine this possibility, cyclopropene **4.6** was mixed with tetrazine **4.2**. Over the course of the reaction, the concentration of 5-phenyl-triazine remained constant, while cyclopropene **4.6** and tetrazine **4.3** were consumed (Figure 4-10). Collectively, these data suggested that the 5-substituted-triazine/TMTH reaction could be used concurrently with cyclopropene/disubstituted-tetrazine cycloadditon.

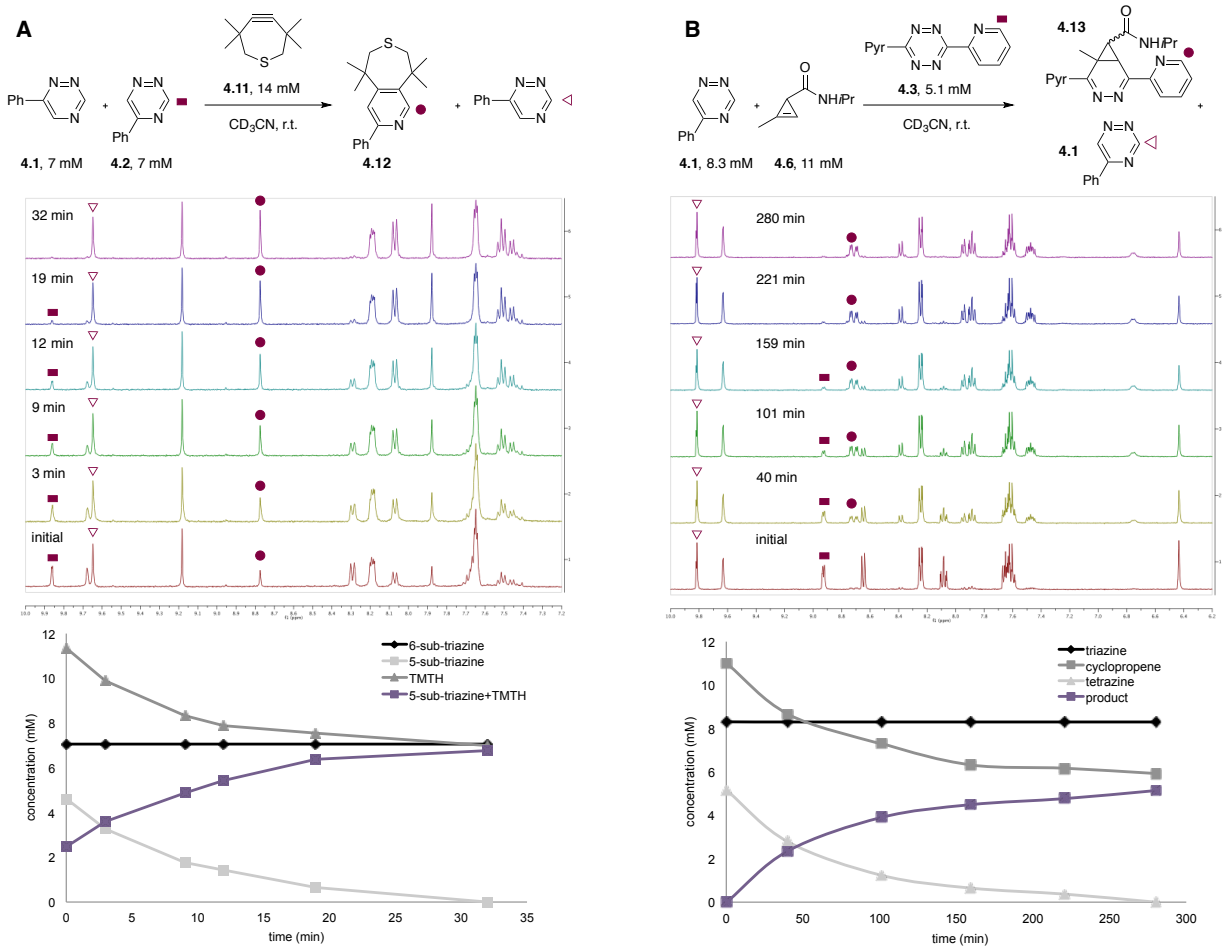

Figure 4-10. Isomeric triazines exhibit unique bioorthogonal reactivities. (A) Triazine **4.2** reacts exclusively with TMTH **4.11**. The reaction was monitored by ^{1}H NMR (top), with the reaction progress is plotted below. (B) 5-Phenyl-triazine **4.2** can be used in combination with disubstituted tetrazine **4.3** and cyclopropene. The reaction was monitored by 1H NMR (top), with the reaction progress plotted below.

To investigate this possibility, we combined all four reagents (2.5 mM) and monitored the reactions by ^{1}H-NMR and HPLC (Figures 4-11 and S4-9 to S4-11). The reactions proceeded quantitatively to the expected two distinct cycloadducts. To our knowledge, this is the first example of a pair of [4+2] IED-DA cycloadditions that can be used simultaneously for bioorthogonal reactivity.[3]

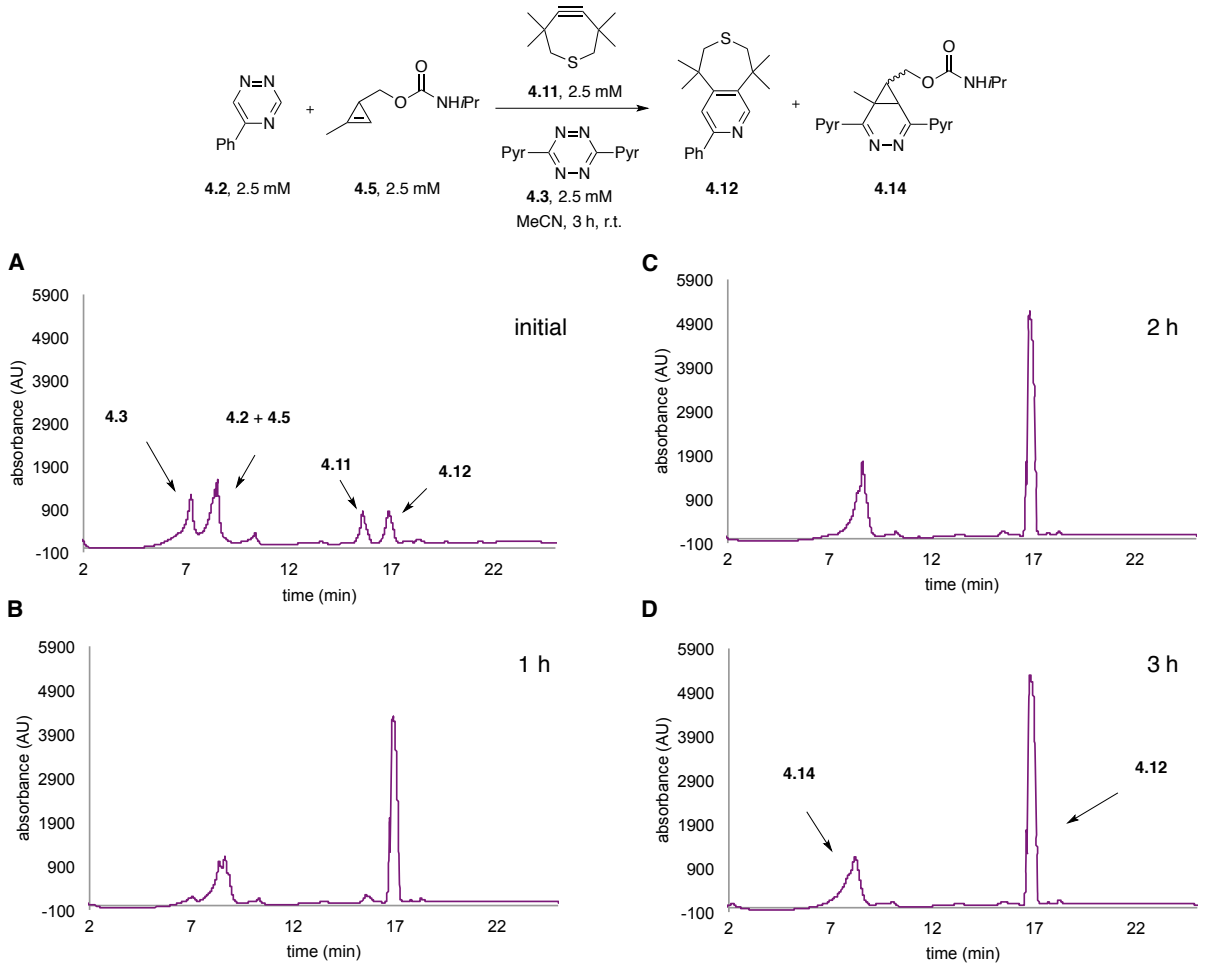

Figure 4-11. Compatible cycloadditions between triazine **4.2**, cyclopropene **4.5**, **4.11**, and **4.3**. All four reagents were combined together (2.5 mM), and the reactions were monitored by HPLC (210 nm) for 3 h.

4.5 Conclusions and future work

In conclusion, computational analyses were used to identify candidate orthogonal reactions, and the predictions were verified experimentally. Notably, 5-substituted triazines were shown to undergo rapid [4+2] cycloadditions with sterically encumbered strained alkynes. This unique, sterically controlled reactivity was exploited for dual bioorthogonal labeling. Mutually orthogonal traizines and cycloaddition chemistries will enable multi-component imaging applications. This reaction could be used in combination with another popular IED-DA reaction, the tetrazine ligation of cyclopropene units. These mutually compatbile chemistries will bolster further multi-component imaging applications and bioorthognoal reaction development.

Collectively, this thesis introduced the development of new bioorthogonal reactions for multicomponent biomolecule labeling. Using a combination of steric and electronic perturbations, new reagents were developed that exhibit selective reactivity and offer the potential to be used together to label multiple targets of interest.

4.6 Materials and methods

4.6a Computational studies

Calculations were performed with Gaussian version 09 [30]. The geometry optimization of the transition states involved was carried at M06-2X level of theory [28-29] with the 6-31G(d) basis set [37]. Vibrational frequencies were computed at the same level to check whether each optimized structure was an energy minimum or a transition state and to evaluate its zero-point vibration energy (ZPVE) and thermal corrections at 298 K. A quasiharmonic correction was applied during the entropy calculation by setting all positive frequencies that were less than 100 cm^{-1} to 100 cm^{-1} [38]. The single-point energies and solvent effects in water were computed at

level of M06-2X/6-311+G(d,p)using the gas-phase optimized structures at the level of M06-2X/6-31G(d). CPCM model was used to evaluate solvation energies by a self-consistent reaction field (SCRF) [39], where UFF radii were used. The frontier molecular orbitals (FMOs) and their energies were computed using M06-2X/6-31G(d) geometries at the HF/6-311+G(d,p) level.

4.6b Rate studies

The reactions between tetrazines **4.3** and 1,2,4-triazine **4.1-4.2** with strained dienophiles **4.4-4.11** were monitored by ^{1}H-NMR. For reactions between tetrazine or 1,2,4-triazine with strained dienophiles, 0.12-0.3 mL of a 20-50 mM solution of the appropriate strained dienophile was added to a solution of the appropriate 1,2,4-triazine or tetrazine in CD_3CN (0.12-0.24 mL, 20-50 mM), and then diluted to a final volume of 0.6 mL. The final concentrations of all reactants were 5-10 mM and reactions were monitored for at least 24 h. No reaction indicates a rate constant of not faster than $k_2 \sim 10^{-5}$ M^{-1} s^{-1}. All reactions were carried out at 25 °C. Representative spectra and experimental conditions for each reaction are shown in the accompanying figures.

4.6c General synthetic procedures

Compounds **S4.1** [12], **S4.3** [12], **4.1** [12], **4.2** [40], **4.4** [15], **4.6** [10], **4.9** [41]**, 4.11** [32] were synthesized as previously reported. All other reagents were obtained from commercial sources and used without further purification. Reactions were run under ambient conditions, unless otherwise indicated. Tetrahydrofuran (THF), diethyl ether (Et_2O), dichloromethane (CH_2Cl_2), and acetonitrile (MeCN) were degassed with argon and run through two 4 x 36 inch columns of anhydrous neutral A-2 (8 x 14 mesh; LaRoche Chemicals; activated under a flow of argon at 350 °C for 12 h). Thin-layer chromatography was performed using Silica Gel 60 F_{254}-

coated glass plates (0.25 mm thickness), and visualization was performed with $KMnO_4$ stain and/or UV irradiation. Chromatography was accomplished with 60 Å (240-400 mesh) silica gel, commercially available from Sorbent Technologies. HPLC purifications were performed on a Varian ProStar equipped with 325 Dual Wavelength UV-Vis Detector. Analytical runs were performed using an Agilent C18 Scalar column (4.6 x 150 mm, 5 μm) with a 1 mL/min flow rate, and visualized with 210nm wavelength. NMR spectra were collected on a Bruker DRX-400 (400 MHz ^{1}H, 100 MHz ^{13}C, 376.5 MHz ^{19}F) or CRYO-500 (500 MHz ^{1}H, 125.7 MHz ^{13}C) instrument. All spectra were collected at 298 K. High-resolution mass spectrometry was performed by the University of California, Irvine Mass Spectrometry Center.

4.6d Synthetic procedures

5,5,9,9-Tetramethyl-3-phenyl-5,6,8,9-tetrahydrothiepino[4,5-*c*]pyridine (4.12): To three separate NMR tubes containing triazine **4.2** (0.3 mL of a 20 mM solution) was added TMTH **4.11** (0.3 mL of a 20 mM solution) in CD_3CN. After the reaction was complete, the solutions were concentrated *in vacuo* to provide the cycloadduct. ^{1}H NMR (400 MHz, CD_3CN): δ 8.73 (s, 1H), 8.03 (d, J = 7.6 Hz, 2H), 7.83 (s, 1H), 7.39-7.49 (m, 3H), 2.87 (s, 2H), 2.86 (s, 2H), 1.58 (s, 6H), 1.57 (s, 6H). ^{13}C NMR (125 MHz, CD_3CN) δ 157.2, 153.6, 151.0, 141.5, 139.1, 128.7, 126.6, 119.7, 42.9, 41.8, 41.4, 41.1, 32.0, 31.7. HRMS (ESI) *m*/*z* calcd for $C_{19}H_{24}NS$ $[M+H]^+$ 298.1629, found 298.1639.

***N*-Isopropyl-2-(3-phenyl-5,6,7,8,9,10-hexahydrocycloocta[*c*]pyridin-8-yl)acetamide S4.2**: To a vial containing TCO-isopropylamine **S4.1** (16.0 mg, 0.0757 mmol) was added a solution of triazine **4.2** (12.0 mg, 0.0763 mmol) in 1 mL MeCN. The vial was placed in a 37 °C incubator for 3 d to facilitate air-oxidation to the pyridine adduct. After 3 d, the crude product was

concentrated *in vacuo* and purified by flash column chromatography (eluting with 10-20% EtOAc in CH_2Cl_2) to provide aromatized cycloadduct **S4.2** as a mixture of two-regioisomers (11.0 mg, 43%) as a light-yellow oil. ^{1}H NMR (400 MHz, $CDCl_3$): δ 8.44 (s, 1H), 8.40 (s, 1H), 7.98 (apparent d, J = 7.4 Hz, 4 H), 7.38-7.51 (m, 8H), 4.39-4.58 (m, 3H), 3.77 (m, 2H), 2.76-2.94 (m, 6H), 1.48-2.20 (m, 17 H), 1.14 (m, 13H). ^{13}C NMR (125 MHz, $CDCl_3$) δ 156.2, 156.0, 150.1, 150.0, 149.8, 139.5, 139.4, 134.5, 134.4, 128.7, 128.7, 128.6, 126.8, 120.8, 74.7, 74.5, 43.0, 37.3, 36.6, 33.0, 31.8, 29.8, 29.1, 28.9, 27.9, 27.2, 25.9, 23.1. HRMS (ESI) *m*/*z* calcd for $C_{21}H_{26}N_2O_2Na$ $[M+Na]^+$ 361.1892, found 361.1882.

4.7 References

(1) Grammel, M.; Hang, H. C: Chemical reporters for biological discovery. *Nat. Chem. Biol.* **2013**, *9*, 475.

(2) Patterson, D. M.; Nazarova, L. A.; Prescher, J. A: Finding the right (bioorthogonal) chemistry. *ACS. Chem. Biol.* **2014**, *9*, 592.

(3) Patterson, D. M.; Prescher, J. A: Orthogonal bioorthogonal chemistries. *Curr. Opin. Chem. Biol.* **2015**, *28*, 141.

(4) Patterson, D. M.; Nazarova, L. A.; Xie, B.; Kamber, D. N.; Prescher, J. A: Functionalized cyclopropenes as bioorthogonal chemical reporters. *J. Am. Chem. Soc.* **2012**, *134*, 18638.

(5) Sachdeva, A.; Wang, K.; Elliott, T.; Chin, J. W: Concerted, rapid, quantitative, and site-specific dual labeling of proteins. *J. Am. Chem. Soc.* **2014**, *136*, 7785.

(6) Hudak, J. E.; Barfield, R. M.; de Hart, G. W.; Grob, P.; Nogales, E.; Bertozzi, C. R.; Rabuka, D: Synthesis of heterobifunctional protein fusions using copper-free click chemistry and the aldehyde tag. *Angew. Chem. Int. Ed.* **2012**, *51*, 4161.

(7) Andersen, K. A.; Aronoff, M. R.; McGrath, N. A.; Raines, R. T: Diazo groups endure metabolism and enable chemoselectivity in cellulo. *J. Am. Chem. Soc.* **2015**, *137*, 2412.

(8) Willems, L. I.; Li, N.; Florea, B. I.; Ruben, M.; van der Marel, G. A.; Overkleeft, H. S: Triple bioorthogonal ligation strategy for simultaneous labeling of multiple enzymatic activities. *Angew. Chem. Int. Ed.* **2012**, *51*, 4431.

(9) Karver, M. R.; Weissleder, R.; Hilderbrand, S. A: Bioorthogonal reaction pairs enable simultaneous, selective, multi-target imaging. *Angew. Chem. Int. Ed.* **2012**, *51*, 920.

(10) Kamber, D. N.; Nazarova, L. A.; Liang, Y.; Lopez, S. A.; Patterson, D. M.; Shih, H. W.; Houk, K. N.; Prescher, J. A: Isomeric cyclopropenes exhibit unique bioorthogonal reactivities. *J. Am. Chem. Soc.* **2013**, *135*, 13680.

(11) Shih, H-W.; Kamber, D. N.; Prescher, J. A: Building better bioorthogonal reactions. *Curr. Opin. Chem. Biol.* **2014**, *21*, 103.

(12) Kamber, D. N.; Liang, Y.; Blizzard, R. J.; Liu, F.; Mehl, R. A.; Houk, K. N.; Prescher, J. A: 1,2,4-Triazines are versatile bioorthogonal reagents. *J. Am. Chem. Soc.* **2015**, *137*, 8388.

(13) Blackman, M. L.; Royzen, M.; Fox, J. M: Tetrazine ligation: fast bioconjugation based on inverse-electron-demand Diels-Alder reactivity. *J. Am. Chem. Soc.* **2008**, *130*, 13518.

(14) Yang, J.; Liang, Y.; Seckute, J.; Houk, K. N.; Devaraj, N. K: Synthesis and reactivity comparisons of 1-methyl-3-substituted cyclopropene mini-tags for tetrazine bioorthogonal reactions. *Chem. Eur. J.* **2014**, *20*, 3365.

(15) Yang, J.; Seckute, J.; Cole, C. M.; Devaraj, N. K: Live-cell imaging of cyclopropene tags with fluorogenic tetrazine cycloadditions. *Angew. Chem. Int. Ed.* **2012**, *51*, 7476.

(16) Seckute, J.; Devaraj, N. K: Expanding room for tetrazine ligations in the in vivo chemistry toolbox. *Curr. Opin. Chem. Biol.* **2013**, *17*, 761.

(17) Karver, M. R.; Weissleder, R.; Hilderbrand, S. A: Synthesis and evaluation of a series of 1,2,4,5-tetrazines for bioorthogonal conjugation. *Bioconjugate Chem.* **2011**, *22*, 2263.

(18) Xiong, D. C.; Zhu, J. J.; Han, M. J.; Luo, H. X.; Wang, C.; Yu, Y.; Ye, Y. Q.; Tai, G. H.; Ye, X. S: Rapid probing of sialylated glycoproteins in vitro and in vivo via metabolic oligosaccharide engineering of a minimal cyclopropene reporter. *Org. Biomol. Chem.* **2015**, *13*, 3911.

(19) Wu, H.; Cisneros, B. T.; Cole, C. M.; Devaraj, N. K: Bioorthogonal tetrazine-mediated transfer reactions facilitate reaction turnover in nucleic acid-templated detection of microRNA. *J. Am. Chem. Soc.* **2014**, *136*, 17942.

(20) Debets, M. F.; van Hest, J. C.; Rutjes, F. P: Bioorthogonal labelling of biomolecules: new functional handles and ligation methods. *Org. Biomol. Chem.* **2013**, *11*, 6439.

(21) Ramil, C. P.; Lin, Q: Bioorthogonal chemistry: strategies and recent developments. *Chem. Commun.* **2013**, *49*, 11007.

(22) Shieh, P.; Bertozzi, C. R: Design strategies for bioorthogonal smart probes. *Org. Biomol. Chem.* **2014**, *12*, 9307.

(23) Lang, K.; Chin, J. W: Bioorthogonal reactions for labeling proteins. *ACS Chem. Biol.* **2014**, *9*, 16.

(24) Lang, K.; Chin, J. W. Cellular incorporation of unnatural amino acids and bioorthogonal labeling of proteins. *Chem. Rev.* **2014**, *114*, 4764.

(25) Sauer, J.; Sustmann, R: Mechanistic Aspects of Diels-Alder Reactions - a Critical Survey. *Angew. Chem. Int. Ed.* **1980**, *19*, 779.

(26) Nikic, I.; Plass, T.; Schraidt, O.; Szymanski, J.; Briggs, J. A.; Schultz, C.; Lemke, E. A: Minimal tags for rapid dual-color live-cell labeling and super-resolution microscopy. *Angew. Chem. Int. Ed.* **2014**, *53*, 2245.

(27) Horner, K. A.; Valette, N. M.; Webb, M. E: Strain-promoted reaction of 1,2,4-triazines with bicyclononynes. *Chem. Eur. J.* **2015**, *21*, 14376.

(28) Zhao, Y.; Truhlar, D. G: The M06 suite of density functionals for main group thermochemistry, thermochemical kinetics, noncovalent interactions, excited states, and transition elements: two new functionals and systematic testing of four M06-class functionals and 12 other functionals. *Theor. Chem. Acc.* **2008**, *120*, 215.

(29) Zhao, Y.; Truhlar, D. G: Density functionals with broad applicability in chemistry. *Acc. Chem. Res.* **2008**, *41*, 157.

(30) Frisch, M. J. T.; *et al. Gaussian Inc.: Wallingford, CT* **2013**.

(31) Liang, Y.; Mackey, J. L.; Lopez, S. A.; Liu, F.; Houk, K. N: Control and design of mutual orthogonality in bioorthogonal cycloadditions. *J. Am. Chem. Soc.* **2012**, *134*, 17904.

(32) de Almeida, G.; Sletten, E. M.; Nakamura, H.; Palaniappan, K. K.; Bertozzi, C. R: Thiacycloalkynes for copper-free click chemistry. *Angew. Chem. Int. Ed.* **2012**, *51*, 2443.

(33) King, M.; Baati, R.; Wagner, A: New tetramethylthiepinium (TMTI) for copper-free click chemistry. *Chem. Commun.* **2012**, *48*, 9308.

(34) Sletten, E. M.; Nakamura, H.; Jewett, J. C.; Bertozzi, C. R: Difluorobenzocyclooctyne: synthesis, reactivity, and stabilization by beta-cyclodextrin. *J. Am. Chem. Soc.* **2010**, *132*, 11799.

(35)Debets, M. F.; van Berkel, S. S.; Dommerholt, J.; Dirks, A. T.; Rutjes, F. P.; van Delft, F. L: Bioconjugation with strained alkenes and alkynes. *Acc. Chem. Res.* **2011**, *44*, 805.

(36) Liu, F.; Liang, Y.; Houk, K. N: Theoretical elucidation of the origins of substituent and strain effects on the rates of Diels-Alder reactions of 1,2,4,5-tetrazines. *J. Am. Chem. Soc.* **2014**, *136*, 11483.

(37) Hehre, W. J.; Radom, L.; Schleyer, P. v. R.; Pople, J. A. *Ab Initio Molecular Orbital Theory*, Wiley: New York, 1986.

(38) (a) Zhao, Y.; Truhlar, D. G: Computational characterization and modeling of buckyball tweezers: density functional study of concave–convex π⋯π interactions. *Phys. Chem. Chem. Phys.* **2008**, *10*, 2813. (b) Ribeiro, R. F.; Marenich, A. V.; Cramer, C. J.; Truhlar, D. G: Use of solution-phase vibrational frequencies in continuum models for the free energy of solvation. *J. Phys. Chem. B* **2011**, *115*, 14556.

(39) (a) Barone, V.; Cossi, M: Quantum calculation of molecular energies and energy gradients in solution by a conductor solvent model. *J. Phys. Chem. A* **1998**, *102*, 1995. (b) Cossi, M.; Rega, N.; Scalmani, G.; Barone, V: Energies, structures, and electronic properties of molecules in solution with the C-PCM solvation model. *J. Comput. Chem.* **2003**, *24*, 669. (c) Takano, Y.; Houk, K. N: Benchmarking the conductor-like polarizable continuum model (CPCM) for aqueous solvation free energies of neutral and ionic organic molecules. *J. Chem. Theory Comput.* **2005**, *1*, 70.

(40) Ernd, M.; Heuschmann, M.; Zipse, H: Cycloadditions of Aryl-Substituted 1,2,4-Triazines with 2-Cyclopropylidene-1,3-dimethylimidazolidine – Zwitterions as Discrete Intermediates. *Helvetica. Chimica. Acta.* **2005**, *88*, 1491.

(41) Sletten, E. M.; Nakamura, H.; Jewett, J. C.; Bertozzi, C. R: Difluorobenzocyclooctyne: synthesis, reactivity, and stabilization by beta-cyclodextrin. *J. Am. Chem. Soc.* **2010**, *132,* 11799.

Appendix A: Computational data for Chapter 2

Table S2.1. Coordinates and Energies of Stationary Points

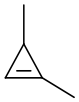

Cp(1,3)

G_{water} = -195.131186 Hartree; E = -195.214932 Hartree

C	-0.685716	0.206784	0.034439
C	0.003444	1.281046	-0.188019
C	0.743755	0.170246	0.498557
H	0.071276	2.282536	-0.585351
C	-1.930745	-0.588044	-0.047853
H	-2.268156	-0.869273	0.955190
H	-2.729430	-0.032687	-0.545229
H	-1.751504	-1.516576	-0.599893
C	1.793558	-0.656829	-0.223730
H	2.785056	-0.196606	-0.147229
H	1.865357	-1.666757	0.195570
H	1.544061	-0.746137	-1.286163
H	0.937560	0.266279	1.572748

Cp(3,3)

G_{water} = -195.125864 Hartree; E = -195.209797 Hartree

C	1.262218	0.000000	-0.647393
C	1.262251	0.000000	0.647586
C	-0.094543	0.000000	-0.000408
H	1.808131	0.000000	1.579301
C	-0.937031	-1.267285	0.000024
H	-1.586720	-1.305168	0.882845
H	-1.585151	-1.306582	-0.883882
H	-0.304718	-2.159209	0.001161
C	-0.937031	1.267285	0.000024
H	-1.585151	1.306582	-0.883882
H	-1.586720	1.305169	0.882845
H	-0.304717	2.159209	0.001161
H	1.809858	0.000000	-1.578546

Ph−C≡N−NPh
⊕ ⊖

NI

G_{water} = -610.561731 Hartree; E = -610.711307 Hartree

C	-0.929904	-0.625562	-0.000063
C	-2.291680	-0.210331	-0.000015
C	-3.315537	-1.171208	0.000353
C	-2.611625	1.156569	-0.000337
C	-4.641117	-0.759662	0.000387

H	-3.061517	-2.225638	0.000609
C	-3.942993	1.549243	-0.000283
H	-1.815938	1.894105	-0.000631
C	-4.960686	0.597031	0.000073
H	-5.429973	-1.504860	0.000667
H	-4.186537	2.606753	-0.000531
H	-5.999156	0.911115	0.000106
N	0.176906	-0.991934	-0.000090
N	1.332102	-1.493421	-0.000138
C	2.389061	-0.569760	-0.000059
C	2.235545	0.823145	0.000151
C	3.681500	-1.113310	-0.000194
C	3.356425	1.647282	0.000221
H	1.241562	1.261702	0.000269
C	4.790834	-0.281467	-0.000124
H	3.783272	-2.193627	-0.000356
C	4.638473	1.105853	0.000084
H	3.222289	2.725176	0.000389
H	5.784936	-0.718636	-0.000231
H	5.508223	1.754449	0.000140

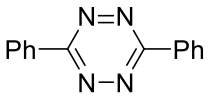

Tz

G_{water} = -758.159878 Hartree; E = -758.329060 Hartree

C	-0.000124	-1.287597	-0.000573
C	0.000124	1.287597	-0.000573
N	1.183187	0.651657	-0.001373
N	1.183061	-0.652015	-0.001280
N	-1.183061	0.652015	-0.001280
N	-1.183187	-0.651657	-0.001373
C	0.000214	2.764533	0.000244
C	1.210798	3.465467	0.001564
C	-1.210325	3.465451	-0.000733
C	1.206617	4.855025	0.001864
H	2.143368	2.912363	0.002220
C	-1.206155	4.855025	-0.000518
H	-2.142875	2.912278	-0.002082
C	0.000214	5.552030	0.000788
H	2.147731	5.395799	0.002879
H	-2.147320	5.395715	-0.001343
H	0.000236	6.637766	0.001079
C	-0.000214	-2.764533	0.000244
C	-1.210798	-3.465467	0.001564
C	1.210325	-3.465451	-0.000733
C	-1.206617	-4.855025	0.001864
H	-2.143368	-2.912363	0.002220
C	1.206155	-4.855025	-0.000518
H	2.142875	-2.912278	-0.002082

C	-0.000214	-5.552030	0.000788
H	-2.147731	-5.395799	0.002879
H	2.147320	-5.395715	-0.001343
H	-0.000236	-6.637766	0.001079

TS-NI-Cp(1,3)

G_{water} = -805.663047 Hartree; E = -805.923388 Hartree

C	-1.173412	-0.139874	-0.328353
N	-0.145854	-0.631460	-0.691817
N	1.010317	-0.484744	-1.181569
C	2.075049	-0.965123	-0.401779
C	3.348352	-0.902504	-0.983126
C	1.939800	-1.451238	0.906149
C	4.465803	-1.302231	-0.262875
H	3.430960	-0.546306	-2.005323
C	3.065449	-1.855517	1.614975
H	0.952720	-1.514932	1.355387
C	4.332338	-1.780592	1.040300
H	5.447333	-1.248232	-0.724170
H	2.950178	-2.232655	2.626913
H	5.206304	-2.098206	1.599535
C	-0.440489	2.075250	-0.336111
C	0.603104	2.033092	0.747529
C	0.821282	2.031780	-0.727709
C	-2.579963	-0.403870	-0.127719
C	-3.217669	-1.462469	-0.789927
C	-3.307490	0.424468	0.733730
C	-4.572573	-1.686128	-0.583552
H	-2.642175	-2.096172	-1.456984
C	-4.662196	0.190347	0.938107
H	-2.795328	1.239307	1.236319
C	-5.294548	-0.861999	0.279477
H	-5.067598	-2.505001	-1.095570
H	-5.225525	0.829661	1.609953
H	-6.353422	-1.041094	0.437645
H	0.725292	1.084579	1.288118
C	1.851316	2.367802	-1.739244
H	2.750391	1.761724	-1.597919
H	1.472953	2.208299	-2.751733
H	2.140212	3.421561	-1.638370
H	-1.415967	2.478544	-0.571165
C	0.952917	3.250770	1.585822
H	0.310411	3.324153	2.470716
H	1.990785	3.206788	1.933727
H	0.828814	4.169623	1.002448

TS-NI-Cp(3,3)

G_{water} = -805.656784 Hartree; E = -805.916333 Hartree

C	-1.078797	-0.204813	-0.303942
N	-0.012448	-0.624510	-0.648565
N	1.114077	-0.400554	-1.168768
C	2.238094	-0.882929	-0.470185
C	3.486651	-0.568000	-1.017951
C	2.174718	-1.633154	0.710887
C	4.650804	-0.985631	-0.388608
H	3.516437	0.010484	-1.936004
C	3.347410	-2.050393	1.330467
H	1.207006	-1.888389	1.133535
C	4.589828	-1.729378	0.789603
H	5.613702	-0.731205	-0.821614
H	3.287934	-2.632911	2.245263
H	5.501282	-2.057901	1.278444
C	-0.617697	2.081795	-0.791772
C	0.417250	2.644638	0.148462
C	0.631905	2.066158	-1.215820
H	1.296174	2.073859	-2.064482
C	-2.462187	-0.569477	-0.102815
C	-2.980298	-1.763066	-0.625560
C	-3.289434	0.295034	0.622280
C	-4.314963	-2.083995	-0.415857
H	-2.329784	-2.423007	-1.190742
C	-4.624245	-0.033266	0.826494
H	-2.868546	1.214490	1.018294
C	-5.136788	-1.220668	0.308217
H	-4.716592	-3.008124	-0.819081
H	-5.264920	0.635775	1.391805
H	-6.180018	-1.474716	0.468441
C	0.845448	1.895736	1.401443
H	1.886629	2.132814	1.651378
H	0.225616	2.186386	2.259528
H	0.772102	0.814177	1.277744
C	0.515306	4.155352	0.327294
H	-0.125164	4.493065	1.151652
H	1.542453	4.453843	0.569651
H	0.210663	4.682799	-0.581313
H	-1.644418	2.210352	-1.107005

TS-Tz-Cp(1,3)

G_{water} = -953.260183 Hartree; E = -953.537839 Hartree

C	-1.168019	-0.701568	-0.339577
N	-0.528455	-0.339192	-1.489289
N	0.755193	-0.324681	-1.462519
C	1.345888	-0.649437	-0.270979
N	0.720682	-1.553830	0.559350
N	-0.556099	-1.569982	0.528386
C	-0.583430	1.175429	0.927905

C	0.754269	1.097658	0.862438
C	0.097072	2.146293	0.015992
H	1.604120	1.012673	1.525837
H	0.052734	1.946539	-1.057971
C	2.824936	-0.558255	-0.197087
C	3.525112	-1.240993	0.800824
C	3.516046	0.244723	-1.107601
C	4.909152	-1.126883	0.877957
H	2.977451	-1.863620	1.500240
C	4.899449	0.354492	-1.024562
H	2.960885	0.769425	-1.878265
C	5.599041	-0.330707	-0.033157
H	5.450108	-1.663751	1.651080
H	5.433906	0.975943	-1.736442
H	6.679495	-0.243312	0.029442
C	-2.643922	-0.631675	-0.326730
C	-3.382484	-1.399324	0.577977
C	-3.302071	0.245473	-1.193458
C	-4.768400	-1.288899	0.611855
H	-2.861431	-2.079305	1.243622
C	-4.687503	0.353161	-1.152705
H	-2.717204	0.835837	-1.891850
C	-5.423588	-0.412428	-0.249747
H	-5.338971	-1.890228	1.312913
H	-5.194522	1.036733	-1.826759
H	-6.505394	-0.325555	-0.218737
C	0.182079	3.617554	0.374496
H	1.060819	4.077632	-0.088078
H	-0.703254	4.157758	0.024022
H	0.258471	3.756619	1.457828
C	-1.693074	1.177910	1.920205
H	-2.669955	1.292368	1.445308
H	-1.688499	0.258257	2.511725
H	-1.541334	2.024637	2.600320

TS-Tz-Cp(3,3)

G_{water} = -953.245086 Hartree; E = -953.522432 Hartree

C	1.257223	-0.750901	-0.261619
C	-1.257232	-0.750883	-0.261616
N	-0.638409	-1.687065	0.536993
N	0.638393	-1.687069	0.536996
N	-0.641253	-0.381130	-1.422918
N	0.641232	-0.381162	-1.422918
C	0.670780	0.911906	1.080881
C	-0.670795	0.911890	1.080694
C	0.000048	2.170409	0.597593
H	-1.489933	0.654327	1.739073
H	1.489765	0.654227	1.739409
C	-2.734369	-0.650963	-0.202746

C	-3.405757	0.196202	-1.088101
C	-3.453225	-1.368257	0.756689
C	-4.788837	0.314957	-1.019240
H	-2.834456	0.749711	-1.826417
C	-4.837391	-1.243873	0.820474
H	-2.921527	-2.026008	1.436102
C	-5.507639	-0.404223	-0.065894
H	-5.307663	0.971329	-1.710816
H	-5.393904	-1.807434	1.562798
H	-6.587795	-0.309019	-0.013673
C	2.734354	-0.650971	-0.202738
C	3.405745	0.196259	-1.088029
C	3.453210	-1.368332	0.756648
C	4.788824	0.315014	-1.019154
H	2.834454	0.749828	-1.826306
C	4.837376	-1.243949	0.820447
H	2.921513	-2.026134	1.436012
C	5.507624	-0.404232	-0.065858
H	5.307649	0.971439	-1.710681
H	5.393887	-1.807562	1.562732
H	6.587781	-0.309029	-0.013628
C	0.000284	2.658925	-0.843496
H	-0.884054	3.284122	-1.011281
H	0.882895	3.286936	-1.009887
H	0.002216	1.866494	-1.586020
C	-0.000191	3.344502	1.571490
H	-0.884261	3.971982	1.411824
H	-0.001083	3.007541	2.611964
H	0.884578	3.971357	1.413170

Appendix B: NMR spectra for Chapter 2

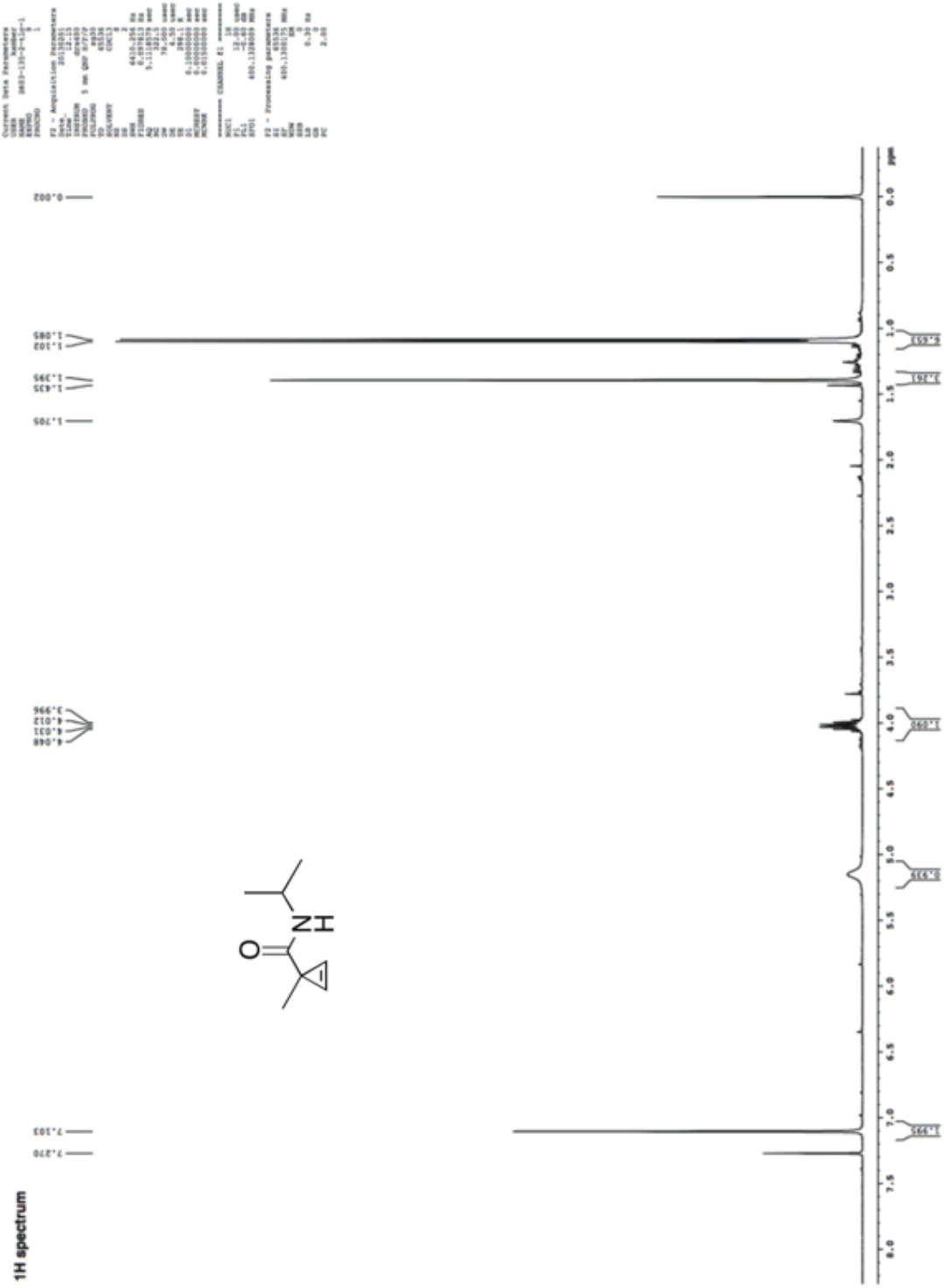
1H spectrum
7.270
7.103
4.068
4.031
4.012
3.996
1.705
1.635
1.395
1.102
1.085
0.002
ppm

13C spectrum with 1H decoupling

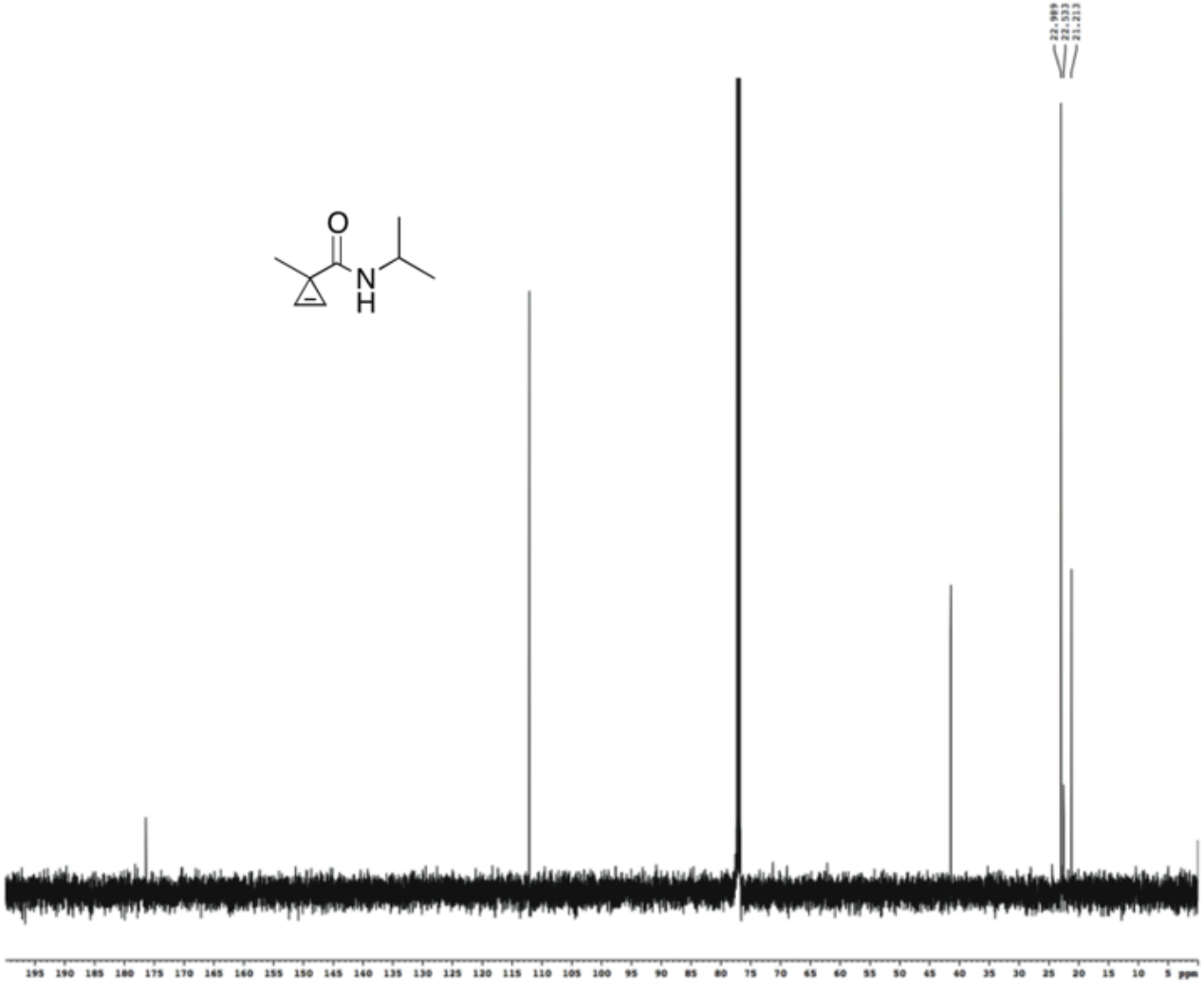


```
Current Data Parameters
USER            kamber
NAME      0803-135-2-tlc-1
EXPNO             22
PROCNO             1

F2 - Acquisition Parameters
Date_        20130201
Time            12.33
INSTRUM         qs300
PROBHD   5 mm broadband
PULPROG       zgpg30
TD             65536
SOLVENT        CDCl3
NS               289
DS                 4
SWH          30303.031 Hz
FIDRES       0.462388 Hz
AQ           1.0813960 sec
RG             14596.5
DW             16.500 usec
DE              4.50 usec
TE             298.0 K
D1           0.25000000 sec
d11          0.03000000 sec
MCREST       0.00000000 sec
MCWRK        0.01500000 sec

======== CHANNEL f1 ========
NUC1             13C
P1              7.70 usec
PL1             0.00 dB
SFO1       125.5880432 MHz

======== CHANNEL f2 ========
CPDPRG2       waltz16
NUC2             1H
PCPD2          80.00 usec
PL2            -3.00 dB
PL12           13.20 dB
SFO2       499.4024970 MHz

F2 - Processing parameters
SI             65536
SF         125.5742300 MHz
WDW              EM
SSB               0
LB             1.00 Hz
GB                0
PC             2.00
```

1H spectrum

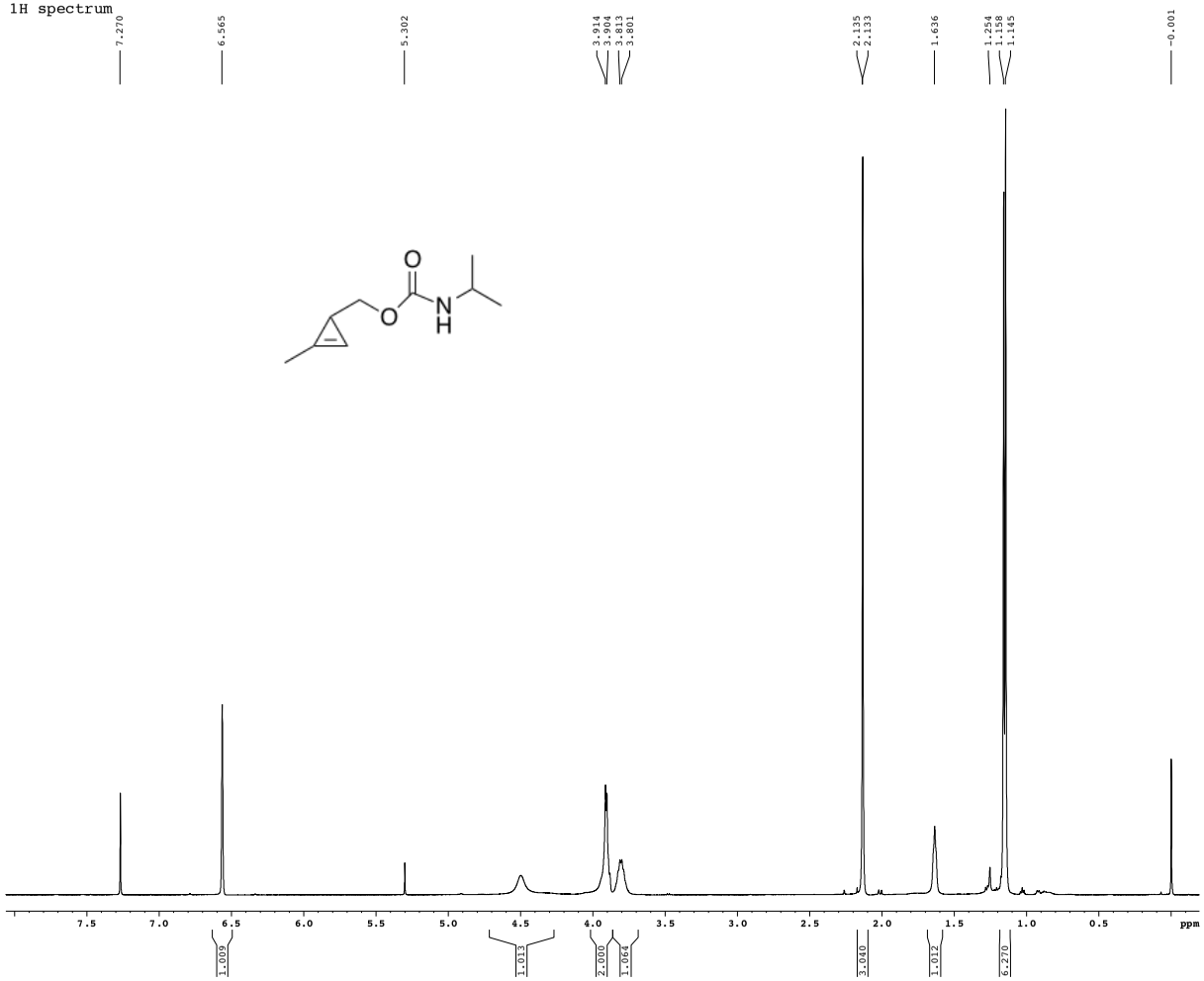


```
Current Data Parameters
USER            dpatte
NAME          DMP3_055
EXPNO                 5
PROCNO                1

F2 - Acquisition Parameters
Date_          20121120
Time              14.51
INSTRUM        cryo500
PROBHD   5 mm CPTCI 1H-
PULPROG          zg30
TD               81728
SOLVENT          CDCl3T
NS                    8
DS                    2
SWH            8012.820 Hz
FIDRES         0.098043 Hz
AQ           5.0998774 sec
RG                   16
DW              62.400 usec
DE               6.00 usec
TE              298.0 K
D1           0.10000000 sec
MCREST       0.00000000 sec
MCWRK        0.01500000 sec

======== CHANNEL f1 ========
NUC1                 1H
P1                7.50 usec
PL1               1.60 dB
SFO1        500.2235015 MHz

F2 - Processing parameters
SI               65536
SF          500.2200258 MHz
WDW                 no
SSB                  0
LB                0.00 Hz
GB                   0
PC                4.00
```

Z-restored spin-echo 13C spectrum with 1H decoupling

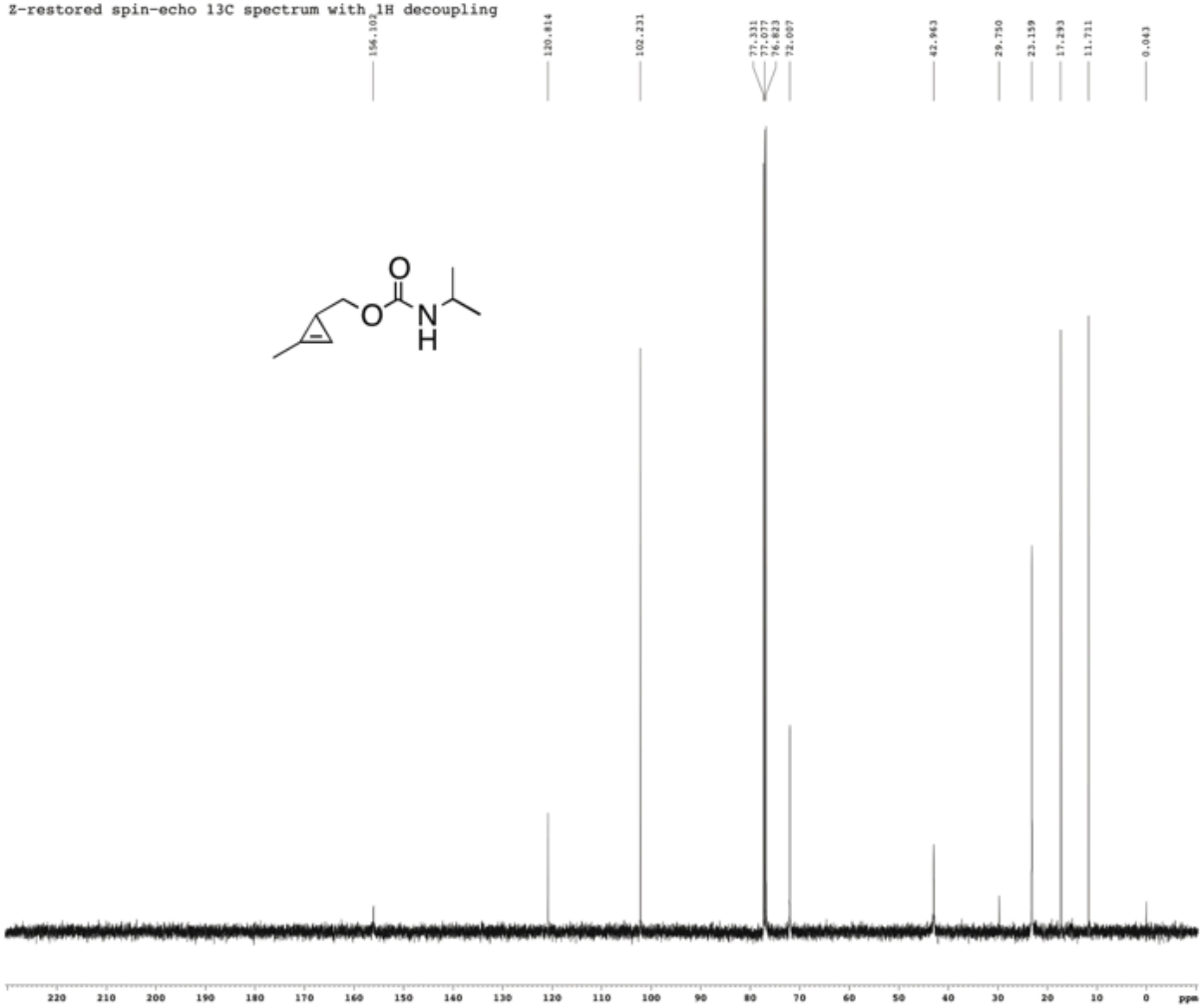


```
Current Data Parameters
USER            dpatse
NAME          DMP3_055
EXPNO                 4
PROCNO                1

F2 - Acquisition Parameters
Date_        20121120
Time            14.41
INSTRUM       cryo500
PROBHD   5 mm CPTCI 1H-
PULPROG  Spin&Echo@30gg.prd
TD              65536
SOLVENT         CDCl3
NS                448
DS                 16
SWH          30303.031 Hz
FIDRES       0.462388 Hz
AQ           1.0813940 sec
RG               3251
DW             16.500 usec
DE              6.00 usec
TE            298.0 K
D1           0.25000000 sec
d11          0.03000000 sec
D16          0.00020000 sec
d17          0.00019600 sec
MCREST       0.00000000 sec
MCWRK        0.01500000 sec
P2             31.00 usec

======== CHANNEL f1 ========
NUC1              13C
P1              15.50 usec
P11            500.00 usec
P12           2000.00 usec
PL0            120.00 dB
PL1             -1.00 dB
SFO1       125.7942548 MHz
SP1             3.20 dB
SP2             3.20 dB
SPNAM1   Crp60,0.5,20.1
SPNAM2     Crp60comp.4
SPOFF1          0.00 Hz
SPOFF2          0.00 Hz

======== CHANNEL f2 ========
CPDPRG2       waltz16
NUC2               1H
PCPD2         100.00 usec
PL2             1.60 dB
PL12           24.60 dB
SFO2       500.2225011 MHz

====== GRADIENT CHANNEL =====
GPNAM1        SINE.100
GPNAM2        SINE.100
GPZ1             0.00 %
GPZ2             0.00 %
GPZ1             0.00 %
GPZ2             0.00 %
GPZ1            30.00 %
GPZ2            50.00 %
p15           500.00 usec
p16          1000.00 usec

F2 - Processing parameters
SI              65536
SF         125.7804150 MHz
WDW               EM
SSB                0
LB              1.00 Hz
GB                 0
PC              2.00
```

1H spectrum

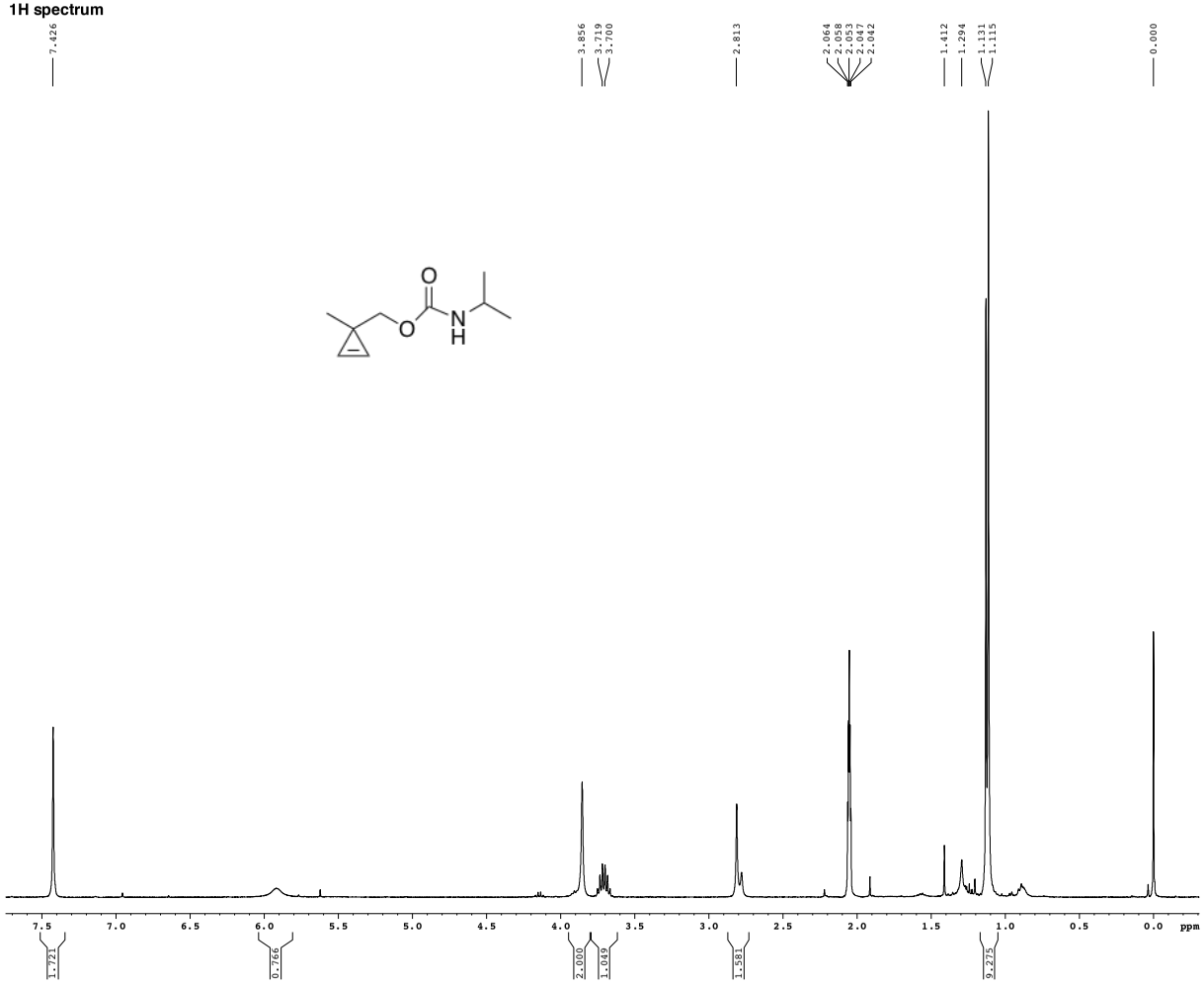


```
Current Data Parameters
USER              kamber
NAME            DK04-029
EXPNO                  3
PROCNO                 1

F2 - Acquisition Parameters
Date_           20130319
Time              14.43
INSTRUM           drx400
PROBHD   5 mm QNP H/F/P
PULPROG            zg30
TD                65536
SOLVENT          Acetone
NS                     8
DS                     2
SWH            6410.256 Hz
FIDRES         0.097813 Hz
AQ            5.1118579 sec
RG                   362
DW               78.000 usec
DE                 4.50 usec
TE               298.0 K
D1           0.10000000 sec
MCREST       0.00000000 sec
MCWRK        0.01500000 sec

======== CHANNEL f1 ========
NUC1                  1H
P1                12.00 usec
PL1               -0.60 dB
SFO1        400.1328009 MHz

F2 - Processing parameters
SI                65536
SF          400.1300094 MHz
WDW                    EM
SSB                    0
LB                  0.30 Hz
GB                     0
PC                  2.00
```

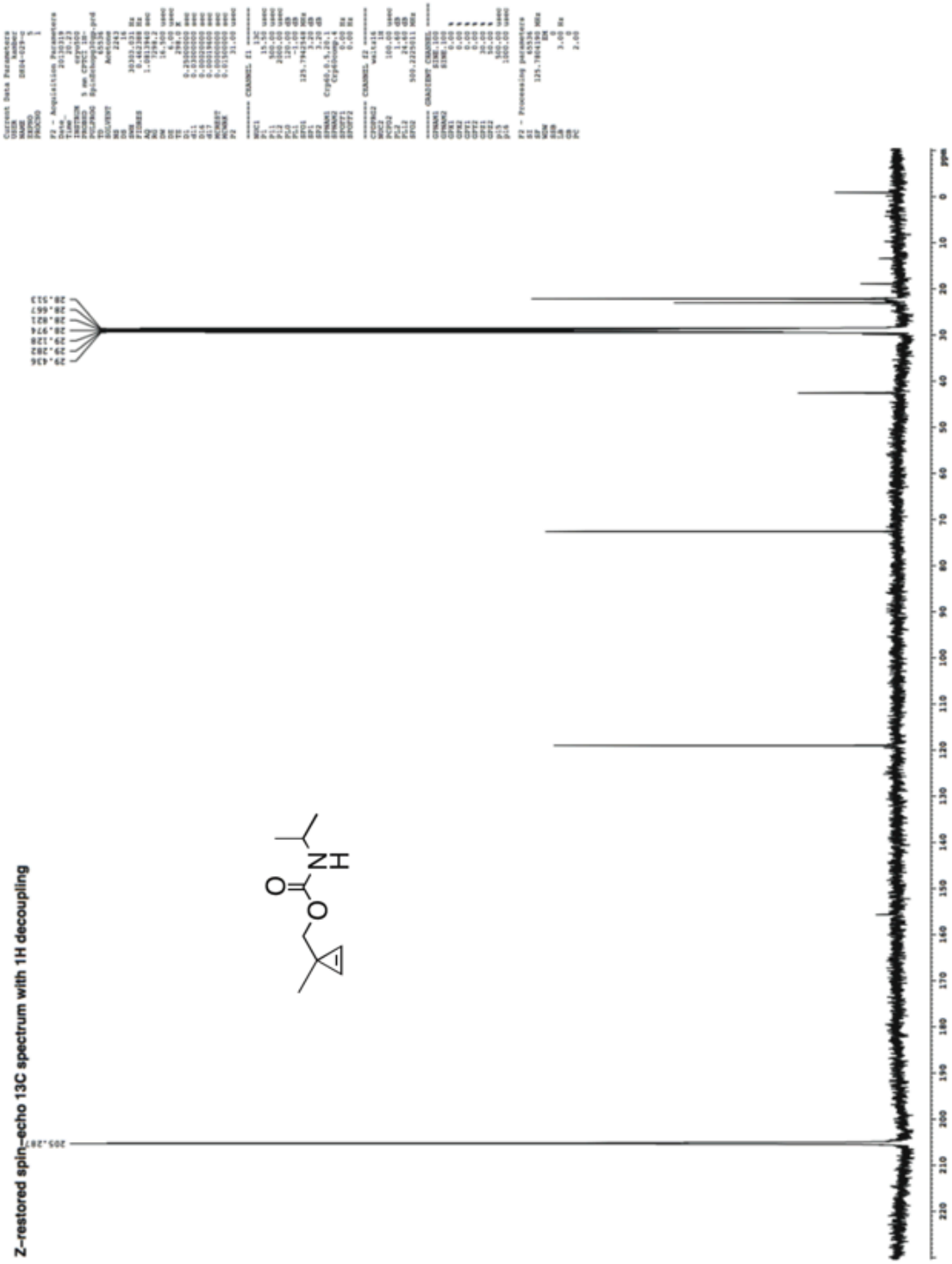
Z-restored spin-echo 13C spectrum with 1H decoupling
205.281
29.436
29.128
29.282
28.974
28.821
28.667
28.513
ppm

1H spectrum

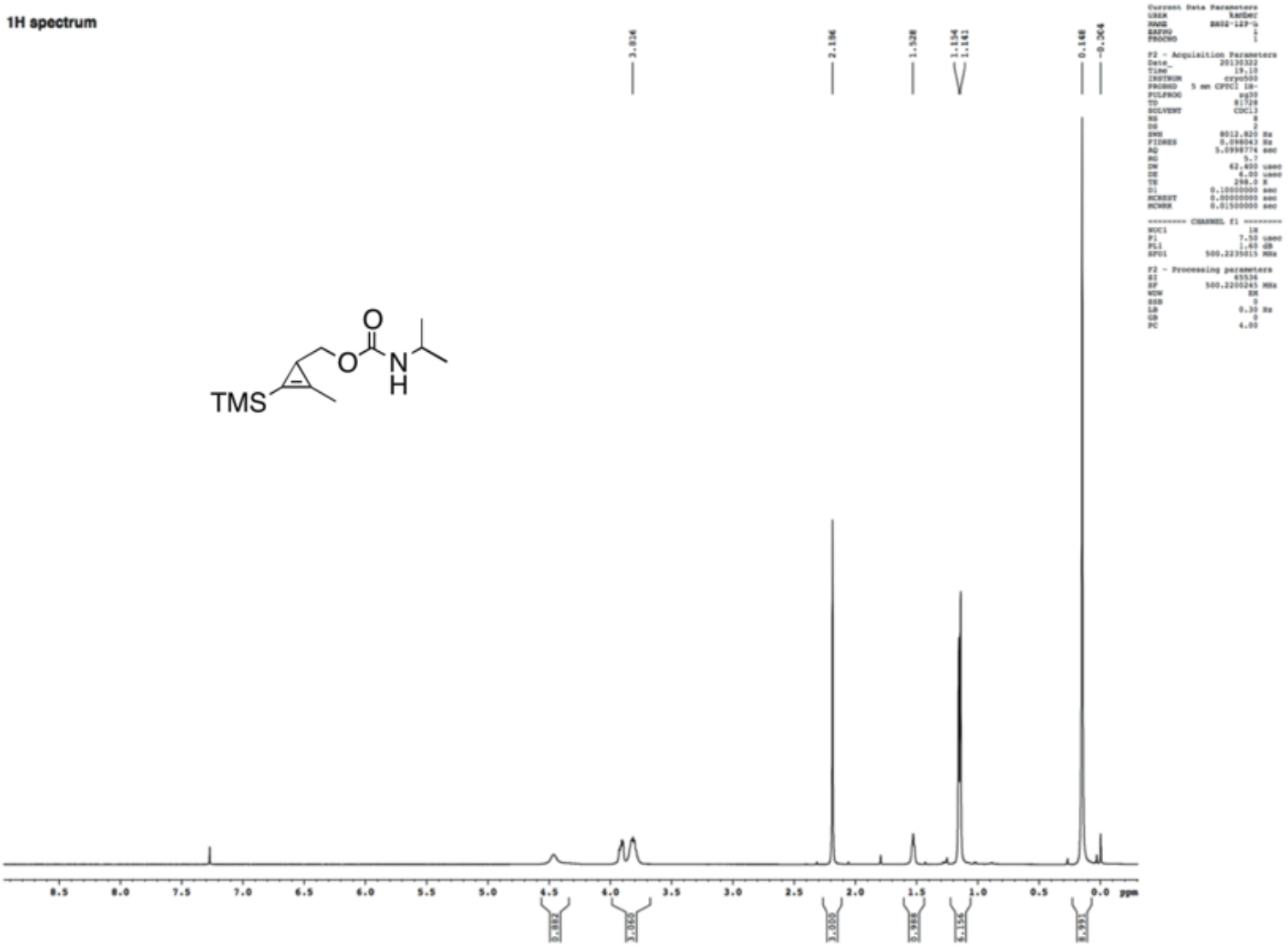
TMS
O
O
N
H
3.934
2.194
1.528
1.154
1.141
0.148
-0.364
8.5
8.0
7.5
7.0
6.5
6.0
5.5
5.0
4.5
4.0
3.5
3.0
2.5
2.0
1.5
1.0
0.5
0.0
ppm
2.893
2.960
3.000
2.988
5.154
8.993

Z–restored spin–echo 13C spectrum with 1H decoupling

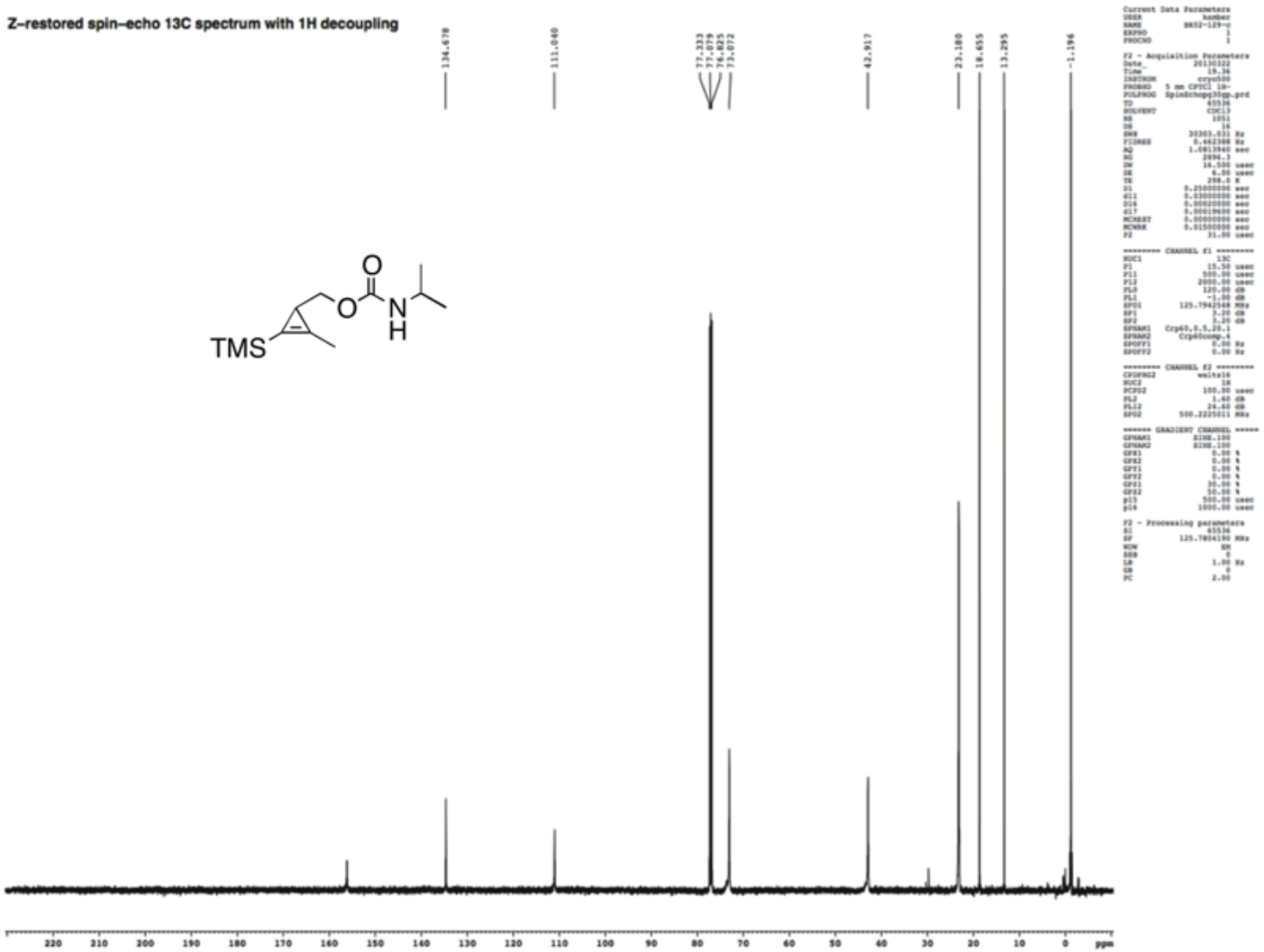

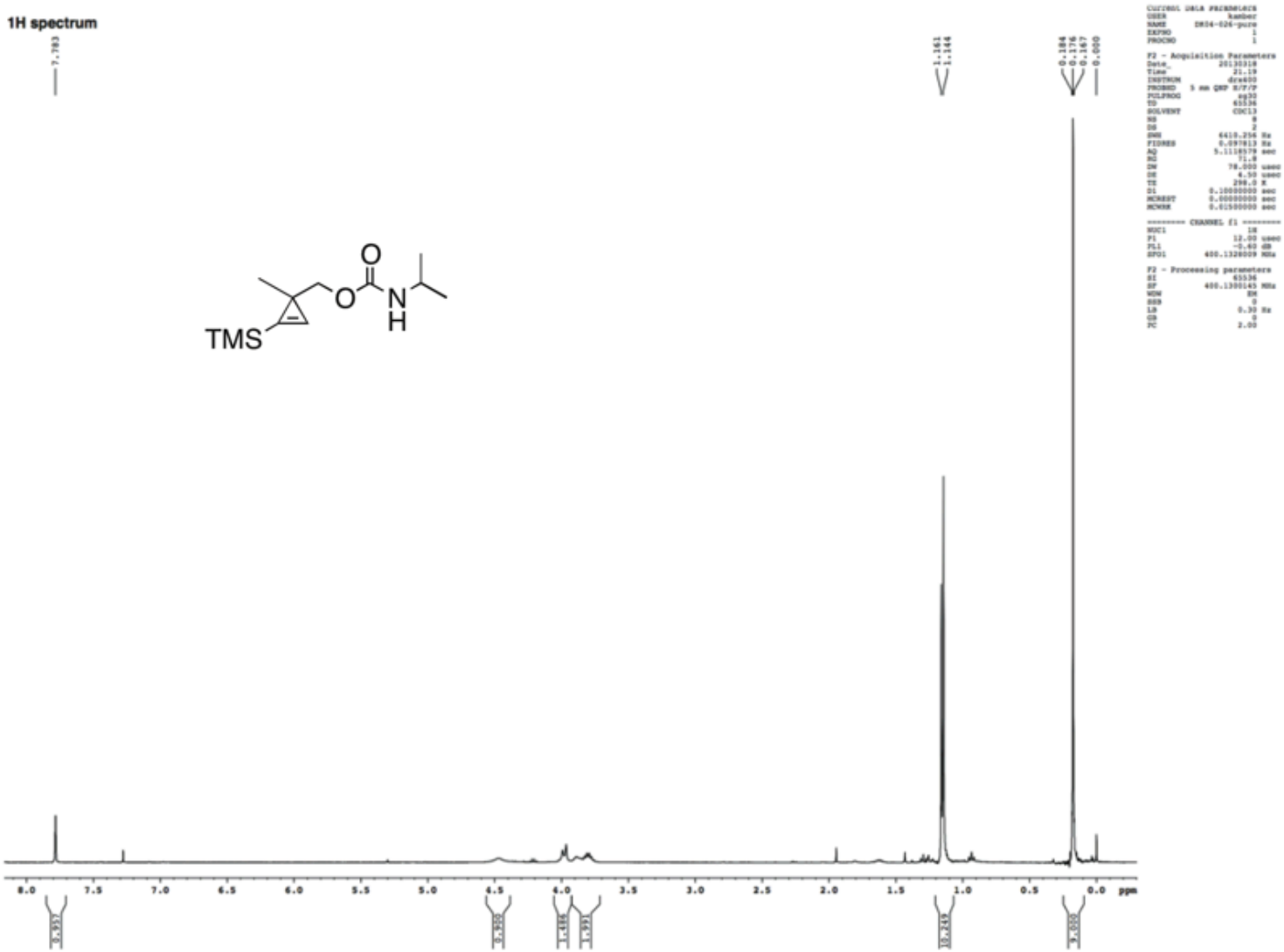
1H spectrum
7.783
1.161
1.144
0.184
0.176
0.147
0.000
TMS
O
O
N
H
8.0
7.5
7.0
6.5
6.0
5.5
5.0
4.5
4.0
3.5
3.0
2.5
2.0
1.5
1.0
0.5
0.0
ppm
3.95
3.00
1.48
1.93
15.43
9.00

Z-restored spin-echo 13C spectrum with 1H decoupling

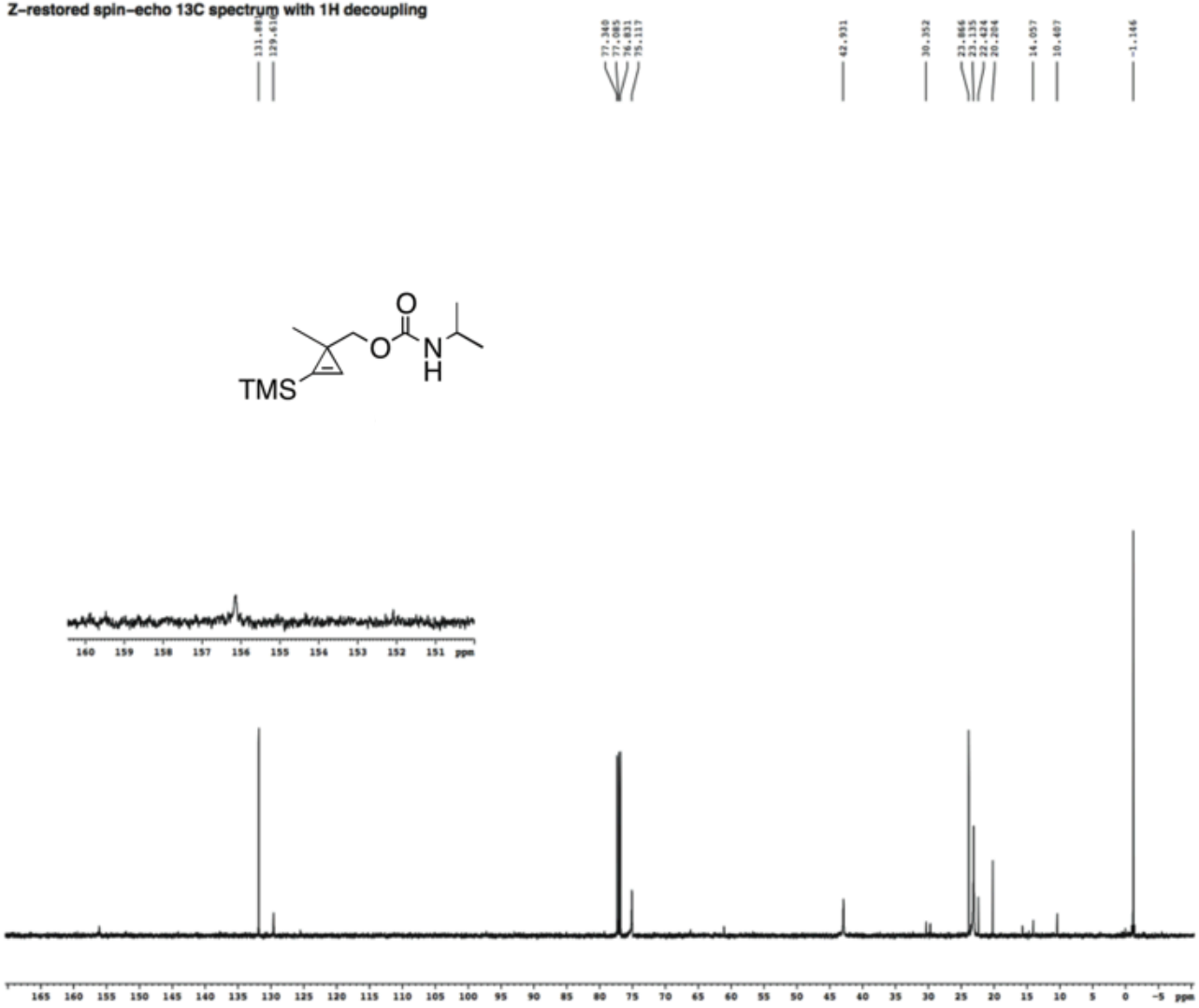


```
Current Data Parameters
USER            hamber
NAME          DR34-026-c
EXPNO                 2
PROCNO                1

F2 - Acquisition Parameters
Date_          20130318
TIME             21.32
INSTRUM        cryo500
PROBHD   5 mm CPTCI 1H-
PULPROG  zgpg30cpd.prd
TD             65536
SOLVENT          CDCl3
NS               239
DS                 16
SWH            33333.331 Hz
FIDRES         0.462388 Hz
AQ             1.0813960 sec
RG               7998.2
DW               16.500 usec
DE                4.00 usec
TE              298.0 K
D1            0.25000000 sec
d11           0.03000000 sec
D16           0.00020000 sec
d17           0.00019600 sec
MCWEST        0.00000000 sec
MCWRK         0.01500000 sec
P2               31.00 usec

======== CHANNEL f1 ========
NUC1               13C
P1               15.50 usec
P11             500.00 usec
P12            2000.00 usec
PL0             120.00 dB
PL1              -1.00 dB
SFO1        125.7942548 MHz
SP1              3.20 dB
SP2              3.20 dB
SPNAM1   Crp60,0.5,20.1
SPNAM2      Crp60comp.4
SPOFF1           0.00 Hz
SPOFF2           0.00 Hz

======== CHANNEL f2 ========
CPDPRG2        waltz16
NUC2                1H
PCPD2           100.00 usec
PL2              1.40 dB
PL12            24.60 dB
SFO2        500.2225011 MHz

====== GRADIENT CHANNEL =====
GPNAM1         SINE.100
GPNAM2         SINE.100
GPX1             0.00 %
GPX2             0.00 %
GPY1             0.00 %
GPY2             0.00 %
GPZ1            30.00 %
GPZ2            50.00 %
p15             500.00 usec
p16            1000.00 usec

F2 - Processing parameters
SI             65536
SF        125.7804190 MHz
WDW              EM
SSB               0
LB             1.00 Hz
GB               0
PC             2.00
```

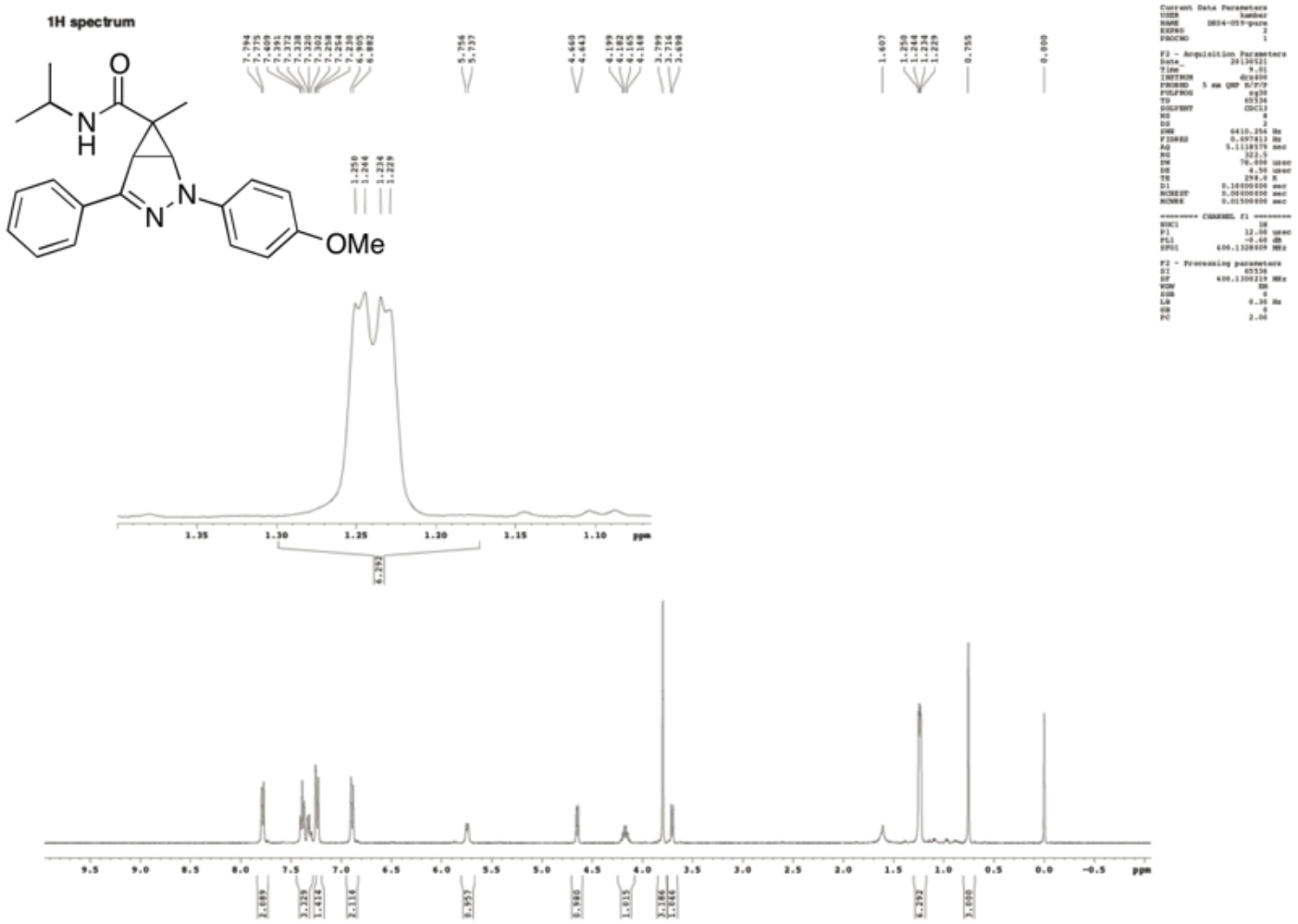
1H spectrum
OMe

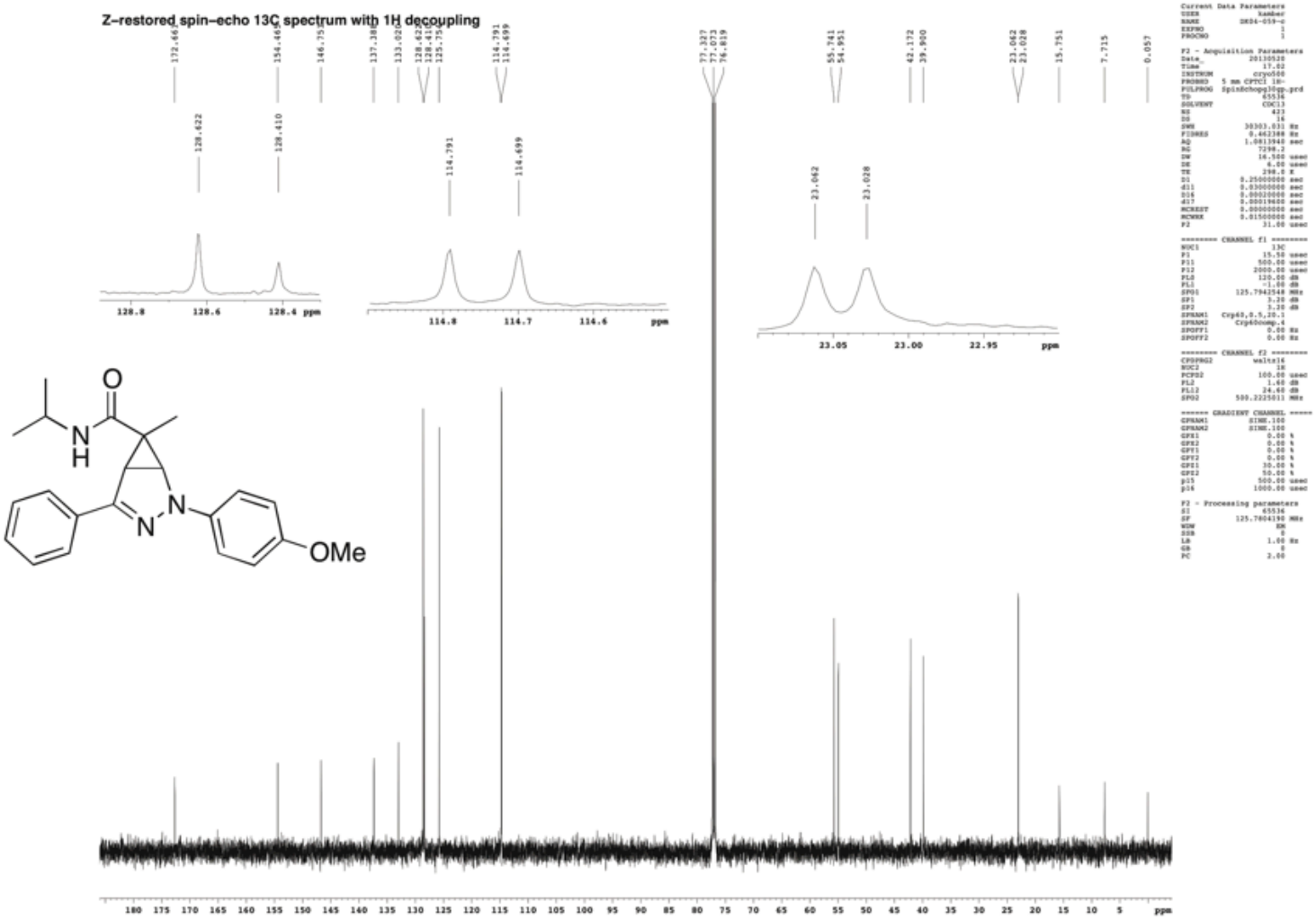
Z-restored spin-echo 13C spectrum with 1H decoupling
172.466
154.460
146.755
137.380
133.020
128.622
128.410
125.755
114.791
114.699
77.327
77.073
76.819
55.741
54.951
42.172
39.900
23.042
23.028
15.751
7.715
0.057
128.622
128.410
114.791
114.699
23.042
23.028
128.8
128.6
128.4 ppm
114.8
114.7
114.6
ppm
23.05
23.00
22.95
ppm
O
N
H
N
N
OMe
180 175 170 165 160 155 150 145 140 135 130 125 120 115 110 105 100 95 90 85 80 75 70 65 60 55 50 45 40 35 30 25 20 15 10 5 ppm
Current Data Parameters
USER kamber
NAME 0604-059-c
EXPNO 1
PROCNO 1
F2 - Acquisition Parameters
Date_ 20130520
Time 17.02
INSTRUM cryo500
PROBHD 5 mm CPTCI 1H-
PULPROG Spinechopg10gp.prd
TD 65536
SOLVENT CDCl3
NS 423
DS 16
SWH 30303.031 Hz
FIDRES 0.462388 Hz
AQ 1.0813940 sec
RG 7298.2
DW 16.500 usec
DE 6.00 usec
TE 298.0 K
D1 0.25000000 sec
d11 0.03000000 sec
D16 0.00020000 sec
d17 0.00019600 sec
MCREST 0.00000000 sec
MCWRK 0.01500000 sec
P2 31.00 usec
======== CHANNEL f1 ========
NUC1 13C
P1 15.50 usec
P11 500.00 usec
P12 2000.00 usec
PL0 120.00 dB
PL1 -1.00 dB
SFO1 125.7942548 MHz
SF1 3.20 dB
SF2 1.28 dB
SPNAM1 Cryp60,0.5,20.1
SPNAM2 Cryp600mp.4
SPOFF1 0.00 Hz
SPOFF2 0.00 Hz
======== CHANNEL f2 ========
CPDPRG2 waltz16
NUC2 1H
PCPD2 100.00 usec
PL2 1.60 dB
PL12 24.40 dB
SFO2 500.2225011 MHz
====== GRADIENT CHANNEL =====
GPNAM1 SINE.100
GPNAM2 SINE.100
GPZ1 0.00 %
GPZ2 0.00 %
GPZ3 0.00 %
GPZ4 0.00 %
GPZ11 30.00 %
GPZ12 50.00 %
p15 500.00 usec
p16 1000.00 usec
F2 - Processing parameters
SI 65536
SF 125.7804190 MHz
WDW EM
SSB 0
LB 1.00 Hz
GB 0
PC 2.00

1H spectrum

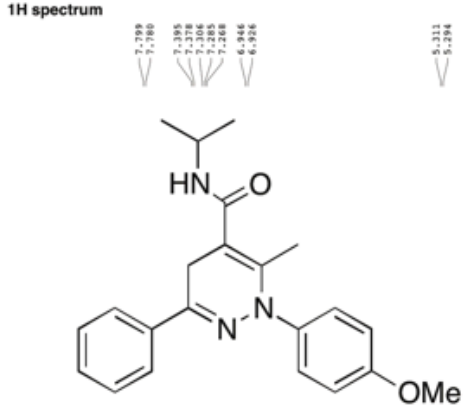

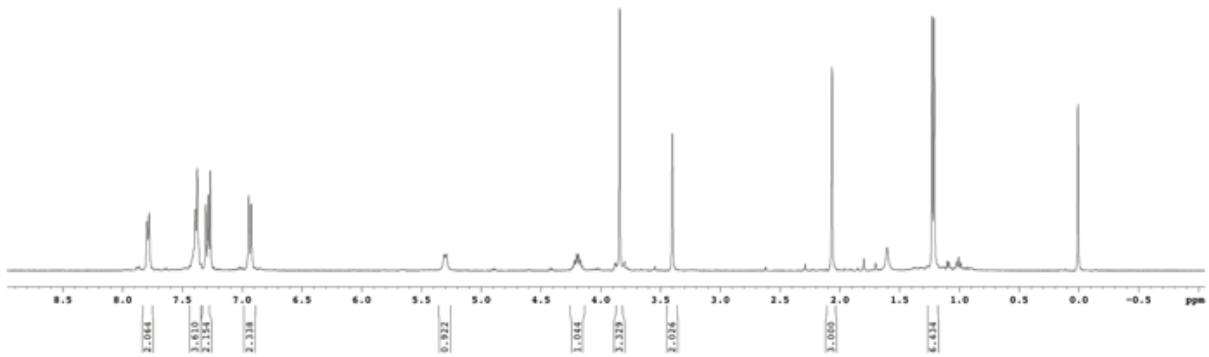


```
Current Data Parameters
USER            kamber
NAME      0834-072-highrac
EXPNO                 1
PROCNO                1

F2 - Acquisition Parameters
Date_           20130601
Time              16.57
INSTRUM           drx400
PROBHD   5 mm QNP H/P/F
PULPROG           zg30
TD                65536
SOLVENT           CDCl3
NS                    8
DS                    2
SWH            6410.256 Hz
FIDRES         0.097813 Hz
AQ             5.1118579 sec
RG               322.5
DW               78.000 usec
DE                4.50 usec
TE               298.1 K
D1             0.10000000 sec
MCREST         0.00000000 sec
MCWRK          0.01500000 sec

======== CHANNEL f1 ========
NUC1                 1H
P1                12.00 usec
PL1               -0.68 dB
SFO1        400.1320009 MHz

F2 - Processing parameters
SI                65536
SF          400.1300175 MHz
WDW                 EM
SSB                  0
LB                0.30 Hz
GB                   0
PC                2.00
```

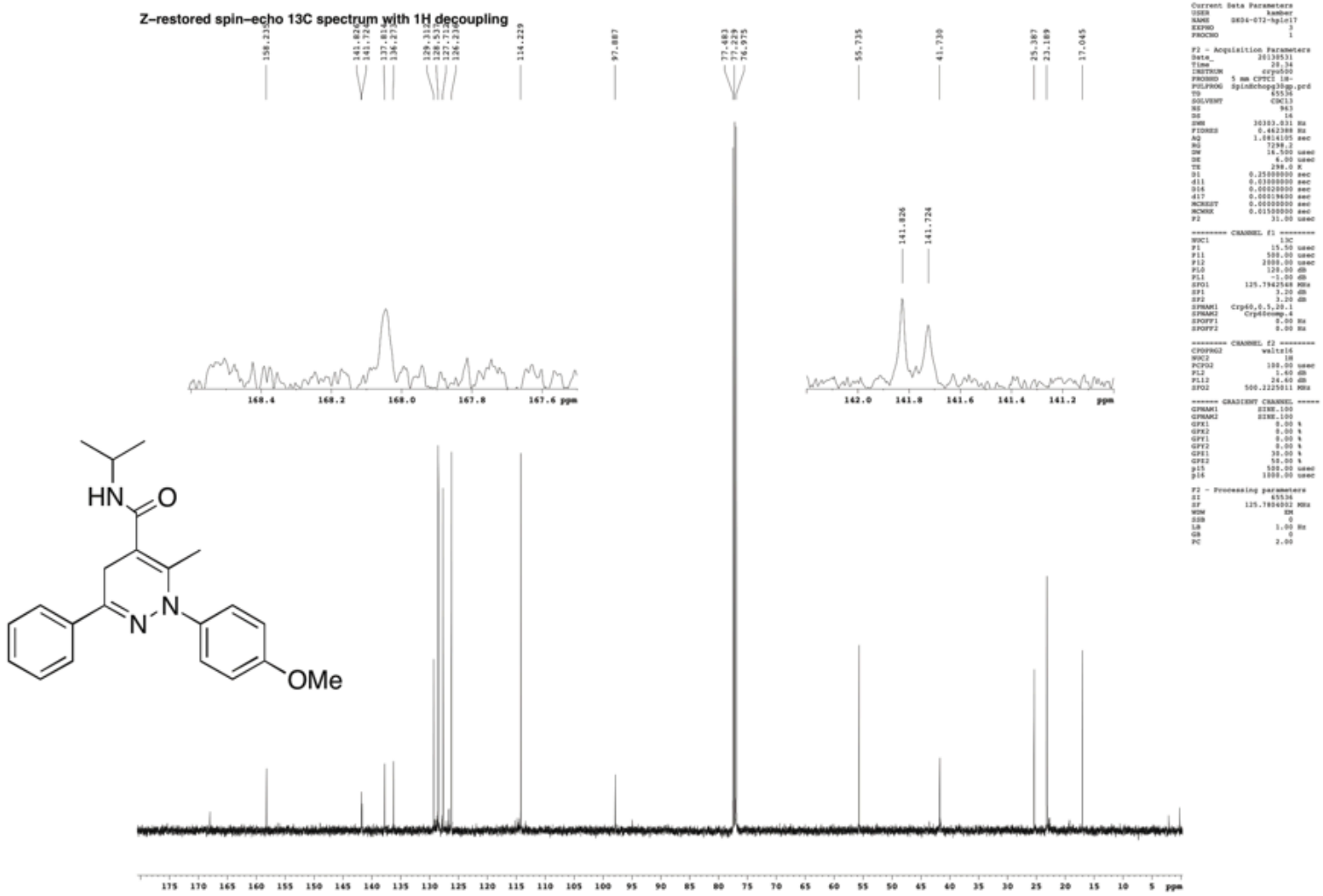
Z-restored spin-echo 13C spectrum with 1H decoupling
HN
O
N
N
OMe
ppm

Appendix C: Additional computational data for Chapter 3

Table S3.1 Coordinates and energies of stationary points

G(water) = -296.264818 Hartree

C	1.260460	0.000000	0.000001
C	-1.260460	0.000000	-0.000001
H	2.345050	0.000000	-0.000003
H	-2.345050	0.000000	0.000003
N	-0.656986	-1.190085	0.000000
N	0.656986	-1.190086	0.000000
N	-0.656986	1.190086	0.000000
N	0.656986	1.190085	0.000000

G(water) = -280.251744 Hartree

C	0.865860	0.992684	0.000004
C	-1.251104	0.275588	-0.000012
C	1.257122	-0.348729	0.000001
H	1.595773	1.799211	0.000000
H	-2.316274	0.488177	0.000018
H	2.300916	-0.646420	-0.000003
N	0.365019	-1.331397	0.000001
N	-0.922299	-1.012485	0.000001
N	-0.415817	1.321278	0.000000

G(water) = -280.227078 Hartree

N	0.000000	0.000000	1.376240
C	0.000000	0.000000	-1.351893
N	0.000000	1.148053	0.732876
N	0.000000	-1.148053	0.732876
C	0.000000	-1.163704	-0.602986
C	0.000000	1.163704	-0.602986
H	0.000000	-2.151344	-1.055436
H	0.000000	2.151344	-1.055436
H	0.000000	0.000000	-2.435883

Ethylene

G(water) = -78.534176 Hartree

C	0.000000	0.000000	0.663557
H	0.000000	0.923717	1.234715
H	0.000000	-0.923717	1.234715
C	0.000000	0.000000	-0.663557
H	0.000000	-0.923717	-1.234715
H	0.000000	0.923717	-1.234715

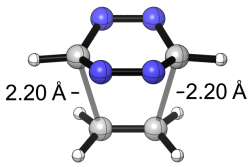

G(water) = -374.764048 Hartree

C	-0.438261	1.227407	0.000016
C	-0.438222	-1.227418	-0.000005
C	1.690521	-0.685849	-0.000037
H	1.854314	-1.233138	-0.922941
H	1.854347	-1.233154	0.922854
C	1.690488	0.685893	-0.000028
H	1.854282	1.233195	0.922869
H	1.854255	1.233204	-0.922926
N	-0.776559	-0.642457	-1.186379
N	-0.776576	0.642460	-1.186370
N	-0.776482	-0.642481	1.186402
N	-0.776501	0.642435	1.186413
H	-0.350803	2.307704	0.000024
H	-0.350729	-2.307711	-0.000020

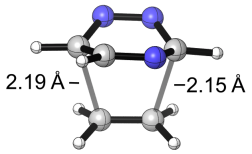

G(water) = -358.739167 Hartree

C	0.521832	1.226127	0.146486
C	0.312709	-1.265939	-0.013119
H	0.535183	2.306020	0.249316
C	-1.704193	-0.557113	-0.216848
H	-2.049022	-1.102806	0.654955
H	-1.818801	-1.059070	-1.172211
C	-1.602373	0.817884	-0.170998
H	-1.640919	1.399118	-1.086396
H	-1.859738	1.351496	0.738041
N	0.505397	-0.746853	1.246935
N	0.618950	0.527748	1.325252
N	0.885417	-0.712235	-1.118812
C	1.003627	0.582696	-1.023977
H	1.449026	1.137517	-1.847256

H 0.126308 -2.334819 -0.039342

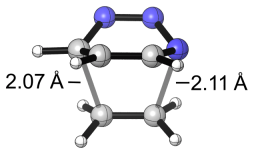

G(water) = -358.695934 Hartree

N -0.382891 -1.311636 0.097615
C 1.585294 0.677893 -0.396304
C -0.329470 1.258773 0.134590
C 1.578341 -0.711931 -0.409931
H 1.592679 1.217764 -1.337605
H -0.196283 2.331676 0.226339
H 1.975968 -1.269965 0.429953
H 2.058387 1.188667 0.436643
H 1.524770 -1.254611 -1.346509
N -0.341475 -0.671919 1.319425
C -1.135150 0.696550 -0.885991
H -1.633121 1.289676 -1.643459
N -0.330511 0.591103 1.358281
C -1.100485 -0.663864 -0.868354
H -1.529443 -1.300550 -1.636670

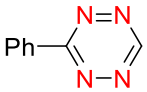

G(water) = -527.213293 Hartree

C 0.795954 -0.000001 -0.000312
C 3.344786 0.000000 0.000332
N 2.735472 -1.186514 0.000292
N 1.426931 -1.186701 -0.000008
N 2.735472 1.186514 -0.000108
N 1.426931 1.186700 -0.000451
C -0.681194 -0.000001 -0.000145
C -1.381274 1.210967 0.000099
C -1.381274 -1.210966 -0.000212
C -2.770752 1.206739 0.000257
H -0.828010 2.143429 0.000139
C -2.770754 -1.206738 -0.000063
H -0.828012 -2.143429 -0.000401
C -3.467186 0.000000 0.000177
H -3.311732 2.147647 0.000449
H -3.311730 -2.147649 -0.000139
H -4.552928 0.000003 0.000302
H 4.428939 0.000000 0.000779

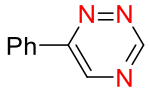

G(water) = -511.197341 Hartree

C	0.779183	0.013130	0.000499
C	3.386889	-0.068209	-0.033570
N	2.863080	1.127688	0.260984
N	2.714818	-1.189031	-0.270907
N	1.393616	-1.143256	-0.258470
C	-0.700656	0.013439	-0.003058
C	-1.392570	-1.183361	0.211540
C	-1.421563	1.190864	-0.224579
C	-2.781702	-1.195642	0.217865
H	-0.826008	-2.094434	0.371487
C	-2.812337	1.174522	-0.219253
H	-0.901160	2.121930	-0.429722
C	-3.495167	-0.017550	0.005618
H	-3.309776	-2.128116	0.390764
H	-3.361531	2.093117	-0.400063
H	-4.580655	-0.029630	0.010384
H	4.469062	-0.146334	-0.073090
C	1.544020	1.158636	0.286596
H	1.072887	2.100691	0.559044

MeSH

G(water) = -438.656253 Hartree

S	-0.662844	-0.086584	0.000048
C	1.154810	0.019179	0.000083
H	1.522202	-1.008042	-0.001406
H	1.525074	0.522090	-0.893925
H	1.526001	0.520821	0.894490
H	-0.896636	1.235410	-0.000422

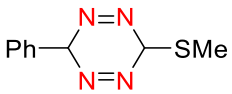

G(water) = -965.832220 Hartree

N	0.295361	1.055955	-0.319223
C	-0.406242	-0.067415	0.343872
C	2.110527	-0.246654	0.221673
N	1.522469	0.970480	-0.380635
N	1.361785	-1.446596	-0.191933
N	0.134549	-1.357621	-0.133431
C	-1.899490	0.017551	0.158156
C	-2.674544	-1.142340	0.183866
C	-2.516225	1.260146	0.009234
C	-4.058050	-1.057451	0.059546

H	-2.190446	-2.107698	0.285751
C	-3.900112	1.339699	-0.114851
H	-1.909368	2.158678	-0.024214
C	-4.673679	0.182377	-0.089842
H	-4.655093	-1.963848	0.075713
H	-4.373562	2.309070	-0.235153
H	-5.752851	0.246310	-0.188635
H	-0.133144	-0.002578	1.411152
S	3.832287	-0.471981	-0.256754
C	4.463002	1.095191	0.405116
H	5.520585	1.144391	0.141199
H	3.938187	1.936981	-0.048551
H	4.369361	1.131611	1.493507
H	1.999466	-0.143376	1.313223

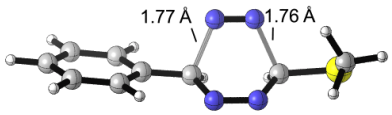

G(water) = -965.824023 Hartree

N	-0.288085	0.910404	-0.640143
C	0.441783	-0.232048	-0.409749
C	-2.148220	-0.401074	-0.450015
N	-1.567975	0.827084	-0.667786
N	-1.423215	-0.934892	1.060935
N	-0.258375	-0.870132	1.082408
C	1.903005	-0.059037	-0.220501
C	2.735347	-1.177408	-0.285256
C	2.449223	1.195822	0.057253
C	4.104846	-1.046402	-0.081080
H	2.307177	-2.155147	-0.494512
C	3.819239	1.325219	0.255801
H	1.792018	2.057449	0.102568
C	4.648558	0.207018	0.188599
H	4.746262	-1.920326	-0.134220
H	4.242241	2.302633	0.465705
H	5.717389	0.312611	0.346440
H	0.175883	-1.130288	-0.980579
S	-3.916392	-0.435442	-0.325637
C	-4.145196	1.056348	0.682681
H	-3.815891	1.938759	0.136349
H	-5.211672	1.123481	0.902580
H	-3.588035	0.961476	1.617491
H	-1.791040	-1.261442	-1.025929

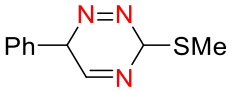

G(water) = -949.812627 Hartree

C	0.453808	0.238583	-0.425344
C	-2.141584	0.019126	-0.343048
N	-1.575505	0.685411	0.801767
N	-1.364701	-1.197005	-0.755538
N	-0.143380	-1.105876	-0.774722
C	1.934568	0.124120	-0.204539
C	2.439400	-0.931446	0.556637
C	2.806578	1.089703	-0.704541
C	3.804276	-1.020139	0.809908
H	1.758452	-1.690625	0.932217
C	4.172328	1.003458	-0.448145
H	2.416117	1.911502	-1.300084
C	4.672457	-0.051986	0.309517
H	4.191253	-1.846819	1.397334
H	4.844943	1.757827	-0.844009
H	5.737421	-0.122263	0.507350
H	0.235319	0.871355	-1.300339
S	-3.829956	-0.570619	-0.042404
C	-4.549450	1.023064	0.435889
H	-5.578309	0.827857	0.742741
H	-3.992559	1.446306	1.272895
H	-4.557676	1.723544	-0.403300
H	-2.121549	0.694558	-1.213184
C	-0.309950	0.783169	0.746875
H	0.236390	1.213036	1.587062

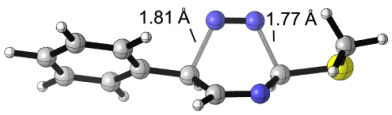

G(water) = -949.803454 Hartree

C	0.494698	-0.490756	-0.255194
C	-2.199810	-0.590460	-0.226819
N	-1.619757	0.314280	-1.066969
N	-1.452844	-0.303093	1.352799
N	-0.288188	-0.239285	1.362252
C	1.940332	-0.204317	-0.130418
C	2.885259	-1.228668	-0.226803
C	2.376380	1.104329	0.099727
C	4.243119	-0.947861	-0.119549
H	2.552459	-2.249834	-0.395304
C	3.733724	1.385450	0.208929
H	1.642952	1.899193	0.212068
C	4.670144	0.360309	0.095681
H	4.968851	-1.750816	-0.203430
H	4.061017	2.404434	0.390865

H	5.729848	0.579050	0.182858
H	0.247764	-1.555062	-0.266841
S	-3.969596	-0.516555	-0.034751
C	-4.139867	1.284149	0.086102
H	-3.768149	1.755506	-0.823265
H	-5.202543	1.495651	0.213731
H	-3.589406	1.653840	0.954506
H	-1.883214	-1.638753	-0.284985
C	-0.316315	0.345547	-1.085918
H	0.153489	1.162027	-1.635184

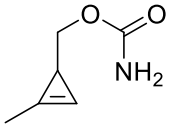

G(water) = -439.038604 Hartree

C	-2.166718	0.175532	0.058874
C	-2.006027	-0.469760	1.170833
C	-1.431480	-1.126459	-0.044027
H	-2.131475	-0.535413	2.240679
C	0.062086	-1.177135	-0.308638
H	0.539951	-2.010779	0.217916
H	0.269937	-1.302805	-1.377421
O	0.637711	0.050638	0.139259
C	1.974764	0.141012	-0.018915
O	2.668768	-0.713420	-0.519492
N	2.429227	1.320799	0.498171
H	3.369185	1.583352	0.247576
H	1.764153	2.052257	0.695037
H	-1.937570	-1.997520	-0.475794
C	-2.622171	1.345280	-0.722413
H	-3.287944	1.031457	-1.532692
H	-3.146818	2.067822	-0.092923
H	-1.758564	1.837471	-1.181998

G(water) = -272.545754 Hartree

C	-1.275344	-0.668267	-0.500391
C	-0.084771	-1.124602	0.325215
C	1.179937	-0.777633	-0.521120
C	1.179960	0.777613	-0.521143
C	-1.275321	0.668278	-0.500390
C	-0.084742	1.124606	0.325239
C	-0.030779	0.000005	1.376394
H	-1.915633	-1.325220	-1.079425
H	-0.114261	-2.151779	0.692510
H	2.080314	-1.172541	-0.039936

H	1.123410	-1.201886	-1.526509
H	1.123255	1.201826	-1.526539
H	2.080396	1.172565	-0.040118
H	-1.915564	1.325267	-1.079429
H	-0.114276	2.151779	0.692547
H	-0.897291	0.000013	2.042551
H	0.896013	-0.000019	1.961528

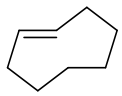

G(water) = -312.998444 Hartree

C	-0.413966	-0.522065	-1.358397
H	-1.490184	-0.336794	-1.334889
C	0.413966	0.522065	-1.358397
H	1.490184	0.336794	-1.334889
C	0.034981	-1.871510	-0.901221
H	-0.510280	-2.704358	-1.358222
H	1.102540	-2.008137	-1.112700
C	-0.034981	1.871510	-0.901221
H	-1.102540	2.008137	-1.112700
H	0.510280	2.704358	-1.358222
C	0.183001	1.877834	0.635533
H	1.260794	1.924503	0.841500
H	-0.248046	2.798155	1.048278
C	-0.413966	0.660993	1.376189
H	-0.560669	0.965017	2.418884
H	-1.420918	0.465721	0.984525
C	-0.183001	-1.877834	0.635533
H	0.248046	-2.798155	1.048278
H	-1.260794	-1.924503	0.841500
C	0.413966	-0.660993	1.376189
H	0.560669	-0.965017	2.418884
H	1.420918	-0.465721	0.984525

For structures of TS1-6, see Figure S1.

TS1

G(water) = -966.219637 Hartree

C	-1.785023	1.002564	0.065584
N	-1.499250	1.599124	1.253867
N	-0.755036	2.653157	1.217687
C	-0.317368	3.018589	-0.016008
N	-1.075656	2.783947	-1.131608
N	-1.818109	1.739234	-1.087522
C	0.488480	0.264690	-0.381988
C	1.117914	1.446633	-0.379553
C	1.295785	0.581859	0.830007
H	1.723713	2.047359	-1.043074
H	0.778461	0.886927	1.744089

C	-2.516616	-0.279705	0.094626
C	-2.515449	-1.054113	1.259192
C	-3.825457	-1.971959	-1.023342
C	-3.167220	-2.281677	1.276707
H	-2.003938	-0.682638	2.141414
C	-3.822644	-2.743702	0.136696
H	-4.338732	-2.326589	-1.911781
H	-3.164317	-2.879842	2.182545
H	-4.330863	-3.703017	0.153526
C	2.598546	-0.135144	1.108721
H	3.266996	0.482748	1.716903
H	2.429443	-1.072951	1.648662
C	0.175577	-0.897472	-1.253360
H	-0.415957	-1.654083	-0.733022
H	-0.361488	-0.579017	-2.151016
H	1.128538	-1.348610	-1.552765
O	3.223891	-0.414042	-0.145919
C	4.426542	-1.030211	-0.049049
O	4.944131	-1.351051	0.994274
N	4.967337	-1.200207	-1.287750
H	5.772273	-1.802837	-1.350644
H	4.390050	-1.076008	-2.104252
C	-3.173886	-0.743971	-1.048182
H	-3.170978	-0.133000	-1.944473
H	0.342527	3.877216	-0.055999

TS2

G(water) = -950.193369 Hartree

C	0.394356	2.963677	0.259283
N	0.830392	2.536526	1.467336
C	1.790983	0.845760	0.129312
N	1.815633	1.690598	-0.955670
N	1.103297	2.755731	-0.898063
C	-1.096567	1.401715	-0.280304
C	-0.357867	0.280304	-0.235414
C	-1.273432	0.522197	0.916120
H	-0.056368	-0.544091	-0.865070
H	-0.835136	0.861498	1.860706
C	2.515768	-0.440316	0.007305
C	2.292948	-1.451136	0.947341
C	4.100378	-1.867707	-1.124248
C	2.978074	-2.657927	0.857740
H	1.561526	-1.297401	1.737747
C	3.886371	-2.867184	-0.177226
H	4.806442	-2.028750	-1.933079
H	2.797761	-3.437212	1.591582
H	4.421776	-3.808903	-0.248732
C	-2.521641	-0.307094	1.121565
H	-2.313588	-1.192030	1.732552
H	-3.305079	0.267341	1.627446
C	-1.956116	2.177822	-1.221824

H	-2.358601	3.081355	-0.756188
H	-1.388527	2.460290	-2.111672
H	-2.799574	1.546105	-1.519784
O	-2.990940	-0.723386	-0.162749
C	-4.102885	-1.494986	-0.132282
O	-4.688640	-1.806126	0.877941
N	-4.436817	-1.885409	-1.393969
H	-5.342865	-2.309923	-1.511721
H	-4.006260	-1.432864	-2.184786
C	3.418244	-0.658957	-1.037211
H	3.577099	0.127807	-1.766636
H	-0.264348	3.826455	0.245086
C	1.559781	1.452984	1.392819
H	1.984466	1.039377	2.305727

TS3

G(water) = -799.723669 Hartree

N	1.142263	1.919608	1.357410
N	-0.013107	1.355546	1.351933
C	-0.587018	1.148580	0.129651
N	-0.356460	2.073407	-0.864681
N	0.792986	2.632801	-0.865547
C	1.648111	2.225818	0.130772
C	0.857358	-0.350557	-0.764744
C	2.088527	0.283851	-0.700373
C	0.948097	-1.582284	0.115451
C	1.882713	-2.540851	-0.686880
C	2.953581	-0.553547	0.232113
C	3.266560	-1.833467	-0.601713
C	1.916913	-1.122017	1.217360
H	0.211892	-0.321464	-1.636914
H	2.520957	0.806585	-1.548608
H	-0.003390	-2.021019	0.421405
H	1.540540	-2.684426	-1.715336
H	1.908690	-3.522249	-0.203607
H	3.828409	-0.056739	0.655118
H	3.683602	-1.594818	-1.584100
H	3.996111	-2.452780	-0.071271
H	2.319585	-1.968255	1.783499
H	1.503226	-0.392867	1.910797
C	-1.839324	0.361439	0.076105
C	-2.622079	0.357630	-1.081906
C	-2.219558	-0.416318	1.173834
C	-3.776806	-0.415336	-1.136746
H	-2.323094	0.971543	-1.925532
C	-3.374506	-1.188224	1.111804
H	-1.607202	-0.399895	2.069855
C	-4.155122	-1.190320	-0.042418
H	-4.384434	-0.410838	-2.036354
H	-3.667253	-1.787974	1.968023
H	-5.056503	-1.793755	-0.088086

H	2.644412	2.653050	0.113445

TS4

G(water) = -783.696583 Hartree

N	1.166999	1.877319	1.317935
N	0.003900	1.337572	1.290625
C	-0.584994	1.136918	0.066953
N	0.922380	2.663078	-0.917169
C	1.712704	2.204533	0.102306
C	0.885437	-0.359166	-0.749060
C	2.129252	0.259500	-0.652840
C	0.928227	-1.580548	0.150686
C	1.860181	-2.569071	-0.615770
C	2.951613	-0.594370	0.305762
C	3.257236	-1.889056	-0.505675
C	1.880831	-1.130861	1.271359
H	0.292385	-0.367295	-1.657900
H	2.598902	0.739804	-1.506495
H	-0.040730	-1.992263	0.440707
H	1.540863	-2.719633	-1.650920
H	1.854534	-3.544824	-0.120105
H	3.826418	-0.113358	0.747226
H	3.701188	-1.670650	-1.481148
H	3.960621	-2.519353	0.047180
H	2.251052	-1.982998	1.851231
H	1.468423	-0.388140	1.949654
C	-1.849145	0.365479	0.042528
C	-2.489021	0.099210	-1.172500
C	-2.399414	-0.138866	1.226072
C	-3.667774	-0.638651	-1.204302
H	-2.060119	0.461830	-2.103774
C	-3.575055	-0.880342	1.190158
H	-1.897013	0.067145	2.164909
C	-4.215043	-1.130245	-0.022178
H	-4.154695	-0.834382	-2.154696
H	-3.995188	-1.263743	2.115010
H	-5.132561	-1.709881	-0.045867
H	2.726592	2.589544	0.149394
C	-0.259571	2.121802	-0.920215
H	-0.986426	2.444823	-1.663839

TS5

G(water) = -840.187486 Hartree

C	-1.012127	1.217003	-0.071701
C	1.047417	2.567439	-0.371057
C	1.880567	0.575300	-0.219291
H	2.301894	0.644720	-1.224137
C	0.787513	-0.247208	-0.067038
H	0.499175	-0.515263	0.950951

N	0.469568	2.641470	0.863788
N	-0.589427	1.933004	1.017422
N	0.277100	2.409408	-1.487025
N	-0.784494	1.704997	-1.329095
C	0.441437	-1.242532	-1.131181
H	-0.624575	-1.491756	-1.144768
H	0.707005	-0.834113	-2.114236
C	2.864215	0.727700	0.908849
H	3.406566	1.679197	0.869204
H	2.327453	0.698150	1.864578
C	1.260192	-2.525979	-0.858926
H	1.094223	-3.215599	-1.694761
H	0.853951	-3.021074	0.032823
C	3.870637	-0.440944	0.833545
H	4.513833	-0.391042	1.719825
H	4.529660	-0.289653	-0.031835
C	3.242632	-1.844236	0.740987
H	3.993536	-2.555743	1.100807
H	2.411428	-1.915586	1.455529
C	2.773122	-2.313278	-0.667130
H	3.263218	-3.268048	-0.885587
H	3.139397	-1.617001	-1.433589
C	-2.143947	0.285067	0.121294
C	-2.909736	-0.135884	-0.970243
C	-2.436058	-0.196976	1.400312
C	-3.958825	-1.028911	-0.779003
H	-2.677083	0.249475	-1.957508
C	-3.484752	-1.090684	1.584596
H	-1.843294	0.144976	2.243113
C	-4.248079	-1.508801	0.496289
H	-4.553973	-1.347923	-1.629055
H	-3.708217	-1.460641	2.580480
H	-5.066011	-2.207653	0.642263
H	1.977325	3.109964	-0.501540

TS6

G(water) = -824.161176 Hartree

C	-1.004112	1.196477	-0.033370
C	1.108634	2.548884	-0.356698
C	1.888700	0.584231	-0.230986
H	2.293339	0.623240	-1.243544
C	0.787732	-0.233873	-0.046927
H	0.545899	-0.521130	0.977526
N	0.563978	2.702192	0.883637
N	0.323478	2.353856	-1.470875
N	-0.743954	1.667165	-1.298483
C	0.409228	-1.227876	-1.103421
H	-0.659754	-1.467032	-1.093211
H	0.649956	-0.814913	-2.090764

C	2.907268	0.704102	0.872285
H	3.463545	1.647422	0.826444
H	2.393532	0.680037	1.841313
C	1.219561	-2.521329	-0.863175
H	1.024334	-3.202316	-1.699960
H	0.830786	-3.020081	0.034723
C	3.893797	-0.477455	0.771737
H	4.559485	-0.439243	1.642191
H	4.534117	-0.333229	-0.108875
C	3.247995	-1.873052	0.690115
H	3.999815	-2.594422	1.028406
H	2.433752	-1.939215	1.424619
C	2.739443	-2.330900	-0.707563
H	3.210456	-3.292118	-0.939937
H	3.097700	-1.637250	-1.479952
C	-2.156963	0.285410	0.131843
C	-3.037336	0.039003	-0.927564
C	-2.358996	-0.367312	1.352473
C	-4.104952	-0.835384	-0.758304
H	-2.870492	0.542631	-1.873575
C	-3.429135	-1.239671	1.518979
H	-1.664743	-0.202934	2.173331
C	-4.305921	-1.475529	0.463185
H	-4.785767	-1.017209	-1.584332
H	-3.573823	-1.740124	2.471415
H	-5.139458	-2.159387	0.589974
H	2.043233	3.067925	-0.548709
C	-0.525669	2.005163	1.039186
H	-1.066059	2.071536	1.982197

Appendix D: NMR spectra for Chapter 3

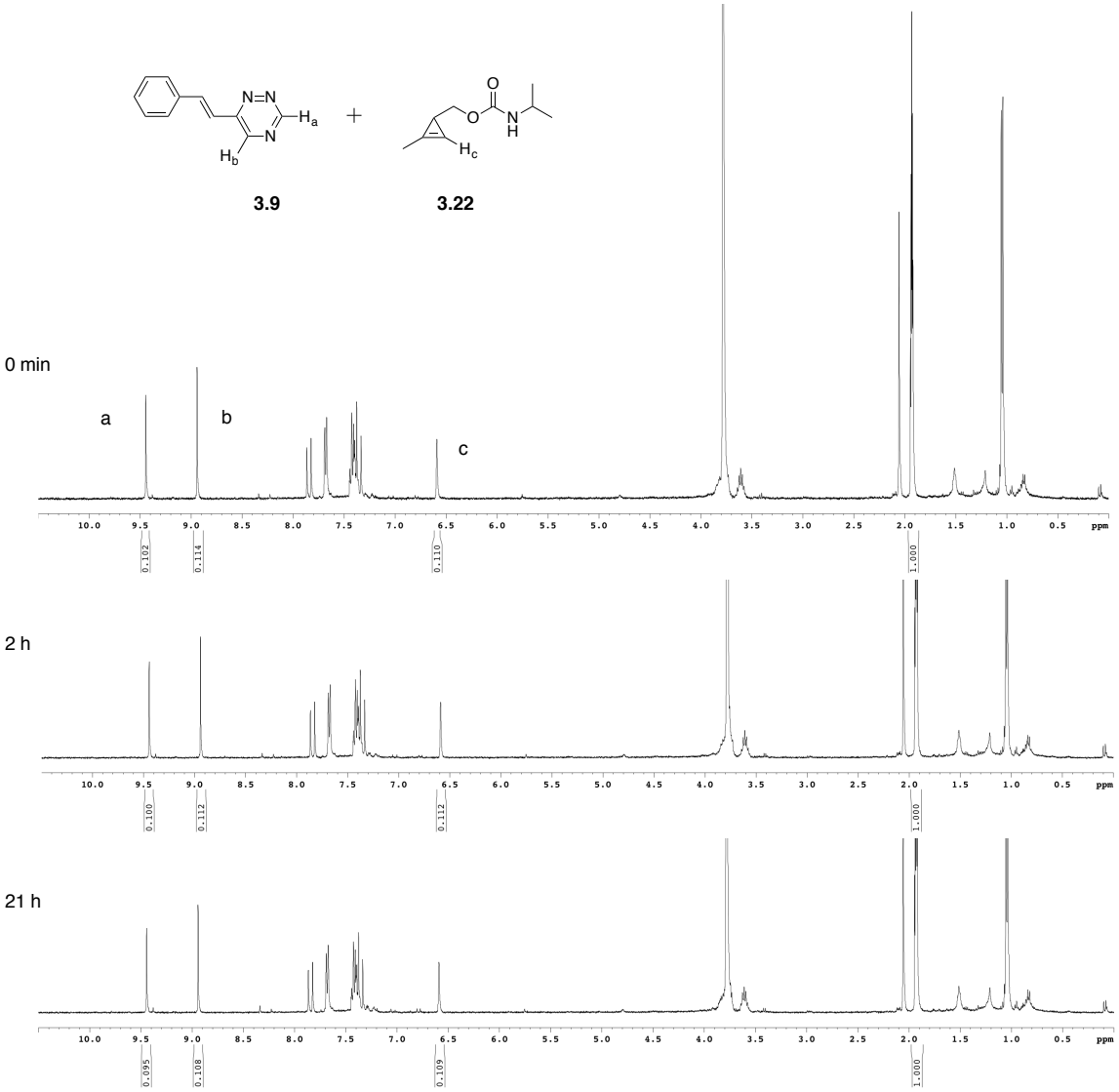

Figure S3-1. Triazine **3.9** does not react with cyclopropene **3.22.** To a solution of triazine **3.9** (0.24 mL of a 25 mM solution CD_3CN) was added cyclopropene **3.22** (0.3 mL of a 20 mM solution in 1:1 CD_3CN:D_2O) and added CD_3CN to a final volume of 0.6 mL. The reaction was monitored over time by ^{1}H-NMR.

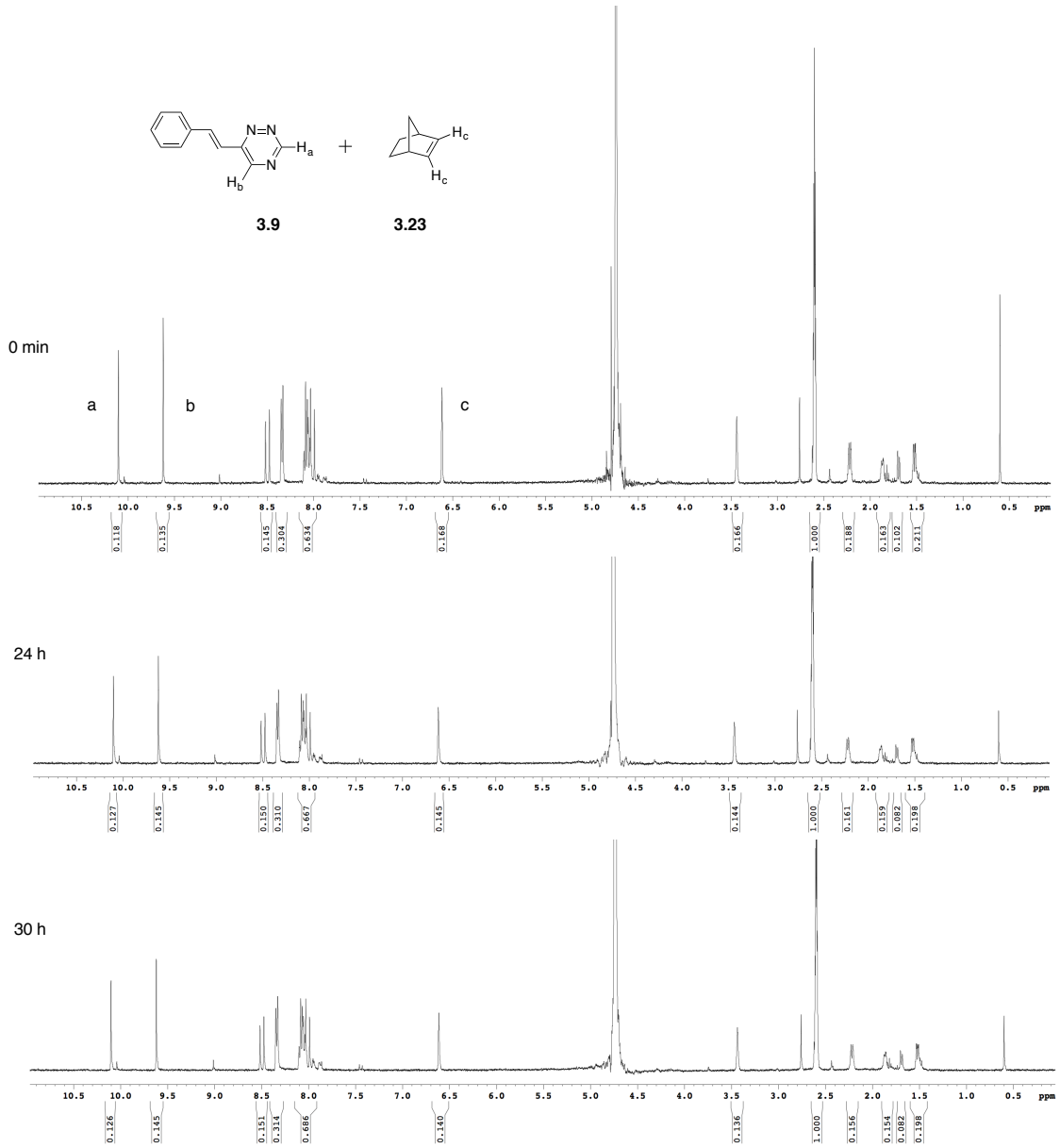

Figure S3-2. Triazine **3.9** does not react with norbornene **3.23.** To a solution of triazine **3.9** (0.12 mL of a 50 mM solution in CD_3CN) was added norbornene **3.23** (0.12 mL of a 40 mM solution in 1:1 CD_3CN:*d*-PBS) and diluted with 0.24 mL CD_3CN and 0.24 mL *d*-PBS to a final volume of 0.72 mL. The reaction was monitored over time by ^{1}H-NMR.

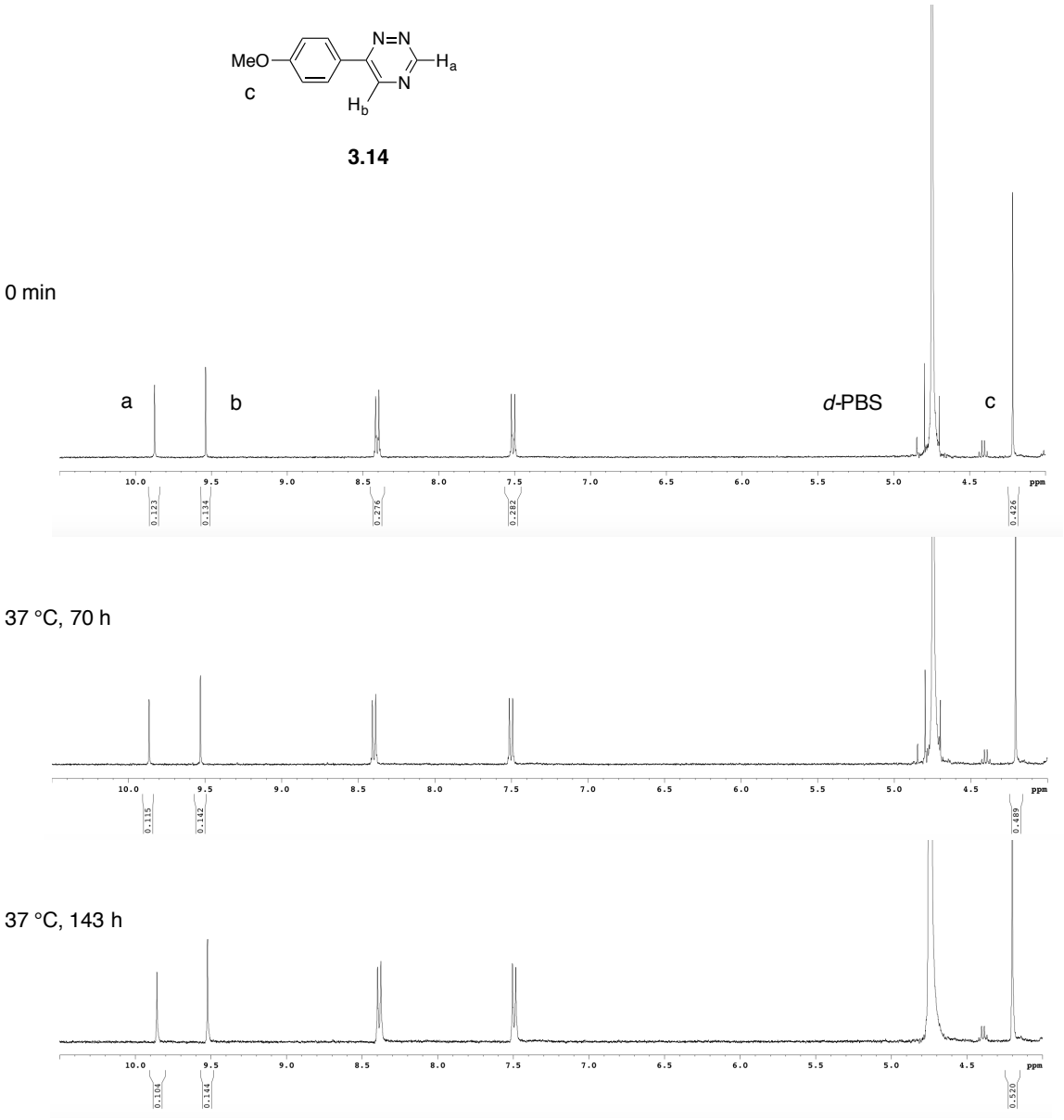

Figure S3-3. Triazine **3.14** is stable in aqueous buffer. A solution of triazine **3.14** (0.2 mL of a 25 mM solution in CD_3CN) was diluted with 0.4 mL *d*-PBS. The reaction was incubated at 37 °C for 0-143 h. The reaction was monitored over time by ^{1}H-NMR.

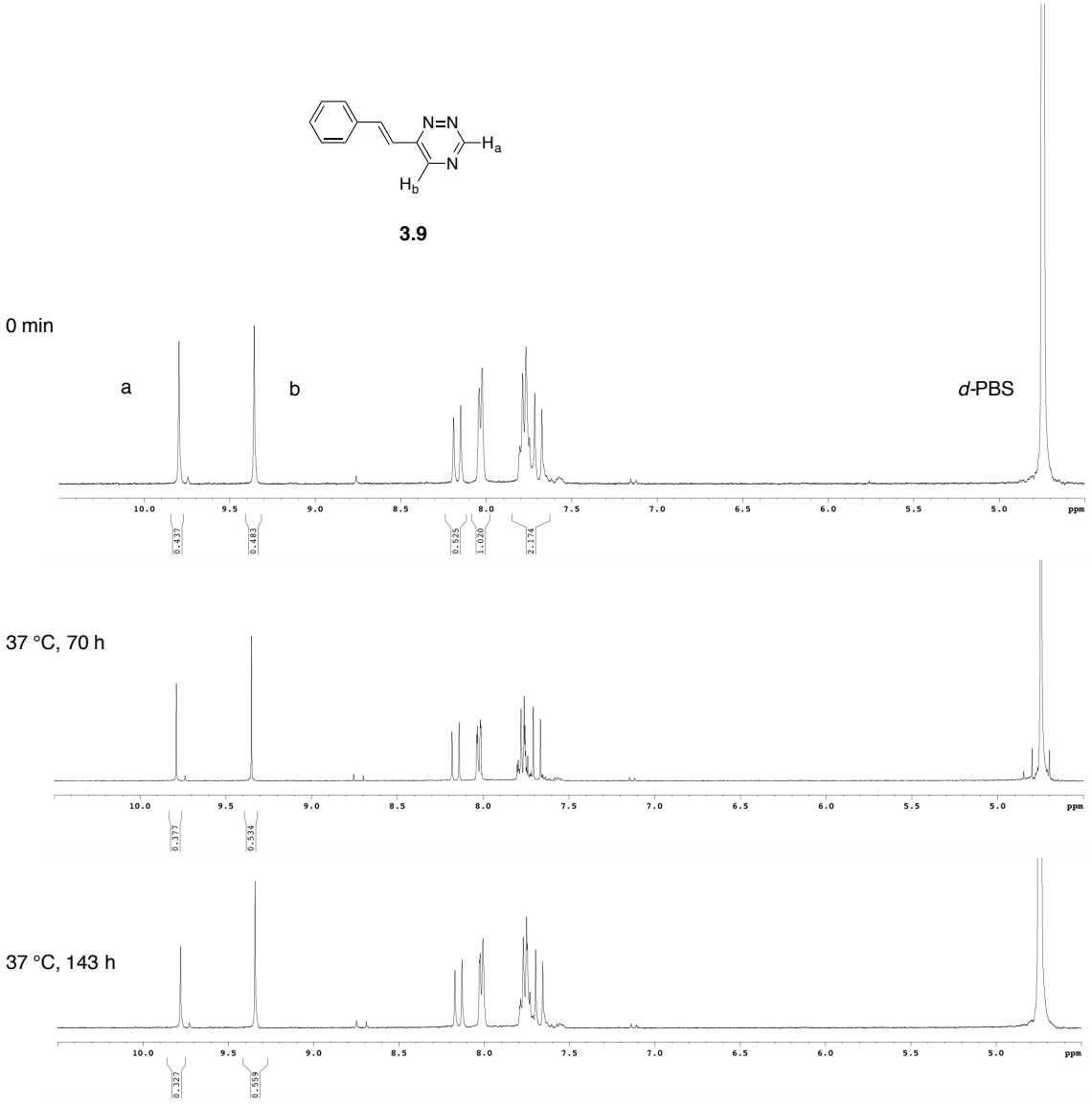

Figure S3-4. Triazine **3.9** is stable in aqueous buffer. A solution of triazine **3.9** (0.2 mL of a 50 mM solution in CD_3CN) was diluted with 0.4 mL *d*-PBS. The reaction was incubated at 37 °C for 0-143 h. The reaction was monitored over time by ^{1}H-NMR.

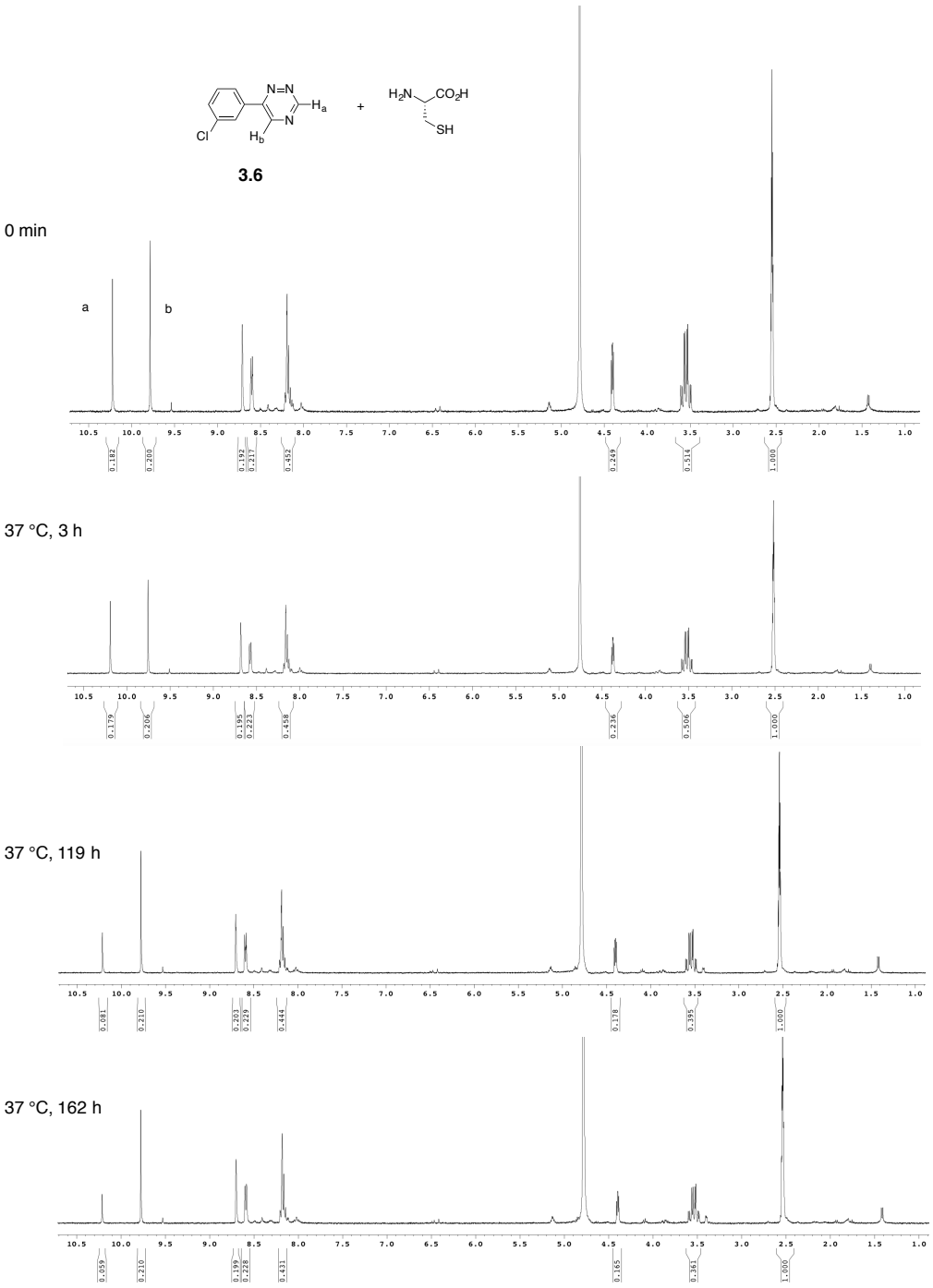

Figure S3-5. Triazine **3.6** is stable in the presence of cysteine. To a solution of triazine **3.6** (0.24 mL of a 25 mM solution in CD_3CN) was added L-cysteine (0.12 mL of a 50 mM solution in D_2O). The reaction was further diluted with 1:1 CD_3CN:D_2O to a final volume of 0.6 mL. The reaction was incubated at 37 °C and monitored over time by ^{1}H-NMR.

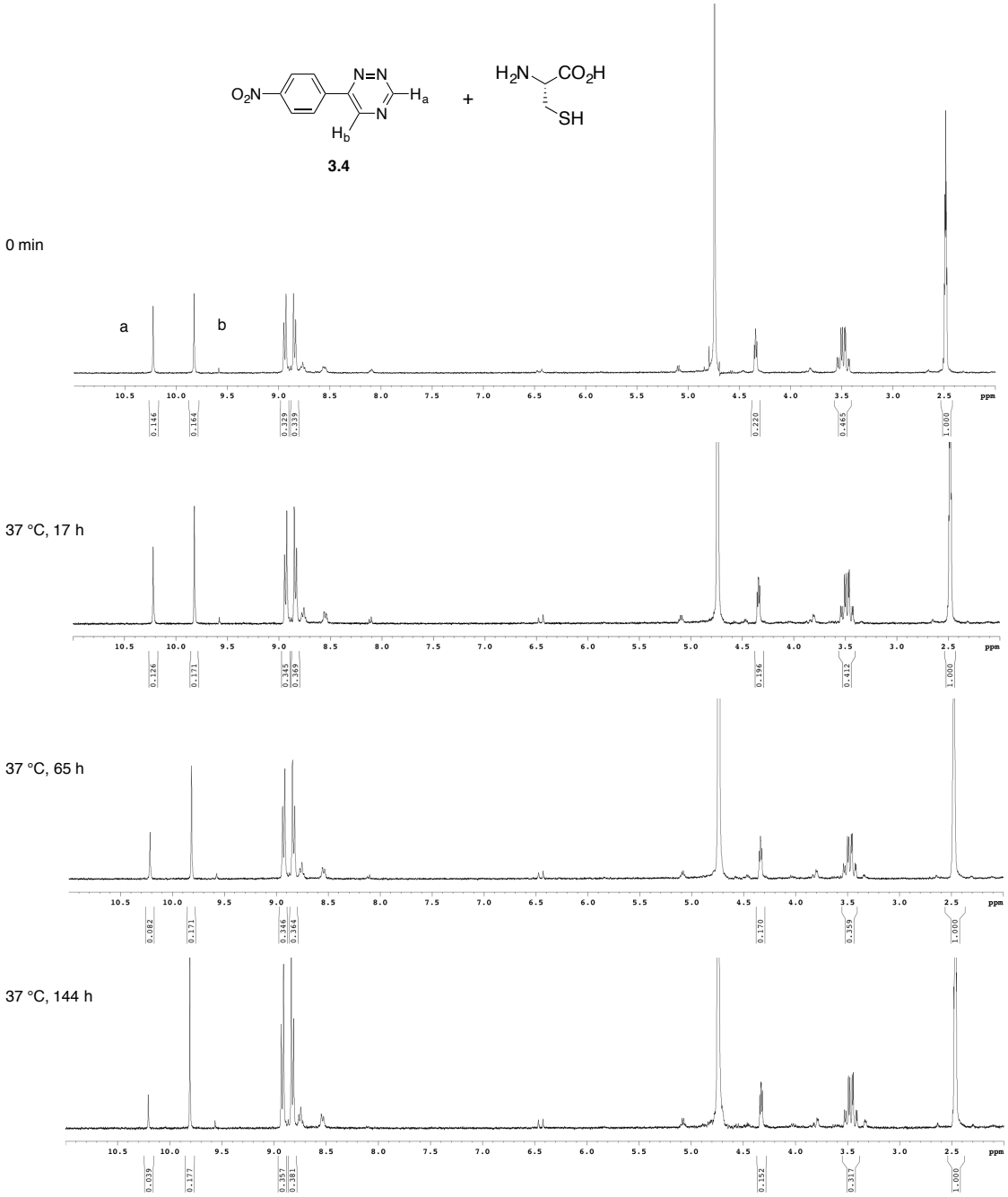

Figure S3-6. Triazine **3.4** is stable in the presence of cysteine. To a solution of triazine **3.4** (0.3 mL of a 20 mM solution in CD_3CN) was added L-cysteine (0.24 mL of a 25 mM solution in D_2O). The reaction was further diluted with 60 μL D_2O to a final volume of 0.6 mL. The reaction was incubated at 37 °C and monitored over time by ^{1}H-NMR.

1H spectrum

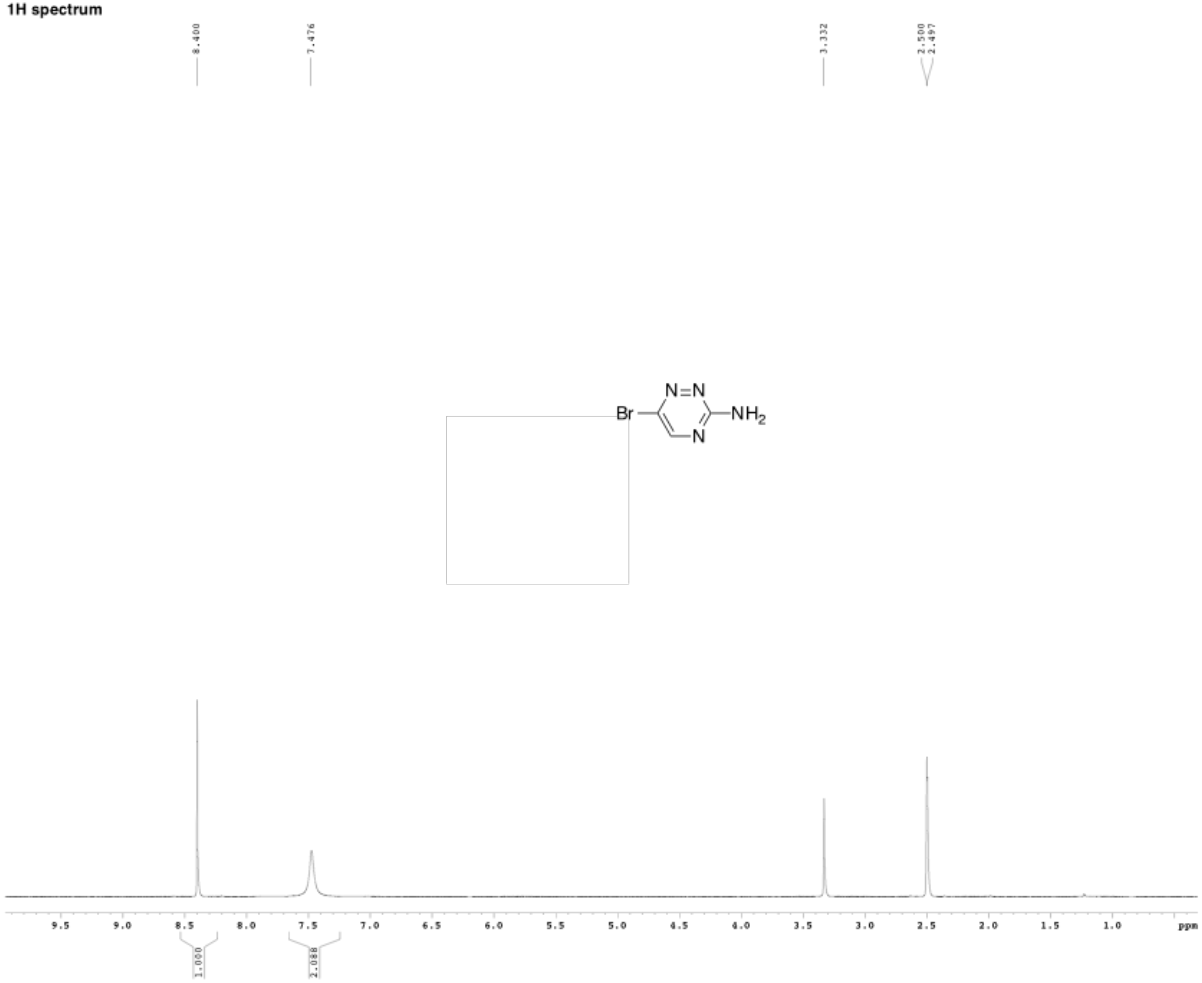


```
Current Data Parameters
USER            kamber
NAME            DK07-049
EXPNO                 2
PROCNO                1

F2 - Acquisition Parameters
Date_           20140713
Time              23.13
INSTRUM         cryo500
PROBHD   5 mm CPTCI 1H-
PULPROG           zg30
TD                81728
SOLVENT            DMSO
NS                    2
DS                    2
SWH            8012.820 Hz
FIDRES         0.098043 Hz
AQ             5.0999398 sec
RG                    8
DW               62.400 usec
DE                6.00 usec
TE              298.0 K
D1            0.10000000 sec
MCREST        0.00000000 sec
MCWRK         0.01500000 sec

======== CHANNEL f1 ========
NUC1                 1H
P1                7.50 usec
PL1               1.60 dB
SFO1        500.2235015 MHz

F2 - Processing parameters
SI                65536
SF          500.2200132 MHz
WDW                 EM
SSB                  0
LB                0.30 Hz
GB                   0
PC                4.00
```

Z-restored spin-echo 13C spectrum with 1H decoupling

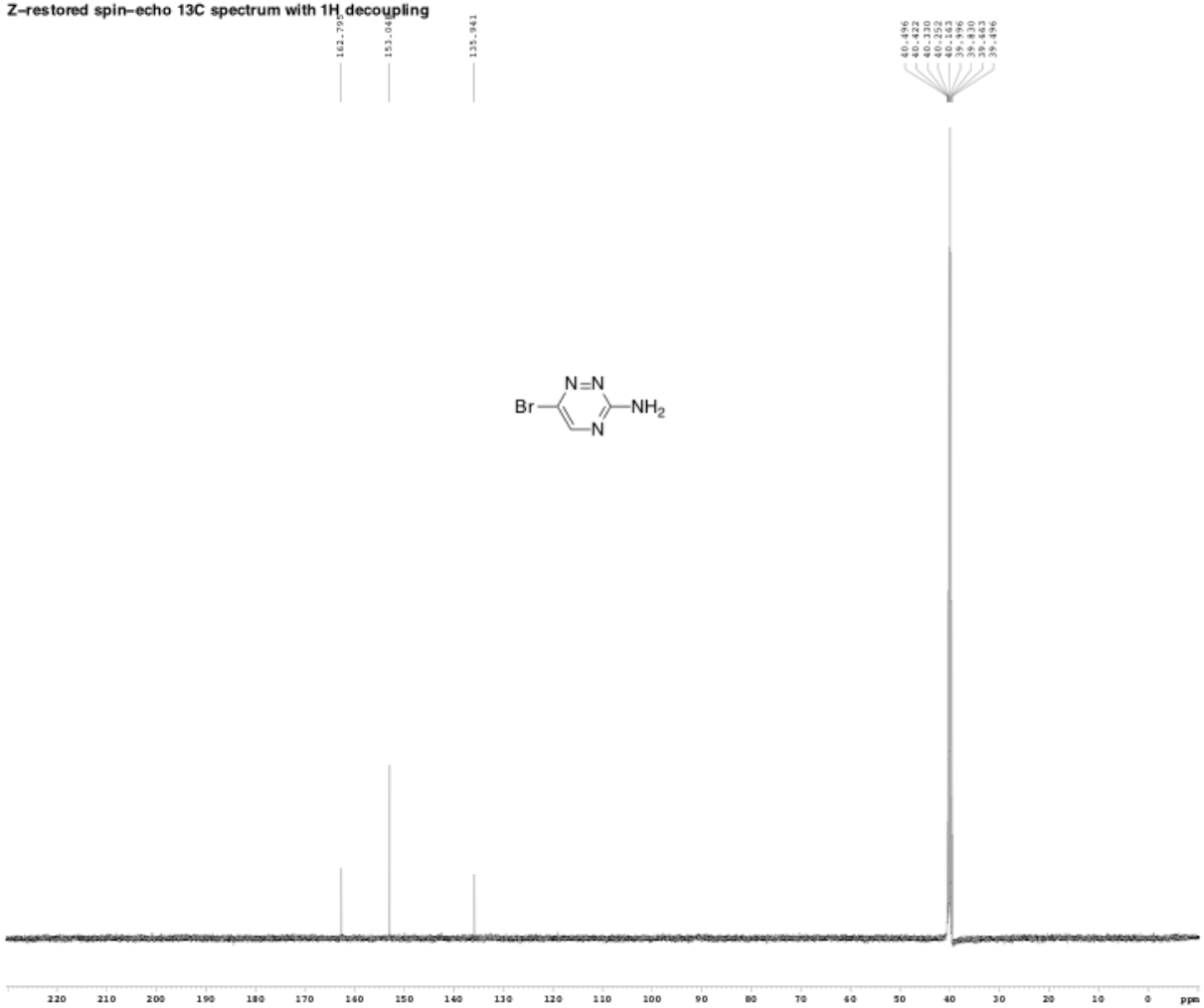


```
Current Data Parameters
USER                 hamber
NAME              D807-049
EXPNO                   3
PROCNO                  1

F2 - Acquisition Parameters
Date_            20140712
Time               22.17
INSTRUM          cryo500
PROBHD   5 mm CPTCI 1H-
PULPROG  zgpg30cgp.prod
TD                 65536
SOLVENT            DMSO
NS                   250
DS                    16
SWH            30303.031 Hz
FIDRES         0.462388 Hz
AQ             1.0814105 sec
RG                7298.2
DW                16.500 usec
DE                 6.00 usec
TE                298.0 K
D1             8.25000000 sec
d11            8.03000000 sec
D16            8.00020000 sec
d17            8.00019600 sec
MCREST         8.00000000 sec
MCWRK          8.01500000 sec
P2                31.00 usec

======== CHANNEL f1 ========
NUC1                 13C
P1                15.50 usec
P11              500.00 usec
P12             2000.00 usec
PL2               120.00 dB
PL1                -1.00 dB
SFO1        125.7942548 MHz
SP1                3.20 dB
SP2                3.20 dB
SPNAM1   Crp48,0.5,20.1
SPNAM2      Crp60comp.4
SPOFF1             0.00 Hz
SPOFF2             0.00 Hz

======== CHANNEL f2 ========
CPDPRG2          waltz16
NUC2                 1H
PCPD2             100.00 usec
PL2                1.60 dB
PL12              24.60 dB
SFO2        599.2225011 MHz

====== GRADIENT CHANNEL =====
GPNAM1          SINE.100
GPNAM2          SINE.100
GPZ1               0.00 %
GPZ2               0.00 %
GPZ3               0.00 %
GPZ4               0.00 %
GPZ11             80.00 %
GPZ12             50.00 %
p15              500.00 usec
p16             1000.00 usec

F2 - Processing parameters
SI                 65536
SF          125.7804190 MHz
WDW                  EM
SSB                   0
LB                 1.00 Hz
GB                    0
PC                 4.00
```

1H spectrum

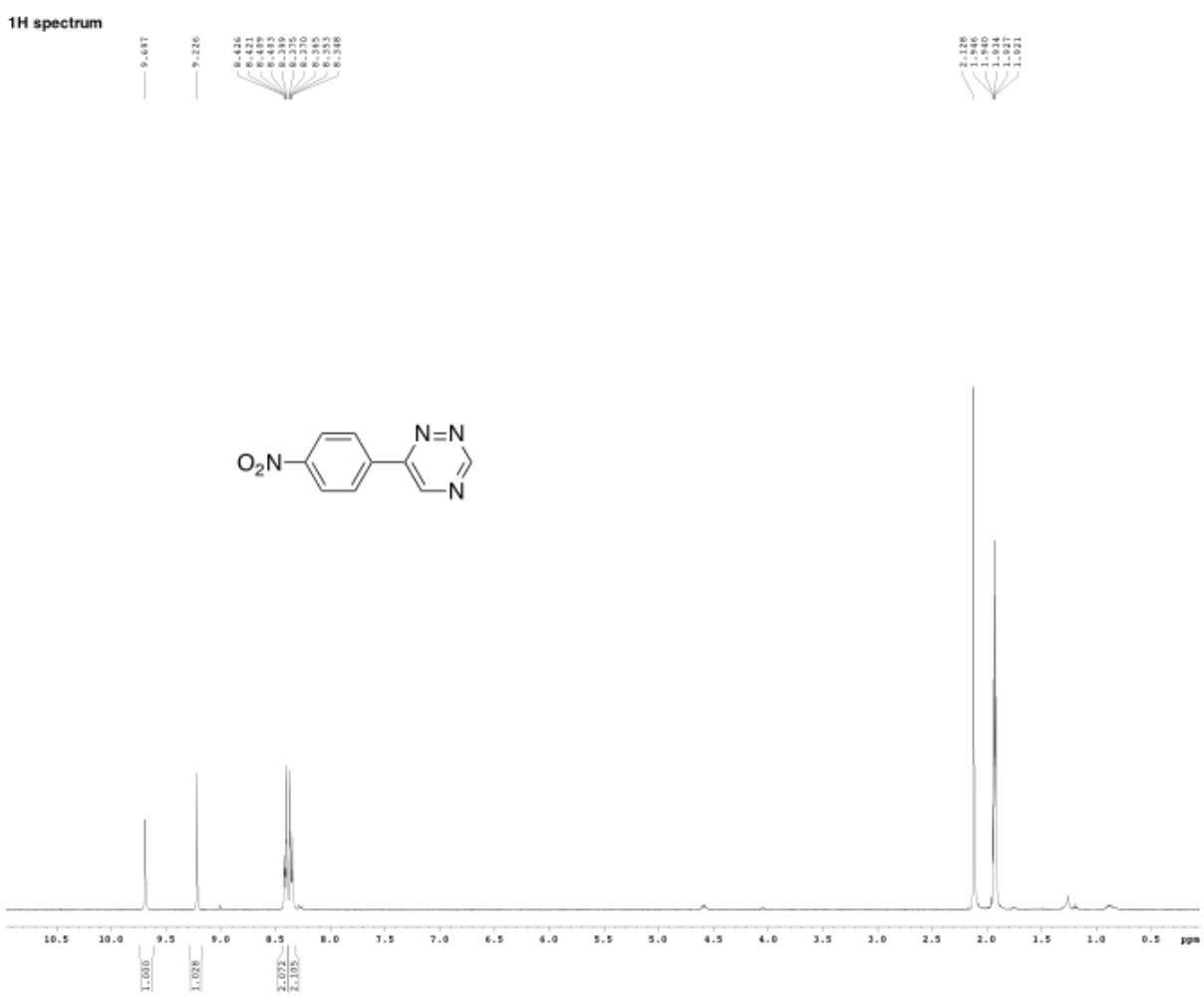


```
Current Data Parameters
USER            kamber
NAME            0837-168
EXPNO                 2
PROCNO                1

F2 - Acquisition Parameters
Date_        20141115
Time             16.15
INSTRUM        dex400
PROBHD   5 mm QNP H/P
PULPROG          zg30
TD               65536
SOLVENT          CDCN
NS                   8
DS                   2
SWH           6410.256 Hz
FIDRES        0.097813 Hz
AQ            5.1118079 sec
RG               1149.4
DW               78.000 usec
DE                4.50 usec
TE              298.0 K
D1            3.10000000 sec
MCREST        0.00000000 sec
MCWRK         0.01500000 sec

======== CHANNEL f1 ========
NUC1                1H
PW               12.00 usec
PL1               0.00 dB
SFO1        400.1320009 MHz

F2 - Processing parameters
SI               65536
SF          400.1300175 MHz
WDW                 EM
SSB                  0
LB                0.30 Hz
GB                   0
PC                2.00
```

Z–restored spin–echo 13C spectrum with 1H decoupling


```
Current Data Parameters
USER                 Esther
NAME              DR37-BS2
EXPNO                    2
PROCNO                   1

F2 - Acquisition Parameters
Date_           20140715
Time              15.32
INSTRUM         qtp500
PROBHD   5 mm CPPTI 3H-
PULPROG   Spin&Echo93bpp.pr4
TD                 65536
SOLVENT            CDCl3
NS                  1824
DS                    16
SWH             30383.811 Hz
FIDRES          0.463380 Hz
AQ              1.081940 sec
RG                 6597.6
DW                 16.500 usec
DE                  6.00 usec
TE                 298.0 K
D1              0.25000000 sec
d11             0.03000000 sec
D16             0.00020000 sec
d17             0.00019400 sec
MCREST          0.00000000 sec
MCWRK           0.01500000 sec
P2                 31.00 usec

======== CHANNEL f1 ========
NUC1                  13C
P1                  15.50 usec
PL1                 500.00 usec
PL12               2000.00 usec
PL2                 120.00 dB
PL13                 -1.00 dB
SFO1            125.7942548 MHz
SW1                   3.20 dB
SW2                   3.20 dB
SPNAM1    Crp60,0.5,20.1
SPNAM2      CspMCwamp.4
SPOFF1                0.00 Hz
SPOFF2                0.00 Hz

======== CHANNEL f2 ========
CPDPRG2          waltz16
NUC2                   1H
PCPD2               100.00 usec
PL2                   1.40 dB
PL12                 24.40 dB
SFO2            500.2225811 MHz

====== GRADIENT CHANNEL ====
GPNAM1            SINE.100
GPNAM2            SINE.100
GPZ1                  8.00 %
GPZ2                  8.00 %
GPZ3                  8.00 %
GPZ4                  8.00 %
GPZ5                 38.00 %
GPZ6                 58.00 %
p15                 500.00 usec
p16                 1000.00 usec

F2 - Processing parameters
SI                  65536
SF              125.7886290 MHz
WDW                    EM
SSB                     0
LB                   1.00 Hz
GB                      0
PC                   2.00
```

1H spectrum


```
Current Data Parameters
NAME              hamdev
EXPNO                  4
PROCNO                 1

F2 - Acquisition Parameters
Date_          20140712
Time              13.34
INSTRUM          dra400
PROBHD   5 mm QNP H/F/P
PULPROG           zg30
TD                65536
SOLVENT           CDCl3
NS                    8
DS                    2
SWH            6410.256 Hz
FIDRES         0.097813 Hz
AQ             5.111879 sec
RG                 406.4
DW               78.000 usec
DE                4.50 usec
TE               297.9 K
D1             8.10000000 sec
MCREST         0.00000000 sec
MCWRK          0.01500000 sec

-------- CHANNEL f1 --------
NUC1                  1H
P1                12.00 usec
PL1                0.00 dB
SFO1          400.1320009 MHz

F2 - Processing parameters
SI                65536
SF            400.1300175 MHz
WDW                  EM
SSB                   0
LB                 0.30 Hz
GB                    0
PC                 2.00
```

Z-restored spin-echo 13C spectrum with 1H decoupling

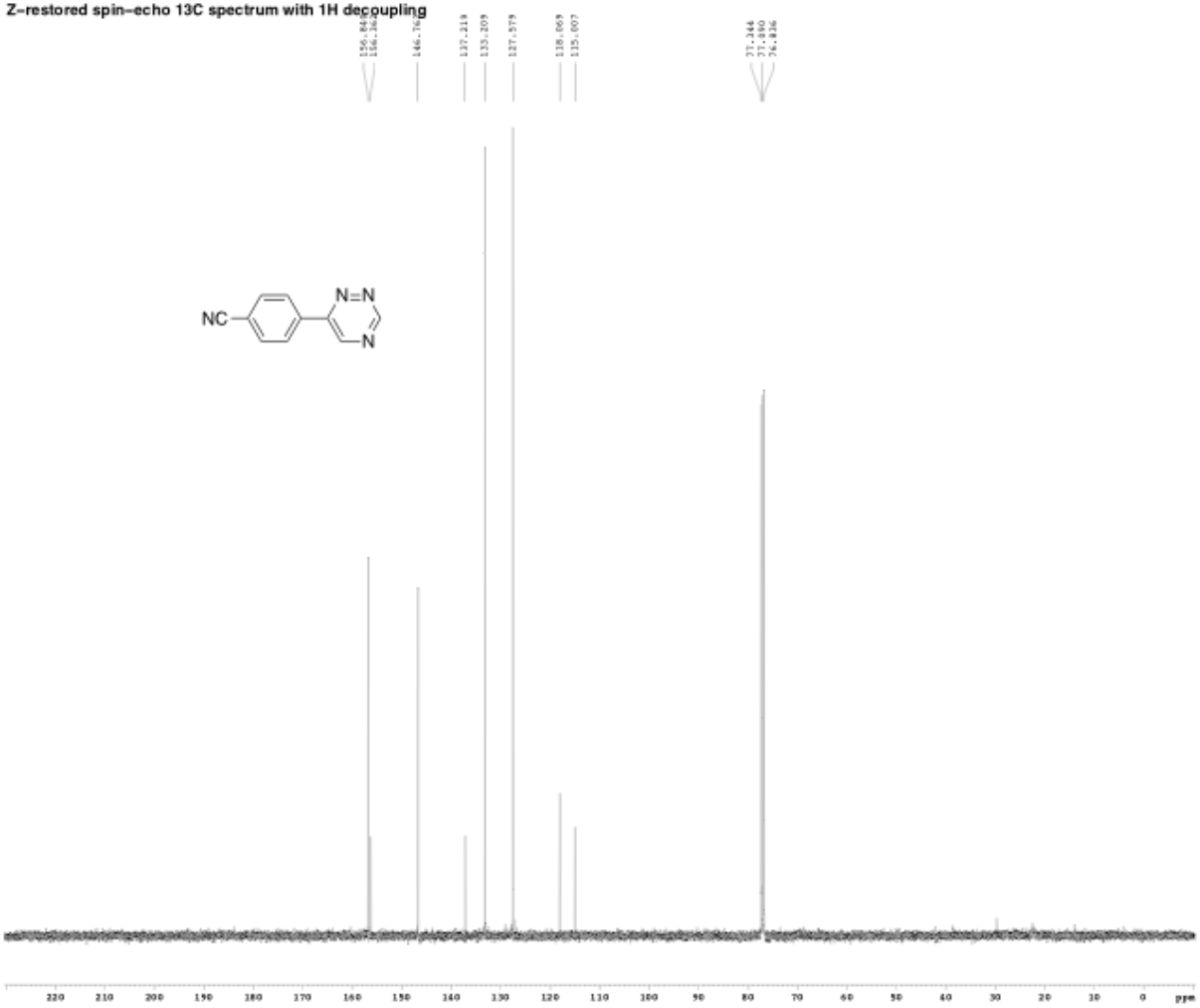


```
Current Data Parameters
NAME              hamkmr
EXPNO                  5
PROCNO                 1

F2 - Acquisition Parameters
Date_           1014712
Time              12.48
INSTRUM           crysm500
PROBHD   5 mm CPTCI 1H-
PULPROG  Spin8chapq36gp.pr6
TD                45536
SOLVENT           CDCl3
NS                  554
DS                   16
SWH            36363.631 Hz
FIDRES         0.442388 Hz
AQ             1.6813948 sec
RG                4597.6
DW               14.500 usec
DE                6.00 usec
TE              298.0 K
D1             0.25000000 sec
d11            0.03000000 sec
D16            0.00020000 sec
d17            0.00019600 sec
MCREST         0.00000000 sec
MCWRK          0.01500000 sec
P2               31.00 usec

======== CHANNEL f1 ========
NUC1                  13C
P1                  15.30 usec
PL1                 500.00 usec
PL12               2000.00 usec
PL16                120.00 dB
PL1                   -1.00 dB
SFO1           125.7642148 MHz
SP1                   3.19 dB
SP2                   2.28 dB
SPNAM1    Crp60,0.5,20.1
SPNAM2       Cpd0comp.4
SPOFF1                0.00 Hz
SPOFF2                0.00 Hz

======== CHANNEL f2 ========
CPDPRG2          waltz16
NUC2                  1H
PCPD2               100.00 usec
PL2                   1.00 dB
PL12                 26.00 dB
SFO2           500.2235011 MHz

====== GRADIENT CHANNEL =====
GPNAM1          SINE.100
GPNAM2          SINE.100
GPZ1                  0.00 %
GPZ2                  0.00 %
GPY1                  0.00 %
GPY2                  0.00 %
GPX1                 10.00 %
GPZ3                 50.00 %
gt5                 500.00 usec
gt6                1000.00 usec

F2 - Processing parameters
SI                    65536
SF             125.7664159 MHz
WDW                      EM
SSB                       0
LB                     1.00 Hz
GB                        0
PC                     2.00
```

1H spectrum

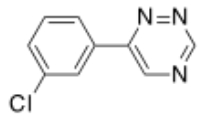
N=N
N
Cl

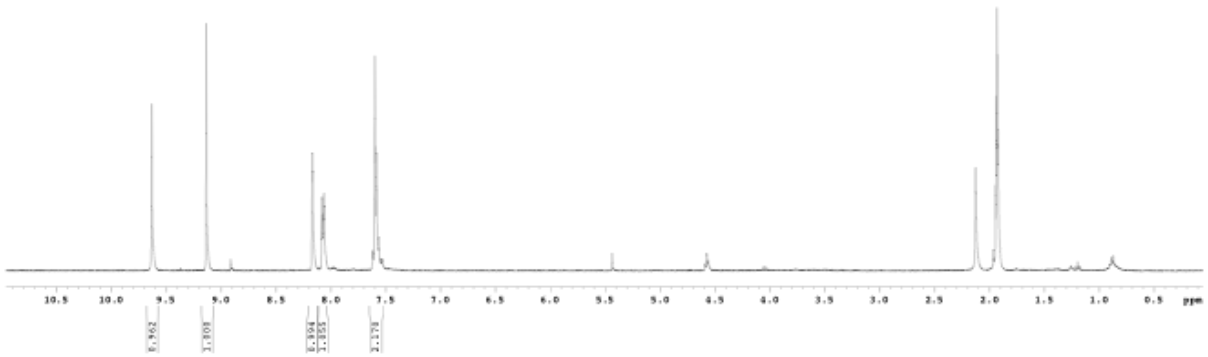
10.5
10.0
9.5
9.0
8.5
8.0
7.5
7.0
6.5
6.0
5.5
5.0
4.5
4.0
3.5
3.0
2.5
2.0
1.5
1.0
0.5
ppm
0.962
1.000
2.994
1.155
2.178

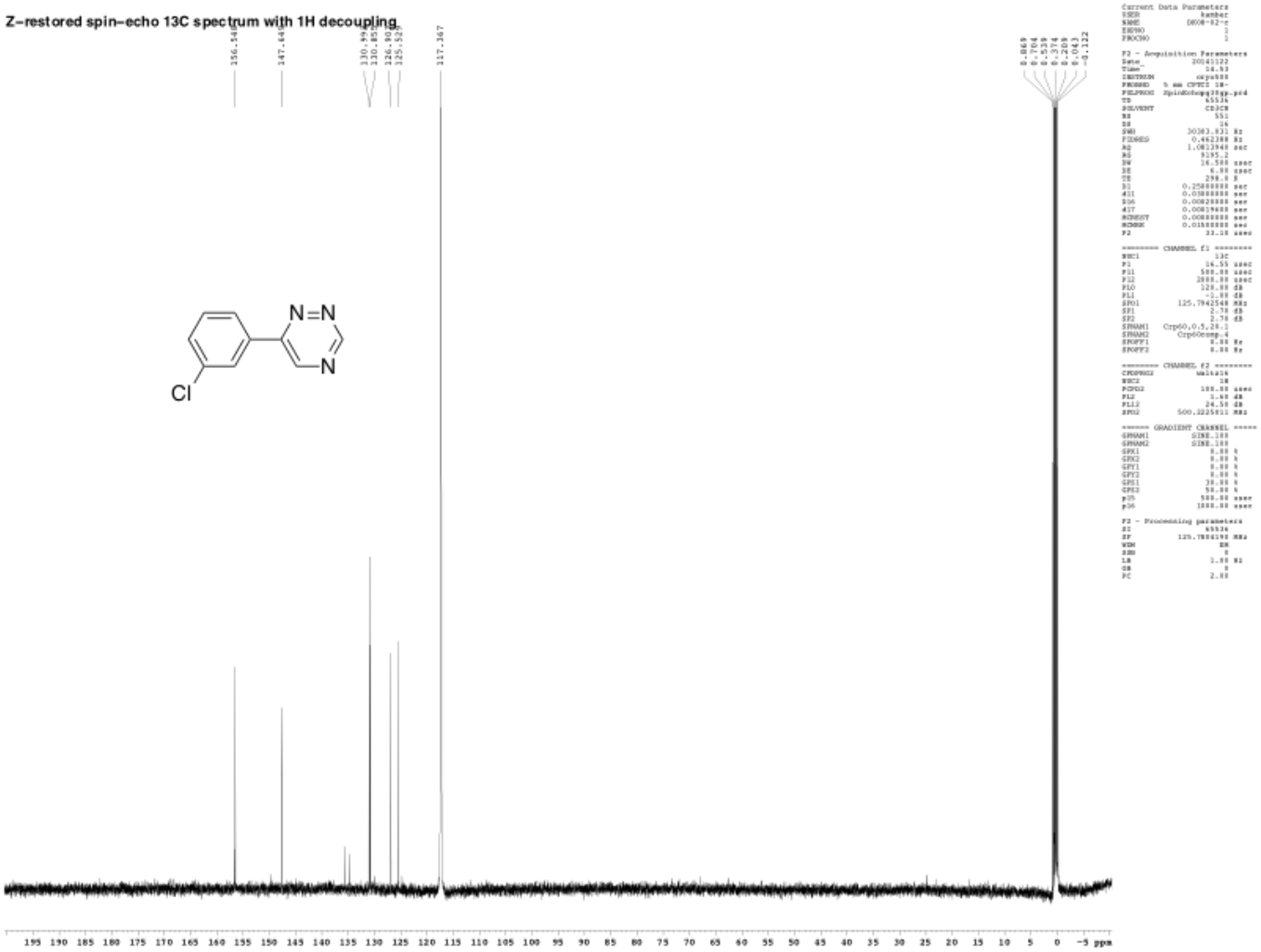
Z-restored spin-echo 13C spectrum with 1H decoupling
156.548
147.148
130.499
130.857
126.800
125.520
117.367
N=N
N
Cl
195 190 185 180 175 170 165 160 155 150 145 140 135 130 125 120 115 110 105 100 95 90 85 80 75 70 65 60 55 50 45 40 35 30 25 20 15 10 5 0 -5 ppm

1H spectrum

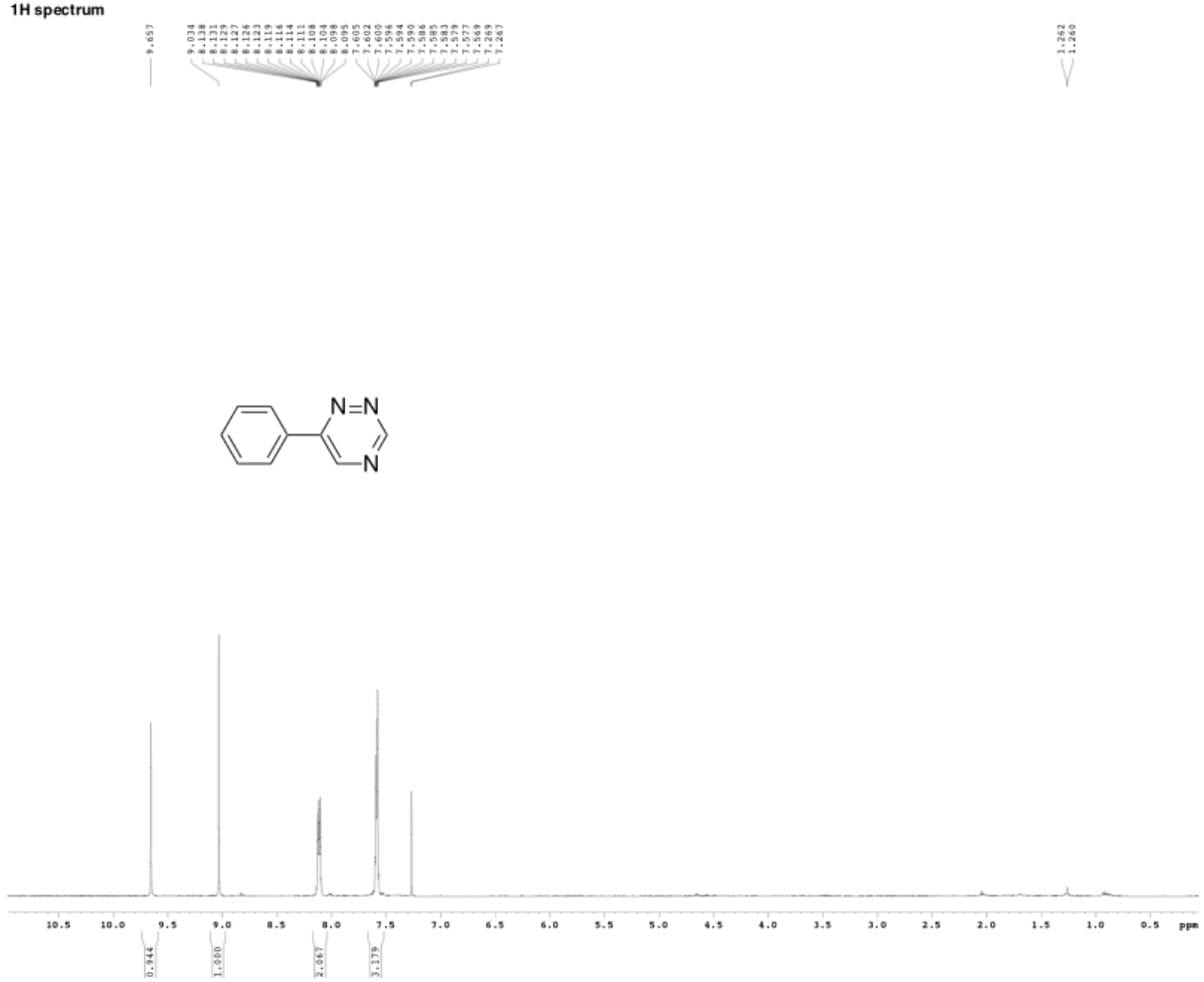


```
Current Data Parameters
USER              kamber
NAME            DK07-123
EXPNO                  1
PROCNO                 1

F2 - Acquisition Parameters
Date_           20141013
Time              17.23
INSTRUM           drx400
PROBHD    5 mm QNP H/P/F
PULPROG            zg30
TD                65536
SOLVENT           CDCl3
NS                     1
DS                     2
SWH            6410.256 Hz
FIDRES         0.097813 Hz
AQ             5.1118579 sec
RG                 456.1
DW               78.000 usec
DE                4.50 usec
TE                298.0 K
D1             0.10000000 sec
MCREST         0.00000000 sec
MCWRK          0.01500000 sec

======== CHANNEL f1 ========
NUC1                  1H
P1                12.00 usec
PL1                0.00 dB
SFO1        400.1328009 MHz

F2 - Processing parameters
SI                65536
SF          400.1300175 MHz
WDW                   EM
SSB                    0
LB                  0.30 Hz
GB                     0
PC                  2.00
```

Z-restored spin-echo 13C spectrum with 1H decoupling

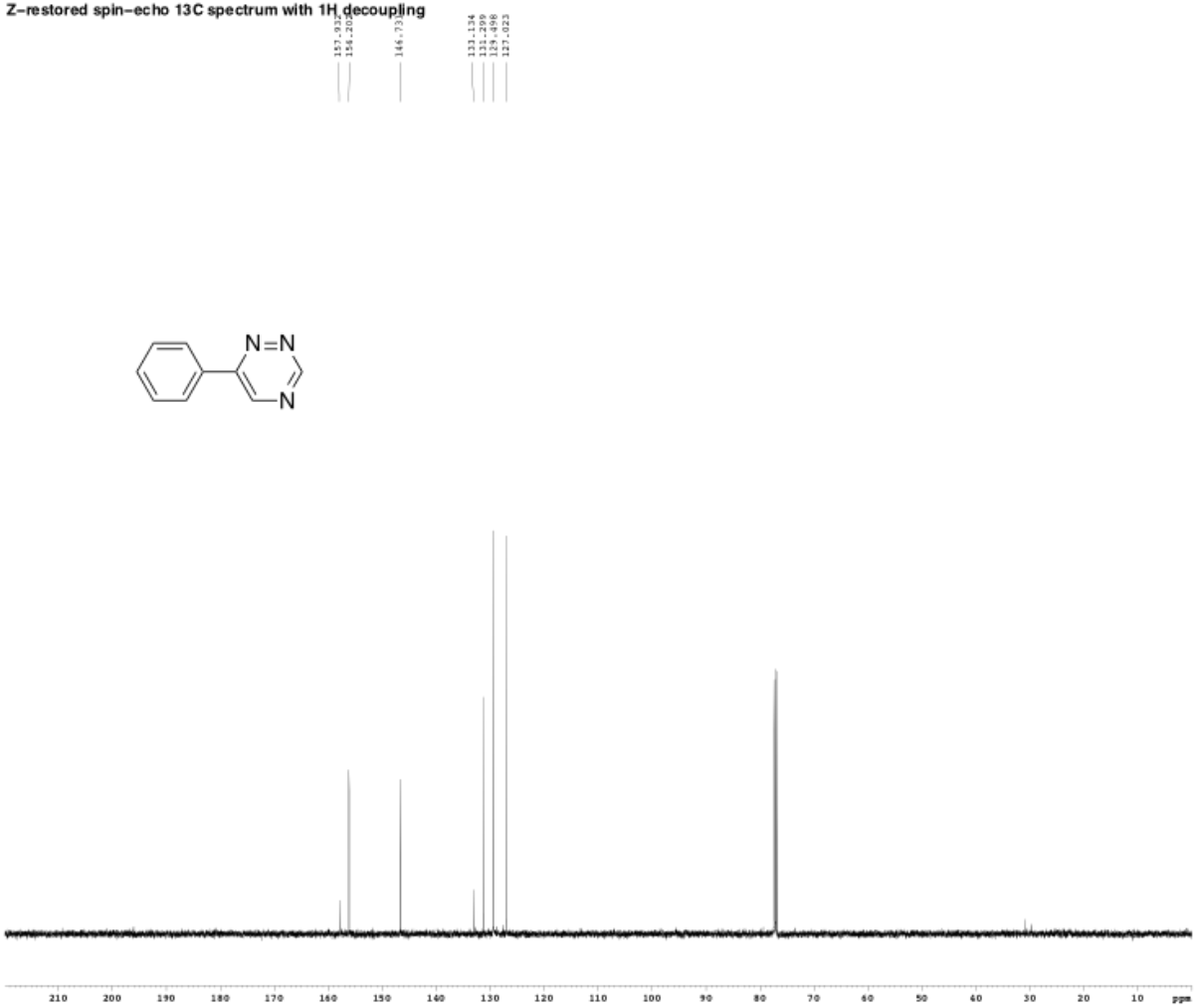


```
Current Data Parameters
USER              kamber
NAME        BR06-014-pure
EXPNO                   2
PROCNO                  1

F2 - Acquisition Parameters
Date_           20140204
Time              12.35
INSTRUM         cryo500
PROBHD   5 mm CPTCI 1H-
PULPROG  SpinEchopg3lsp.pcd
TD                  65536
SOLVENT             CDCl3
NS                    256
DS                     16
SWH             30303.031 Hz
FIDRES           0.462388 Hz
AQ               1.0813948 sec
RG                  7298.2
DW                  16.500 usec
DE                   6.00 usec
TE                  298.0 K
D1               0.25000000 sec
d11              0.03000000 sec
D16              0.00020000 sec
d17              0.00019400 sec
MCREST           0.00000000 sec
MCWRK            0.01500000 sec
P2                  31.00 usec

======== CHANNEL f1 ========
NUC1                  13C
P1                  15.50 usec
P11                 500.00 usec
P12                3000.00 usec
PL0                  120.00 dB
PL1                   -1.00 dB
SFO1           125.7942548 MHz
SP1                   3.20 dB
SP2                   3.20 dB
SPNAM1   crp60,0.5,28.1
SPNAM2      Crp60comp.4
SPOFF1                0.00 Hz
SPOFF2                0.00 Hz

======== CHANNEL f2 ========
CPDPRG2          waltz16
NUC2                   1H
PCPD2                100.00 usec
PL2                   1.00 dB
PL12                 24.00 dB
SFO2           500.2225811 MHz

====== GRADIENT CHANNEL =====
GPNAM1            SINE.100
GPNAM2            SINE.100
GPX1                  8.00 %
GPX2                  8.00 %
GPY1                  8.00 %
GPY2                  8.00 %
GPZ1                 30.00 %
GPZ2                 50.00 %
p15                 500.00 usec
p16                1000.00 usec

F2 - Processing parameters
SI                  65536
SF             125.7864190 MHz
WDW                    EM
SSB                     0
LB                   1.00 Hz
GB                      0
PC                   2.00
```

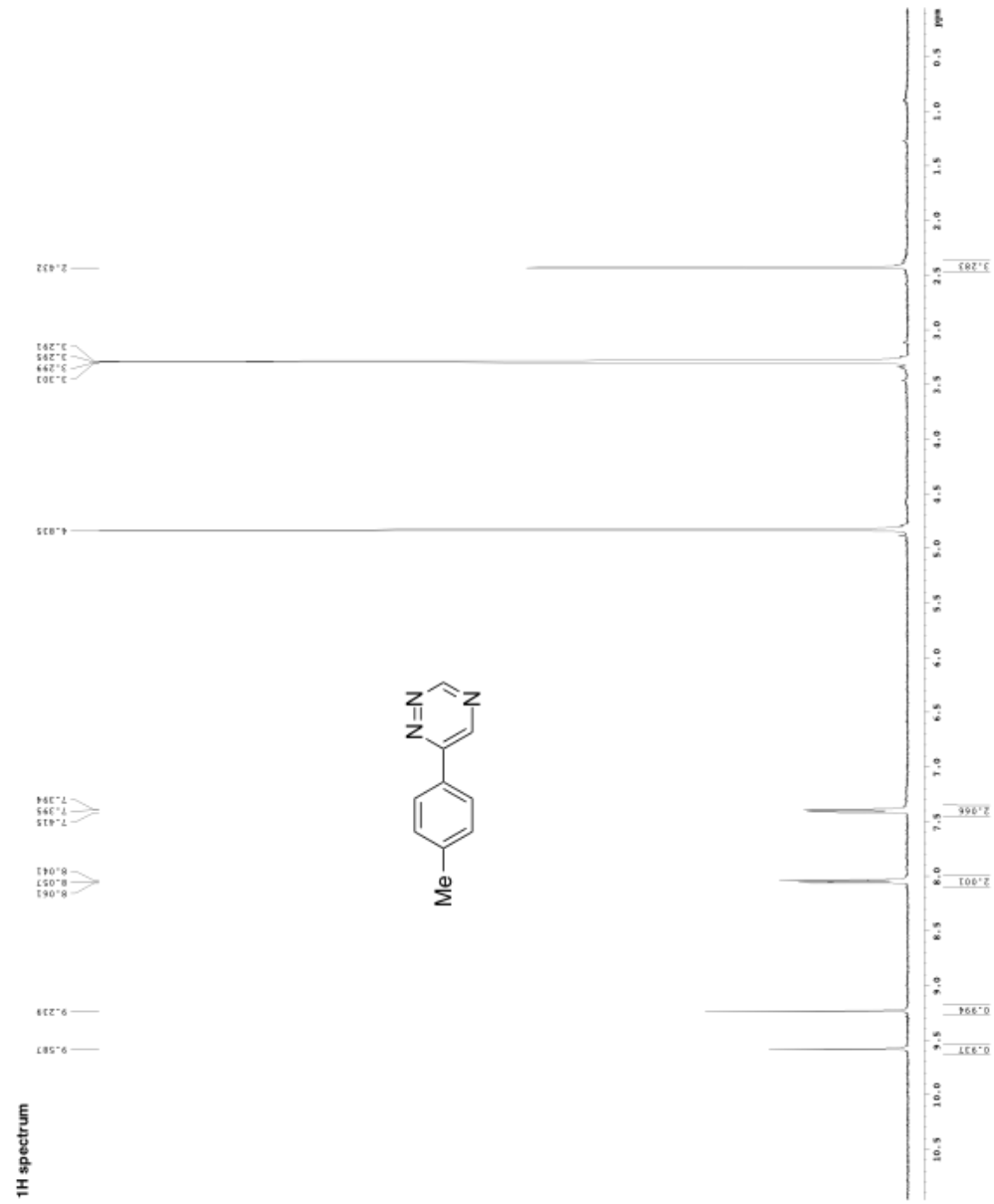
1H spectrum
Me
N
N
N
9.581
9.239
8.061
8.057
8.041
7.415
7.395
7.394
4.825
3.302
3.299
3.295
3.291
2.432
0.937
0.994
2.001
2.066
3.283
ppm

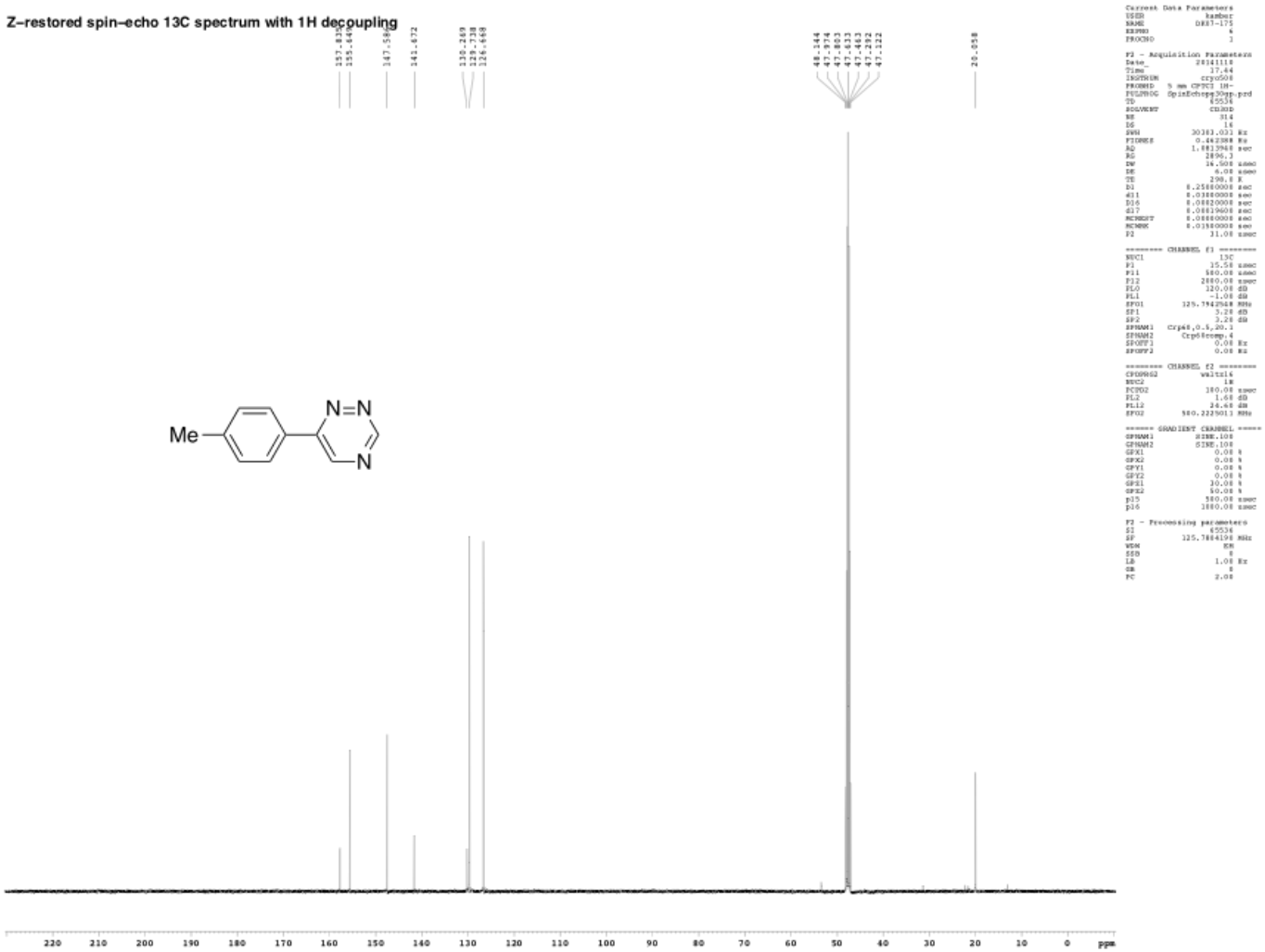
Z-restored spin-echo 13C spectrum with 1H decoupling
157.833
155.640
147.580
141.872
130.269
129.738
126.668
48.144
47.974
47.803
47.633
47.463
47.292
47.122
20.658
Me
N=N
N
220 210 200 190 180 170 160 150 140 130 120 110 100 90 80 70 60 50 40 30 20 10 0 ppm
Current Data Parameters
USER kamber
NAME D887-175
EXPNO 4
PROCNO 3
F2 - Acquisition Parameters
Date_ 20141118
Time 17.44
INSTRUM cryo500
PROBHD % mm CPTC1 1H-
PULPROG SpinEchepg30mp.prd
TD 65536
SOLVENT CDCl3
NS 314
DS 16
SWH 30383.031 Hz
FIDRES 0.462388 Hz
AQ 1.0813948 sec
RG 2896.3
DW 16.500 usec
DE 6.00 usec
TE 298.0 K
D1 0.25000000 sec
d11 0.03000000 sec
D16 0.00020000 sec
d17 0.00019600 sec
MCREST 0.00000000 sec
MCWRK 0.01500000 sec
P2 31.00 usec
======== CHANNEL f1 ========
NUC1 13C
P1 15.50 usec
P11 580.00 usec
P12 2880.00 usec
PL0 120.00 dB
PL1 -1.00 dB
SFO1 125.7942548 MHz
SP1 3.28 dB
SP2 3.28 dB
SPNAM1 Crp48,0.4,20.1
SPNAM2 Crp60comp.4
SPOFF1 0.00 Hz
SPOFF2 0.00 Hz
======== CHANNEL f2 ========
CPDPRG2 waltz16
NUC2 1H
PCPD2 180.00 usec
PL2 1.68 dB
PL12 24.68 dB
SFO2 500.2229011 MHz
====== GRADIENT CHANNEL =====
GPNAM1 SINE.100
GPNAM2 SINE.100
GPX1 0.00 %
GPX2 0.00 %
GPY1 0.00 %
GPY2 0.00 %
GPZ1 10.00 %
GPZ2 50.00 %
p15 580.00 usec
p16 1880.00 usec
F2 - Processing parameters
SI 65536
SF 125.7864198 MHz
WDW EM
SSB 0
LB 1.00 Hz
GB 0
PC 2.00

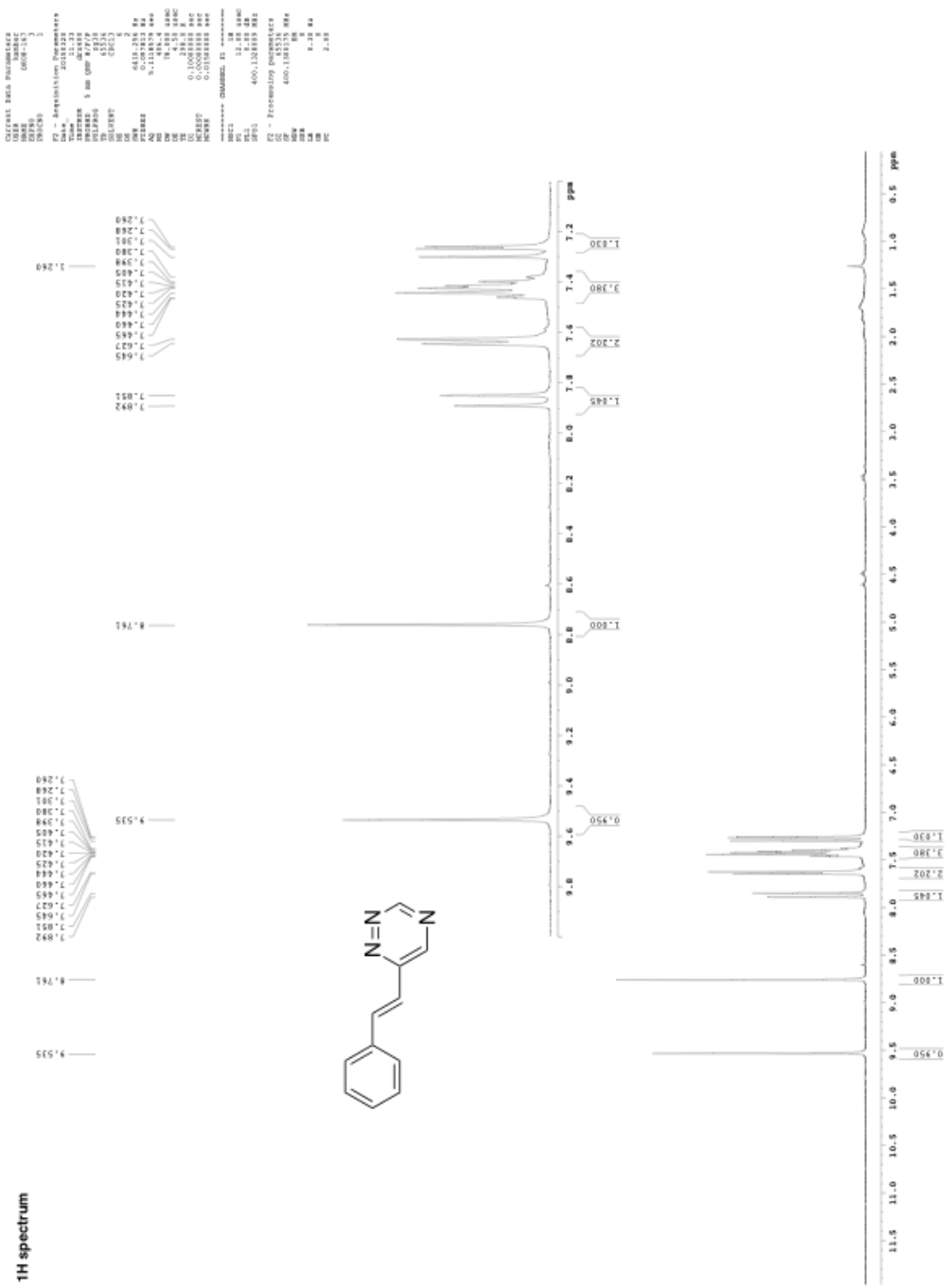
1H spectrum

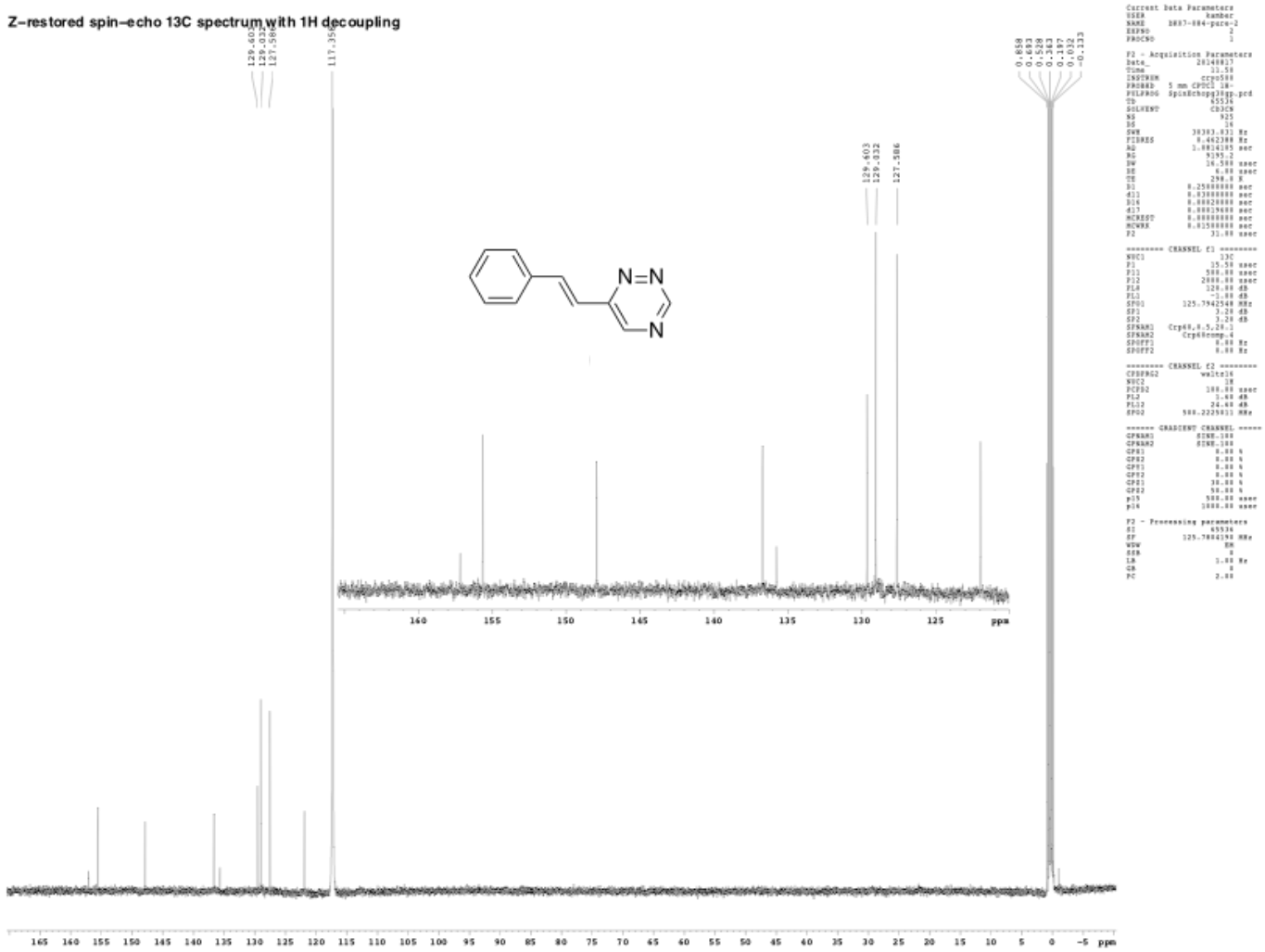
Z-restored spin-echo 13C spectrum with 1H decoupling
129.603
129.032
127.586
117.350
0.858
0.693
0.568
0.549
0.187
0.032
-0.133
N=N
N
ppm

1H spectrum

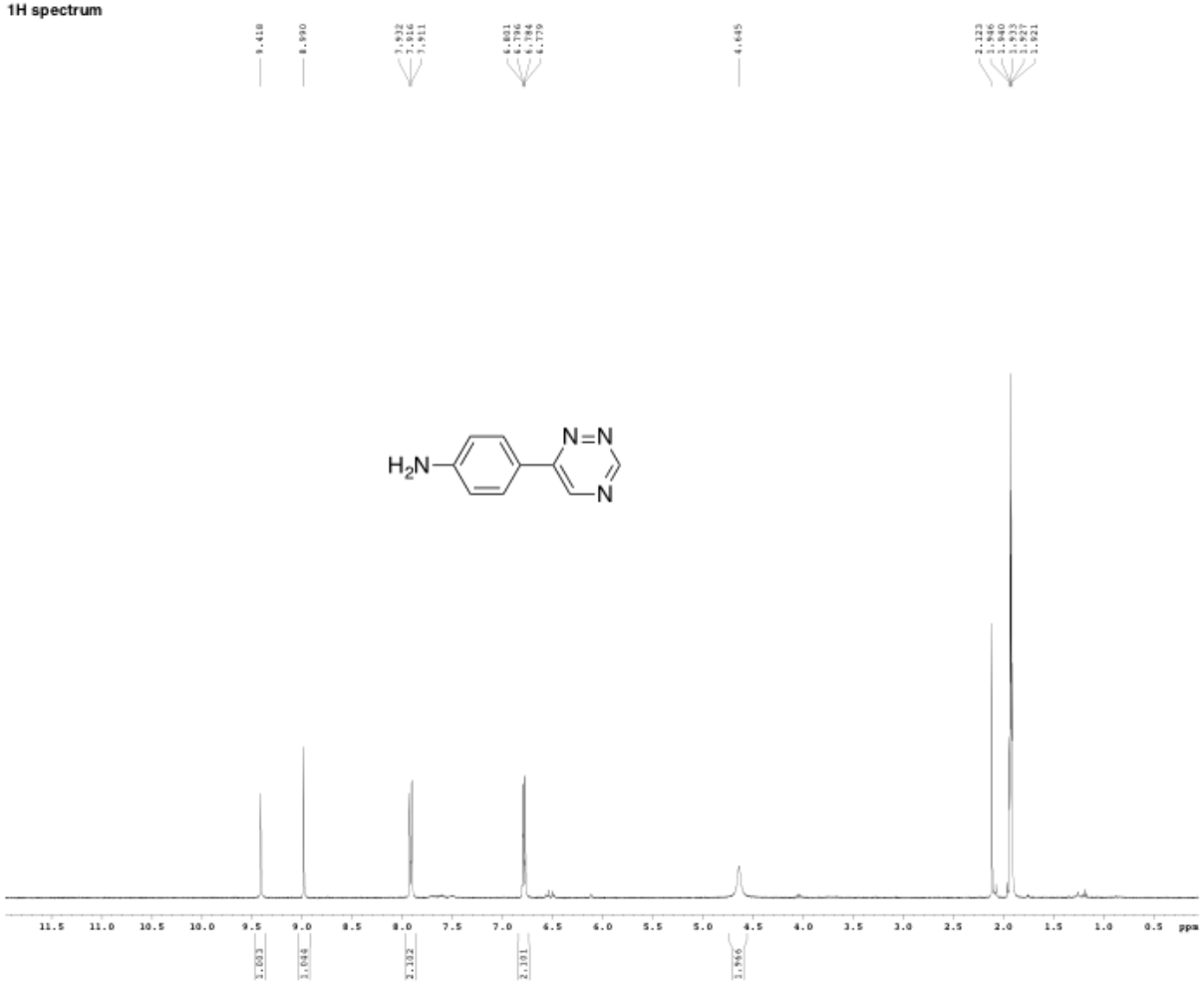

Current Data Parameters
USER kamker
NAME DEB-76
EXPNO 5
PROCNO 1

F2 - Acquisition Parameters
Date_ 20159106
Time 12.24
INSTRUM drx400
PROBHD 5 mm QNP 1/H/D
PULPROG zg30
TD 65536
SOLVENT CD3OD
NS 5
DS 2
SWH 6410.256 Hz
FIDRES 0.097813 Hz
AQ 5.1118579 sec
RG 1298.2
DW 78.000 usec
DE 6.50 usec
TE 293.9 K
D1 0.10000000 sec
MCREST 0.00000000 sec
MCWRK 0.01500000 sec

======== CHANNEL f1 ========
NUC1 1H
P1 12.80 usec
PL1 0.00 dB
SFO1 400.1328999 MHz

F2 - Processing parameters
SI 65536
SF 400.1300175 MHz
WDW EM
SSB 0
LB 0.30 Hz
GB 0
PC 2.00

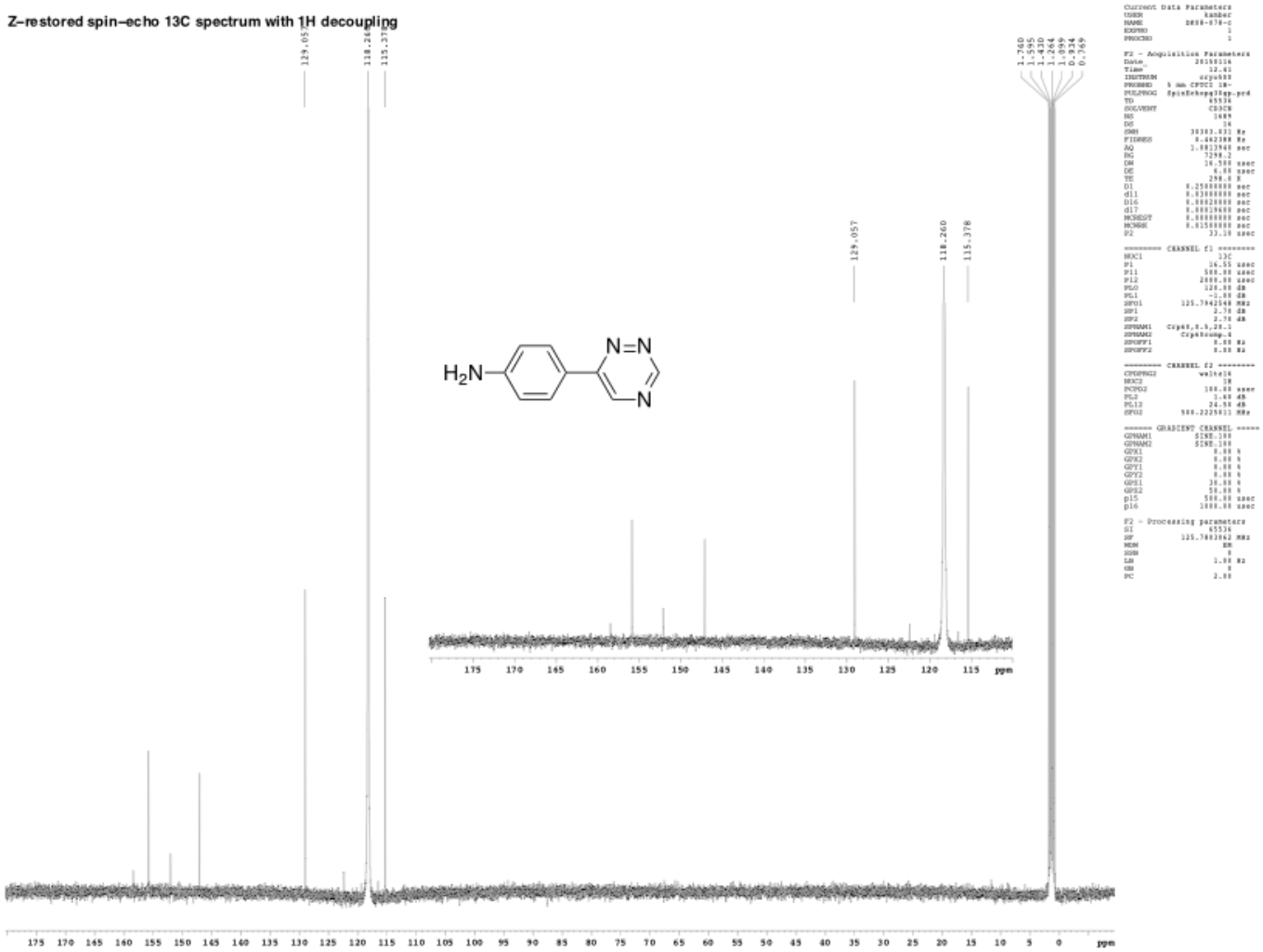
Z-restored spin-echo 13C spectrum with 1H decoupling
129.057
118.260
115.378
1.760
1.595
1.430
1.264
1.098
0.934
0.769
H_2N
N=N
N
ppm

1H spectrum

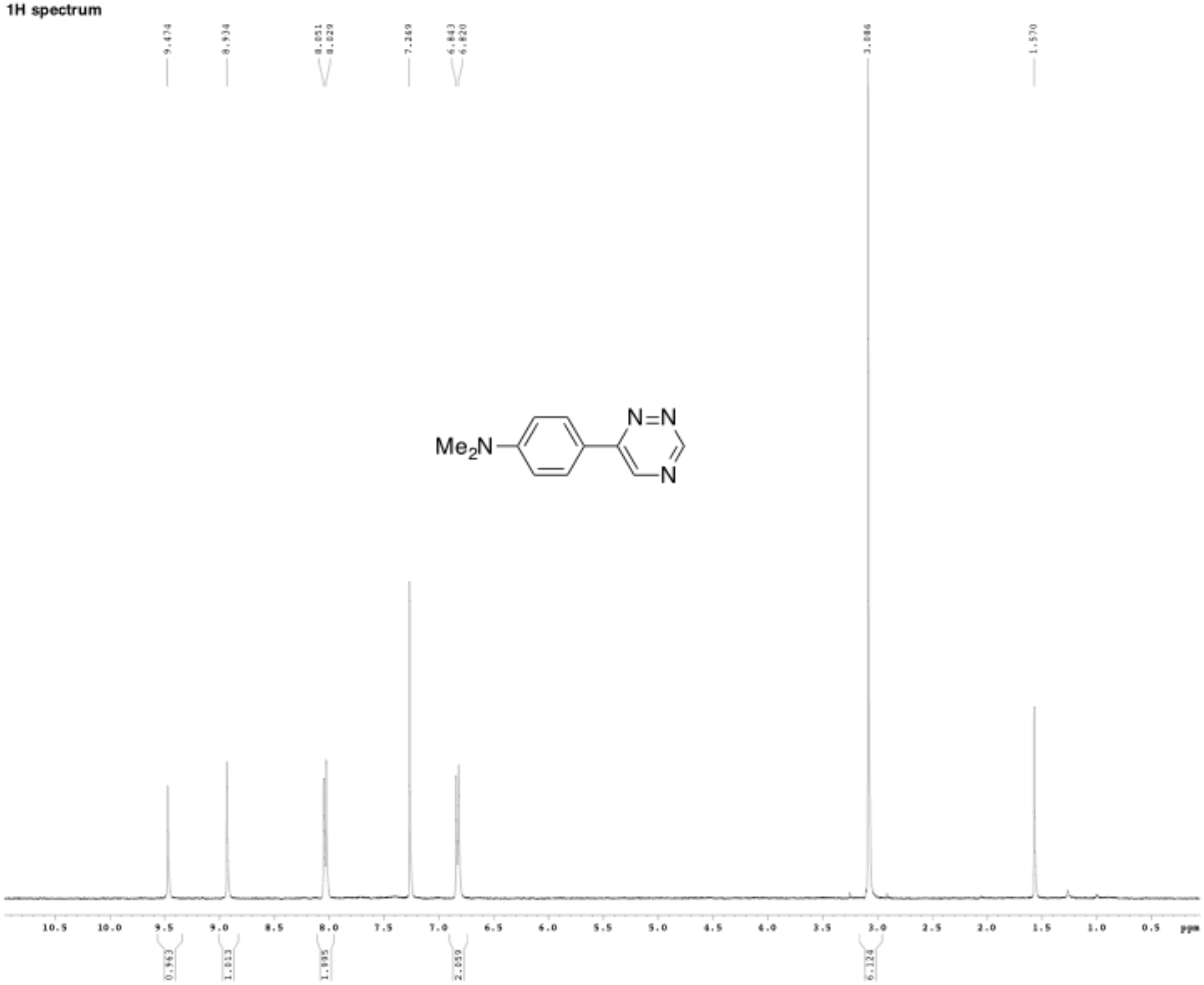


```
Current Data Parameters
USER                 kamber
NAME              3887-163
EXPNO                    2
PROCNO                   1

F2 - Acquisition Parameters
Date_             20141029
Time                 16.42
INSTRUM             drx400
PROBHD   5 mm QNP 1H/19/F
PULPROG              zg30
TD                   65536
SOLVENT              CDCl3
NS                       4
DS                       2
SWH               6410.256 Hz
FIDRES            0.097813 Hz
AQ                5.1118579 sec
RG                   1149.4
DW                   78.000 usec
DE                    6.50 usec
TE                   298.0 K
D1                0.10000000 sec
MCWRGT            0.00000000 sec
MCWNK             0.01500000 sec

======== CHANNEL f1 ========
NUC1                    1H
P1                   12.00 usec
PL1                   0.00 dB
SFO1            400.1320009 MHz

F2 - Processing parameters
SI                   65536
SF              400.1300175 MHz
WDW                     EM
SSB                      0
LB                    0.30 Hz
GB                       0
PC                    2.00
```

Z–restored spin–echo 13C spectrum with 1H decoupling

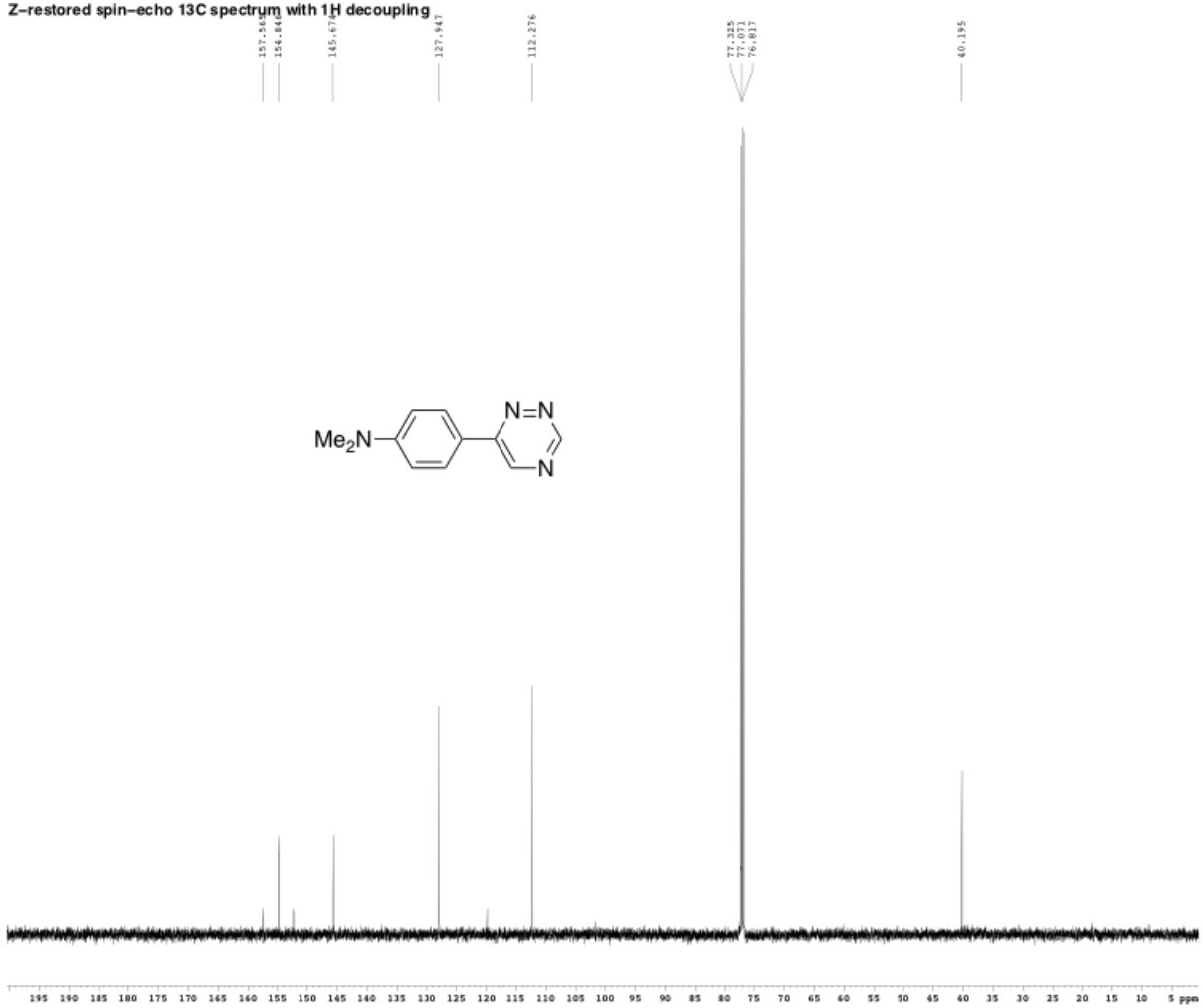


```
Current Data Parameters
USER                 kamber
NAME              1887-163
EXPNO                    5
PROCNO                   1

F2 - Acquisition Parameters
Date_            20141029
Time               16.49
INSTRUM            cryo500
PROBHD    5 mm CPTCI 1H-
PULPROG   zgpnscbsqg30gp.prd
TD                  65536
SOLVENT             CDCl3
NS                    787
DS                     16
SWH              38383.031 Hz
FIDRES           0.462388 Hz
AQ               1.4812948 sec
RG                  4597.4
DW                  16.588 usec
DE                   6.00 usec
TE                  298.0 K
D1               0.25000000 sec
d11              0.03000000 sec
D16              0.00020000 sec
d17              0.00019600 sec
MCREST           0.00000000 sec
MCWRK            0.01500000 sec
P2                  31.00 usec

======== CHANNEL f1 ========
NUC1                   13C
P1                   15.50 usec
P11                 500.00 usec
P12                2000.00 usec
PL0                 120.00 dB
PL1                  -1.00 dB
SFO1            125.7542548 MHz
SP1                  3.20 dB
SP2                  3.20 dB
SPNAM1    Crp60,0.5,20.1
SPNAM2       Crp60comp.4
SPOFF1               0.00 Hz
SPOFF2               0.00 Hz

======== CHANNEL f2 ========
CPDPRG2            waltz16
NUC2                   1H
PCPD2               100.00 usec
PL2                  1.00 dB
PL12                 26.40 dB
SFO2            500.2225011 MHz

====== GRADIENT CHANNEL =====
GPNAM1             SINE.100
GPNAM2             SINE.100
GPX1                 0.00 %
GPX2                 0.00 %
GPY1                 0.00 %
GPY2                 0.00 %
GPZ1                20.00 %
GPZ2                50.00 %
p15                500.00 usec
p16                1000.00 usec

F2 - Processing parameters
SI                  65536
SF            125.7804193 MHz
WDW                    EM
SSB                     0
LB                   1.00 Hz
GB                      0
PC                   2.00
```

1H spectrum

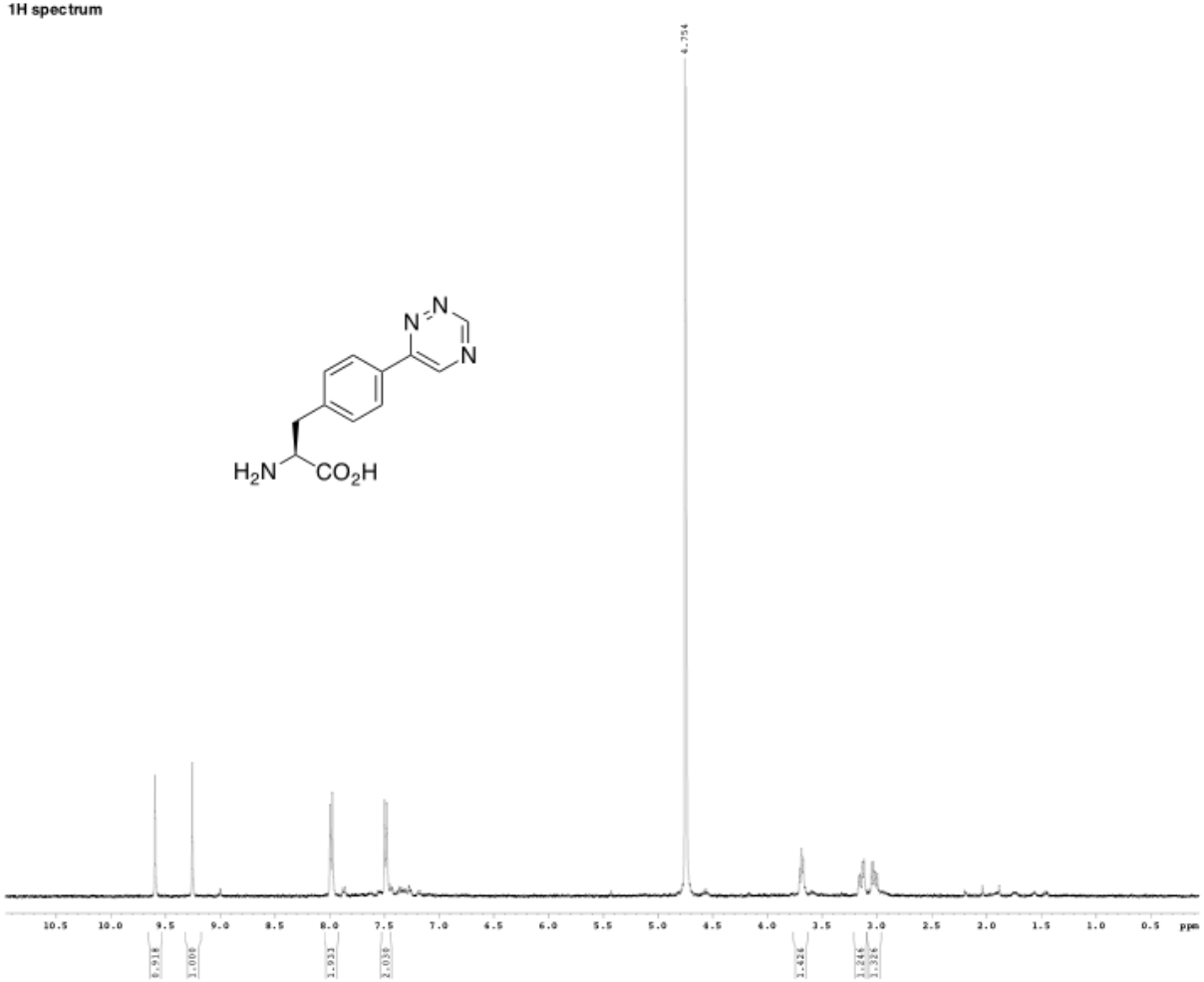


```
Current Data Parameters
USER            kamber
NAME          DR07-126-5
EXPNO                 1
PROCNO                1

F2 - Acquisition Parameters
Date_          20141002
Time             12.51
INSTRUM        drx400
PROBHD   5 mm QNP H/F/P
PULPROG          zg30
TD              65536
SOLVENT           D2O
NS                  5
DS                  2
SWH          6410.256 Hz
FIDRES       0.097813 Hz
AQ           5.1118579 sec
RG              1149.4
DW               78.000 usec
DE                4.50 usec
TE              297.9 K
D1           0.100000000 sec
MCREST       0.000000000 sec
MCWRK        0.01500000 sec

======== CHANNEL f1 ========
NUC1               1H
P1               12.00 usec
PL1               0.00 dB
SFO1        400.1328009 MHz

F2 - Processing parameters
SI              65536
SF          400.1300175 MHz
WDW               EM
SSB                0
LB              0.30 Hz
GB                 0
PC              2.00
```

Z-restored spin-echo 13C spectrum with 1H decoupling

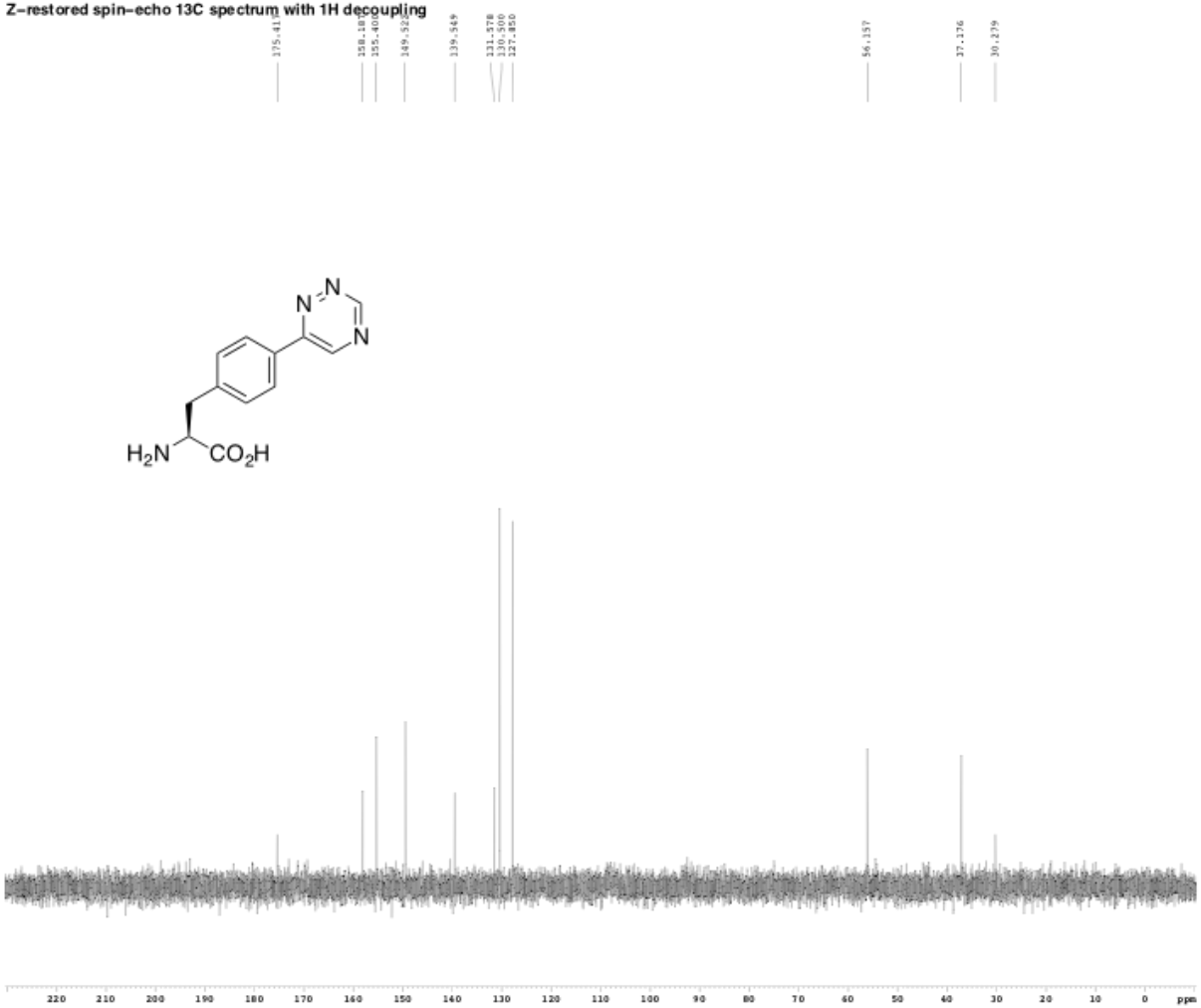


```
Current Data Parameters
USER            kamber
NAME         8887-145-c
EXPNO              2
PROCNO             1

F2 - Acquisition Parameters
Date_        20141019
Time            18.04
INSTRUM       spect500
PROBHD   5 mm CPDCI 1H-
PULPROG  Spin8ehsqp18qp.pr4
TD            65536
SOLVENT         D20
NS              1129
DS                 16
SWH          38383.831 Hz
FIDRES       0.462388 Hz
AQ           1.8812948 sec
RG             11585.2
DW              16.586 usec
DE               6.00 usec
TE             298.0 K
D1           0.25000000 sec
d11          0.03000000 sec
D16          0.00020000 sec
d17          0.00019600 sec
MCREST       0.00000000 sec
MCWRK        0.01500000 sec
P2              33.00 usec

======== CHANNEL f1 ========
NUC1              13C
P1              15.50 usec
P11            500.00 usec
P12           2000.00 usec
PL0             120.00 dB
PL1              -1.00 dB
SFO1        125.7942548 MHz
SP1               3.20 dB
SP2               3.20 dB
SPNAM1   Crp60,0.5,20.1
SPNAM2      Crp60comp.4
SPOFF1            0.00 Hz
SPOFF2            0.00 Hz

======== CHANNEL f2 ========
CPDPRG2         waltz16
NUC2              1H
PCPD2           100.00 usec
PL2               1.40 dB
PL12             24.40 dB
SFO2        499.2228811 MHz

====== GRADIENT CHANNEL =====
GPNAM1         SINE.100
GPNAM2         SINE.100
GPX1              8.00 %
GPX2              8.00 %
GPY1              8.00 %
GPY2              8.00 %
GPZ1             20.00 %
GPZ2             50.00 %
p15             500.00 usec
p16            1000.00 usec

F2 - Processing parameters
SI                65536
SF          125.7846198 MHz
WDW                EM
SSB                 0
LB               1.00 Hz
GB                  0
PC               2.00
```

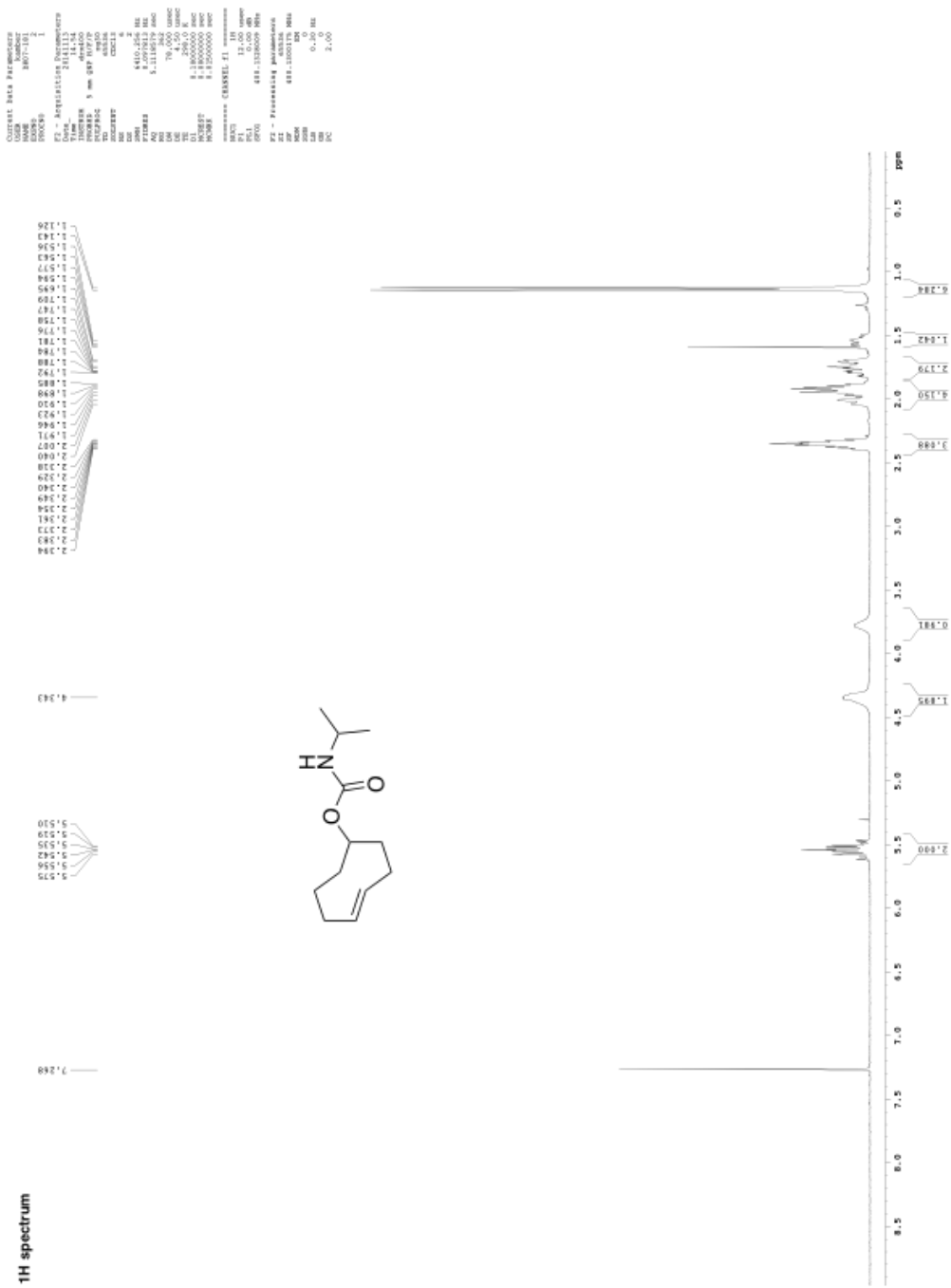
1H spectrum
ppm

Z-restored spin-echo 13C spectrum with 1H decoupling

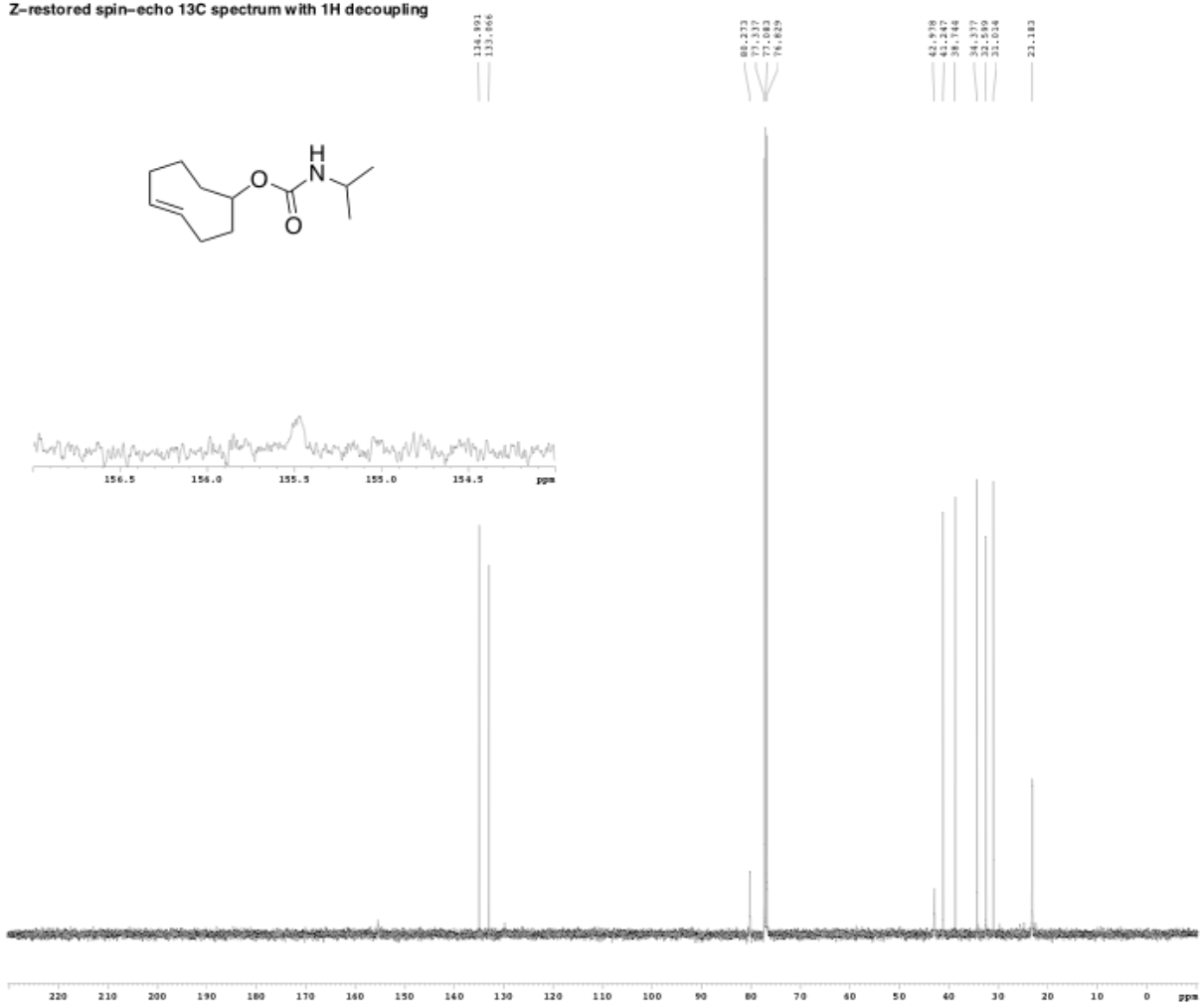


```
Current Data Parameters
NAME          DR07-181-c
EXPNO                   1
PROCNO                  1

F2 - Acquisition Parameters
Date_          20141113
Time             15.14
INSTRUM          cryo500
PROBHD   5 mm CPTCI 1H-
PULPROG  SpinEchopg1kgp.prd
TD             65536
SOLVENT          CDCl3
NS               1857
DS                  16
SWH          30303.031 Hz
FIDRES       0.462388 Hz
AQ           1.0813948 sec
RG               4896
DW             16.500 usec
DE              6.00 usec
TE            298.0 K
D1           0.25000000 sec
d11          0.03000000 sec
D16          0.00020000 sec
d17          0.00019000 sec
MCREST       0.00000000 sec
MCWRK        0.01500000 sec
P2              30.00 usec

======== CHANNEL f1 ========
NUC1              13C
P1               15.50 usec
P11             500.00 usec
P12            2000.00 usec
PL0             120.00 dB
PL1              -1.00 dB
SFO1         125.7942548 MHz
SP1              3.28 dB
SP2              3.28 dB
SPNAM1   Crp40,0.5,28.1
SPNAM2      Crp60comp.4
SPOFF1           0.00 Hz
SPOFF2           0.00 Hz

======== CHANNEL f2 ========
CPDPRG2        waltz16
NUC2              1H
PCPD2           108.00 usec
PL2              1.00 dB
PL12            24.40 dB
SFO2         500.2225811 MHz

====== GRADIENT CHANNEL =====
GPNAM1         SINE.100
GPNAM2         SINE.100
GPX1             8.00 %
GPX2             8.00 %
GPY1             8.00 %
GPY2             8.00 %
GPZ1            50.00 %
GPZ2            50.00 %
p15            500.00 usec
p16           1000.00 usec

F2 - Processing parameters
SI               65536
SF          125.7904139 MHz
WDW                 EM
SSB                  0
LB                1.00 Hz
GB                   0
PC               2.00
```

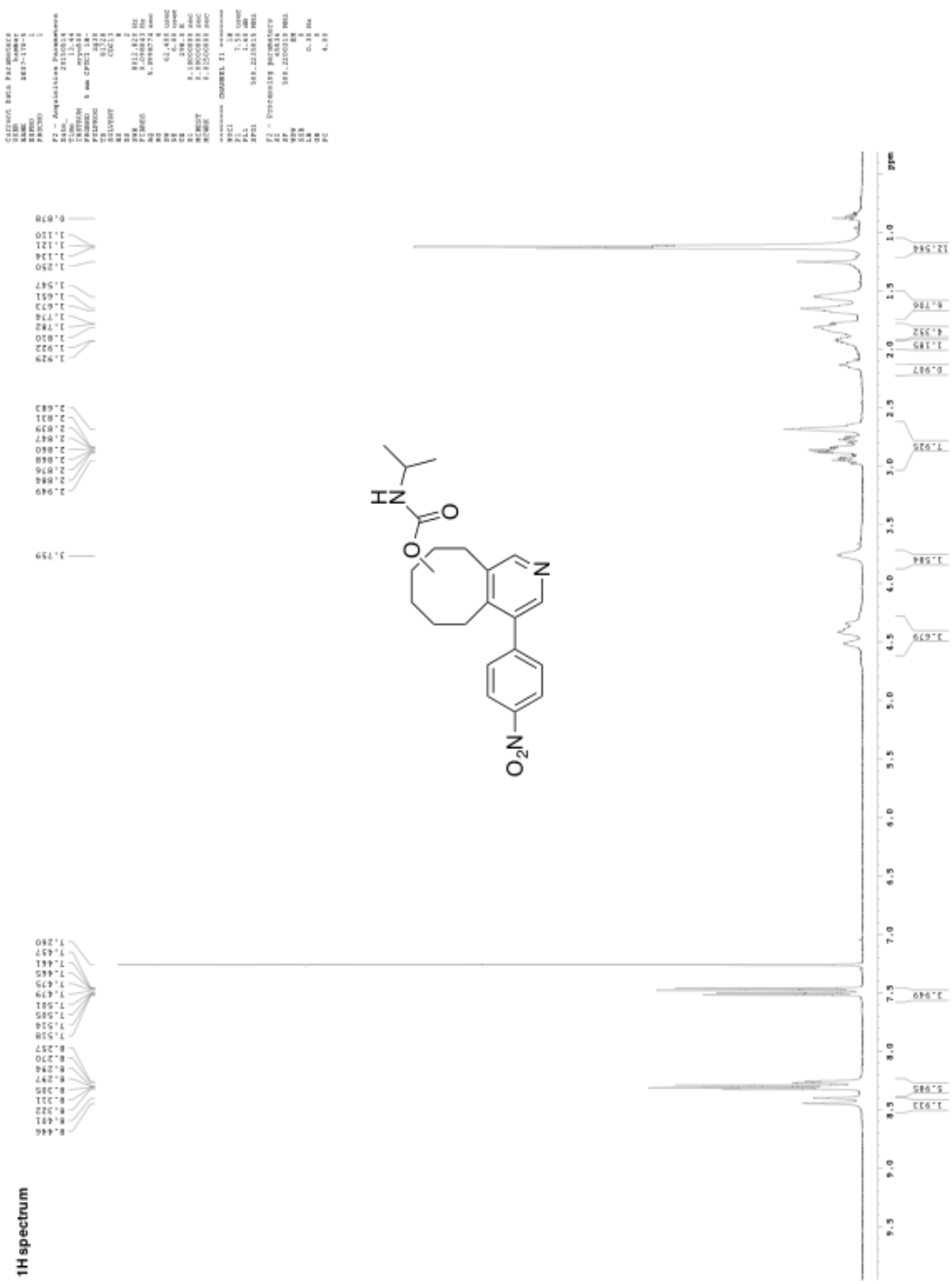
1H spectrum

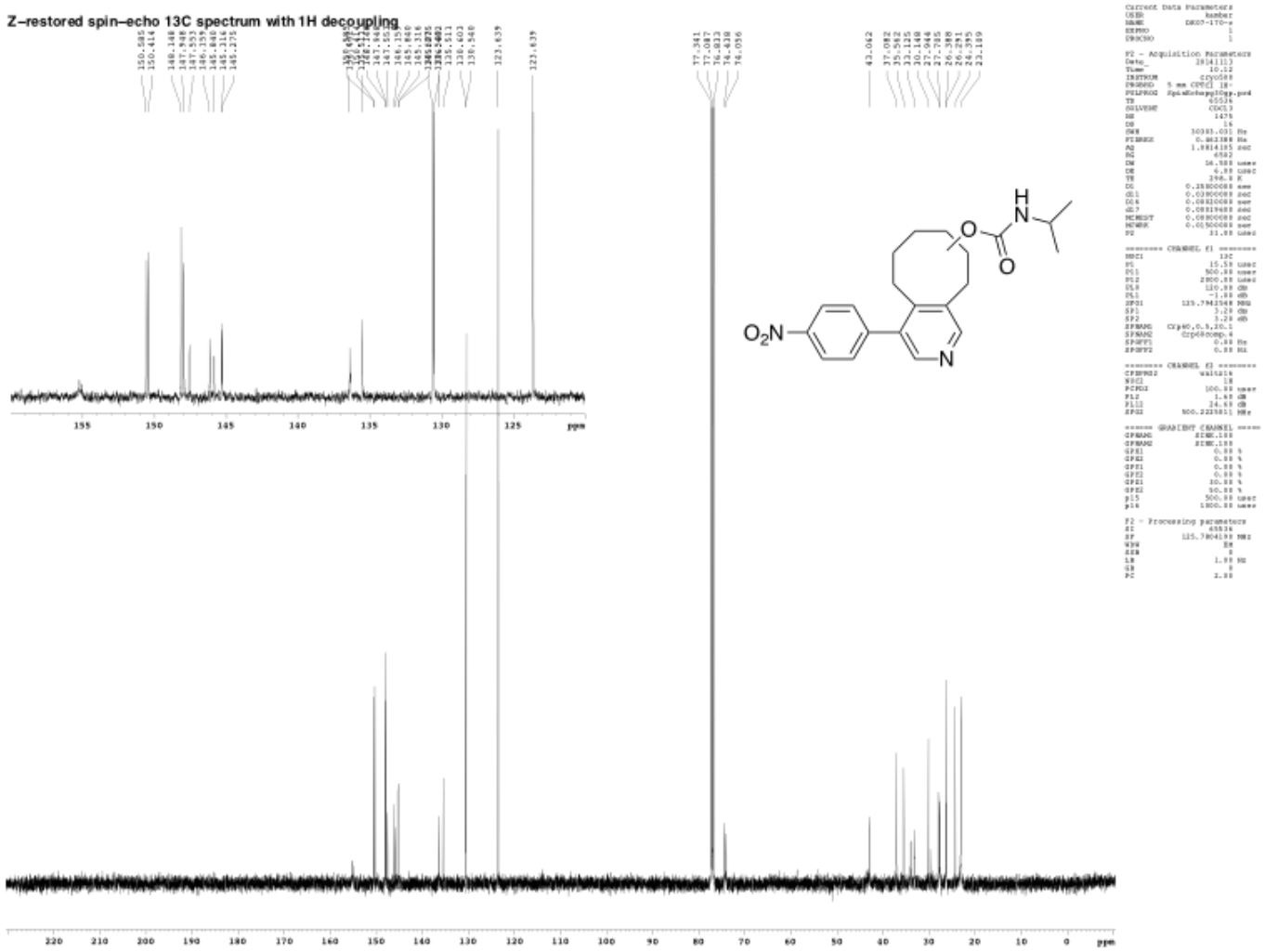
Z-restored spin-echo 13C spectrum with 1H decoupling
150.885
150.414
148.348
147.948
147.555
146.359
145.840
145.316
145.275
147.844
147.155
145.846
145.316
136.603
136.540
123.639
123.639
77.341
77.087
76.833
74.438
74.056
43.042
37.082
35.562
33.135
30.148
27.944
27.795
26.388
24.331
23.935
23.169
155
150
145
140
135
130
125
ppm
220
210
200
190
180
170
160
150
140
130
120
110
100
90
80
70
60
50
40
30
20
10
0
ppm
O
O
H
N
N
O_2N

1H spectrum

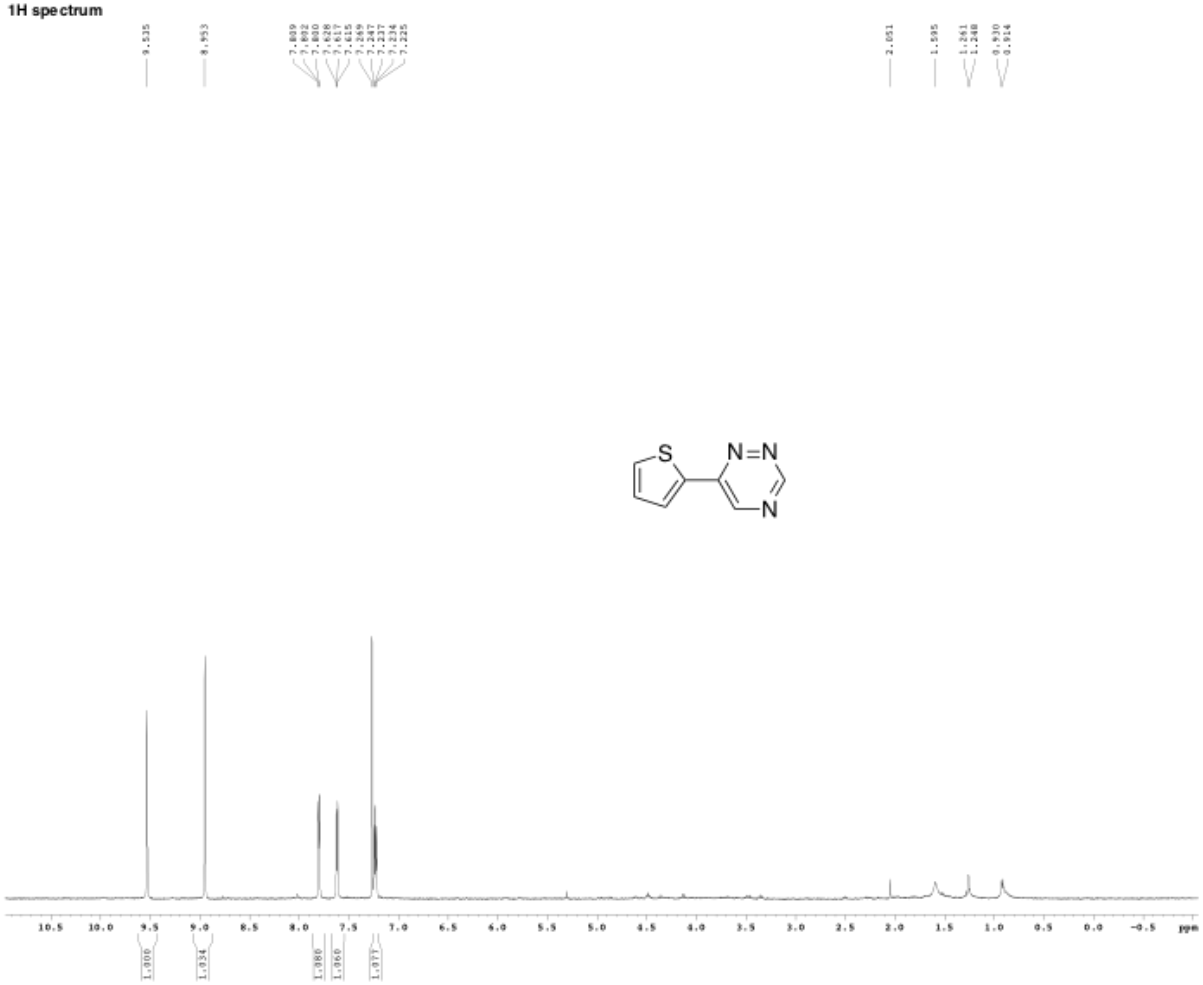


```
Current Data Parameters
NAME              hamber
EXPNO                  1
PROCNO                 1

F2 - Acquisition Parameters
Date_          20140721
Time               12.51
INSTRUM          dmx400
PROBHD   5 mm QNP H/P/F
PULPROG            zg30
TD                 65536
SOLVENT            CDCl3
NS                     4
DS                     2
SWH             6410.256 Hz
FIDRES          0.097903 Hz
AQ              5.1118579 sec
RG                 1149.4
DW                 78.088 usec
DE                  4.50 usec
TE                 296.0 K
D1              8.00000088 sec
MCREST          8.00000088 sec
MCWRK           8.01500088 sec

======== CHANNEL f1 ========
NUC1                  1H
P1                 12.00 usec
PL1                 0.00 dB
SFO1          400.1320009 MHz

F2 - Processing parameters
SI                 65536
SF          400.1300175 MHz
WDW                   EM
SSB                    0
LB                  0.30 Hz
GB                     0
PC                  1.00
```

Z-restored spin-echo 13C spectrum with 1H decoupling

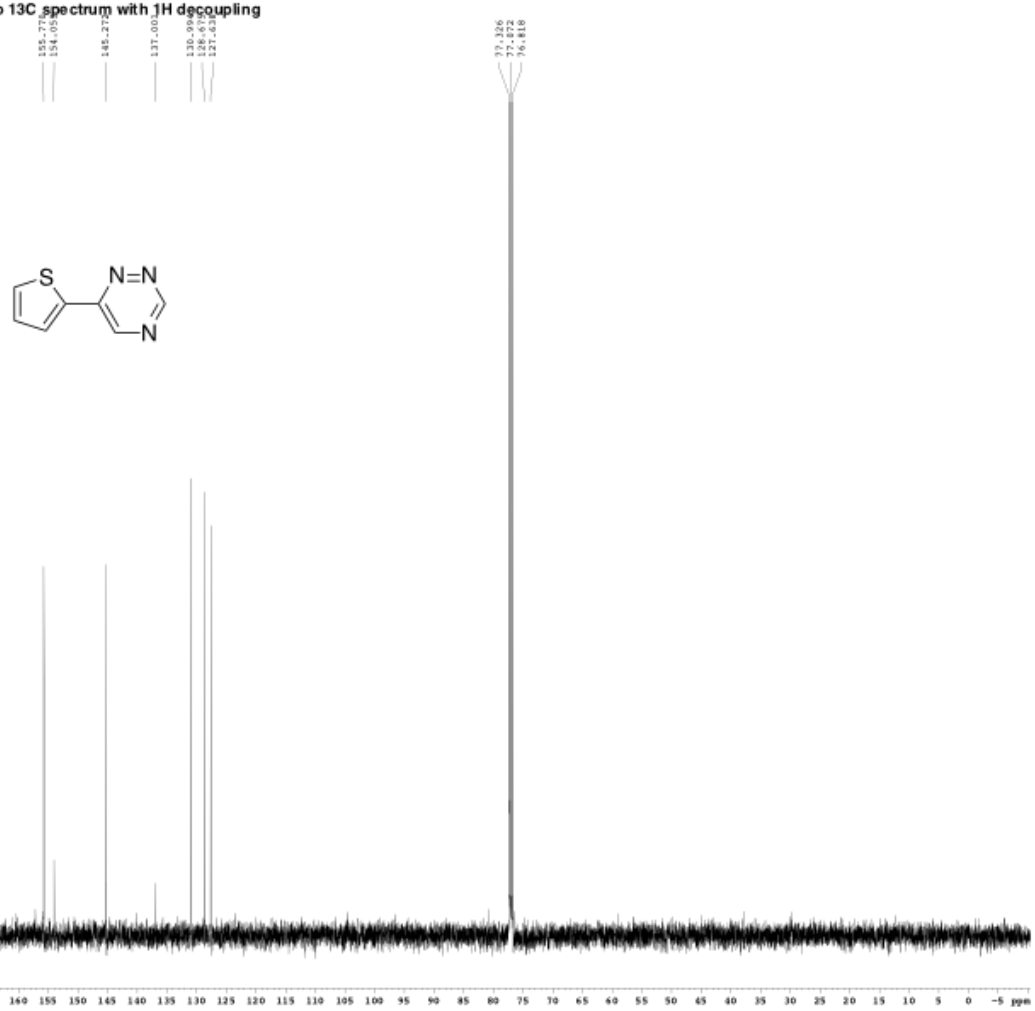


```
Current Data Parameters
NAME                 kamber
EXPNO                     3
PROCNO                    1

F2 - Acquisition Parameters
Date_             20140721
Time                 14.12
INSTRUM            spect600
PROBHD   5 mm CPTCI 1H-
PULPROG  zgpg30cgp.pr4
TD                    65536
SOLVENT               CDCl3
NS                      923
DS                       16
SWH                30303.031 Hz
FIDRES             0.462388 Hz
AQ                 1.0814105 sec
RG                    4597.6
DW                    16.500 usec
DE                     6.00 usec
TE                    298.0 K
D1                 0.35000000 sec
d11                0.03000000 sec
D16                0.00020000 sec
d17                0.00019600 sec
MCREST             0.00000000 sec
MCWRK              0.01500000 sec
P2                    31.00 usec

======== CHANNEL f1 ========
NUC1                     13C
P1                     15.50 usec
PL1                   500.00 usec
PL12                 2000.00 usec
PL2                   120.00 dB
PL13                   -1.00 dB
SFO1            125.7942548 MHz
SP1                      3.20 dB
SP2                      3.20 dB
SPNAM1     crp60,0.5,20.1
SPNAM2        crp60comp.4
SPOFF1                   0.00 Hz
SPOFF2                   0.00 Hz

======== CHANNEL f2 ========
CPDPRG2             waltz16
NUC2                      1H
PCPD2                   100.00 usec
PL2                       1.60 dB
PL12                     24.60 dB
SFO2            500.2225011 MHz

====== GRADIENT CHANNEL =====
GPNAM1              SINE.100
GPNAM2              SINE.100
GPZ1                     0.00 %
GPZ2                     0.00 %
GPZ3                     0.00 %
GPZ4                     0.00 %
GPZ11                   30.00 %
GPZ12                   50.00 %
pl15                   500.00 usec
pl16                  1000.00 usec

F2 - Processing parameters
SI                       65536
SF                 125.7904190 MHz
WDW                         EM
SSB                          0
LB                        1.00 Hz
GB                           0
PC                        2.00
```

1H spectrum

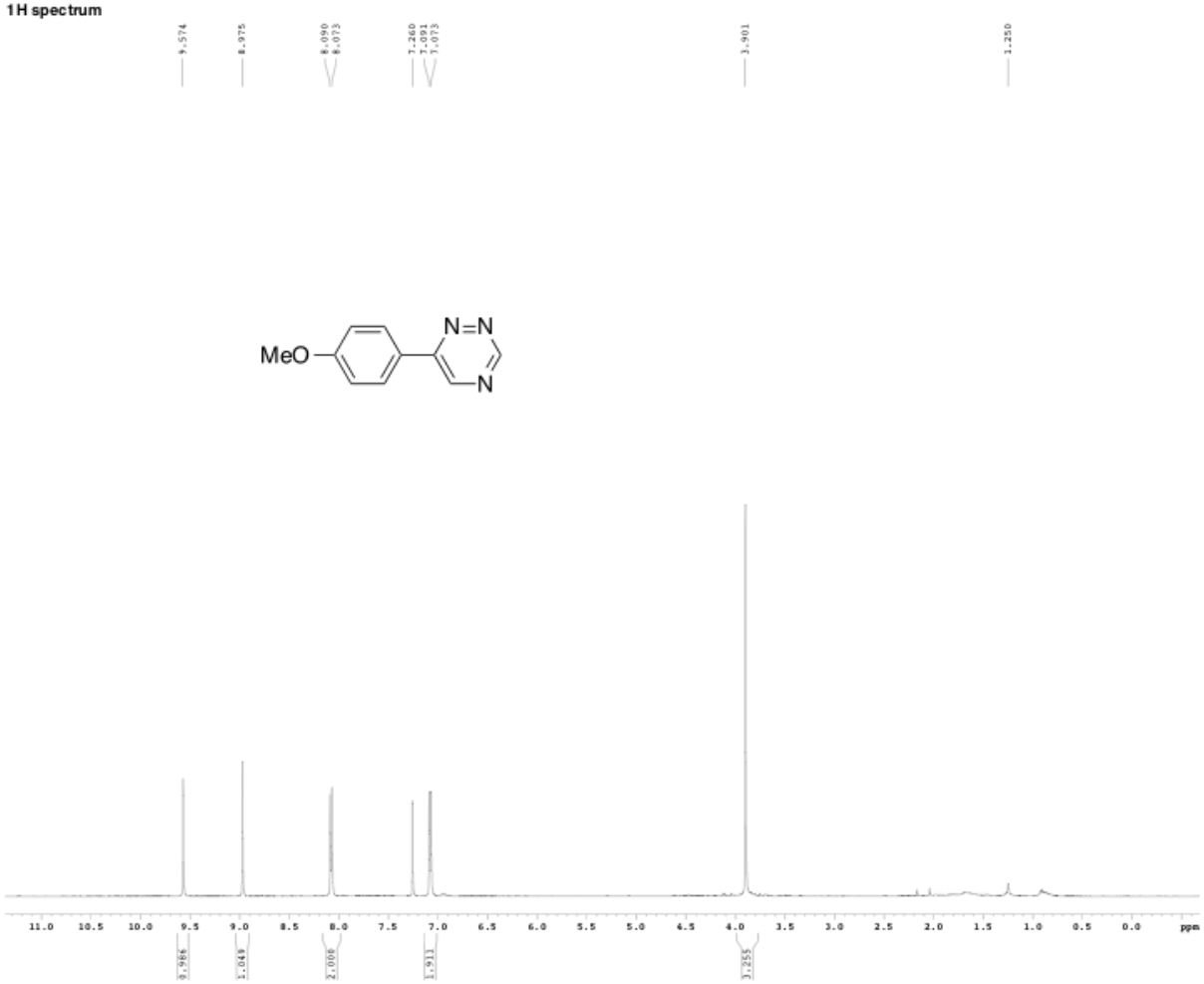


```
Current Data Parameters
USER              kamber
NAME              2E07-034
EXPNO                   4
PROCNO                  1

F2 - Acquisition Parameters
Date_          20140715
Time               16.18
INSTRUM        ergu500
PROBHD   5 mm CPTCI 1H-
PULPROG            zg30
TD                 81728
SOLVENT            CDCl3
NS                     4
DS                     2
SWH             8012.820 Hz
FIDRES          0.098043 Hz
AQ              5.0998772 sec
RG                   7.1
DW                 62.400 usec
DE                  6.00 usec
TE                 298.0 K
D1              0.10000000 sec
MCREST          0.00000000 sec
MCWRK           0.01500000 sec

======== CHANNEL f1 ========
NUC1                  1H
P1                 7.50 usec
PL1                3.60 dB
SFO1          500.2235835 MHz

F2 - Processing parameters
SI                 65536
SF            500.2200316 MHz
WDW                   EM
SSB                    0
LB                  0.30 Hz
GB                     0
PC                  4.00
```

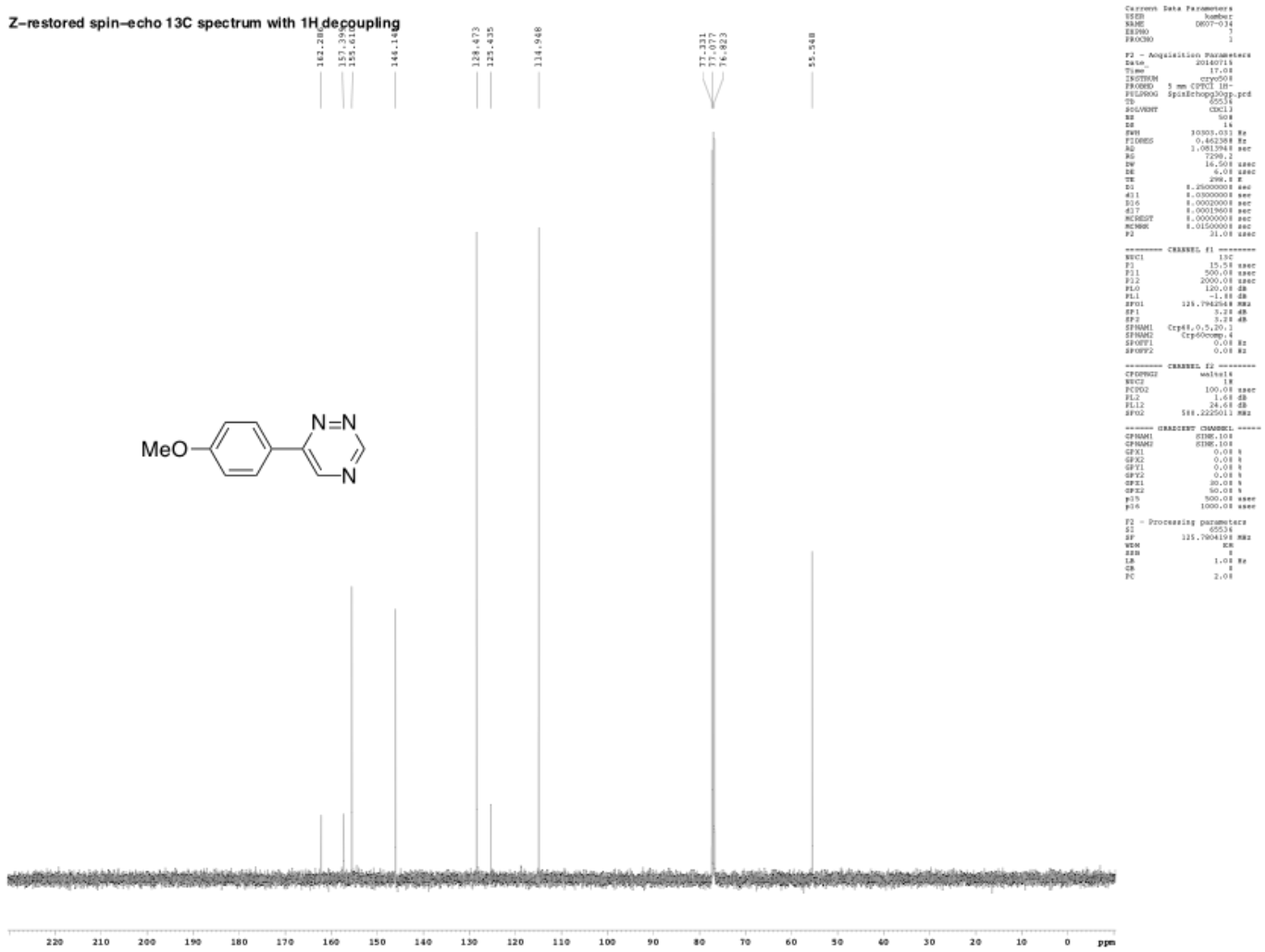
Z-restored spin-echo 13C spectrum with 1H decoupling
162.280
157.399
155.611
146.149
128.673
125.435
114.948
77.331
77.077
76.823
55.548
MeO
N=N
N
220 210 200 190 180 170 160 150 140 130 120 110 100 90 80 70 60 50 40 30 20 10 0 ppm
Current Data Parameters
USER kamber
NAME 0807-034
EXPNO 1
PROCNO 1
F2 - Acquisition Parameters
Date_ 20140716
Time 17.08
INSTRUM cryo500
PROBHD 5 mm CPTCI 1H-
PULPROG SpinEchopg30cpg.pcd
TD 65536
SOLVENT CDCl3
NS 508
DS 16
SWH 30303.031 Hz
FIDRES 0.462388 Hz
AQ 1.0813948 sec
RG 7298.2
DW 16.500 usec
DE 6.08 usec
TE 298.8 K
D1 8.25000000 sec
d31 8.03000000 sec
D16 8.00020000 sec
d17 8.00019600 sec
MCREST 8.00000000 sec
MCWRK 8.01500000 sec
P2 31.08 usec
======== CHANNEL f1 ========
NUC1 13C
P1 15.58 usec
P11 500.08 usec
P12 2000.08 usec
PL0 120.08 dB
PL1 -1.88 dB
SFO1 125.7942548 MHz
SP1 3.28 dB
SP2 3.28 dB
SPNAM1 Crp48,0.5,20.1
SPNAM2 Crp60comp.4
SFOFF1 0.08 Hz
SFOFF2 0.08 Hz
======== CHANNEL f2 ========
CPDPRG2 waltz16
NUC2 1H
PCPD2 100.08 usec
PL2 1.68 dB
PL12 24.68 dB
SFO2 500.2225011 MHz
====== GRADIENT CHANNEL =====
GPNAM1 SINE.100
GPNAM2 SINE.100
GPX1 0.08 %
GPX2 0.08 %
GPY1 0.08 %
GPY2 0.08 %
GPZ1 80.08 %
GPZ2 50.08 %
p15 500.08 usec
p16 1000.08 usec
F2 - Processing parameters
SI 65536
SF 125.7904192 MHz
WDW EM
SSB 0
LB 1.08 Hz
GB 0
PC 2.08

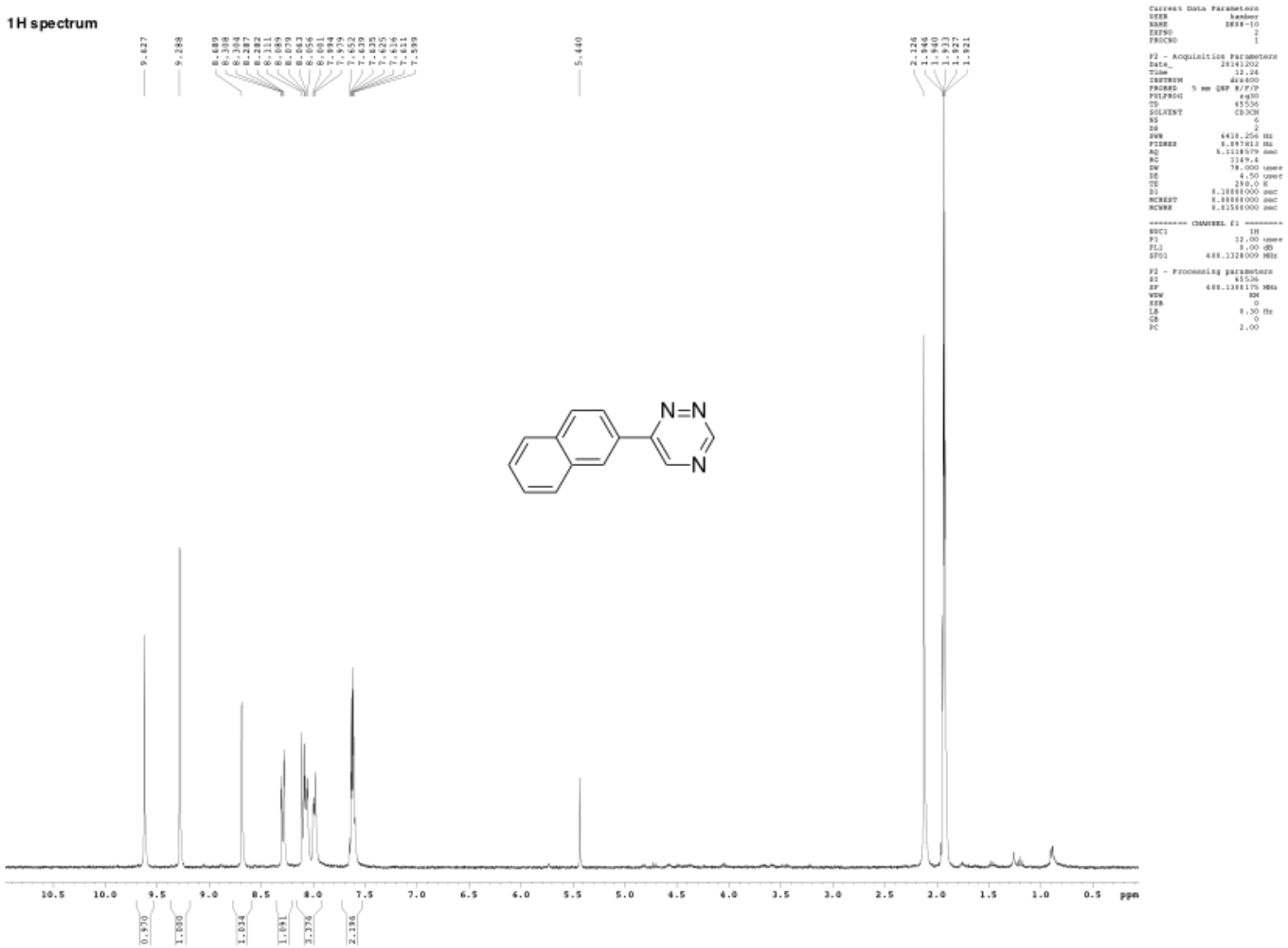
1H spectrum
9.627
9.288
8.689
8.388
8.284
8.287
8.282
8.111
8.099
8.089
8.063
8.056
8.001
7.994
7.979
7.652
7.639
7.635
7.625
7.616
7.611
7.599
5.440
2.126
2.046
1.940
1.933
1.927
1.921
N=N
N
10.5
10.0
9.5
9.0
8.5
8.0
7.5
7.0
6.5
6.0
5.0
4.5
4.0
3.5
3.0
2.5
2.0
1.5
1.0
0.5
ppm
0.970
1.000
1.034
1.041
3.276
2.196
Current Data Parameters
NAME Ember
EXPNO 10
PROCNO 2
1
F2 - Acquisition Parameters
Date_ 20141202
Time 12.24
INSTRUM spect
PROBHD 5 mm QNP H/F/P
PULPROG zg30
TD 65536
SOLVENT CDCl3
NS 16
DS 2
SWH 6410.256 Hz
FIDRES 0.097813 Hz
AQ 5.1118979 sec
RG 1149.6
DW 78.000 usec
DE 4.50 usec
TE 298.0 K
D1 0.10000000 sec
RCREST 0.00000000 sec
RCWRE 0.01500000 sec
======== CHANNEL f1 ========
NUC1 1H
P1 12.00 usec
PL1 0.00 dB
SFO1 400.1328009 MHz
F2 - Processing parameters
SI 65536
SF 400.1300175 MHz
WDW EM
SSB 0
LB 0.30 Hz
GB 0
PC 1.00

Z–restored spin–echo 13C spectrum with 1H decoupling

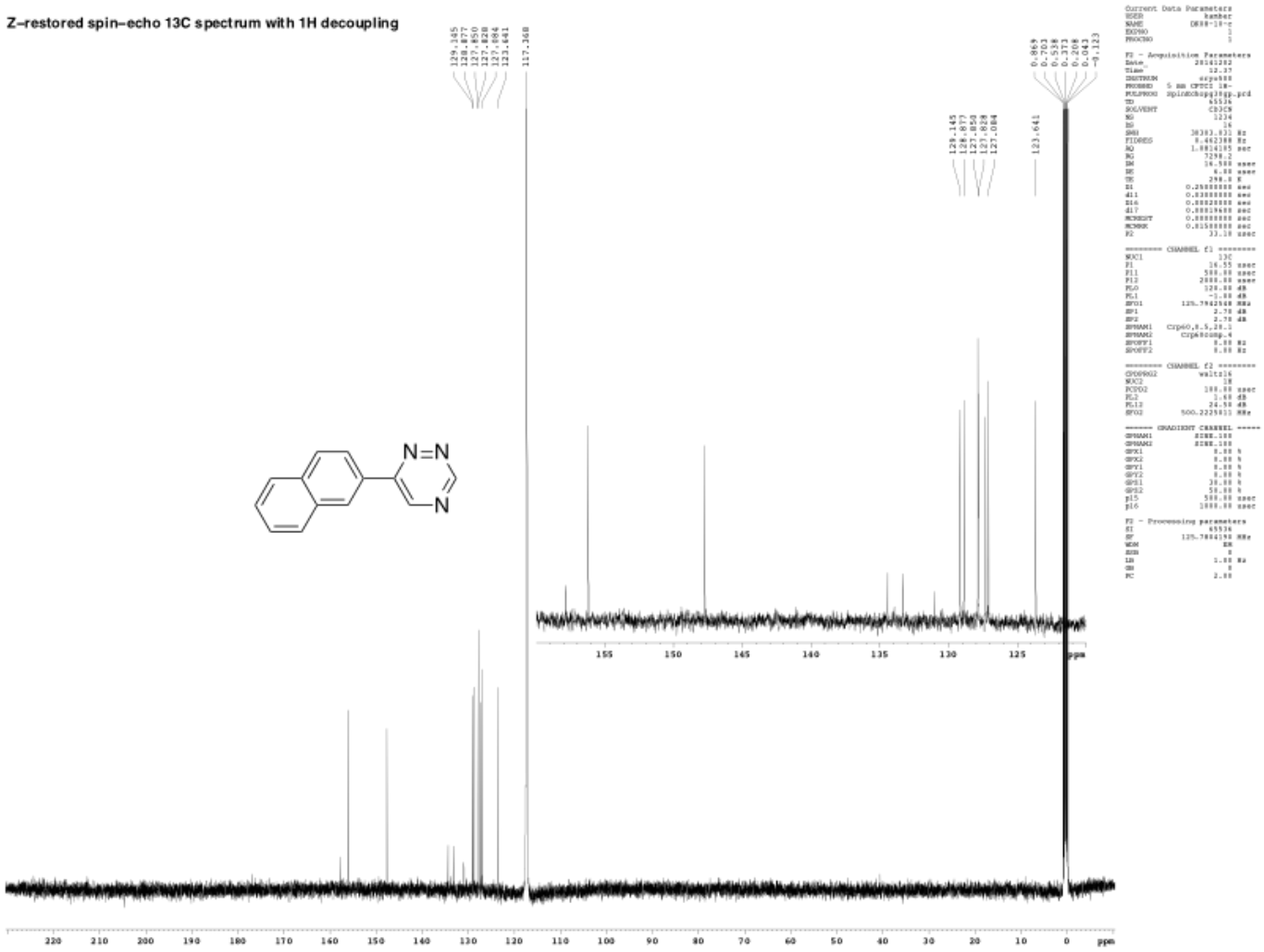

1H spectrum

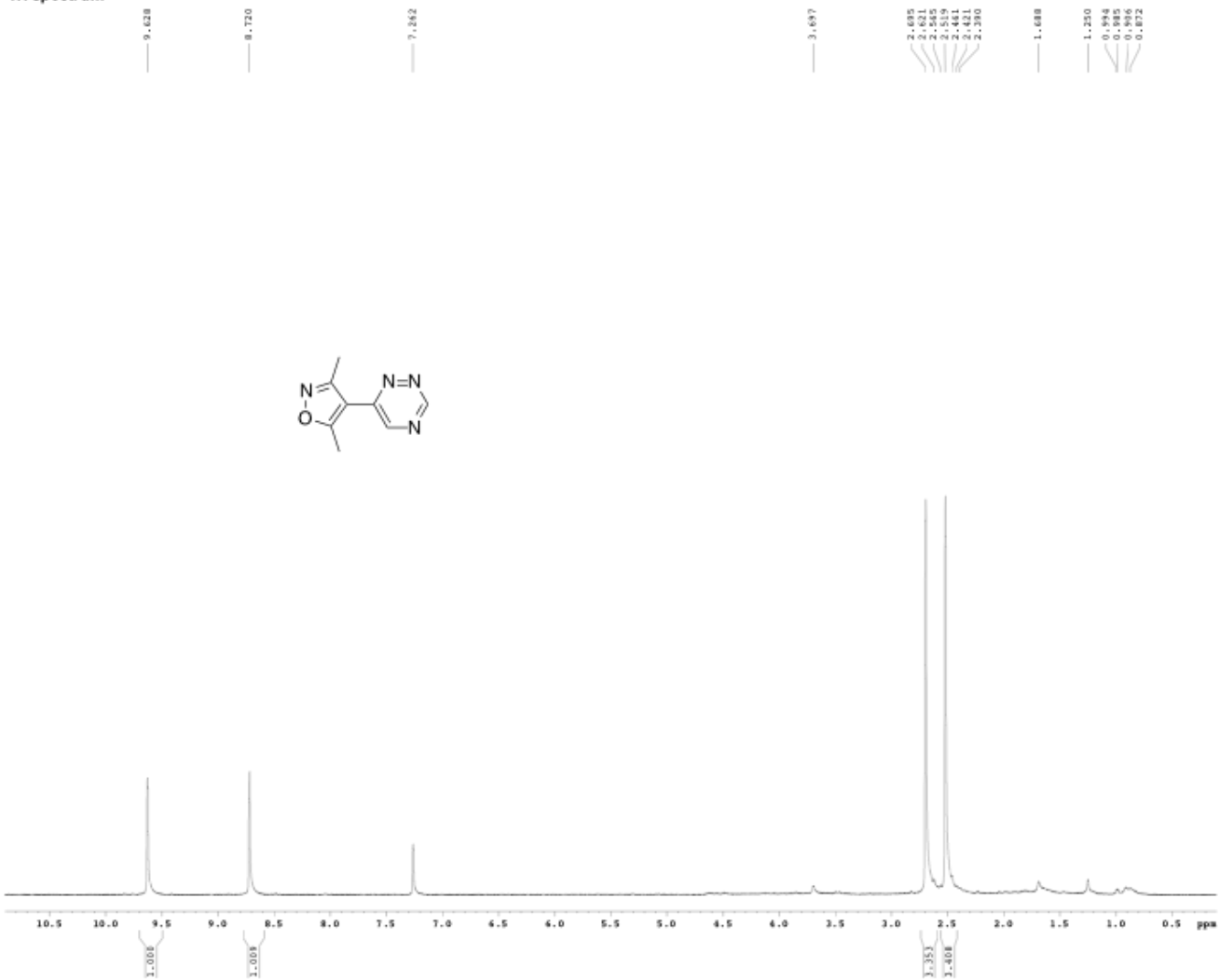


```
Current Data Parameters
USER            kamber
NAME          DB08-022
EXPNO                1
PROCNO               1

F2 - Acquisition Parameters
Date_        20141206
Time            12.51
INSTRUM        qn500
PROBHD   5 mm broadband
PULPROG         zg30
TD             81728
SOLVENT        CDCl3
NS                 4
DS                 2
SWH          8012.820 Hz
FIDRES       0.098043 Hz
AQ         5.0998774 sec
RG            1149.4
DW             62.400 usec
DE              6.00 usec
TE            298.0 K
D1         0.10000000 sec
MCREST     0.00000000 sec
MCWRK      0.01500000 sec

======== CHANNEL f1 ========
NUC1              1H
P1             12.00 usec
PL1            -5.80 dB
SFO1      499.1834943 MHz

F2 - Processing parameters
SI             65536
SF       499.1800256 MHz
WDW              EM
SSB               0
LB             0.30 Hz
GB                0
PC             1.00
```

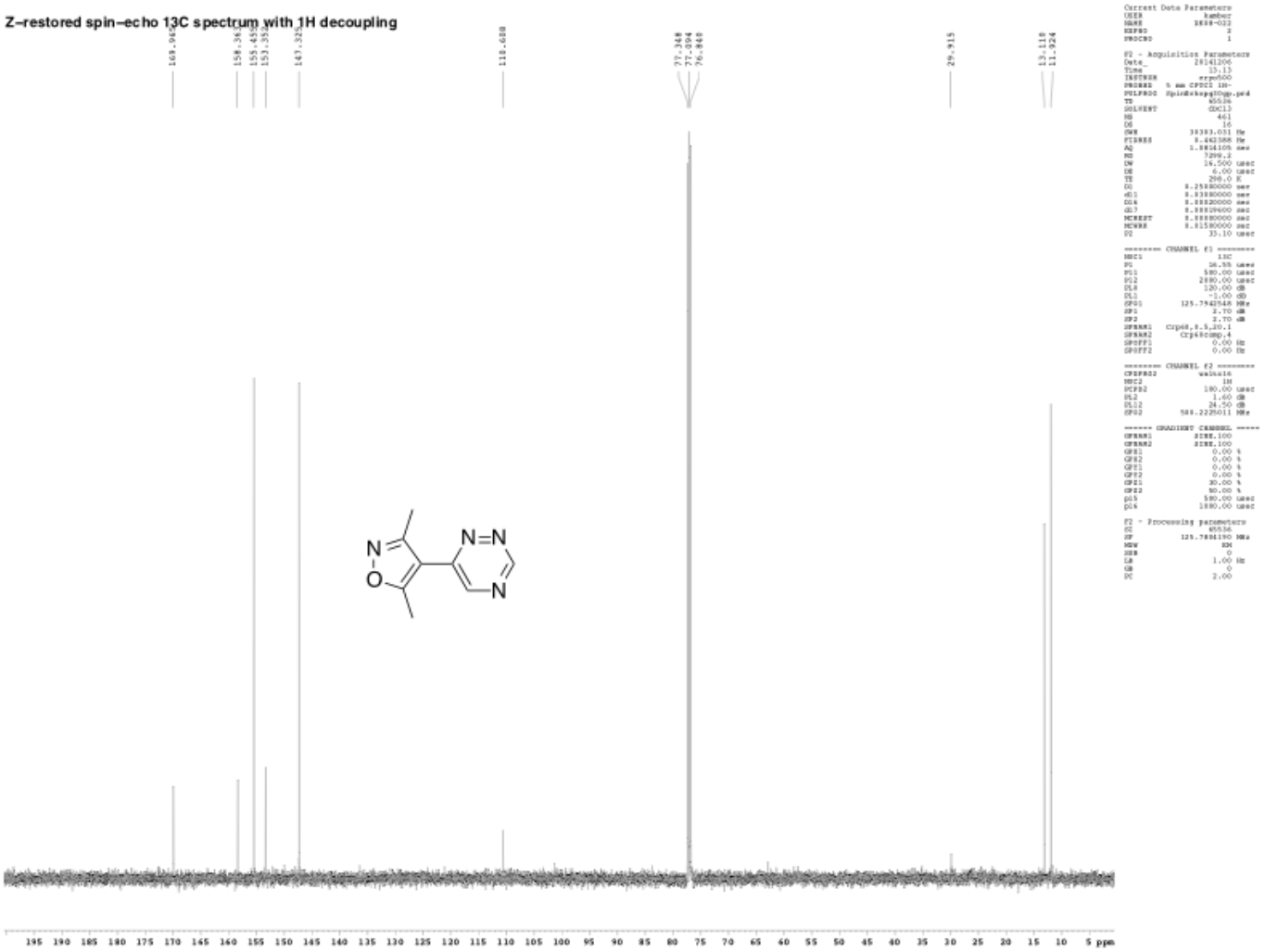

Current Data Parameters
USER kember
NAME 1888-033
EXPNO 2
PROCNO 1

F2 - Acquisition Parameters
Date_ 20141206
Time 13.13
INSTRUM spe500
PROBHD 5 mm CPTCI 1H-
PULPROG Spin2ekpg30ngp.pe4
TD 65536
SOLVENT CDCl3
NS 461
DS 16
SWH 39383.031 Hz
FIDRES 0.442388 Hz
AQ 1.6814105 sec
RG 3298.2
DW 16.500 usec
DE 6.00 usec
TE 298.0 K
D1 0.25000000 sec
d61 0.03000000 sec
D16 0.00020000 sec
d17 0.00029600 sec
MCREST 0.00000000 sec
MCWRK 0.01500000 sec
P2 33.10 usec

======== CHANNEL f1 ========
NUC1 13C
PL 56.55 usec
PL1 580.00 usec
PL2 2880.00 usec
PL8 120.00 dB
PL13 -1.00 dB
SFO1 125.7942548 MHz
SP1 2.70 dB
SP2 2.70 dB
SPNAM1 Crp68,0.5,20.1
SPNAM2 Crp480mp.4
SPOFF1 0.00 Hz
SPOFF2 0.00 Hz

======== CHANNEL f2 ========
CPDPRG2 waltz16
NUC2 1H
PCPD2 180.00 usec
PL2 1.60 dB
PL12 24.50 dB
SFO2 599.2225011 MHz

====== GRADIENT CHANNEL =====
GPNAM1 SINE.100
GPNAM2 SINE.100
GPZ1 0.00 %
GPZ2 0.00 %
GPZ3 0.00 %
GPZ4 0.00 %
GPZ5 30.00 %
GPZ6 50.00 %
pl5 580.00 usec
pl6 1880.00 usec

F2 - Processing parameters
SI 65536
SF 125.7886190 MHz
WDW EM
SSB 0
LB 1.00 Hz
GB 0
PC 2.00

1H spectrum

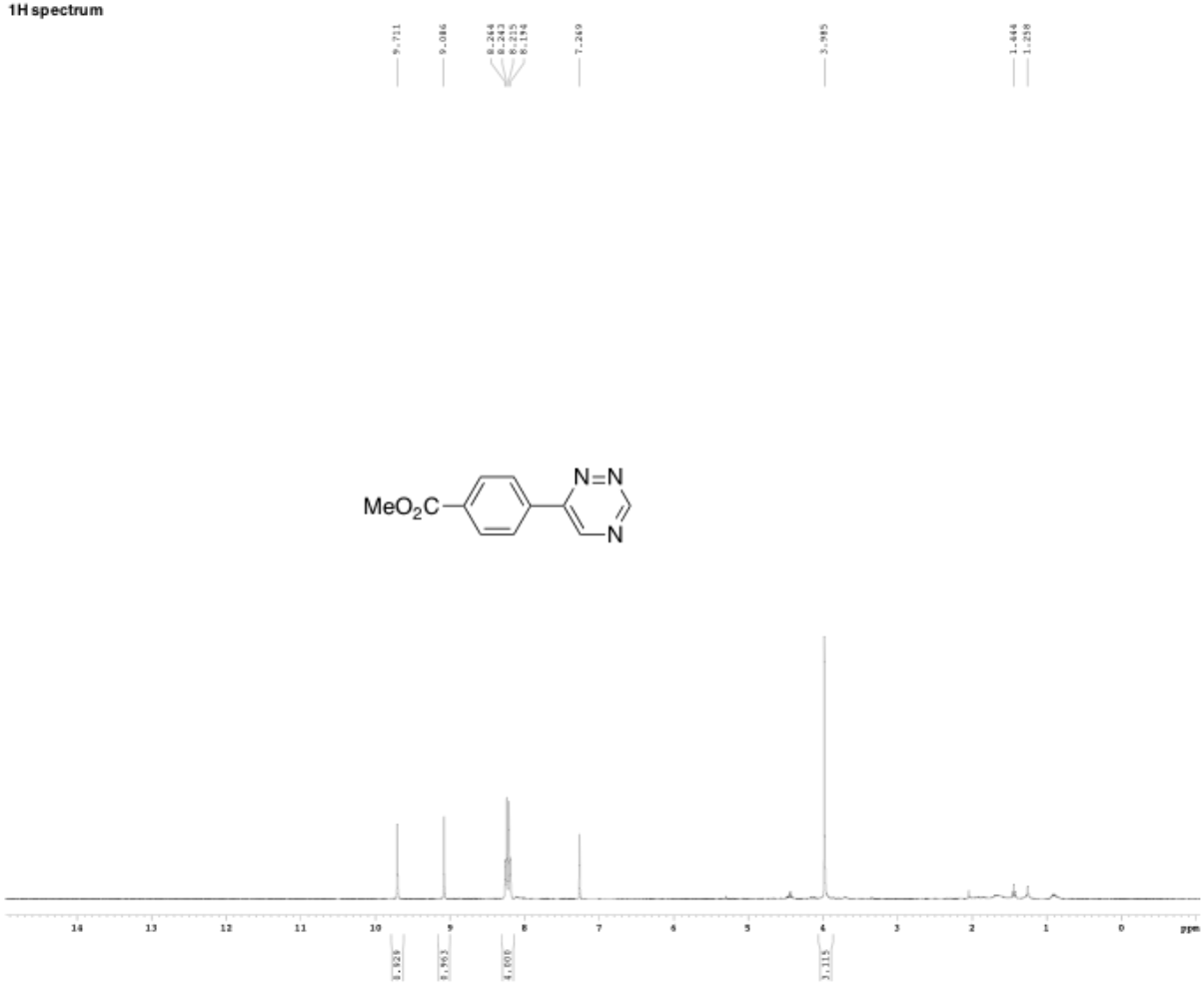
9.711
9.086
8.244
8.243
8.235
8.134
7.269
3.995
1.444
1.258
MeO2C
N=N
N
14
13
12
11
10
9
8
7
6
5
4
3
2
1
0
ppm
0.928
0.963
4.000
3.115

Z–restored spin–echo 13C spectrum with 1H decoupling

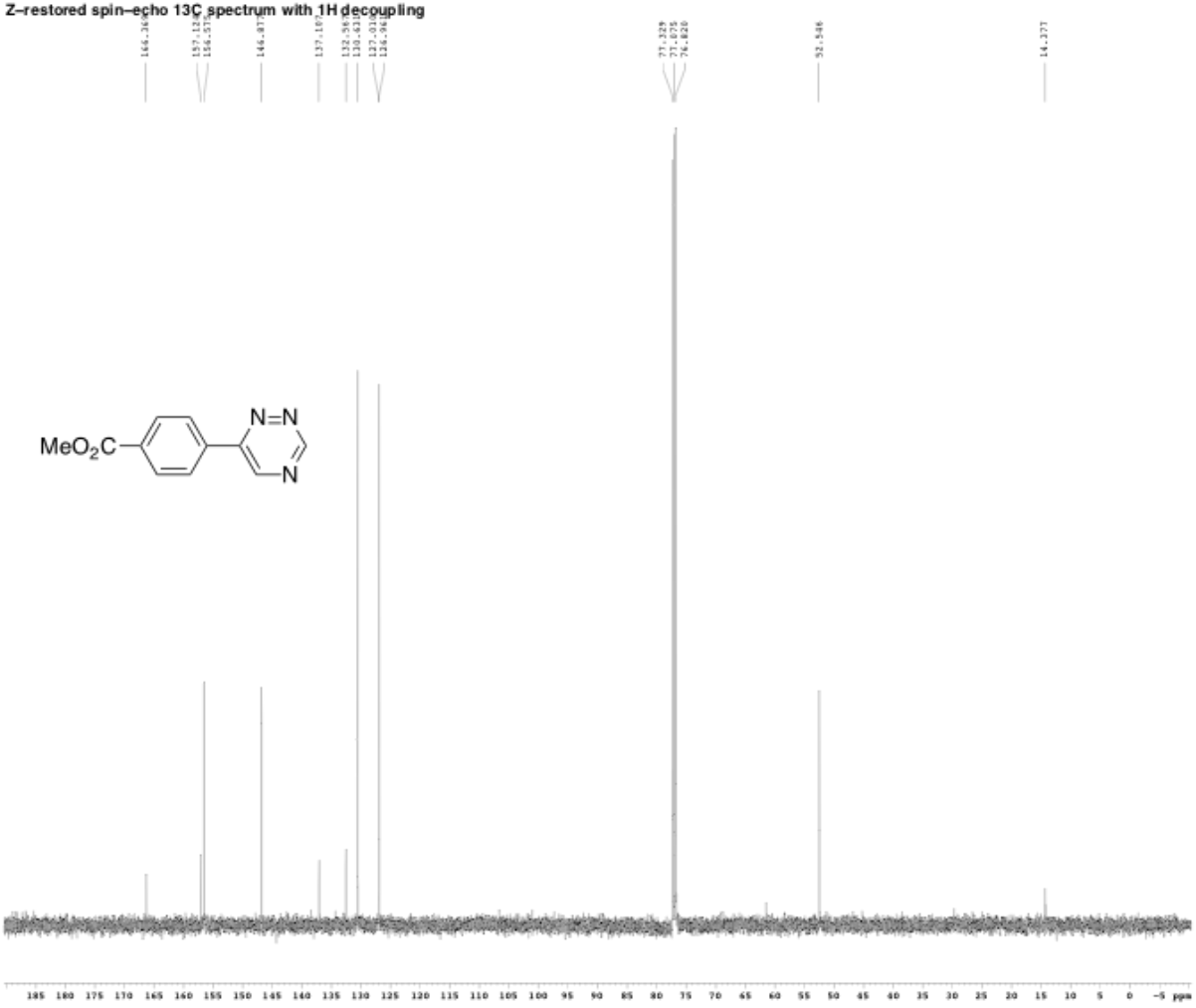


```
Current Data Parameters
USER            kamber
NAME            0807-059
EXPNO                 2
PROCNO                1

F2 - Acquisition Parameters
Date_        20140719
Time              18.38
INSTRUM       exp400
PROBHD   5 mm CPTCI 1H-
PULPROG  SpinEchoqc3Cgp.prd
TD                65536
SOLVENT           CDCl3
NS                  557
DS                   16
SWH           30382.031 Hz
FIDRES        0.463388 Hz
AQ            1.0814105 sec
RG                 7298.2
DW               16.500 usec
DE                6.00 usec
TE               298.0 K
D1            0.25000000 sec
d21           0.03000000 sec
D16           0.00020000 sec
d13           0.00019600 sec
MCREST        0.00000000 sec
MCWRK         0.01500000 sec
P2                  31.00 usec

======== CHANNEL f1 ========
NUC1                 13C
P1                  15.50 usec
PCPD1              588.00 usec
PLW2              3888.00 usec
PLW8               129.00 dB
PLW9                -1.00 dB
SFO1          125.7942548 MHz
SF1                  3.20 dB
SF2                  3.20 dB
SPNAM1     Crp4,0.5,20.1
SPNAM2       Crp60comp.4
SPOFF1               0.00 Hz
SPOFF2               0.00 Hz

======== CHANNEL f2 ========
CPDPRG2          waltz16
NUC2                  1H
PCPD2              188.00 usec
PL2                  1.60 dB
PLW12                24.60 dB
SFO2          590.3225011 MHz

====== GRADIENT CHANNEL =====
GPNAM1          SINE.100
GPNAM2          SINE.100
GPZ1                 8.00 %
GPZ2                 8.00 %
GPZ3                 8.00 %
GPZ4                 8.00 %
GPZ5                 39.00 %
GPZ6                 53.00 %
gt5                588.00 usec
gt6                1888.00 usec

F2 - Processing parameters
SI                  65536
SF            125.7894198 MHz
WDW                    EM
SSB                     0
LB                   1.00 Hz
GB                      0
PC                   2.00
```

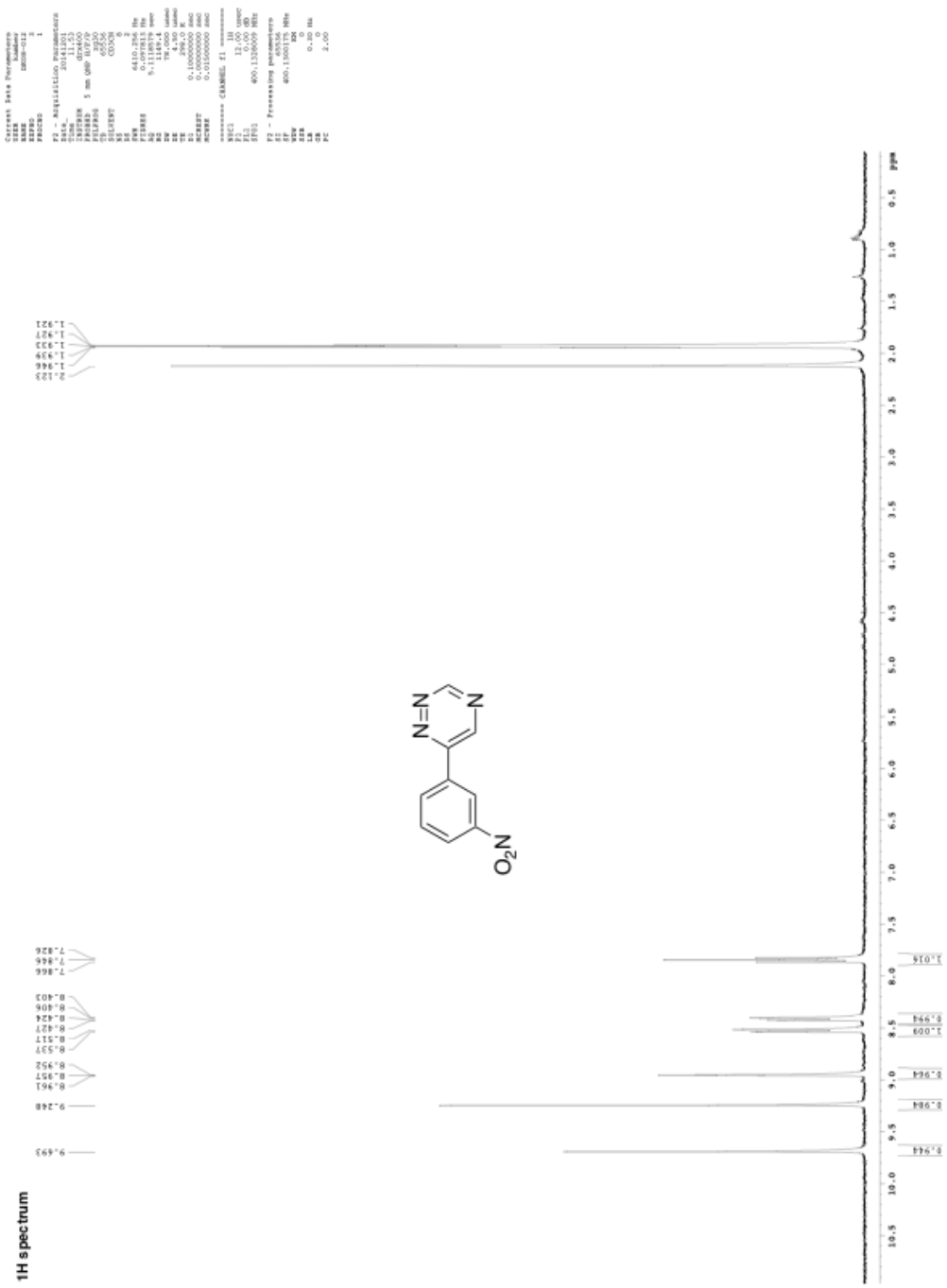
1H spectrum
9.695
9.248
8.961
8.957
8.952
8.537
8.517
8.427
8.424
8.406
8.403
7.866
7.846
7.826
2.123
1.966
1.939
1.933
1.927
1.921
1.016
0.994
1.009
0.964
0.984
0.944
O_2N
N
N
N
ppm

Z–restored spin–echo 13C spectrum with 1H decoupling

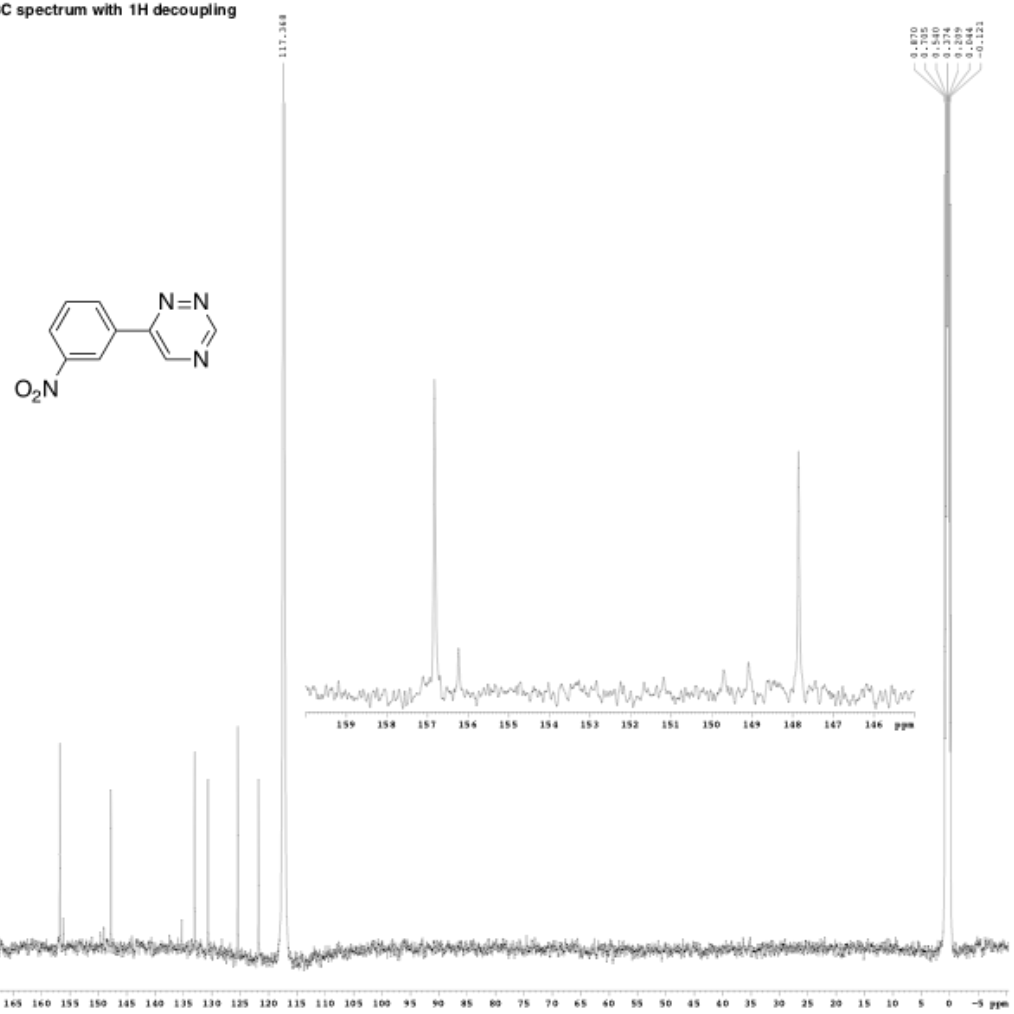


```
Current Data Parameters
USER            hamber
NAME          DEEE-12-c
EXPNO                 2
PROCNO                1

F2 - Acquisition Parameters
Date_          20141201
Time              12.09
INSTRUM         spect600
PROBHD   5 mm CPTCI 1H-
PULPROG  zgpiracbsp30cgp.prd
TD                65536
SOLVENT           CDCl3
NS                 1947
DS                   16
SWH            38383.031 Hz
FIDRES         0.462388 Hz
AQ             1.8812940 sec
RG                 2048
DW               13.020 usec
DE                6.00 usec
TE                298.0 K
D1             0.25000000 sec
d11            0.03000000 sec
D16            0.00020000 sec
d17            0.00019600 sec
MCREST         0.00000000 sec
MCWRK          0.01500000 sec
P2                33.10 usec

======== CHANNEL f1 ========
NUC1                 13C
P1                 16.55 usec
P11               598.00 usec
P12              2988.00 usec
PL0                120.00 dB
PL1                 -1.00 dB
SFO1        125.7942548 MHz
SP1                 2.70 dB
SP2                 2.70 dB
SPNAM1   Crp60.8.5.20.1
SPNAM2      Crp48comp.4
SPOFF1              0.00 Hz
SPOFF2              0.00 Hz

======== CHANNEL f2 ========
CPDPRG2         waltz16
NUC2                 1H
PCPD2              100.00 usec
PL2                 1.40 dB
PL12               24.50 dB
SFO2        500.2229011 MHz

====== GRADIENT CHANNEL =====
GPNAM1          SINE.100
GPNAM2          SINE.100
GPX1                0.00 %
GPX2                0.00 %
GPY1                0.00 %
GPY2                0.00 %
GPZ1               38.00 %
GPZ2               59.00 %
p15               500.00 usec
p16               1000.00 usec

F2 - Processing parameters
SI                65536
SF          125.7884190 MHz
WDW                    EM
SSB                     0
LB                   5.00 Hz
GB                      0
PC                   2.00
```

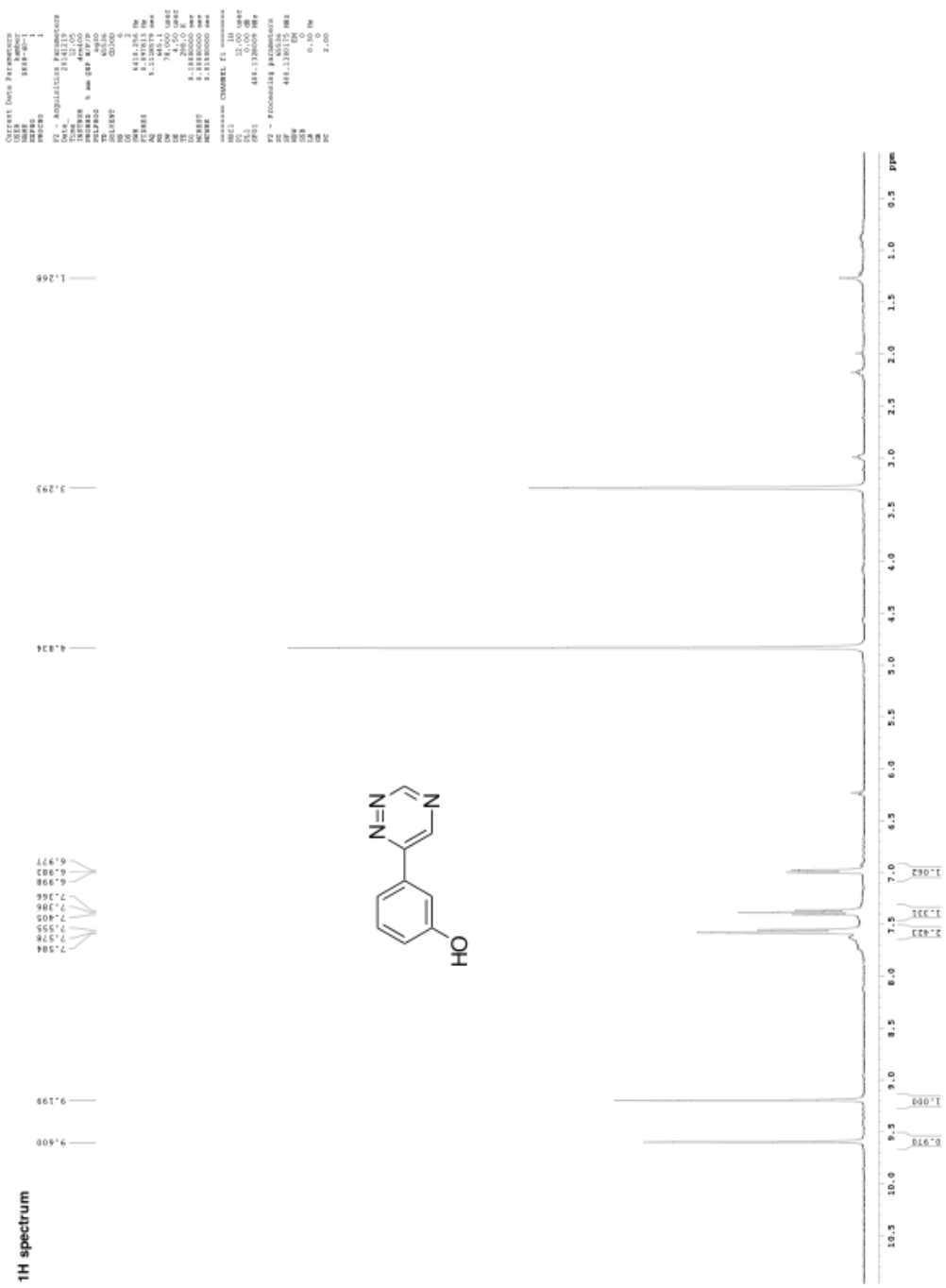
1H spectrum
9.600
9.199
7.584
7.576
7.555
7.405
7.386
7.366
6.983
6.977
6.834
3.293
1.268
0.910
1.000
2.923
1.331
1.062
ppm

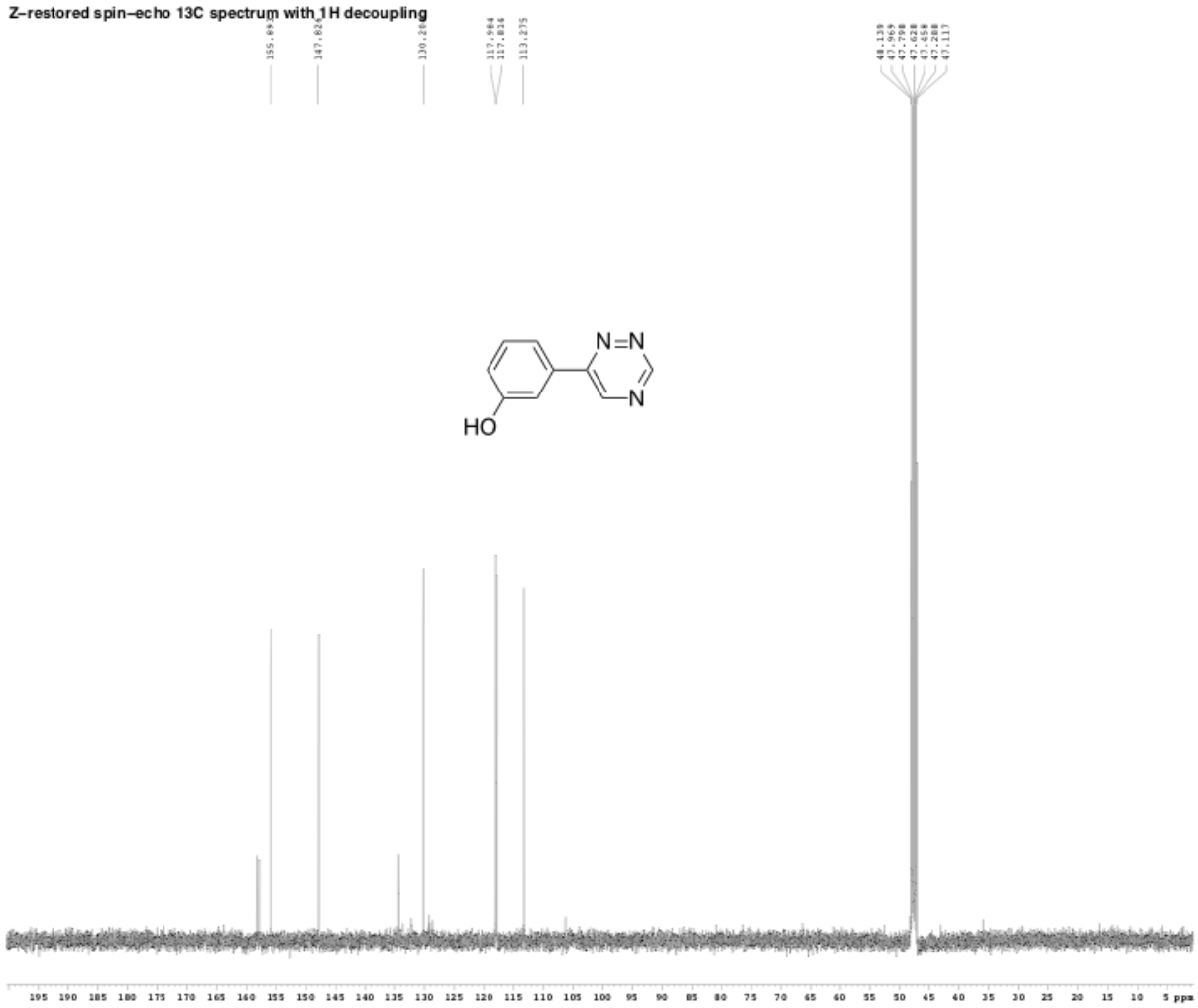

Current Data Parameters
NAME kamber
EXPNO 1
PROCNO 1

F2 - Acquisition Parameters
Date_ 20141219
Time 12.52
INSTRUM cryo500
PROBHD 5 mm CPTCI 1H-
PULPROG Spin2echopg30gp.prd
TD 65536
SOLVENT CDCl3
NS 281
DS 16
SWH 30303.031 Hz
FIDRES 0.462388 Hz
AQ 1.0814105 sec
RG 7298.2
DW 16.500 usec
DE 6.00 usec
TE 298.0 K
D1 0.25000000 sec
d11 0.03000000 sec
D16 0.00020000 sec
d17 0.00019600 sec
MCREST 0.00000000 sec
MCWRK 0.01500000 sec
P2 33.10 usec

======== CHANNEL f1 ========
NUC1 13C
P1 16.95 usec
P11 500.00 usec
P12 2000.00 usec
PL2 120.00 dB
PL1 -1.00 dB
SFO1 125.7942848 MHz
SF1 2.70 dB
SF2 2.70 dB
SPNAM1 Crp40,0.5,20.1
SPNAM2 Crp60comp.4
SPOFF1 0.00 Hz
SPOFF2 0.00 Hz

======== CHANNEL f2 ========
CPDPRG2 waltz16
NUC2 1H
PCPD2 100.00 usec
PL2 1.60 dB
PL12 24.50 dB
SFO2 500.2225011 MHz

====== GRADIENT CHANNEL =====
GPNAM1 SINE.100
GPNAM2 SINE.100
GPZ1 0.00 %
GPZ2 0.00 %
GPZ3 0.00 %
GPZ4 0.00 %
GPZ5 20.00 %
GPZ6 50.00 %
p15 500.00 usec
p16 1000.00 usec

F2 - Processing parameters
SI 65536
SF 125.7804190 MHz
WDW EM
SSB 0
LB 1.00 Hz
GB 0
PC 2.00

Appendix E: NMR spectra and additional data for Chapter 4

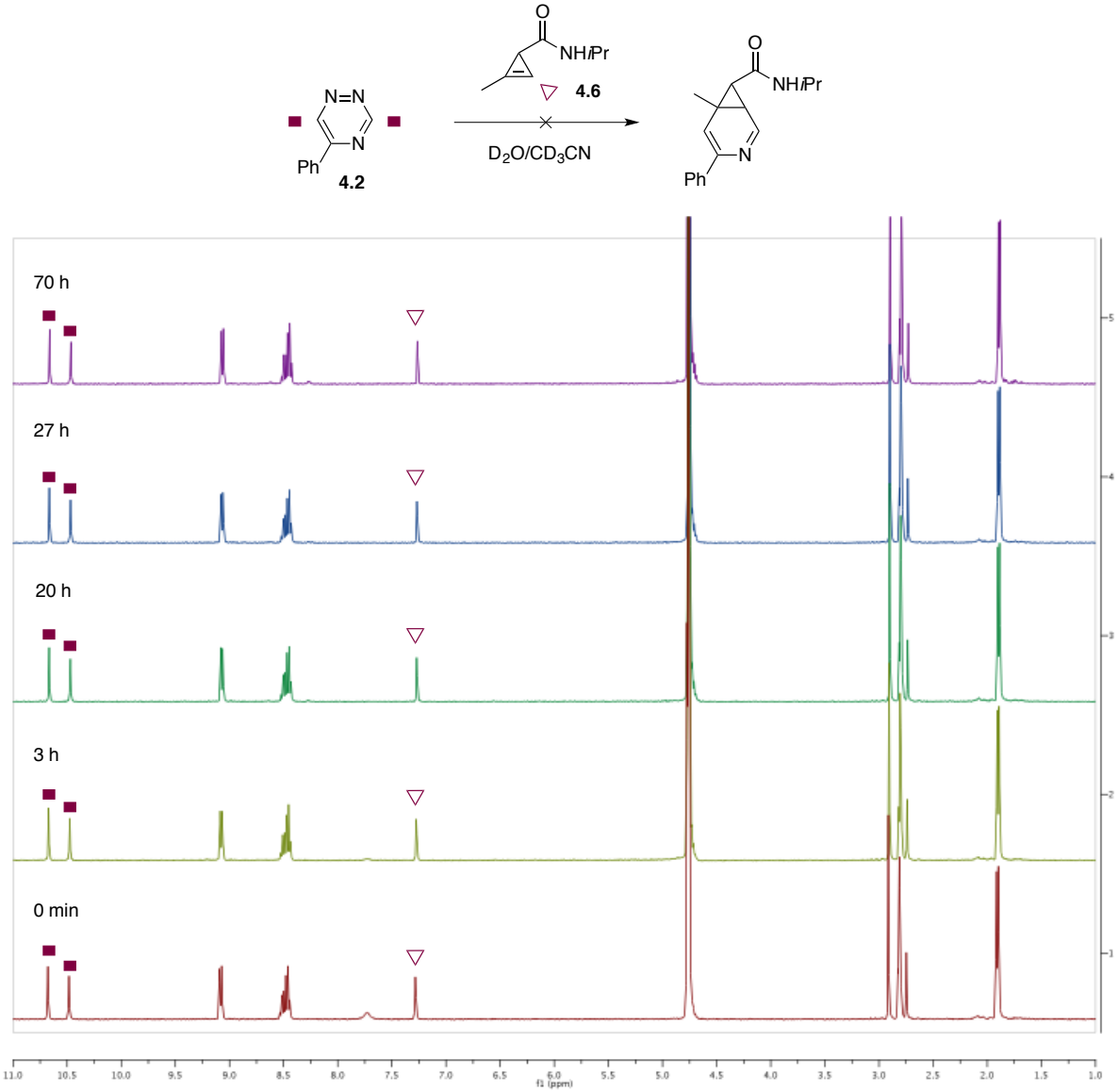

Figure S4.1. 5-Substituted triazine **4.2** is orthogonal to cyclopropene **4.6**. Triazine **4.2** (0.24 mL of a 25 mM solution in CD_3CN) was added a solution of cyclopropene **4.6** (0.17 mL of a 35 mM solution in CD_3CN) and diluted with 0.19 mL of D_2O. The reaction was monitored over time by ^{1}H-NMR.

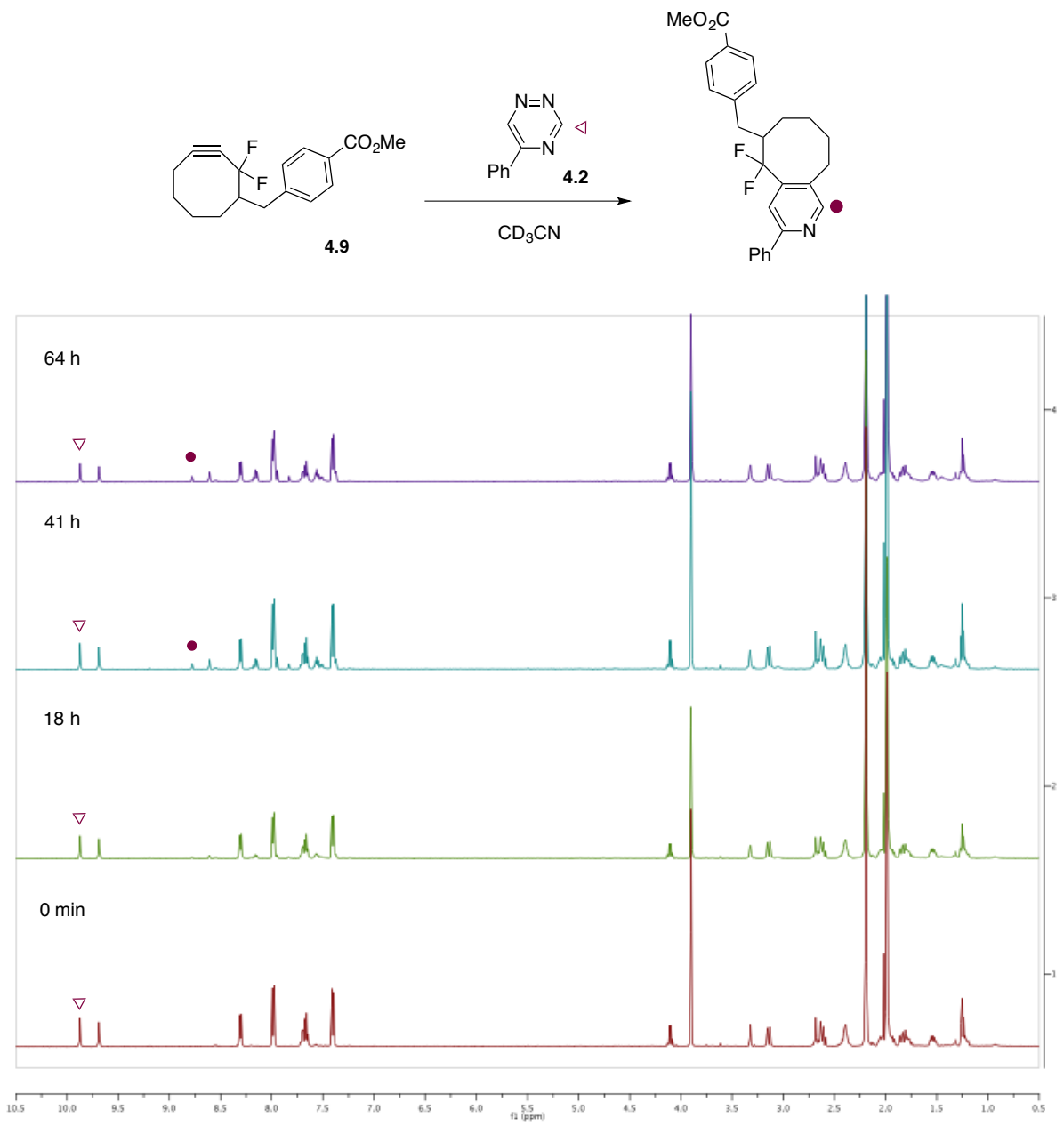

Figure S4.2. Minimum reactivity is observed between triazine **4.2** and DIFO **4.9**. Triazine **4.2** (0.20 mL of a 25 mM solution in CD_3CN) was added a solution of DIFO **4.3** (0.20 mL of a 25 mM solution in CD_3CN) and diluted with 0.15 mL CD_3CN. The reaction was monitored over time by ^{1}H-NMR.

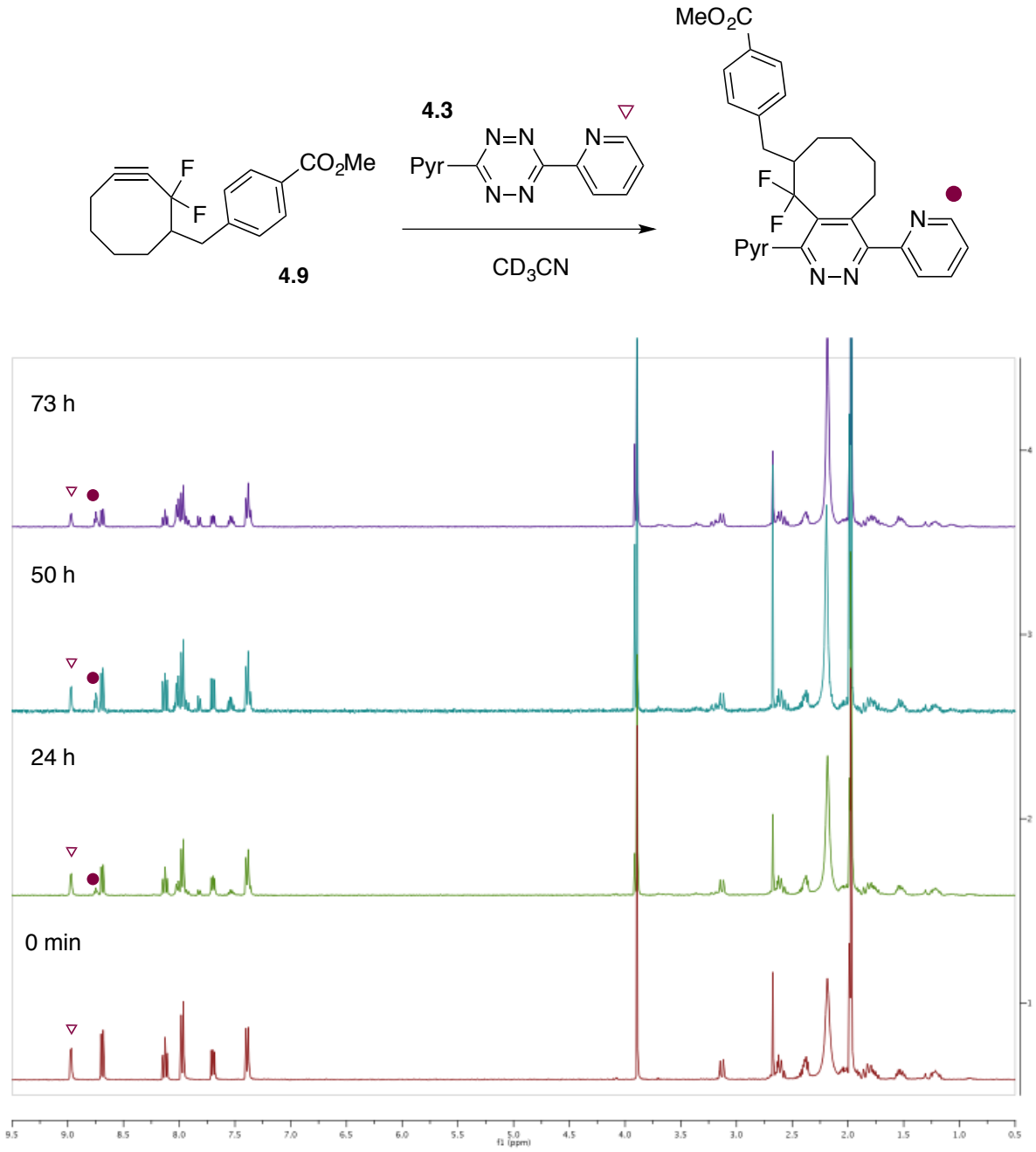

Figure S4.3. Minimum reactivity is observed between tetrazine **4.3** and DIFO **4.9**. Tetrazine **4.2** (0.30 mL of a 20 mM solution in CD_3CN) was added a solution of DIFO **4.3** (0.30 mL of a 20 mM solution in CD_3OD). The reaction was monitored over time by ^{1}H-NMR.

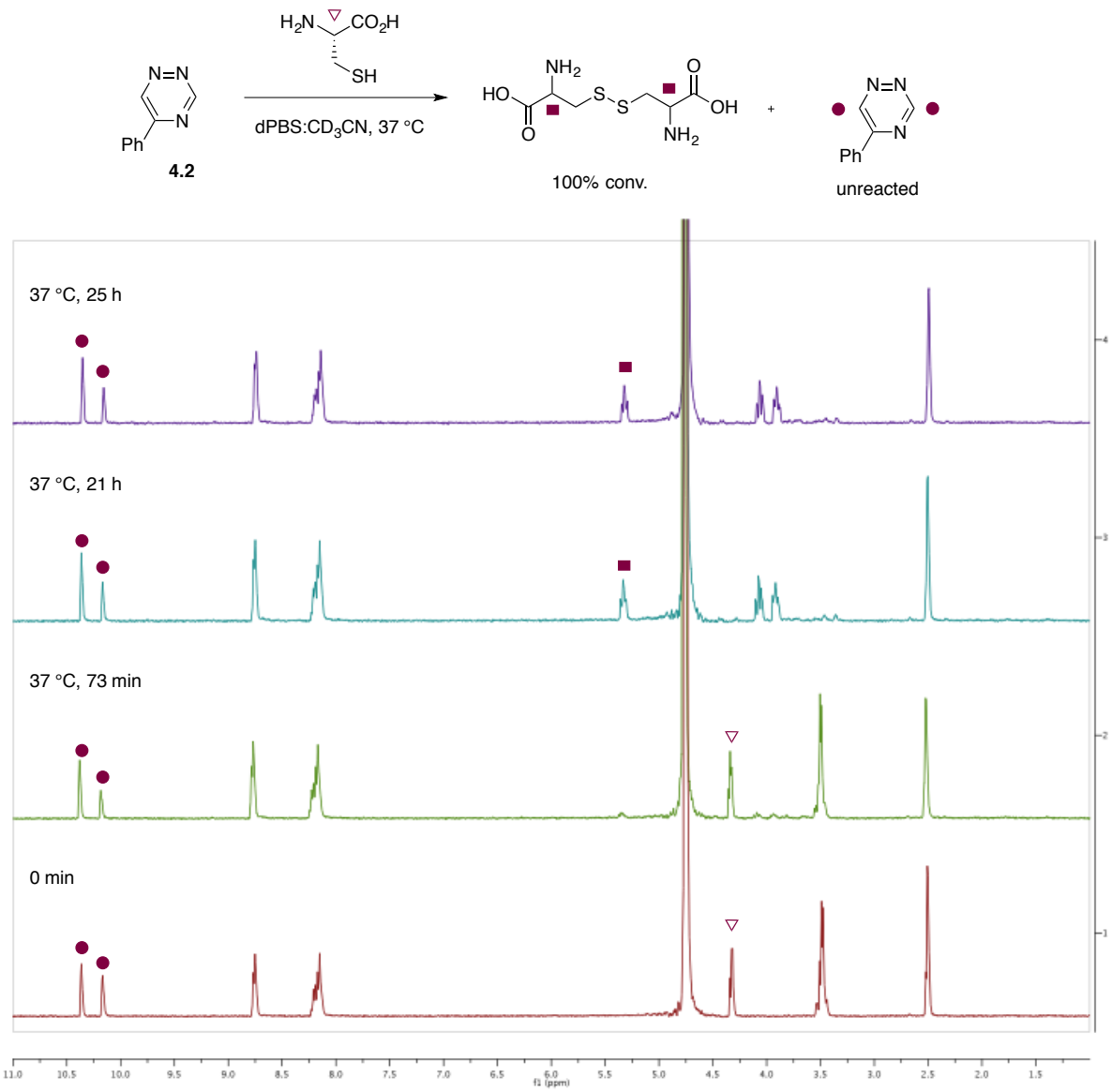

Figure S4.4. Tetrazine **4.2** is stable to L-cys. Triazine **4.2** (0.30 mL of a 20 mM solution in CD_3CN) was added a solution of L-cys (0.24 mL of a 50 mM solution in dPBS) and diluted with 60 µL dPBS. The reaction was monitored over time by ^{1}H-NMR at 37 °C.

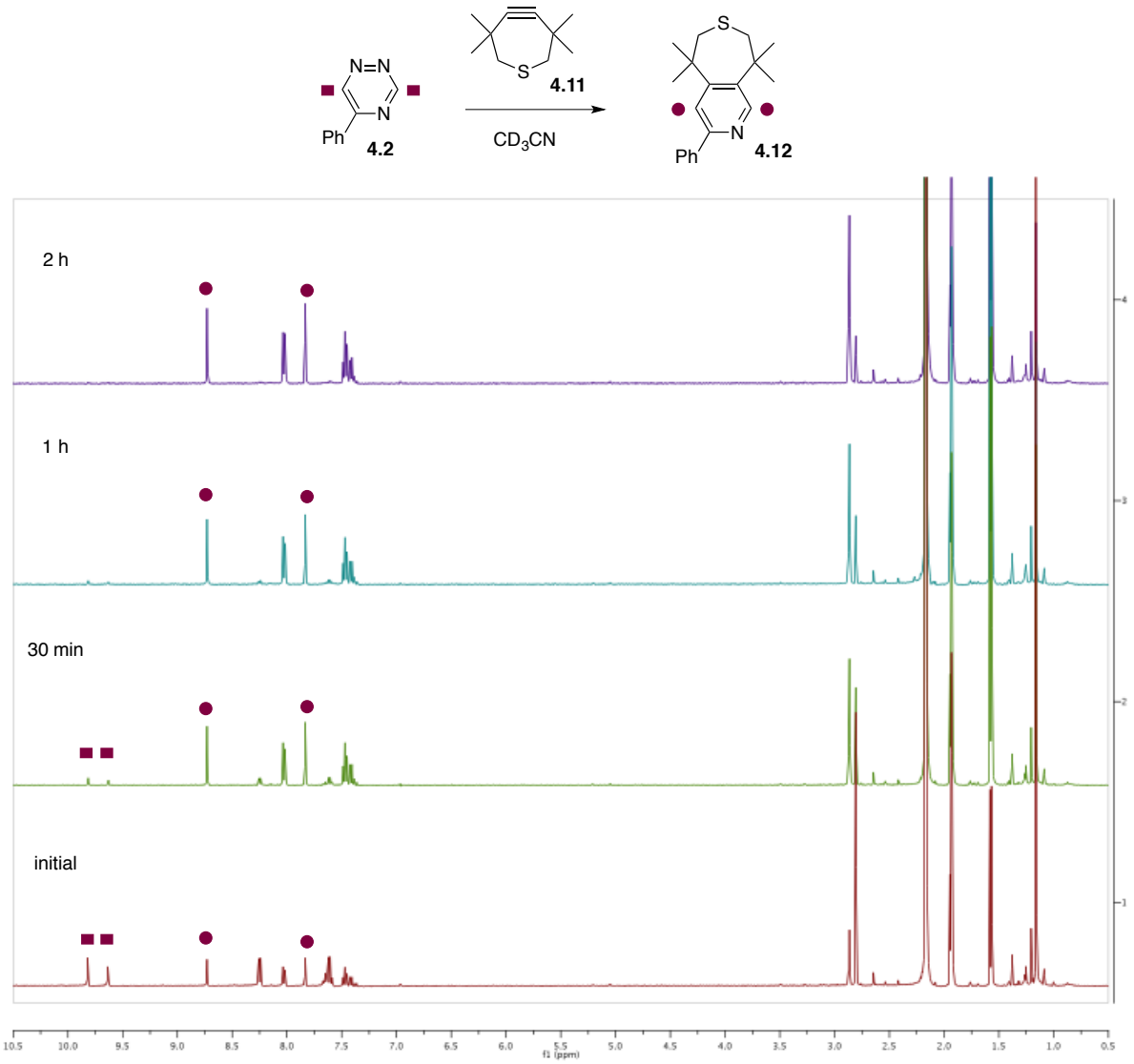

Figure S4.5. Reaction between triazine **4.2** and TMTH **4.11**. Triazine **4.2** (0.12 mL of a 50 mM solution in CD_3CN) was added a solution of TMTH **4.11** (0.12 mL of a 50 mM solution in CD_3CN) and diluted with 0.36 mL of CD_3CN. The reaction was monitored over time by ^{1}H-NMR.

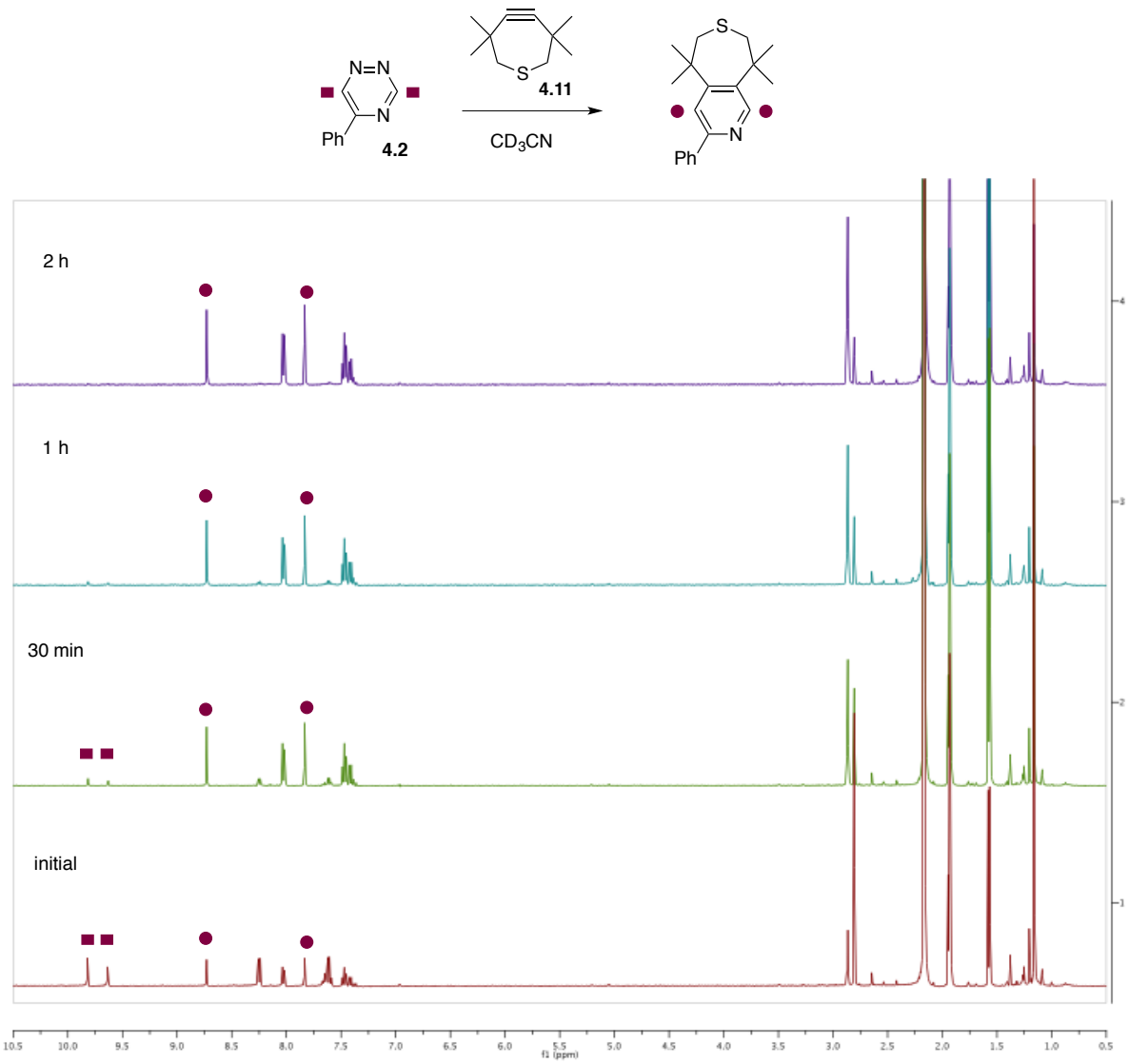

Figure S4-6. Tetrazine **4.2** is orthogonal to TMTH **4.11**. Triazine **4.2** (0.30 mL of a 20 mM solution in CD_3OD) was added a solution of TMTH **4.11** (0.12 mL of a 50 mM solution in CD_3CN) and diluted with 0.18 mL CD_3CN. The reaction was monitored over time by ^{1}H-NMR.

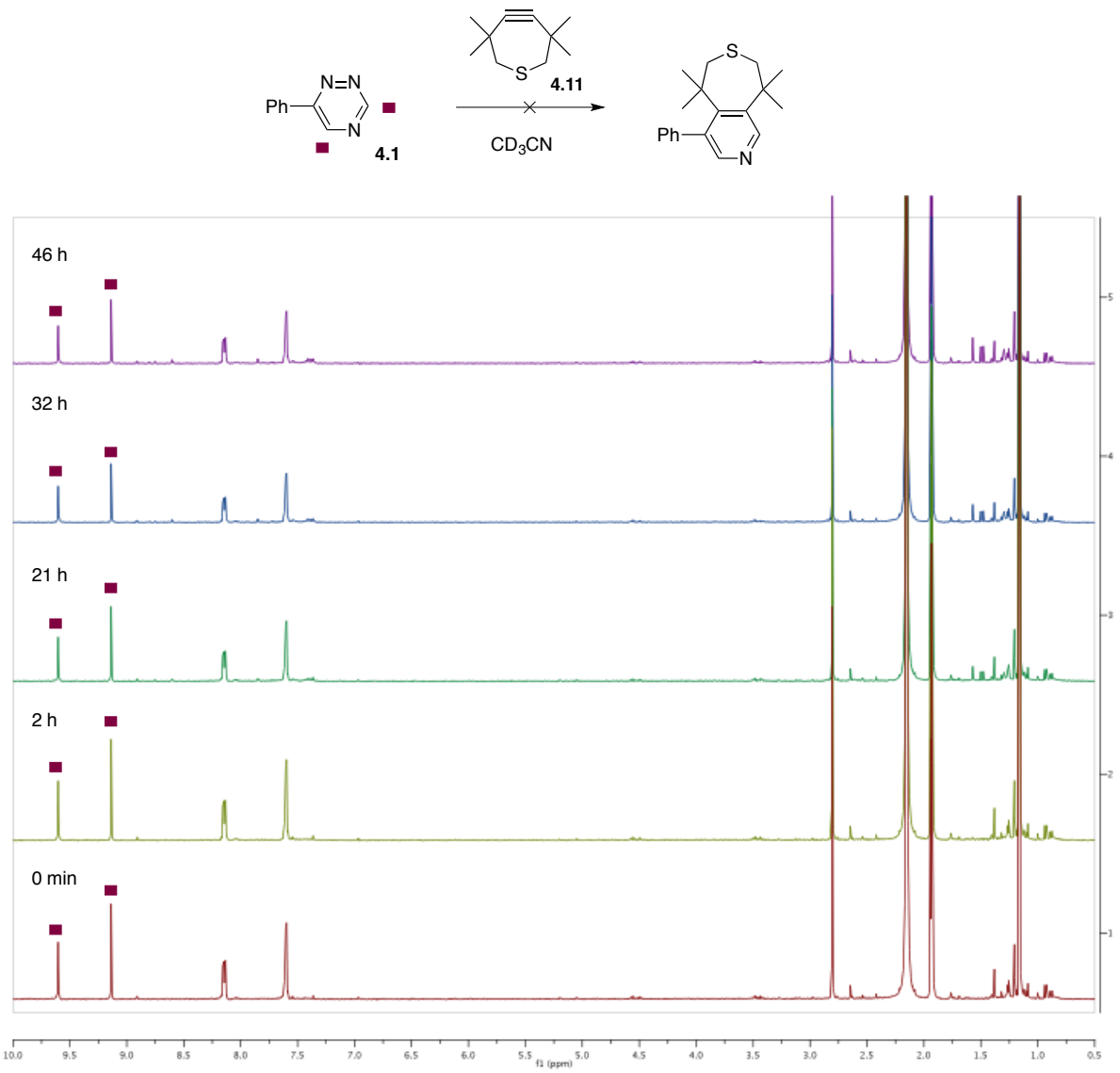

Figure S4.7. Triazine **4.1** is orthogonal to TMTH **4.11**. Triazine **4.1** (0.24 mL of a 25 mM solution in CD_3CN) was added a solution of TMTH **4.11** (0.12 mL of a 50 mM solution in CD_3CN) and diluted with 0.24 mL CD_3CN. The reaction was monitored over time by ^{1}H-NMR.

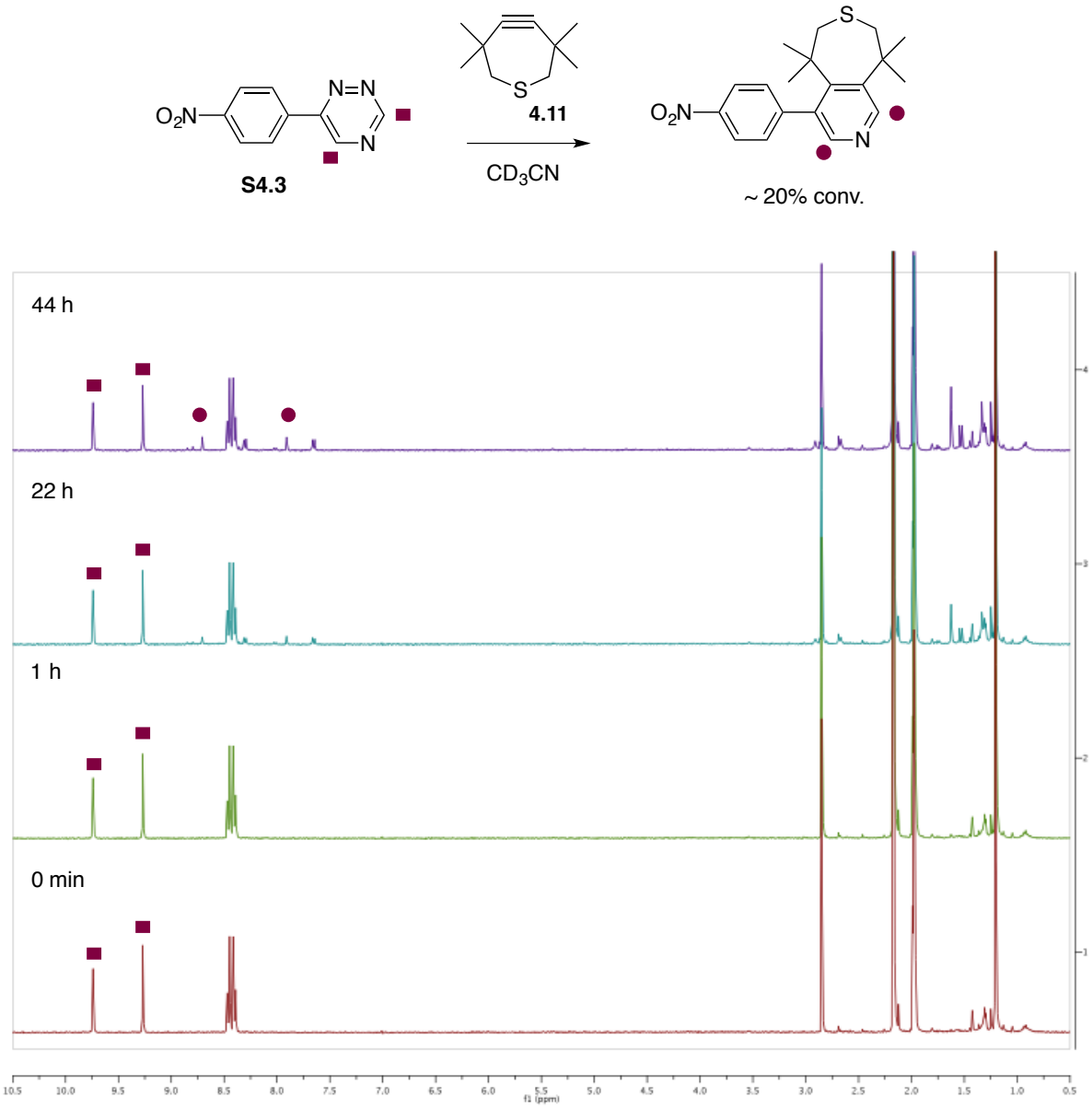

Figure S4.8. Minimum reactivity is observed between triazine **S4.3** and TMTH **4.11**. Triazine **S4.3** (0.30 mL of a 20 mM solution in CD_3CN) was added a solution of TMTH **4.11** (0.12 mL of a 50 mM solution in CD_3CN) and diluted with 0.18 mL CD_3CN. The reaction was monitored over time by ^{1}H-NMR.

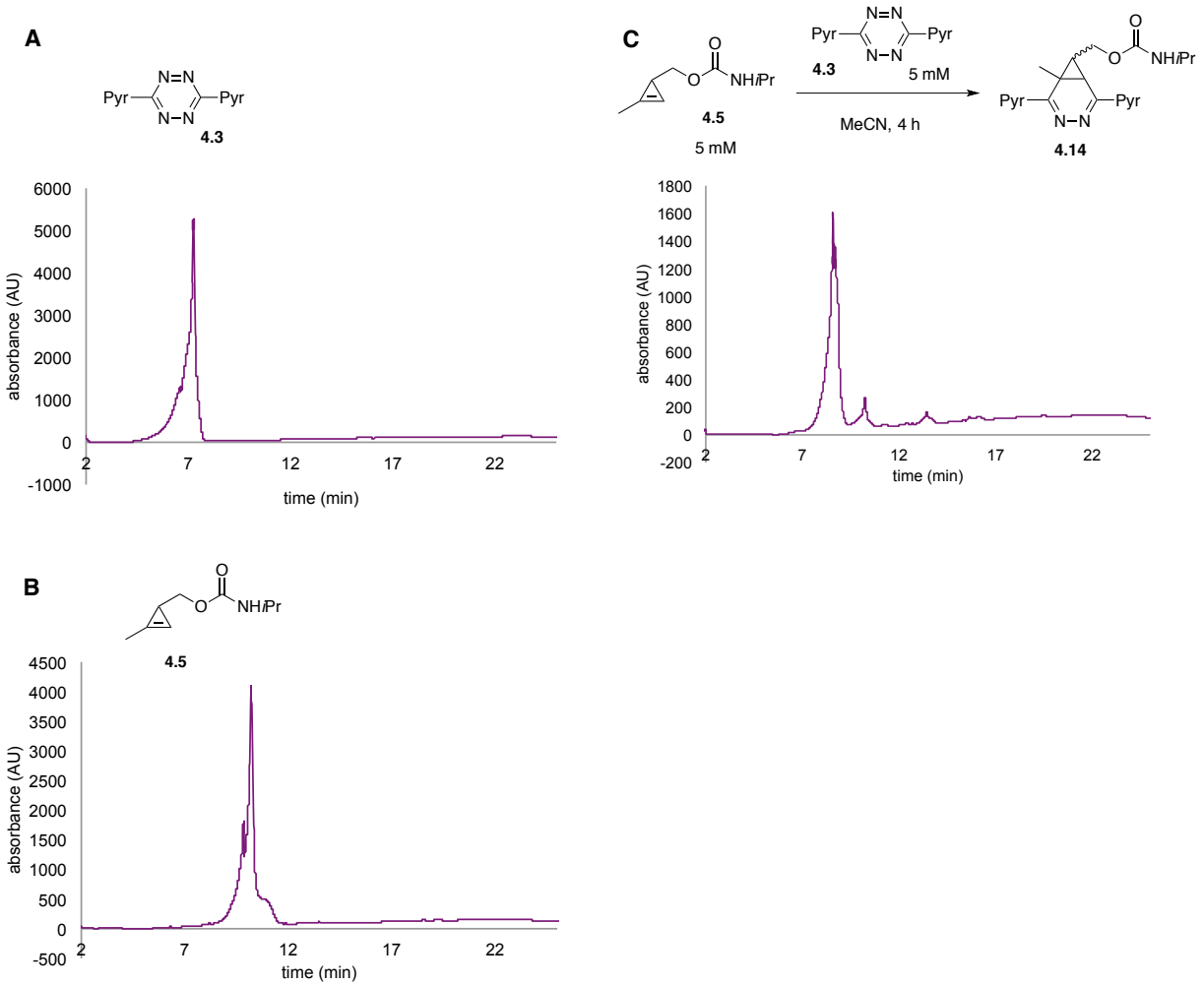

Figure S4.9. Tetrazine **4.3** reacts quantitatively with cyclopropene **4.5**. (A) HPLC trace of starting tetrazine **4.3** reagent. (B) HPLC trace of starting cyclopropene **4.5** trace. (C) Tetrazine **4.3** (5mM in MeCN) was reacted with 1,3-disubstituted cyclopropene **4.5** (5 mM in MeCN) for 4 h, and monitored by HPLC. The initial cycloadduct formed between **4.3** and **4.5** can undergo further rearrangement [4]. HPLC traces are monitored at 210 nm wavelength.

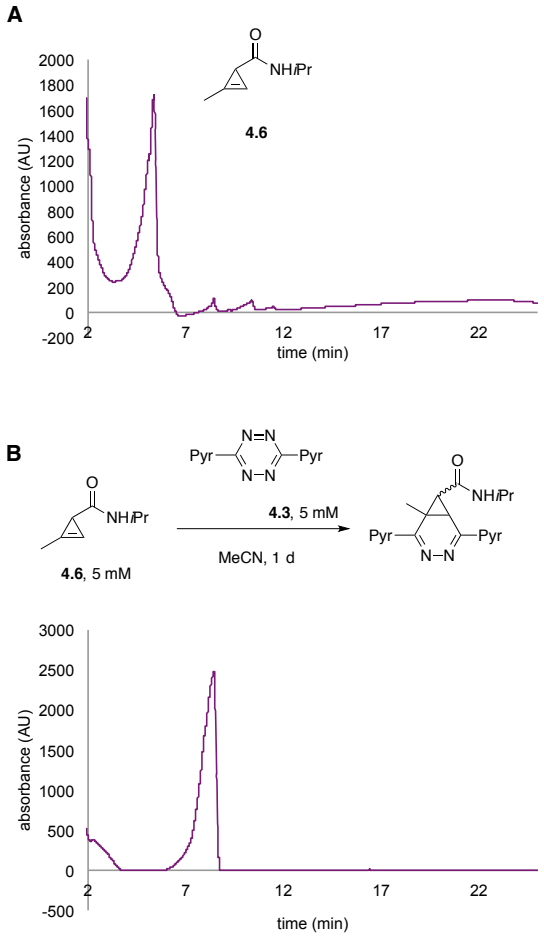

Figure S4.10. Tetrazine **4.3** reacts quantitatively with cyclopropenen **4.6**. (A) HPLC trace of starting cyclopropene **xx** trace. (B) Tetrazine **4.3** (5mM in MeCN) was reacted with cyclopropene **4.6** (5 mM in MeCN) for 4 h, and monitored by HPLC. The initial cycloadduct formed between **4.3** and **4.6** can undergo further rearrangement [4]. HPLC traces are monitored at 210 nm wavelength.

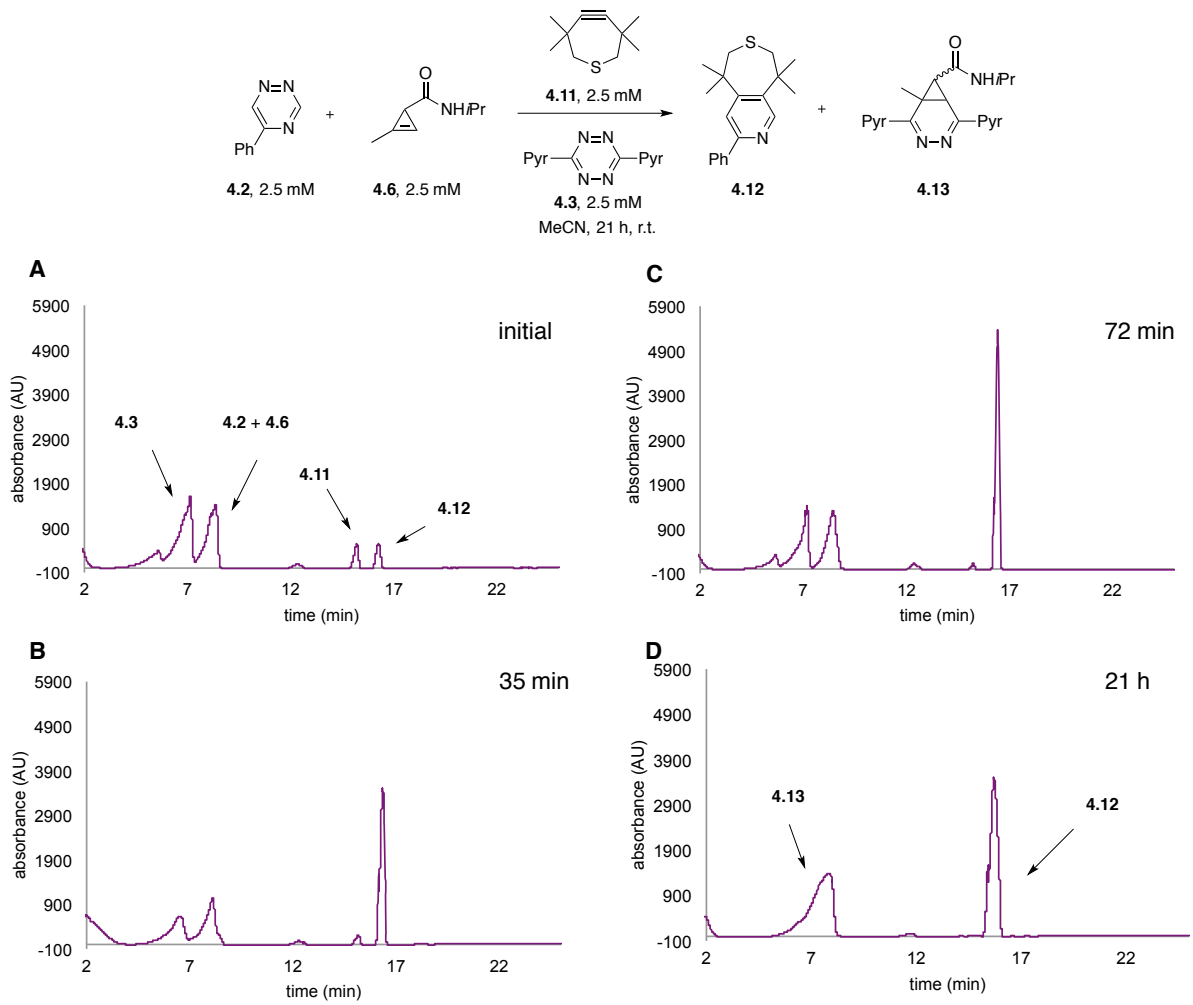

Figure S4.11. Compatible cycloadditions between triazine **4.2**, cyclopropene **4.6**, **4.11**, and **4.3**. All four reagents were combined (2.5 mM), and the reaction monitored by HPLC (210 nm) for 1 d.

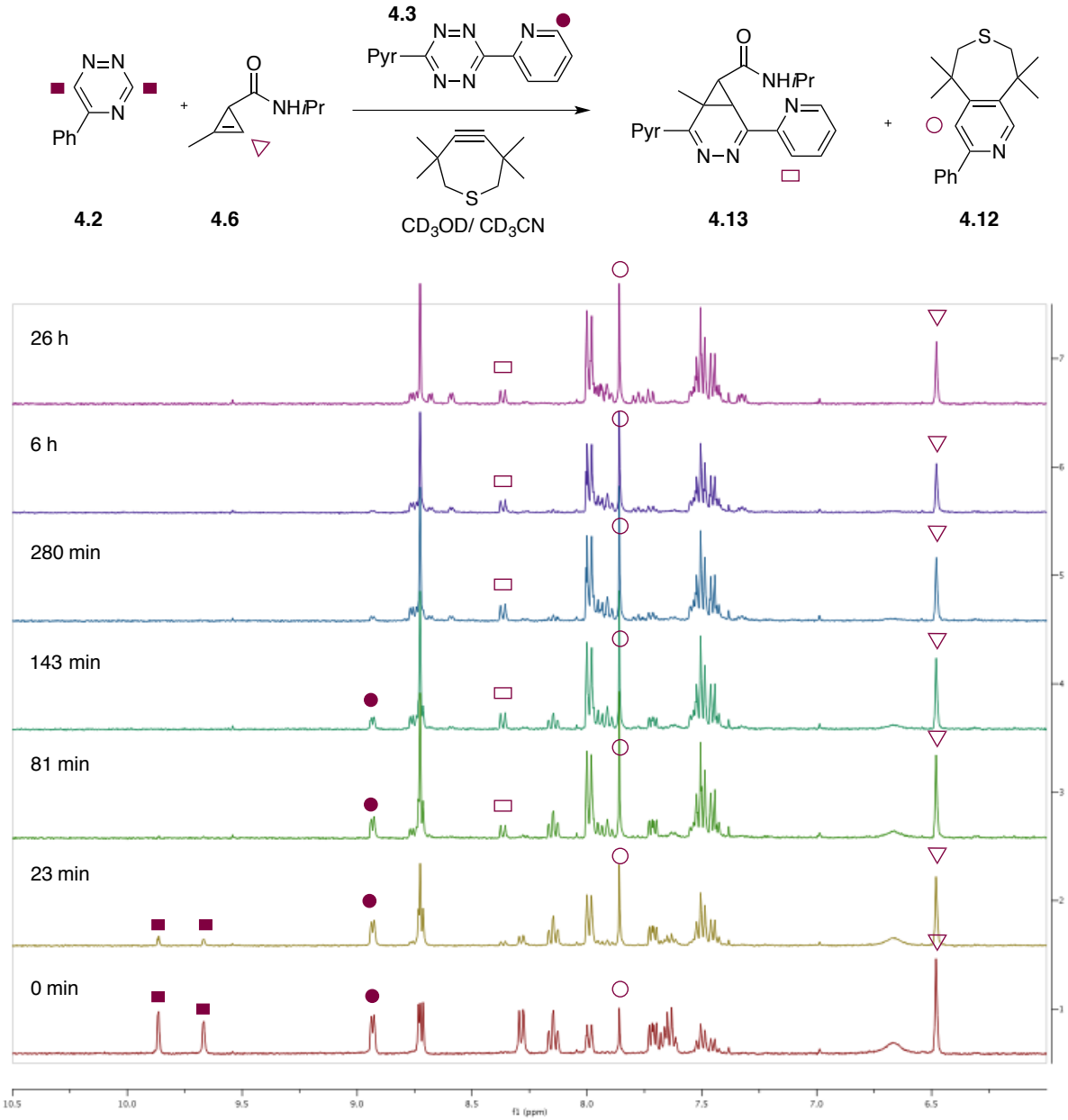

Figure S4.12. One-pot reaction. Triazine **4.2** (0.30 mL of a 25 mM solution in CD_3CN), cyclopropene **4.6** (0.30 mL of a 35 mM solution in CD_3CN), tetrazine **4.3** (0.30 mL of a 20 mM solution in CD_3OD), and TMTH **4.11** (0.30 mL of a 50 mM solution in CD_3CN) were mixed together. The reaction was monitored over time by ^{1}H-NMR.

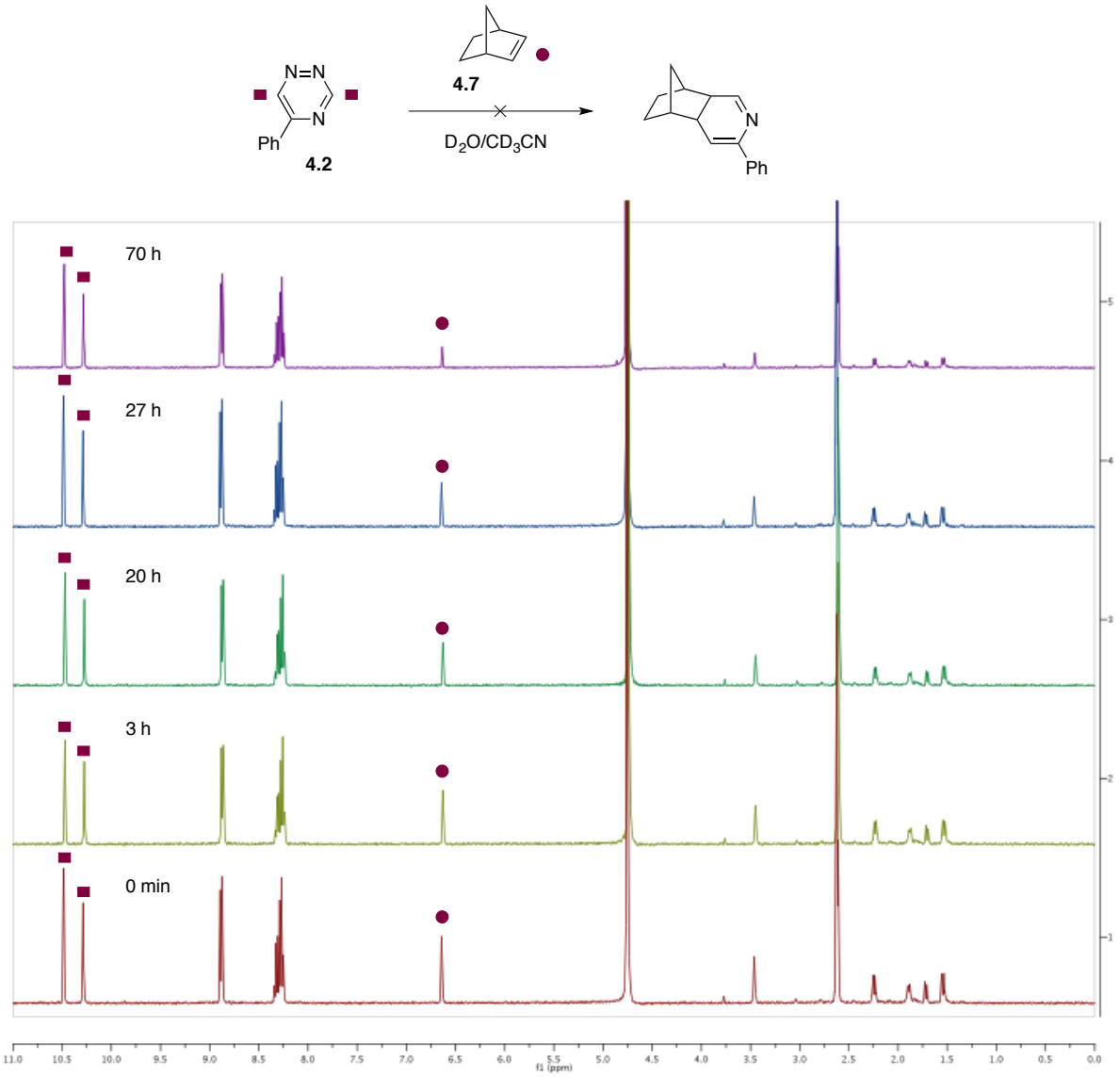

Figure S4.13. 5-Substituted triazine **4.2** is orthogonal to norbornene **4.7**. Triazine **4.2** (0.24 mL of a 25 mM solution in CD_3CN) was added a solution of **4.7** (0.24 mL of a 9.4 mM solution in D_2O:CD_3CN) and diluted with 0.12 mL of D_2O. The reaction was monitored over time by ^{1}H-NMR.

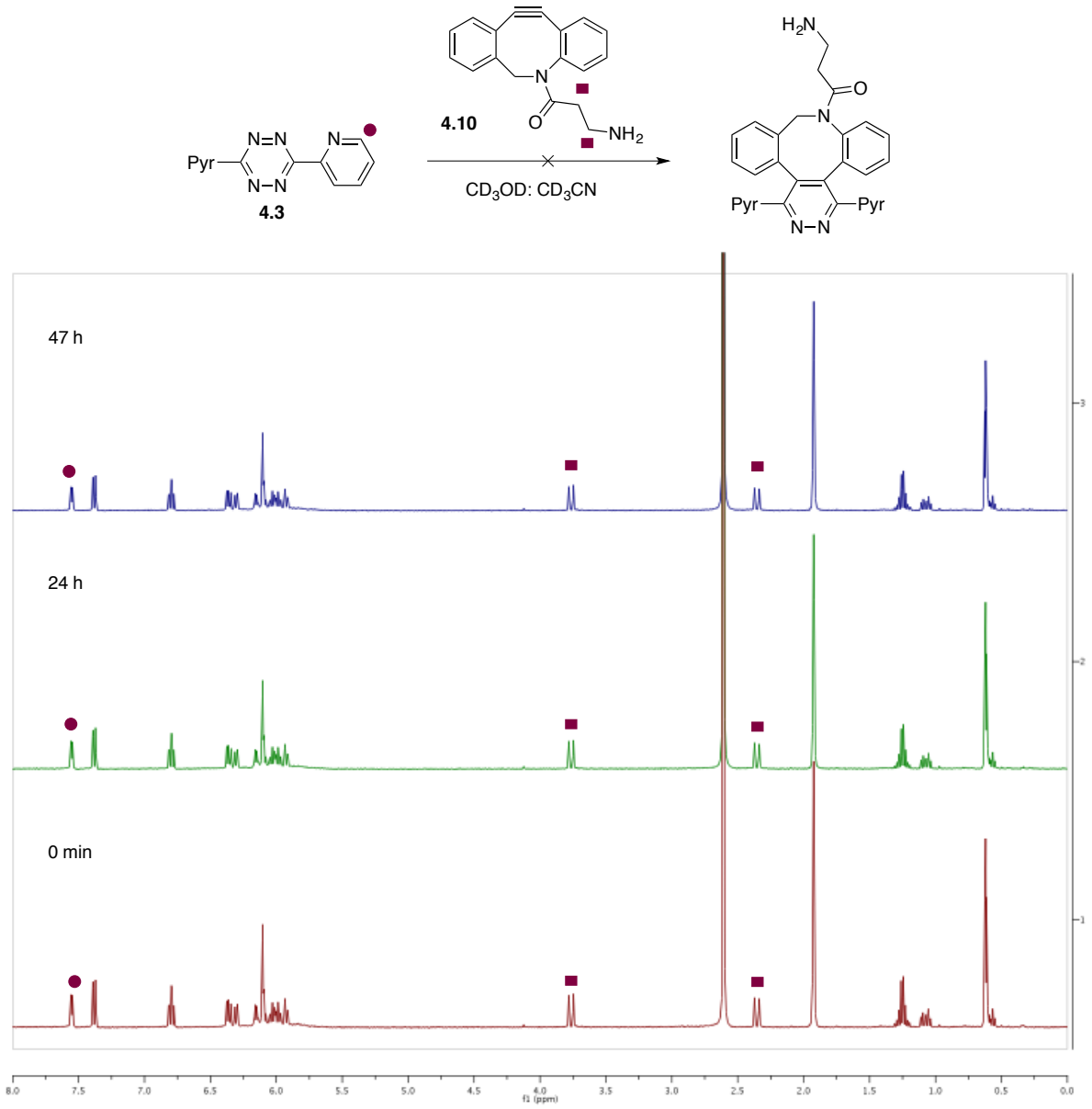

Figure S4-14. Tetrazine **4.3** is orthogonal to DIBAC **4.10**. tetrazine **4.3** (0.30 mL of a 20 mM solution in CD_3CN) was added a solution of **4.10** (0.30 mL of a 20 mM solution in CD_3OD). The reaction was monitored over time by ^{1}H-NMR.

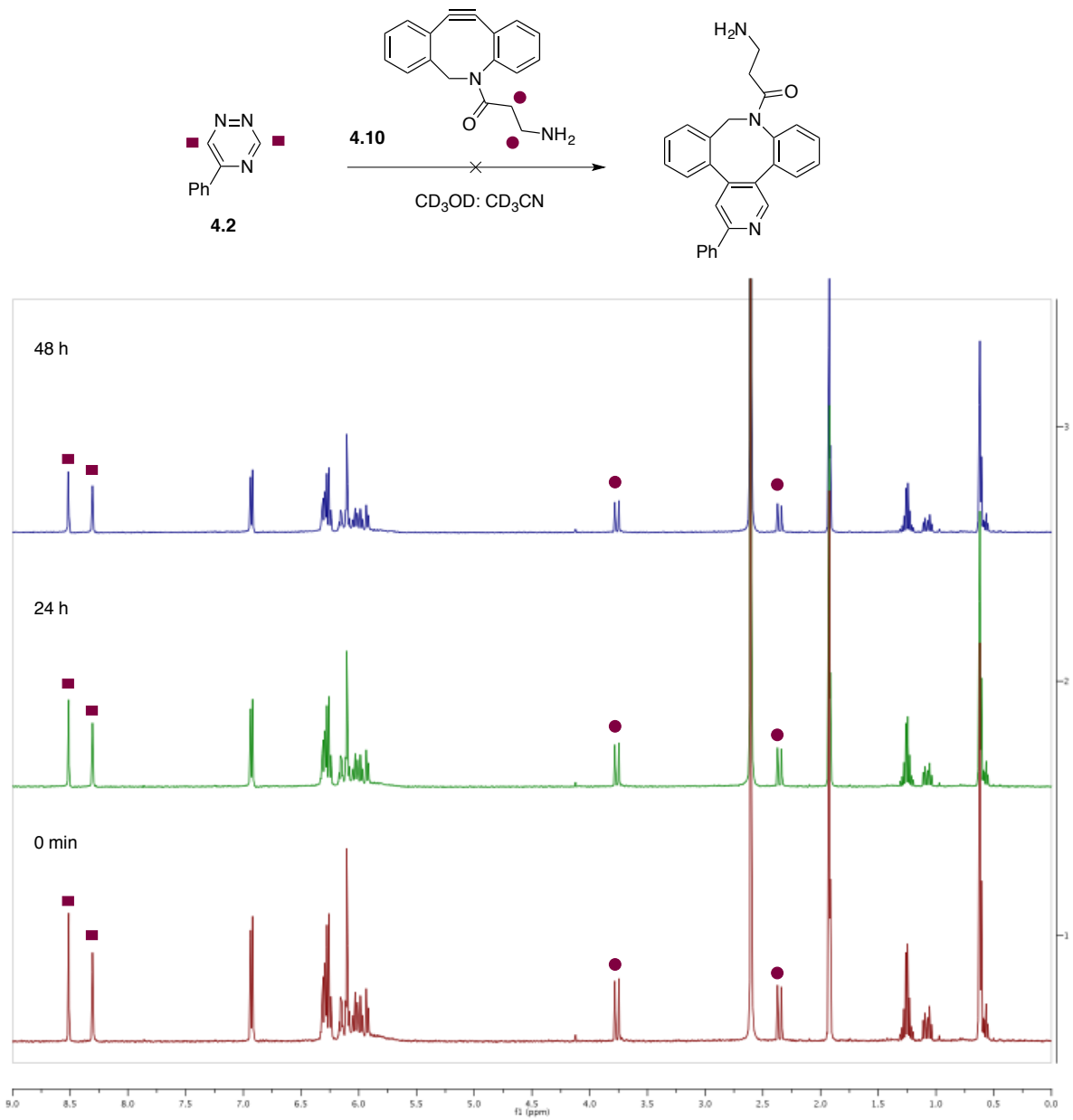

Figure S4-15. Tetrazine **4.2** is orthogonal to **DIBAC**. Triazine **4.2** (0.30 mL of a 20 mM solution in CD_3CN) was added a solution of **DIBAC** (0.30 mL of a 20 mM solution in CD_3OD). The reaction was monitored over time by ^{1}H-NMR.

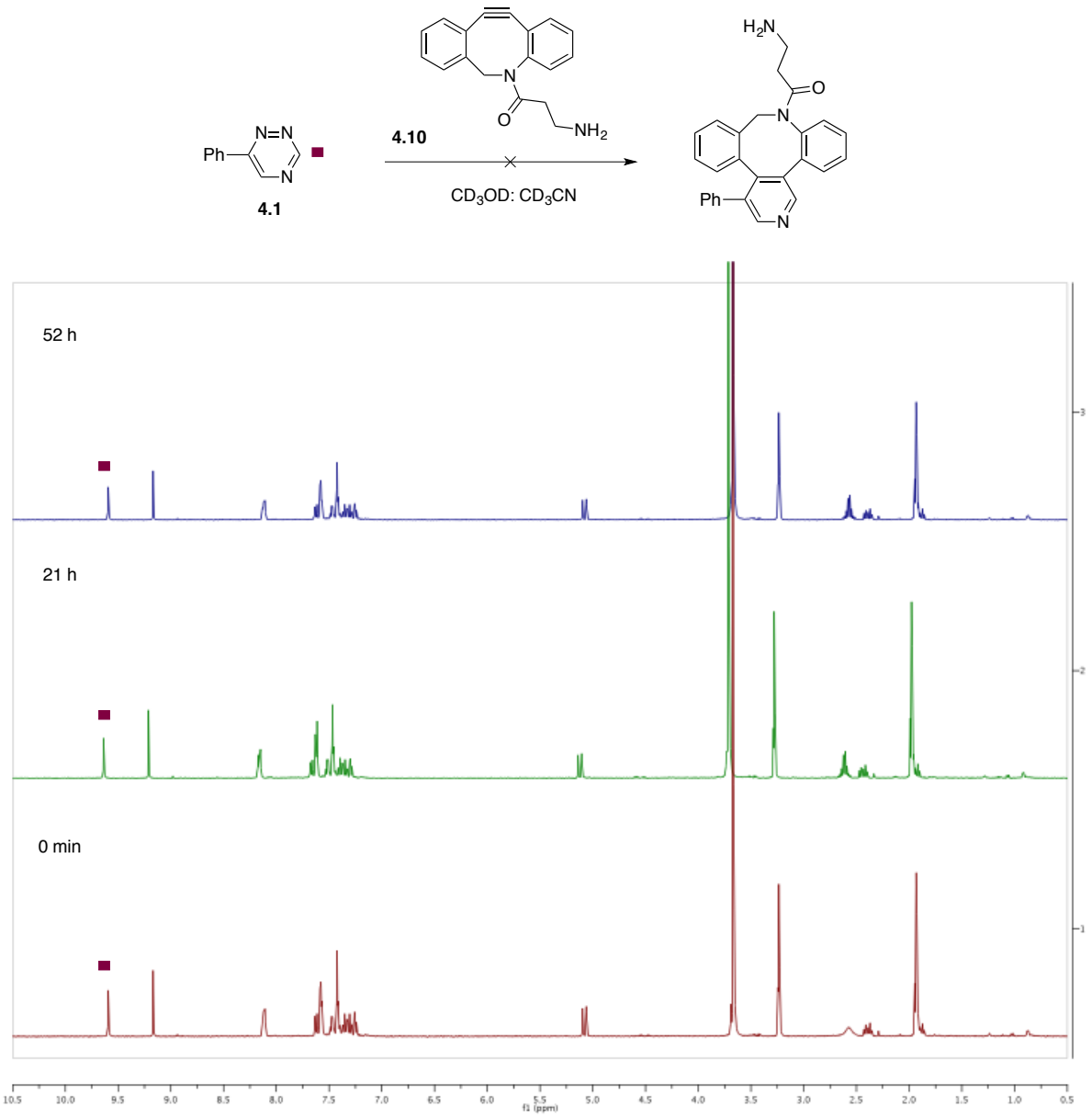

Figure S4-16. Tetrazine **4.1** is orthogonal to DIBAC **4.10**. Triazine **4.1** (0.24 mL of a 25 mM solution in CD_3CN) was added a solution of DIBAC **4.10** (0.24 mL of a 25 mM solution in CD_3OD), and diluted to 0.6 mL with CD_3CN. The reaction was monitored over time by ^{1}H-NMR.

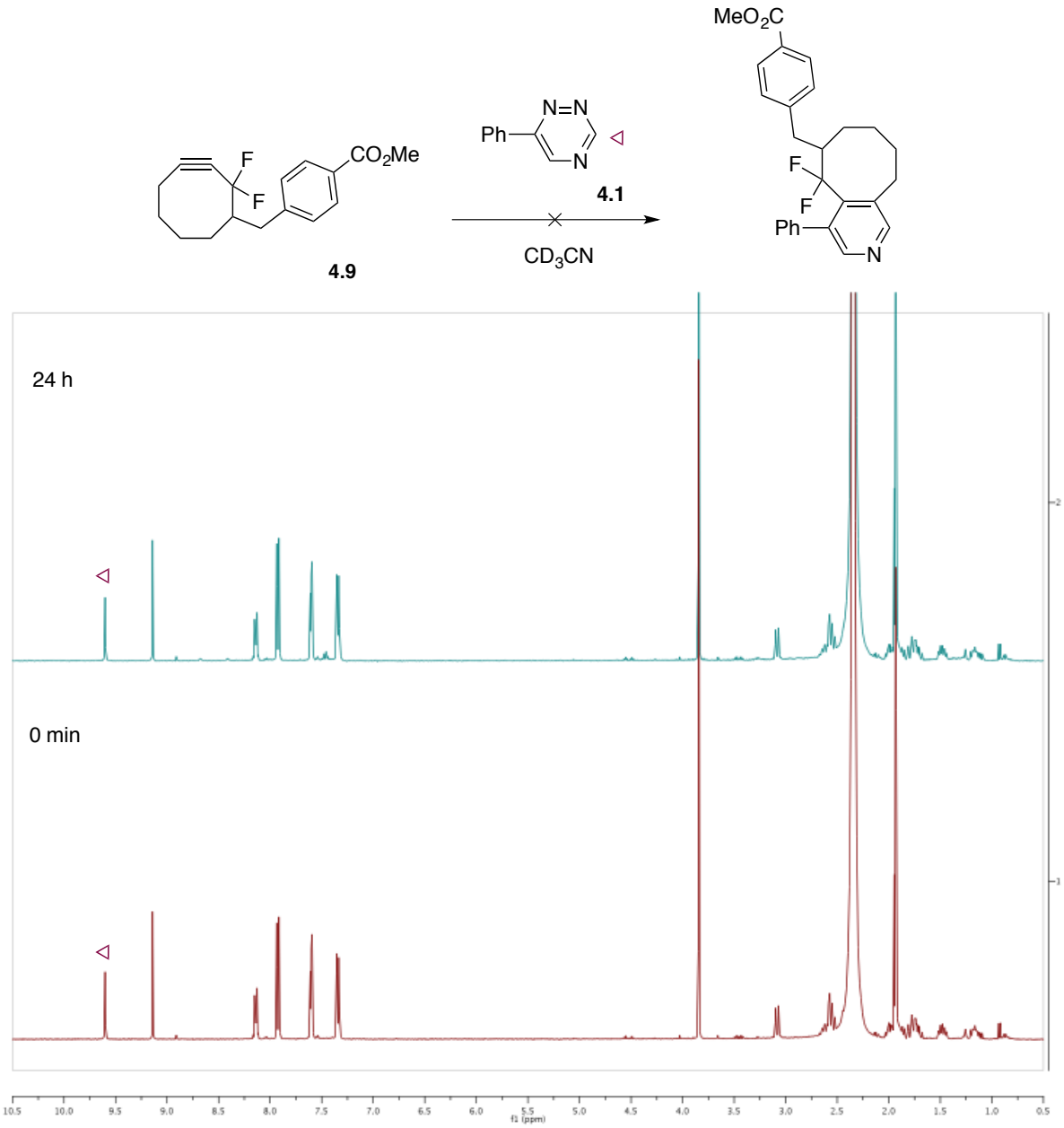

Figure S4-17. Tetrazine **4.1** is orthogonal to DIFO **4.9**. Triazine **4.2** (0.24 mL of a 25 mM solution in CD_3CN) was added a solution of DIFO **4.9** (0.24 mL of a 25 mM solution in CD_3CN) and diluted to 0.6 mL with CD_3CN. The reaction was monitored over time by ^{1}H-NMR.

1H spectrum

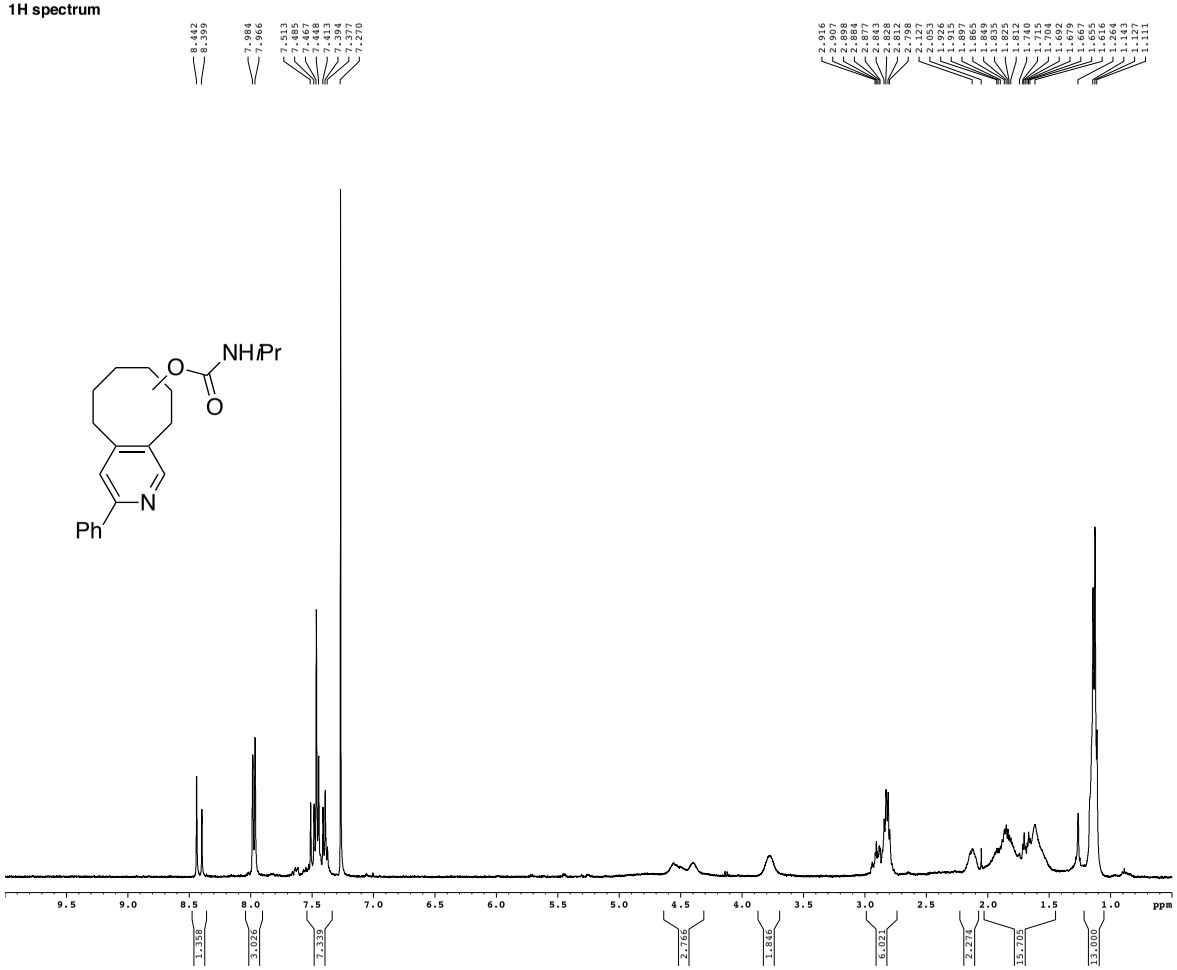


```
Current Data Parameters
USER              kamber
NAME            DK09-146
EXPNO                 15
PROCNO                 1

F2 - Acquisition Parameters
Date_           20150911
Time               11.43
INSTRUM          drx400
PROBHD   5 mm QNP H/F/P
PULPROG            zg30
TD                65536
SOLVENT           CDCl3
NS                    8
DS                    2
SWH            6410.256 Hz
FIDRES         0.097813 Hz
AQ           5.1118579 sec
RG                812.7
DW               78.000 usec
DE                4.50 usec
TE               298.0 K
D1          0.10000000 sec
MCREST      0.00000000 sec
MCWRK       0.01500000 sec

======== CHANNEL f1 ========
NUC1                 1H
P1                12.00 usec
PL1                0.00 dB
SFO1        400.1328009 MHz

F2 - Processing parameters
SI                65536
SF          400.1300175 MHz
WDW                  EM
SSB                   0
LB                 0.30 Hz
GB                    0
PC                 2.00
```

Z-restored spin-echo 13C spectrum with 1H decoupling

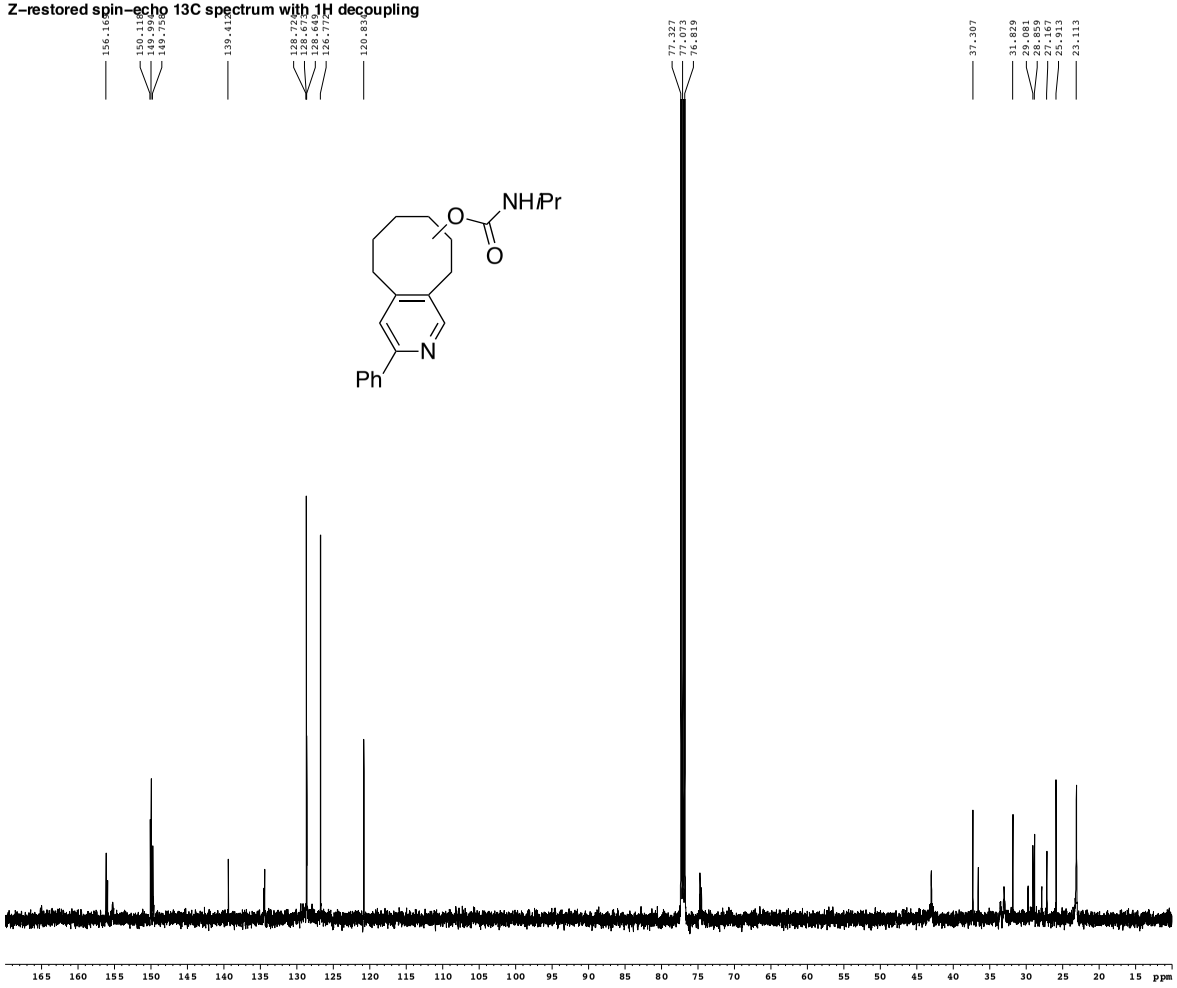


```
Current Data Parameters
USER            kamber
NAME         DK09-146-C
EXPNO               20
PROCNO               1

F2 - Acquisition Parameters
Date_         20150915
Time             11.11
INSTRUM        cryo500
PROBHD   5 mm CPTCI 1H-
PULPROG  SpinEchopg30gp.prd
TD              65536
SOLVENT           CDCl3
NS                 1524
DS                   16
SWH          30303.031 Hz
FIDRES        0.462308 Hz
AQ           1.0813940 sec
RG              2896.3
DW             16.500 usec
DE              6.00 usec
TE             298.0 K
D1          0.25000000 sec
d11         0.03000000 sec
D16         0.00020000 sec
d17         0.00019600 sec
MCREST      0.00000000 sec
MCWRK       0.01500000 sec
P2             33.10 usec

======== CHANNEL f1 ========
NUC1              13C
P1              16.55 usec
P11            500.00 usec
P12           2000.00 usec
PL0            120.00 dB
PL1             -1.00 dB
SFO1       125.7942548 MHz
SP1              2.70 dB
SP2              2.70 dB
SPNAM1   Crp60,0.5,20.1
SPNAM2     Crp60comp.4
SPOFF1           0.00 Hz
SPOFF2           0.00 Hz

======== CHANNEL f2 ========
CPDPRG2        waltz16
NUC2              1H
PCPD2          100.00 usec
PL2              1.60 dB
PL12            24.50 dB
SFO2       500.2225011 MHz

====== GRADIENT CHANNEL =====
GPNAM1        SINE.100
GPNAM2        SINE.100
GPX1             0.00 %
GPX2             0.00 %
GPY1             0.00 %
GPY2             0.00 %
GPZ1            30.00 %
GPZ2            50.00 %
p15            500.00 usec
p16           1000.00 usec

F2 - Processing parameters
SI              65536
SF         125.7804190 MHz
WDW               EM
SSB                0
LB              1.00 Hz
GB                 0
PC              2.00
```

1H spectrum

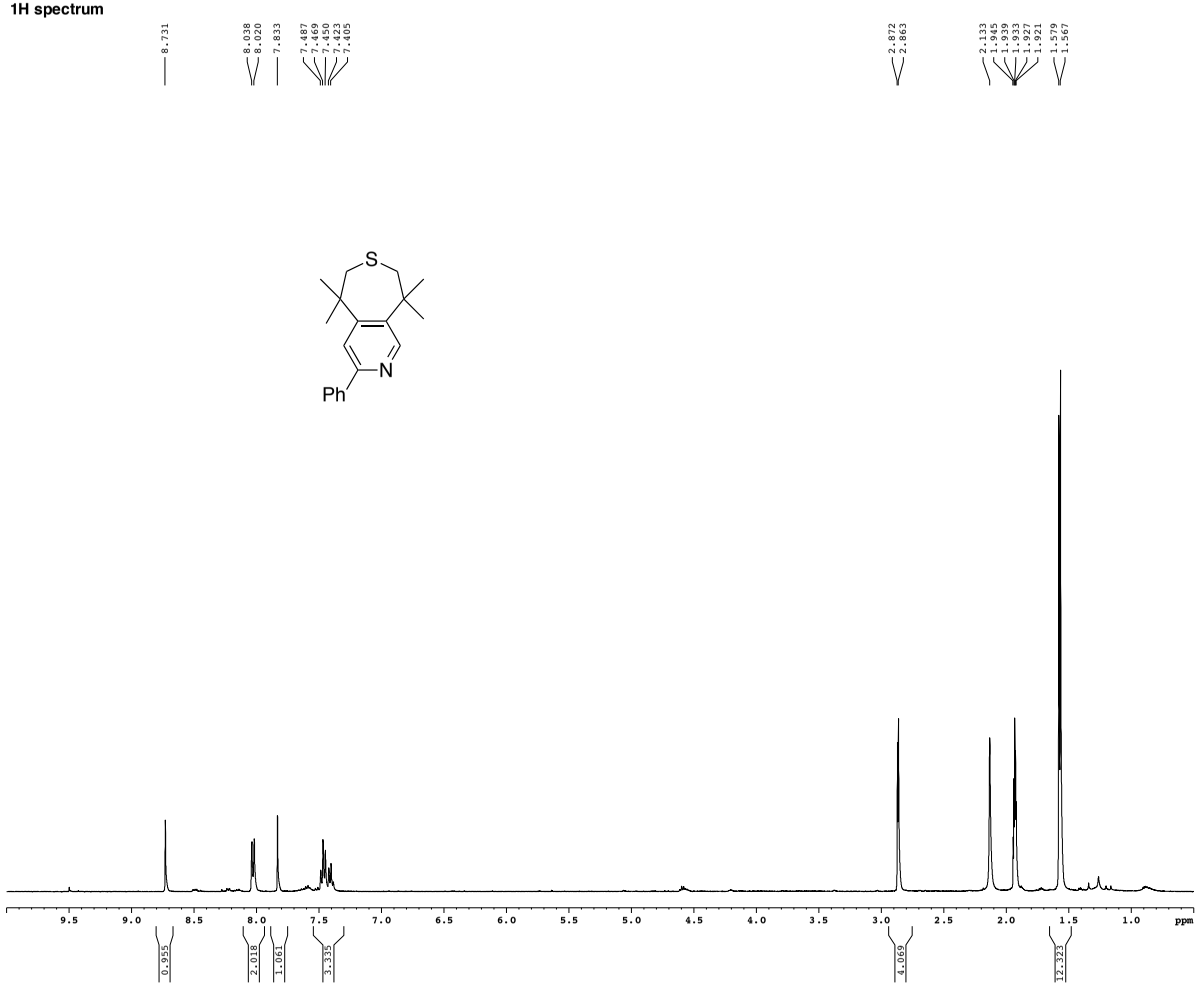


```
Current Data Parameters
USER              kamber
NAME      DK06-186-combine
EXPNO                   1
PROCNO                  1

F2 - Acquisition Parameters
Date_          20140609
Time              11.31
INSTRUM          drx400
PROBHD   5 mm QNP H/F/P
PULPROG           zg30
TD               65536
SOLVENT          CD3CN
NS                    8
DS                    2
SWH            6410.256 Hz
FIDRES         0.097813 Hz
AQ            5.1118579 sec
RG              574.7
DW              78.000 usec
DE               4.50 usec
TE              298.0 K
D1           0.10000000 sec
MCREST       0.00000000 sec
MCWRK        0.01500000 sec

======== CHANNEL f1 ========
NUC1                 1H
P1               12.00 usec
PL1               0.00 dB
SFO1        400.1328009 MHz

F2 - Processing parameters
SI               65536
SF          400.1300175 MHz
WDW                 EM
SSB                  0
LB                0.30 Hz
GB                   0
PC                2.00
```

Z–restored spin–echo 13C spectrum with 1H decoupling

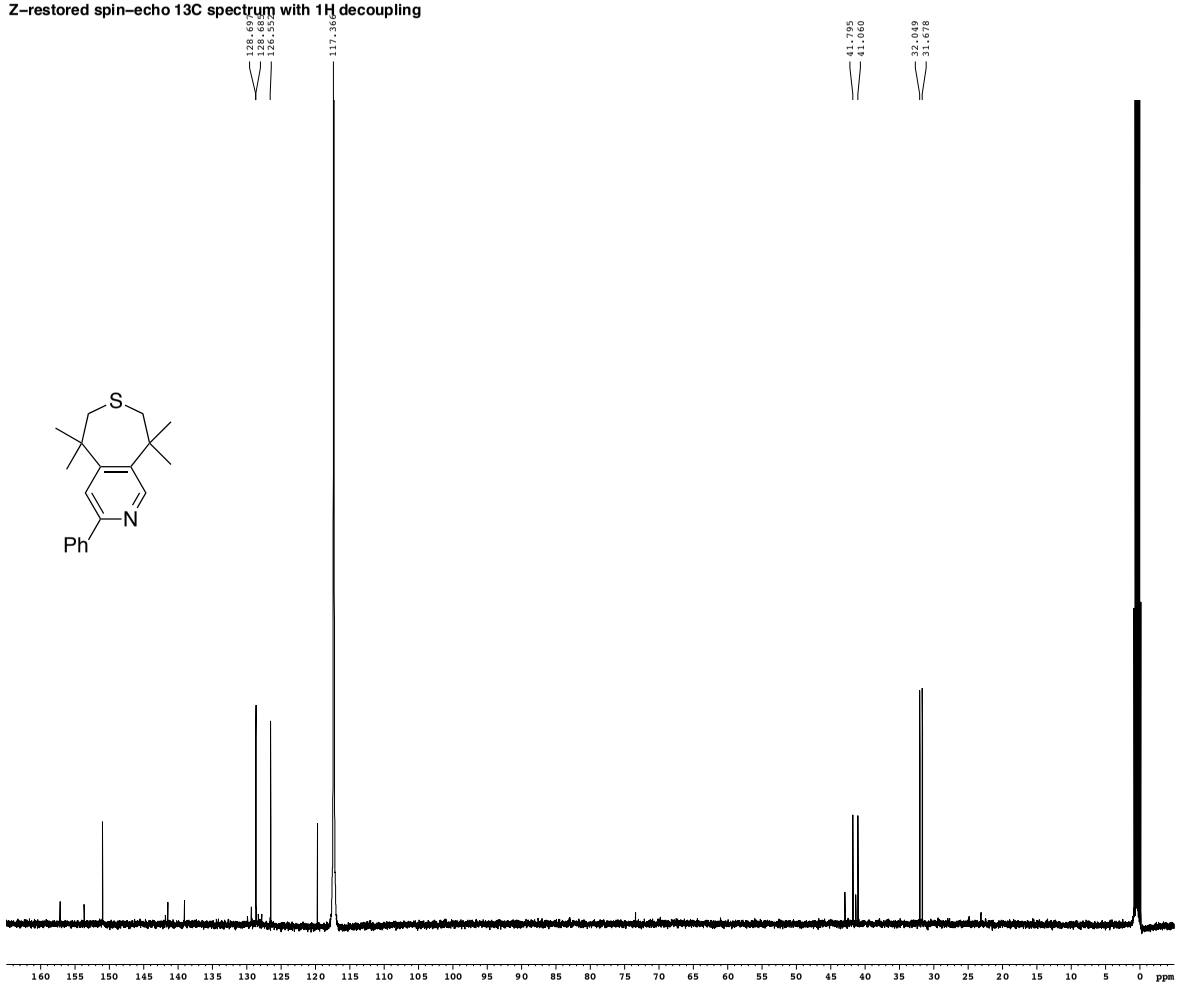


```
Current Data Parameters
USER                kamber
NAME        DK06-186-combine
EXPNO                       2
PROCNO                      1

F2 - Acquisition Parameters
Date              20140609
Time                 17.40
INSTRUM            cryo500
PROBHD    5 mm CPTCI 1H-
PULPROG   SpinEchopg30gp.prd
TD                   65536
SOLVENT              CD3CN
NS                    1896
DS                      16
SWH               30303.031 Hz
FIDRES             0.462388 Hz
AQ                1.0813960 sec
RG                   7298.2
DW                   16.500 usec
DE                    6.00 usec
TE                   298.0 K
D1              0.25000000 sec
d11             0.03000000 sec
D16             0.00020000 sec
d17             0.00019600 sec
MCREST          0.00000000 sec
MCWRK           0.01500000 sec
P2                   31.00 usec

======== CHANNEL f1 ========
NUC1                    13C
P1                    15.50 usec
P11                  500.00 usec
P12                 2000.00 usec
PL0                  120.00 dB
PL1                   -1.00 dB
SFO1            125.79425548 MHz
SP1                    3.20 dB
SP2                    3.20 dB
SPNAM1     Crp60,0.5,20.1
SPNAM2        Crp60comp.4
SPOFF1                 0.00 Hz
SPOFF2                 0.00 Hz

======== CHANNEL f2 ========
CPDPRG2            waltz16
NUC2                     1H
PCPD2                 100.00 usec
PL2                    1.60 dB
PL12                  24.60 dB
SFO2            500.2225011 MHz

===== GRADIENT CHANNEL =====
GPNAM1            SINE.100
GPNAM2            SINE.100
GPX1                   0.00 %
GPX2                   0.00 %
GPY1                   0.00 %
GPY2                   0.00 %
GPZ1                  30.00 %
GPZ2                  50.00 %
p15                  500.00 usec
p16                 1000.00 usec

F2 - Processing parameters
SI                   65536
SF              125.7804190 MHz
WDW                     EM
SSB                      0
LB                    1.00 Hz
GB                       0
PC                    2.00
```